2017

A Roadmap for Development of Novel Antipsychotic Agents Based on a Risperidone Scaffold

Urjita H. Shah
Virginia Commonwealth University

A ROADMAP FOR DEVELOPMENT OF NOVEL ANTIPSYCHOTIC AGENTS

BASED ON A RISPERIDONE SCAFFOLD

A dissertation submitted in partial fulfillment of the requirements for the degree of Doctor of Philosophy at Virginia Commonwealth University.

by

URJITA H. SHAH
Bachelor of Pharmacy, University of Mumbai, India, 2012

Director: DR. RICHARD A. GLENNON, PHD
PROFESSOR, AND CHAIRMAN, MEDICINAL CHEMISTRY

Virginia Commonwealth University
Richmond, Virginia
May 2017

Acknowledgment

I would like to thank my advisor Dr. Richard A. Glennon for being an excellent mentor, and for his unending support, guidance, encouragement and constant patience over the last five years. I am extremely grateful to Dr. Małgorzata Dukat for her constructive inputs and support. Thank you, Drs. Dukat and Glennon for molding me both professionally and personally.

A special thank you to all the lab members over the years: Renata, Atul, Osama, Kavita, Malaika, Farhana, Supriya, Abdelrahman, Rachel, Ahmed, Umberto, Alessandro, Pallavi and Barkha for all their help, and for making the lab a great place to work in. I would like to thank Dr. Osama I. Alwassil, Dr. Kavita A. Iyer and Dr. Philip Mosier for their help with molecular modeling. I would like to express my gratitude to Dr. Javier González-Maeso for giving me the opportunity to test our compounds in his lab, and Dr. Supriya A. Gaitonde for teaching me the techniques necessary to perform radioligand binding assays. I am thankful to Drs. Javier González-Maeso and Diomedes Logothetis as well as their lab members for providing us with biological data. I would also like to thank my committee members Dr. Glen E. Kellogg and Dr. Dana E. Selley.

I am grateful to the Department of Medicinal Chemistry, School of Pharmacy and Virginia Commonwealth University for giving me the opportunity to pursue this degree.

Mom, Dad, Chintal and Dakshil, I cannot thank you enough for your unconditional love, and constant support and encouragement throughout this endeavor. Kavita and Malaika, I am fortunate to have met you both, and I am extremely thankful to the two of you for being my support system and family in Richmond. A big thank you to Manizaay and Urvi for standing by me through the best and the worst. I would also like to thank my friends Bhavi, Nidhi, Sweta and Piyusha for all the good memories, and for making Richmond feel like home. Lastly, I am thankful to my entire family for their support.

Table of Contents

List of Tables

List of Figures

List of Schemes

List of Abbreviations

5-HT	Serotonin
5-HT_{1A}	Serotonin type 1A receptor
5-HT_{1C}	Serotonin type 2C receptor
5-HT_{2A}	Serotonin type 2A receptor
5-HT_{2C}	Serotonin type 2C receptor
α_1	Adrenoceptor type 1
α_2	Adrenoceptor type 2
μ	Micro
Å	Angstrom(s)
Ac_2O	Acetic anhydride
ACh	Acetylcholine
AcOH	Acetic acid
$AlCl_3$	Aluminium chloride
AMPA	α-Amino-3-hydroxy-5-methyl-4-isoxazolepropionic acid
BINAP	2,2'-Bis(diphenylphosphino)-1,1'-binaphthyl
°C	Degrees Celsius
cAMP	Cyclic adenosine monophosphate

CB_1	Cannabinoid type 1 receptor
CB_2	Cannabinoid type 2 receptor
$CHCl_3$	Chloroform
CH_2Cl_2	Dichloromethane
$(COOH)_2$	Oxalic acid
CNS	Central nervous system
CPZ	Chlorpromazine
d	Doublet
dd	Doublet of doublets
D_2	Dopamine type 2 receptor
D_3	Dopamine type 3 receptor
DA	Dopamine
DAG	Diacyl glycerol
DMF	*N*,*N*-Dimethylformamide
DMSO	Dimethylsulfoxide
DOI	1-(2,5-Dimethoxy-4-iodophenyl)-2-aminopropane
DSM-5	Diagnostic and Statistical Manual for Mental Disorders, fifth edition
EC_{50}	Effective concentration to achieve 50% response
ECL	Extracellular loop
EPS	Extrapyramidal symptoms
Et_2O	Diethyl ether
EtOH	Absolute ethanol

EtOAc	Ethyl acetate
Et_3N	Triethylamine
USFDA	The Food and Drugs Administration
$G_{\alpha q}$, $G_{i/o}$, $G_{q/11}$	G-Protein subunits
GABA	Gamma-Aminobutyric acid
GPCRs	G-Protein coupled receptors
GLU	Glutamate
h	Hour(s)
HCHO	Formaldehyde
HCOOH	Formic acid
HCl	Hydrochloric acid
HEK 293	Human embryonic kidney cells
HINT	Hydropathic INTeraction
IC_{50}	Inhibitory concentration to achieve 50% inhibition
ICD-10	International Classification of Diseases, tenth addition
i-PrOH	Isopropyl alcohol
IR	Infrared spectroscopy
GIRK4*	G-Protein sensitive inwardly-rectifying potassium channel
IP_3	Inositol 1,4,5-triphosphate
J	Coupling constant
KI	Potassium iodide
K_i	Inhibitory constant

K_2CO_3	Potassium carbonate
KOH	Potassium hydroxide
LSD	Lysergic acid diethylamide
$LiAlH_4$	Lithium aluminium hydride
m	Multiplet
M_1	Muscarinic type 1 receptor
M_4	Muscarinic type 4 receptor
MARTAs	Multi-acting receptor-targeted antipsychotics
MeCN	Acetonitrile
MeOH	Methanol
$mGlu_2$	Metabotropic glutamate type 2 receptor
$mGlu_2$	Metabotropic glutamate type 2 receptor
$mGlu_3$	Metabotropic glutamate type 3 receptor
mp	Melting point
$NaBH_4$	Sodium borohydride
NaOH	Sodium hydroxide
NAM	Negative allosteric modulator
NCS	*N*-Chlorosuccinimide
$NiCl_2$	Nickel chloride
nM	Nanomolar
NMDA	N-Methyl-D-aspartate
NMR	Nuclear magnetic resonance

PAMs	Positive allosteric modulators
Pd/C	Palladium on carbon
PLC	Phospholipase C
pI3K	Phosphoinositide-3 kinase
q	Quartet
RMSD	Root-mean-square deviation
MAPK	Mitogen-activated protein kinases
s	Singlet
SAR	Structure-activity relationship(s)
SDAs	Serotonin-dopamine antagonists
t	Triplet
td	Triplet of doublets
t-BuOH	*tert*-Butyl alcohol
TEVC	Two-electrode voltage clamp
THF	Tetrahydrofuran
TLC	Thin layer chromatography
TM	Transmembrane
TMD	Transmembrane domain
UniProt	Universal Protein Resource

Abstract

A ROADMAP FOR DEVELOPMENT OF NOVEL ANTIPSYCHOTIC AGENTS BASED ON A RISPERIDONE SCAFFOLD

By Urjita H. Shah, Ph. D.

A dissertation submitted in partial fulfillment of the requirements for the degree of Doctor of Philosophy at Virginia Commonwealth University.

Virginia Commonwealth University, 2017

Major Director: Dr. Richard A. Glennon, Ph. D.
Professor and Chairman, Department of Medicinal Chemistry

Schizophrenia is a chronic psychotic illness affecting ~21 million people globally. Currently available antipsychotic agents act through a dopamine D_2 receptor mechanism, and produce extrapyramidal or metabolic side effects. Hence, there is a need for novel targets and agents. The $mGlu_2$/5-HT_{2A} receptor heteromer has been implicated in the action of antipsychotic agents, and represents a novel and attractive therapeutic target for the treatment of

schizophrenia. A long-term goal of this project is to synthesize bivalent ligands where a 5-HT_{2A} receptor antagonist is tethered to an $mGlu_2$ PAM via a linker.

The goals of the investigation were to study the SAR of risperidone (an atypical antipsychotic agent) at 5-HT_{2A} receptors using a "deconstruction-reconstruction-elaboration" approach to determine the minimal structural features of risperidone that contribute to its 5-HT_{2A} receptor affinity and antagonism, and to determine where on the "minimized risperidone" structure an $mGlu_2$ PAM can be introduced. Additional goals included studying the binding modes of various $mGlu_2$ PAMs and identifying where on an $mGlu_2$ PAM a risperidone "partial" structure could be introduced.

Biological studies of deconstructed/elaborated analogs of risperidone suggest that the entire structure of risperidone is not necessary for 5-HT_{2A} receptor affinity and antagonism, and that a fluoro group contributes to 5-HT_{2A} binding. 6-Fluoro-3-(4-piperidinyl)-1,2-benz[*d*]isoxazole that has only half the structural features of risperidone retains 5-HT_{2A} receptor affinity and antagonist activity, and represents the "minimized risperidone" structure with the piperidine nitrogen atom representing a potential linker site for eventual construction of bivalent ligands. Molecular modeling studies at 5-HT_{2A} receptors suggest that risperidone and its analogs have more than one binding mode.

Modeling studies to evaluate binding modes of various PAMs at $mGlu_2$ receptors, coupled with known SAR information, were used to identify a PAM (JNJ-40411813), and the

pyridone nitrogen atom of JNJ-40411813 as a potential linker site. Additionally, potential synthetic routes for JNJ-40411813 were explored that might be of value in the synthesis of bivalent ligands.

Based on the structural features of 6-fluoro-3-(4-piperidinyl)-1,2-benz[*d*]isoxazole, a new pharmacophore for 5-HT_{2A} receptor antagonists, consisting of one aromatic region, a basic protonated amine and hydrogen bond acceptors, has been proposed.

I. INTRODUCTION

Schizophrenia is a chronic, recurring psychotic illness with an enigmatic etiology that remains a significant health problem and affects ~1% of the global population.[1,2] There is emerging evidence to show that schizophrenia might be a part of a larger group of disorders called "schizophrenia spectrum disorder" that is prevalent in ~6% of the general population.[1,2] The clinical symptoms of schizophrenia can be classified into positive symptoms such as hallucinations and delusions, negative symptoms that include anhedonia and apathy, and cognitive deficits that are related to working memory, and attention.[1,3,4]

Several hypotheses have been proposed to link altered brain function and schizophrenia and there could be abnormalities in dopamine (DA), serotonin (5-HT), glutamate (GLU), γ-aminobutyric acid (GABA), and acetylcholine (ACh) receptor pathways.[4–6] However, most clinically available antipsychotic agents act through a dopamine D_2 receptor mechanism.[7]

The introduction of chlorpromazine (a "typical" antipsychotic agent) in 1952 marked a new era of drug treatment in psychiatry.[8,9] Chlorpromazine is a dopamine D_2 receptor antagonist that is effective against the positive symptoms of schizophrenia;[10] however, extrapyramidal symptoms (EPS) are a common side effect of chlorpromazine therapy.[11]

The introduction of clozapine in 1990 was a hallmark in antipsychotic therapy.[12] Clozapine can ameliorate both the positive and negative attributes of schizophrenia with a lower propensity to cause EPS.[12] The introduction of clozapine led to the development of the concept of "atypical" antipsychotics, and its clinical success prompted the development of other atypical antipsychotic agents such as risperidone.[13]

Risperidone is effective in treating the positive and negative symptoms of schizophrenia and has a lower propensity to cause EPS.[14] It is a dopamine D_2 receptor (K_i = 3.1 nM) and 5-HT_{2A} receptor (K_i = 0.16 nM) antagonist.[15] Moderate D_2 receptor occupancy, and predominantly 5-HT_{2A} receptor occupancy, might be the mechanism for its effectiveness against the positive, and negative symptoms of schizophrenia, with reduced side effects.[14] Even though risperidone has a much lower tendency to cause EPS than typical antipsychotic agents, therapy with risperidone is associated with other side effects such as hyperprolactinemia, and weight gain.[13,16,17]

Nearly all currently available antipsychotic agents act through a dopamine D_2 receptor mechanism, and cause either extrapyramidal or metabolic side effects.[7] Hence, there is a pressing need for novel therapeutic targets and agents.

Literature precedent exists for the formation of a functional 5-HT_{2A}/$mGlu_2$ receptor heterocomplex[18–21] that has been implicated in the mechanism of action of antipsychotic agents.[22] Roles for the 5-HT_{2A} receptor and the $mGlu_2$ receptor in the pathophysiology of schizophrenia

have been well established.[14,23] 5-HT_{2A} receptor antagonists/inverse agonists, and $mGlu_2$ receptor orthosteric agonists and PAMs, possess antipsychotic character.[14,23] The atypical antipsychotic agent risperidone has been shown to mediate its effects by binding to the 5-HT_{2A}/$mGlu_2$ receptor heteromer which then balances $G_{i/o}$ and $G_{q/11}$ signaling.[22] Gonzalez-Maeso et al.[18] have shown that the 5-HT_{2A} receptor is upregulated and the $mGlu_2$ receptor is downregulated in postmortem brain samples of untreated schizophrenic patients. These changes suggest that the 5-HT_{2A}/$mGlu_2$ receptor heteromer may be involved in the altered cortical processes in schizophrenia, and represents an attractive novel therapeutic target for the treatment of schizophrenia.[18] A long-term goal of the project is to synthesize bivalent ligands having a 5-HT_{2A} receptor antagonist portion based on a risperidone scaffold connected to an $mGlu_2$ receptor PAM via a linker.

Goals of the current investigation are to study structure activity relationships of risperidone at 5-HT_{2A} receptors to determine the minimal structural features required for risperidone to retain 5-HT_{2A} receptor affinity and antagonist activity, and to identify where on the risperidone "partial structure" an $mGlu_2$ receptor PAM might be attached. Additional goals include studying the binding modes of various PAMs at the $mGlu_2$ receptor and identifying a PAM as well as a potential site to install the "minimized" risperidone structure that will contribute towards the long-term goal of synthesizing a bivalent molecule that can target the $mGlu_2$/5-HT_{2A} receptor heteromeric complex.

II. BACKGROUND

1. Schizophrenia

Schizophrenia is a chronic, recurring psychotic illness that remains a significant health problem affecting more than 21 million people worldwide are affected by schizophrenia,[1,2,24] and the Global Burden of Disease study has ranked schizophrenia as the ninth leading cause of disability-adjusted life-years for those aged 15-44.[8] There is emerging evidence to show that schizophrenia might be a part of a larger group of disorders called "schizophrenia spectrum disorder" that is prevalent in ~6% of the general population.[1] These disorders are related to each other in terms of pathophysiology, cognitive characteristics, symptom expression, and genetics, with schizophrenia being the most severe of the class.[1]

The concept of schizophrenia as a disease is of recent origin and has been grouped with conditions such as mania, melancholia and generic "insanity" since ancient times.[8,25] During the 19th century Kraeplin, as reviewed by Jablensky,[25] first used the term "dementia praecox' to describe the illness. Bleuler, as reviewed by Kuhn and Cahn,[26] subsequently changed the name from dementia to schizophrenia and provided the disease with a distinct diagnostic profile. The word schizophrenia has Greek origins and translates as "splitting of the mind" (shizein = splitting; phren = soul, spirit, mind).[26]

The diagnosis of schizophrenia is solely based on the presentation of clinical symptoms that can be classified into positive and negative symptoms, and cognitive deficits.[1,3,4] The positive symptoms include delusions (persecutory, referential, somatic, nihilistic, and grandiose delusions), hallucinations, reality distortion, paranoia, disorganized speech and grossly disorganized or catatonic behavior.[1,3,4] The negative attributes include anhedonia, asociality, alogia, avolition, inappropriate social skills, and affective flattening.[1,3,4] Cognitive deficits that are sometimes classified as a part of the negative symptoms are related to working memory, executive functions, and attention.[1,3,4] There can also be neurophysiological disturbances such as abnormal smooth pursuit and saccadic eye movements and abnormal evoked potentials (P300, P50) in patients with schizophrenia.[1] Various modifications have been made to the diagnosis of schizophrenia over the years and the current diagnosis of schizophrenia is based on the criteria of the Diagnostic and Statistical Manual for Mental Disorders, fifth edition (DSM-5)[27] or of the older International Classification of Diseases, tenth addition (ICD-10),[28] published by the American Psychiatric Association and the World Health Organization, respectively.

Schizophrenia is a neurodevelopmental rather than a neurodegenerative disorder and an interplay between several environmental factors such as substance abuse, trauma, and pre- or perinatal stressors, developmental factors, and genetic factors (where a risk for schizophrenia is inherited) contribute to the development of schizophrenia.[1,29] There is altered brain function and structure in schizophrenia, and patients with schizophrenia show enlarged cerebral ventricles, a 5% reduction in the size of the medial temporal cortex, decreased volume of the superior temporal gyrus, and

hippocampal shape irregularities.[1] Cerebral cortical atrophy is a hallmark feature of schizophrenia.[1,5] Proper functionality of connections between the different spatially-distributed brain regions is important for higher- order brain function and changes throughout the connected neural networks rather than damage to a single brain area that might result in schizophrenia.[8] At the neurotransmitter level, there could be abnormalities in dopamine (DA), serotonin (5-HT), glutamate (GLU), γ-aminobutyric acid (GABA), and acetylcholine (ACh) receptor pathways.[4–6] Several hypotheses have been proposed to link altered brain function and schizophrenia.

2. Theories of schizophrenia

a. The dopamine (DA) hypothesis of schizophrenia

DA (**1**) **(Fi**gure 1) functions as a neurotransmitter in the brain and plays an important role in maintaining normal physiological function.[30] DA's effects are mediated via G-protein coupled DA receptors (D_1-D_5).[30] The physiological functions of DA include, but are not limited to, sleep regulation, affect, cognitive function, attention, voluntary movement, reward, feeding, and hormonal regulation.[30] The DA hypothesis is central to the pathophysiology of schizophrenia and has undergone refinement and modification over the years.[31] The initial DA hypothesis was formulated on the basis of the observed antipsychotic effects of drugs such as chlorpromazine (CPZ) (**2**) (Figure 1) that act as DA receptor blockers (i.e.; antagonists).[31] The ability of psychostimulants such as amphetamine (**3**) (Figure 1) to induce psychosis by increasing the synaptic concentrations of monoamine neurotransmitters,[32] and the effectiveness of the indole alkaloid reserpine (**4**) (Figure 1) in treating psychosis by blocking the reuptake of DA and other monoamine neurotransmitters by irreversibly blocking the vesicular monoamine transporters,[33]

provided further evidence for the DA hypothesis of schizophrenia. In the 1970s it was realized that the effectiveness of clinical antipsychotics such as CPZ (**2**) and haloperidol (**5**) (Figure 1) was related to their affinity for the D_2 dopamine receptor.[10,31,34] The "first" version of the DA hypothesis assumed a general dopaminergic hyperfunction.[31] A major drawback of the initial DA hypothesis was that it focused on blockade of DA receptors to treat psychosis, but there was no relation between abnormal dopaminergic activity and expression of positive and negative symptoms, and little was known about where the abnormality occurred in the brain.[31] The hypothesis was also unable to explain the inability of antipsychotics to treat the negative symptoms and cognitive deficits of schizophrenia.[31]

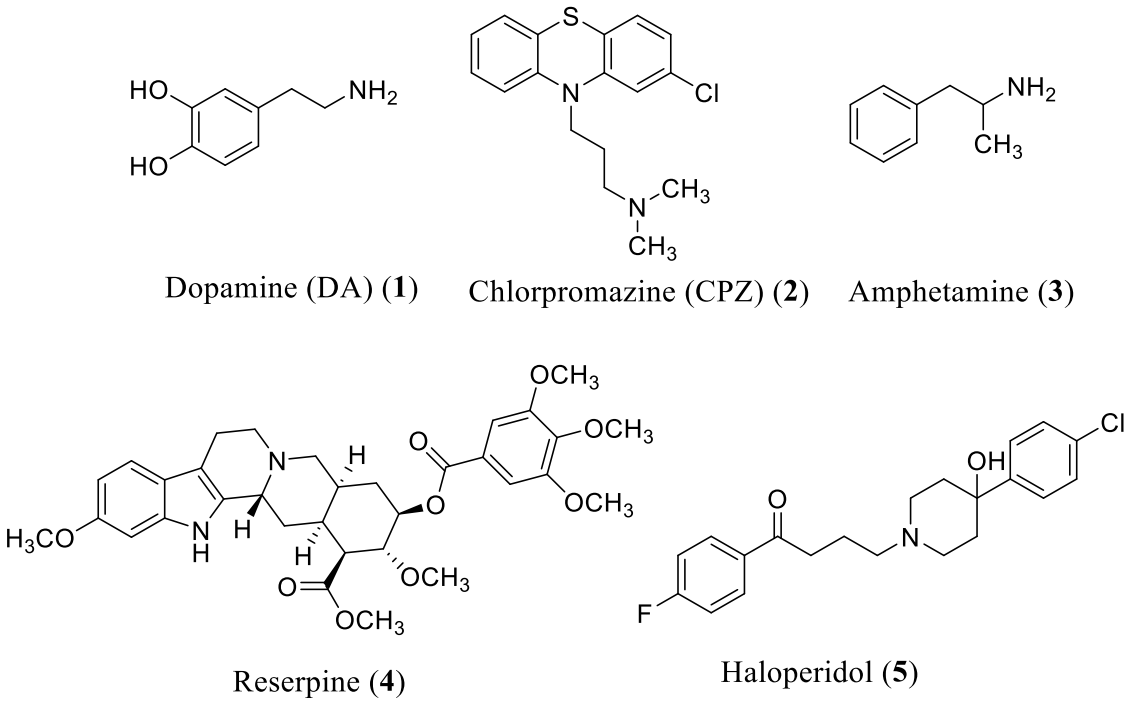

Figure 1. Structures of the neurotransmitter dopamine (DA) (**1**), the typical antipsychotic agents chlorpromazine (CPZ) (**2**), and haloperidol (**5**), the psychostimulant amphetamine (**3**), and the indole alkaloid reserpine (**4**).

In 1991, a "modified hypothesis of schizophrenia" was proposed by Davis et al.[35] They hypothesized that there is hyperdopaminergia in the subcortical DA pathway that is responsible for the positive attributes of schizophrenia, and hypodopaminergia in the prefrontal cortex that accounts for the negative attributes of schizophrenia. They also proposed that the excessive dopaminergic activity in the mesolimbic region might be a result of low dopaminergic activity in the prefrontal cortex.[35]

Based on the availability of newer evidence, Howes et al.[31] further modified the DA hypothesis. They postulated that the DA hypothesis has four distinct components that are as follows: 1. Psychosis in schizophrenia is the result of DA dysregulation due to the interaction of "multiple hits" such as stress, genes, drugs and fronto-temporal dysfunction. 2. DA dysfunction is at the presynaptic control level rather than at the D_2 receptor level. 3. The DA hypothesis does not explain all facets of schizophrenia; rather, it explains the "psychosis" associated with schizophrenia.[31] 4. Dysregulation of the dopaminergic system may lead to an altered appraisal of stimuli by a process of aberrant salience.[31,36]

The DA model of schizophrenia has been a leading hypothesis, and the role of dopamine in the pathophysiology of schizophrenia is well established.[37,38] However, D_2 receptor antagonism alone did not seem to be addressing the core pathophysiology of schizophrenia, since typical antipsychotic agents were unable to alleviate the negative and cognitive symptoms of schizophrenia.[37,38] A dysfunction of multiple neural networks and transmitter systems might be responsible for the negative symptoms and cognitive deficits in patients with schizophrenia.[37,38]

The DA hypothesis addressed a more downstream effect and did not account for the neurocognitive deficits and, the wide range of symptoms, thus eliciting a need for newer hypotheses.[37,38]

b. The serotonin (5-HT) hypothesis of schizophrenia

Serotonin or 5-hydroxytryptamine (5-HT; **6**) (Figure 2) is a monoamine neurotransmitter that is essential for maintaining normal brain function.[39] 5-HT receptors are classified into seven main classes that are further divided into subtypes.[39] The 5-HT_1, 5-HT_2, and 5-HT_{4-7} receptors are G-protein coupled receptors (GPCRs) whereas the 5-HT_3 receptor is a ligand-gated ion channel receptor.[39] Lysergic acid diethylamide (LSD; **7**) (Figure 2), a hallucinogenic agent, is structurally similar to 5-HT (**6**), was found to produce symptoms that resembled the psychotic symptoms of schizophrenia.[40] The hallucinogenic effects of LSD (**7**) were thought to be a result of its ability to antagonize 5-HT in the CNS and the initial 5-HT hypothesis of schizophrenia attributed the symptoms of schizophrenia to a 5-HT deficit in the CNS.[40] It was soon realized that LSD (**7**) could not only antagonize but also mimic the effects of 5-HT[41] and the hypothesis was revised such that a surplus or deficit of 5-HT could be responsible for the psychosis associated with schizophrenia.[42,43]

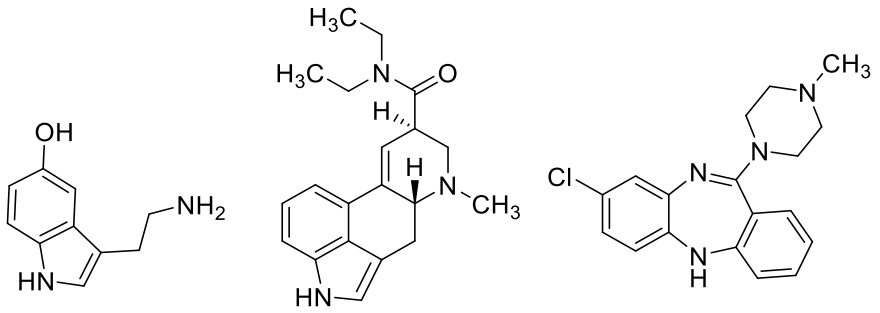

Serotonin (5-HT; **6**) Lysergic acid diethyl amide (LSD; **7**) Clozapine (**8**)

Figure 2. Structures of the monoamine neurotransmitter serotonin (5-HT; **6**), the hallucinogenic agent lysergic acid diethylamide (LSD; **7**), and the atypical antipsychotic agent clozapine (**8**).

The focus of schizophrenia research shifted to the DA hypothesis of schizophrenia with the discovery that neuroleptics (i.e., antipsychotic agents) such as CPZ (**2**), with DA blocking properties, were effective antipsychotic agents. The 5-HT hypothesis of schizophrenia took a back seat and it was only with the discovery of the ability of atypical antipsychotic agents such as clozapine (**8**) (Figure 2) to block certain subtypes of the 5-HT receptors, that attention was refocused on the role of 5-HT in schizophrenia and resulted in a mixed 5-HT/DA hypothesis of schizophrenia.[44]

Per the current 5-HT hypothesis of schizophrenia there is a stress-induced serotonergic overdrive coming from the dorsal raphe nucleus that can disrupt cortical neuronal function in schizophrenia. This, along with the hyperactivity of 5-HT in the cerebral cortex (mainly in the anterior cingulate cortex and the dorsolateral frontal lobe), is the upstream cause of schizophrenia.[5]

Among the 5-HT receptors, the 5-HT_2 (5-HT_{2A}) receptor has been suggested to be most important for the efficacy of antipsychotic agents.[45] The 5-HT_{2A} receptor is widely distributed in many regions of the brain such as the cerebral cortex and the nucleus accumbens, with high density in the frontal cortex.[10,43] Activation of 5-HT_{2A} receptors in the prefrontal cortex can lead to an increase in the release of glutamate that is indicated by the enhanced spontaneous excitatory postsynaptic potentials/currents in layer V pyramidal cells, an effect that can be blocked by α-amino-3-hydroxy-5-methyl-4-isoxazolepropionic acid (AMPA)/kainate glutamate receptor agonists and by group II/III metabotropic glutamate receptor agonists.[10,43,46,47] Hence, the 5-HT hypothesis by itself cannot explain the symptoms of schizophrenia and a number of other hypotheses have been postulated, one of which was the glutamate hypothesis of schizophrenia

c. The glutamate (GLU) hypothesis of schizophrenia

GLU (**9**) (Figure 3) is an amino acid that is the most abundant and primary excitatory neurotransmitter in the brain and accounts for ~40% of neurons and ~60% of synapses in the brain.[48,49] Almost all cortical pyramidal neurons use GLU as the primary excitatory neurotransmitter.[48] Glutamatergic neurotransmission is modulated via two main types of receptors: the ligand-gated ion channel receptors that include N-methyl-D-aspartate (NMDA), α-amino-3-hydroxy-5-methyl-4-isoxazolepropionic acid (AMPA) and kainate receptors, and the G-protein coupled metabotropic glutamate receptors that are divided into 3 groups (I-III) and eight subtypes.[50] The similarity between the psychosis induced by dissociative anesthetics such as phencyclidine (**10**) and ketamine (**11**) (Figure 3) and the psychotic syndrome associated with schizophrenia has been appreciated since the introduction of these agents in the early 1960s. [51,52]

Based on the knowledge that dissociative anesthetics are non-competitive NMDA receptor antagonists, and the emerging pharmacology of the NMDA receptor, it was proposed that schizophrenia might result from a hypofunction of NMDA receptors.[38,51,53]

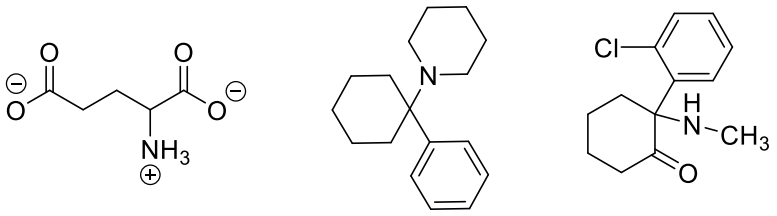

Glutamate (GLU) (**9**) Phencyclidine (**10**) Ketamine (**11**)

Figure 3. Structures of glutamate (GLU) (**9**) and the dissociative anesthetics: phencyclidine (**10**) and ketamine (**11**).

The glutamate hypofunction hypothesis suggested that the positive or psychotic symptoms of schizophrenia might be linked to excessive release of DA from neurons in the mesolimbic pathway due to an abnormal functioning of the GLU-GABA-GLU-DA circuit. (Figure 4) The defective and hypofunctioning NMDA receptors do not receive adequate stimuli form the primary GLU neuron resulting in a loss of GABA output to the secondary GLU neuron leading to excessive firing of the neuron and an ultimate excess of DA in the mesolimbic pathway.[54]

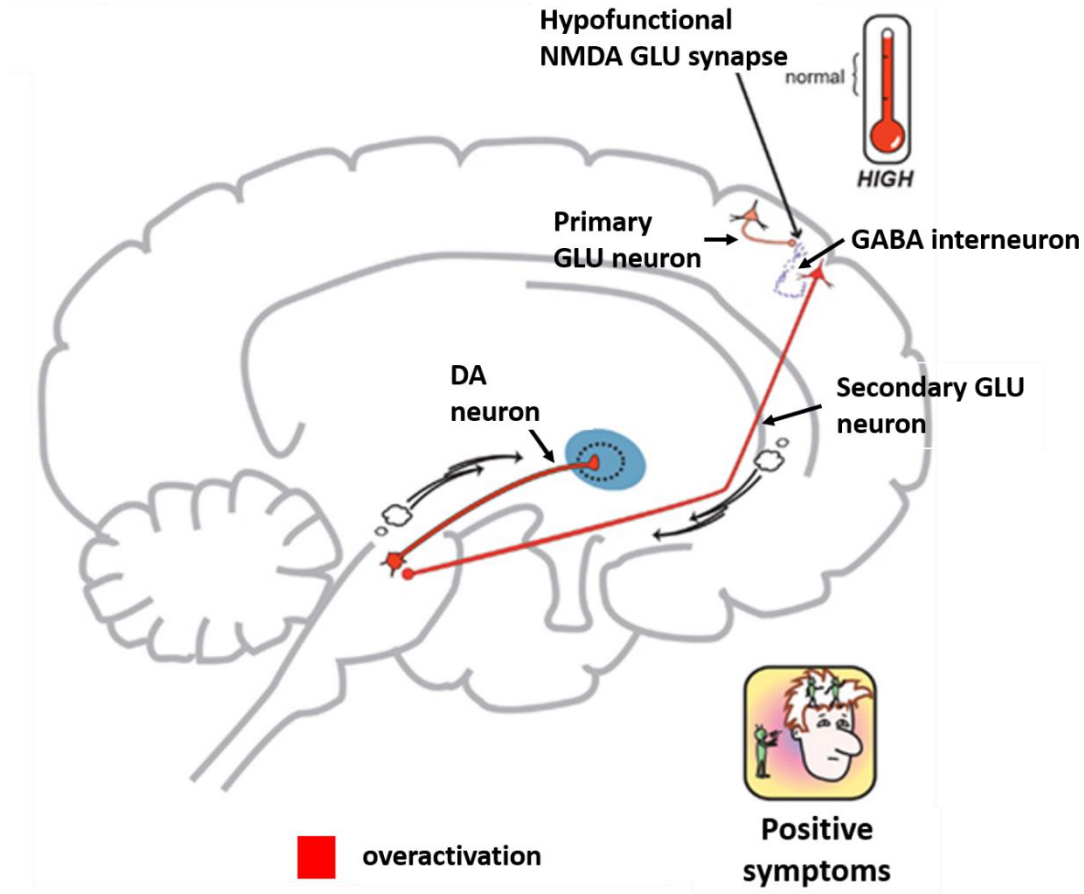

Figure 4. NMDA receptor hypofunction hypothesis for the positive symptoms of schizophrenia (adapted from Schwartz et al.[54]).

The negative and cognitive symptoms of schizophrenia can be attributed to the malfunctioning of another GLU neurocircuit (GLU-GABA-GLU-GABA-DA neuronal circuit) leading to insufficient release of DA in the mesocortical region (Figure 5).[37,54] Hypofunction of the NMDA receptor on the GABA interneuron may lead to an increased tone of the secondary GLU neuron and an increased firing of the GABAergic interneuron in the ventral tegmental area resulting in an inadequate release of DA by the dopaminergic neurons in the mesocortical DA pathway.[37,55]

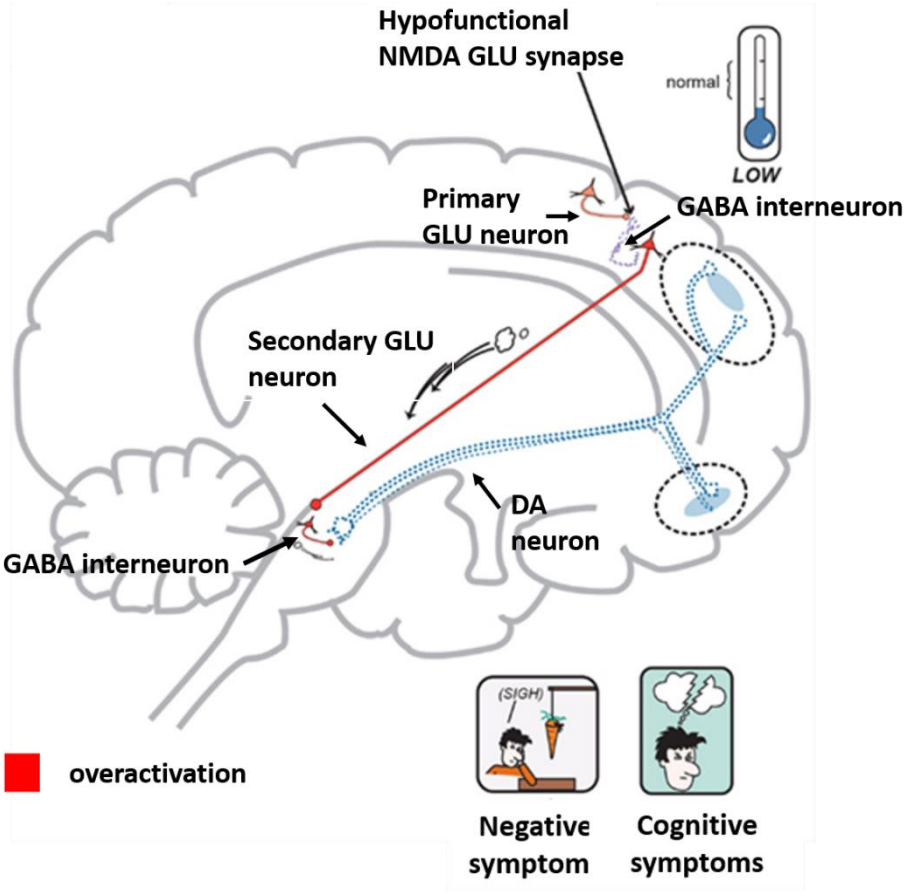

Figure 5. NMDA receptor hypofunction hypothesis for the negative and cognitive symptoms of schizophrenia (adapted from Schwartz et al.[54]).

Direct NMDA receptor agonists or metabotropic glutamate receptor type 2/3 ($mGlu_{2/3}$) agonists or PAMs of $mGlu_2$ could be therapeutically useful in patients with schizophrenia, and some of these agents have advanced into clinical trials.[54] $mGlu_{2/3}$ receptors are autoreceptors located on the secondary GLU neuron.[54] Activation of these receptors with $mGlu_{2/3}$ receptor agonists or $mGlu_2$ receptor PAMs would lead to a decrease in firing of the overactivated GLU neuron resulting in modulation of DA release and an amelioration of the positive, negative and cognitive symptoms of schizophrenia.[54]

5-HT (5-HT_{1A} and 5-HT_{2A}) receptors are widely distributed in the prefrontal cortex and can regulate NMDA receptor activity, and a change in 5-HT signaling in the prefrontal cortex could alter NMDA receptor activity and also contribute to the cognitive and negative symptoms of schizophrenia.[37,56]

The GLU hypofunction hypothesis of schizophrenia looks at more upstream effects that ultimately leads to a final common pathway culminating in the release of DA. GLU- manipulating agents may prove to be therapeutically useful in treating both the positive, negative and cognitive symptoms of schizophrenia.[54]

d. The GABA hypothesis of schizophrenia

GABA (**12**) (Figure 6) is an inhibitory neurotransmitter in the central nervous system and plays an important role in reducing neuronal excitability.

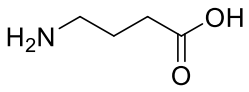

γ-Aminobutyric acid (GABA) (**12**)

Figure 6. Structure of the inhibitory neurotransmitter GABA (**12**).

GABAergic neurons play a crucial role in maturation of neural circuitry during the postnatal period, and impaired maturation of the GABAergic neurons could result in psychiatric disorders

such as schizophrenia.[29] Additionally, the GABAergic interneurons are important for maintaining proper cortical functioning[29] as well as supporting cortical functions that include maintaining a balance between excitation and inhibition,[57] and proper synaptic inhibition at dendrites and somata.[58] The imbalance between excitation and inhibition in the cerebral cortex due to GABAergic dysfunction might lead to increased sub-cortical DA and underlie a part of the pathophysiology of schizophrenia.[29,59]

e. The cholinergic hypothesis of schizophrenia

The nicotinic and muscarinic cholinergic systems interact with one other as well as other neurotransmitter systems such as GABA, GLU and DA in a complex and bi-directional manner.[6] The cholinergic system is important for maintaining normal dopaminergic tone in the cortex and striatum.[60] The glutamatergic neurons in the mesolimbic and mesocortical dopaminergic pathways have alpha 7 nicotinic receptors located on them.[60] Activation of the alpha 7 nicotinic receptors (by alpha 7 receptor agonists and PAMs[61]) on hypofunctional glutamatergic neurons can alleviate the positive, negative symptoms, and the cognitive deficits of schizophrenia by normalizing dopaminergic tone in the cortex and striatum.[60] The muscarinic agents can have antipsychotic effects via both direct muscarinic effects (pro-cognitive effects) and by modulating the dopaminergic system (effects on the positive symptoms of schizophrenia).[6] M_1 and M_4 muscarinic cholinergic agonists might be therapeutically useful in schizophrenia.[6,62]

f. The adenosine hypothesis of schizophrenia

Adenosine (**13**) (Figure 7) is a homeostatic bioenergetic network modulator and affects brain DA and GLU activities.[63,64]

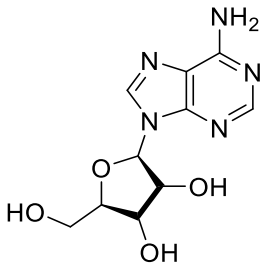

Adenosine (**13**)

Figure 7. Structure of the bioenergetic network modulator adenosine (**13**).

Adenosine (**13**) is relevant to the etiology of schizophrenia because it is not only important for regulation of immune responses but also for early brain development. The adenosine hypothesis suggests that a dysfunction of the purinergic system, resulting in reduced adenosinergic activity, might be responsible for the dysfunctioning of multiple neurotransmitter systems that are associated with schizophrenia. Adenosine (**13**) can be controlled and rebalanced in multiple ways to modulate brain function and restore the homeostatic bioenergetic network balance. Some of the targets include enzymes such as adenosine kinase and transporters that control the tone of adenosine levels.[64]

g. The α-adrenoceptor hypothesis of schizophrenia

α_1-, α_2-Adrenoceptor blockade might contribute to the antipsychotic efficacy of atypical agents such as clozapine (**8**) (Figure 2).[65] α_1-Adrenoceptor blockade leads to a reduction of striatal DA and a reduction in the positive symptoms of schizophrenia. α_2-Adrenoceptor blockade can

ameliorate the negative and cognitive symptoms of schizophrenia by improving prefrontal dopaminergic functioning.[66]

The ability of the atypical antipsychotics such as clozapine (**8**) and risperidone (**14**) (Figure 8) to antagonize α_2- adrenoceptors might be important for their superior clinical profiles.[66,67]

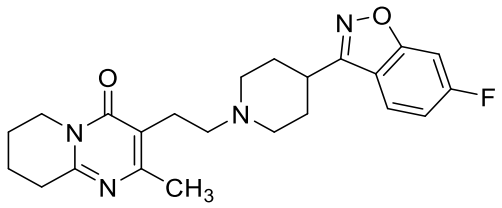

Risperidone (**14**)

Figure 8. Structure of the atypical antipsychotic agent risperidone (**14**).

g. The cannabinoid hypothesis of schizophrenia

The relationship between the use of cannabinoids and schizophrenia is complex and not completely understood. It has been proposed that hyperactivity of the central cannabinoid system might be involved in the pathogenesis of schizophrenia and that the endogenous cannabinoid system could represent a novel therapeutic target for the treatment of schizophrenia.[68,69] The CB_1 receptor system and the dopaminergic system interact in a complex manner and studies have suggested that cannabidiol (**15**) (Figure 9) (a CB_1 and CB_2 receptor antagonist) and SR141716 (**16**) (Figure 9) (a selective CB_1 receptor antagonist), have a pharmacological profile similar to that of atypical antipsychotic agents.[68,70] The antipsychotic agent-like profile of cannabidiol might also be due to its actions at other targets.

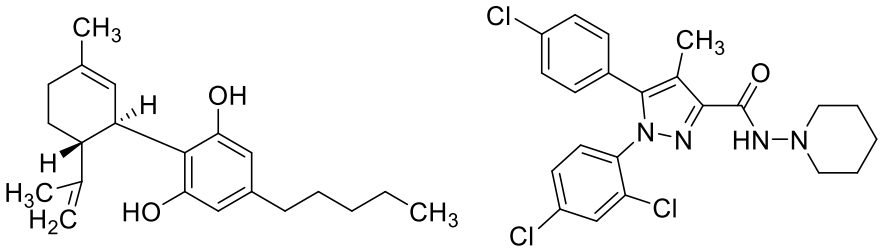

Cannabidiol (**15**) SR141716 (**16**)

Figure 9. Structures of cannabidiol (**15**) and SR141716 (**16**).

2. Antipsychotic agents

a. History

Psychiatric states have been associated with specific areas of the cerebral cortex since the late 19th century, and the process of lobotomy was common practice for the treatment of neuropsychiatric disorders in the early 1900s.[8] Lobotomies involve localized lesions or surgical destruction of certain cerebral sites, and were based on the hypothesis that their anatomical location correlated with functional effects, and severance of certain sections of the brain, especially the frontal lobes, would modify the affective expression of psychosis or neurosis.[71,72]

The introduction of CPZ (**2**) (Figure 1) by Rhône-Poulenc in 1952 marked a new era of drug treatment in psychiatry and resulted in the demise of psychosurgery.[8,9] CPZ (**2**) was initially developed as an antihistaminic agent that was used to potentiate the effect of other anesthetic agents; its antipsychotic effects were discovered serendipitously by Delay and Deniker, as reviewed by Shen[13] and Tamminga.[73] Patients that were administered CPZ (**2**) behaved in a manner that was similar to lobotomized patients, and CPZ (**2**) was regarded as a non-permanent pharmacological lobotomy.[9]

In 1952, extrapyramidal symptoms (EPS) were observed as a side effect associated with CPZ (**2**) therapy, and led clinicians and pharmacologists to believe that antipsychotic efficacy and EPS were linked.[11] EPS include dystonia, akathisia, parkinsonism, tardive dystonia, and tardive dyskinesia.[11] The introduction of haloperidol (**5**) (Figure 1) in 1958 further bolstered this belief.[74] The widespread use of CPZ (**2**) resulted in large decreases in psychiatric inpatient populations worldwide, and fueled a search for other antipsychotic drugs.[13] By the 1970s, at least 40 new antipsychotic agents were introduced worldwide.[13] These agents were "typical" antipsychotic agents (Figure 10) that exerted their antipsychotic effects by blocking DA (particularly D_2) receptors and included drugs such as CPZ (**2**), haloperidol (**5**) (Figure 1), thioridazine (**17**), trifluoperazine (**18**), thiothixene (**19**), and loxapine (**20**) (Figure 10) among others.[13,73,75]

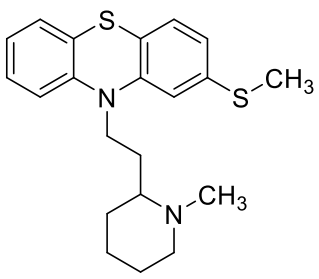

Thioridazine (**17**)

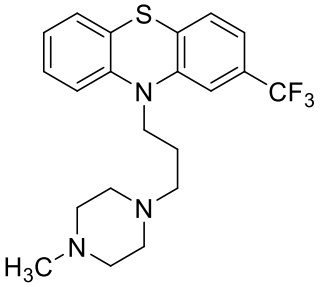

Trifluoperazine (**18**)

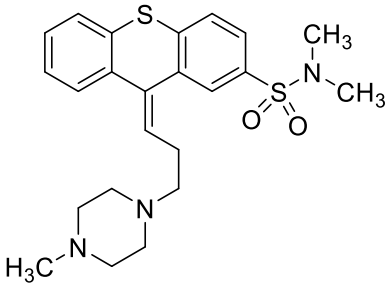

Thiothixene (**19**)

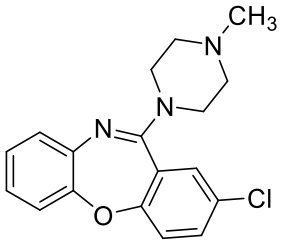

Loxapine (**20**)

Figure 10. Examples of typical antipsychotic agents.

There was a lull in antipsychotic drug development from 1975 to 1990. The introduction of clozapine (**8**) (Figure 2) in 1990 was a hallmark in antipsychotic therapy. Clozapine (**8**) was initially introduced as an antipsychotic in the mid-1960s.[76] However, it was withdrawn from the market for two reasons: it produced life-threatening agranulocytosis as a side effect, and it did not produce EPS, a side-effect that was thought to be correlated with antipsychotic efficacy.[13] Clozapine (**8**) was reintroduced to the market in the 1990s following a successful double-blind study in treatment-resistant patients whose blood levels were carefully monitored. Clozapine (**8**) was different from the previously marketed antipsychotics in being able to ameliorate both the positive and negative attributes of schizophrenia, as well as in having a lower propensity to cause

EPS.[12] The introduction of clozapine (**8**) led to the development of the concept of "atypical" antipsychotics, and its clinical success prompted the development of other atypical antipsychotic agents (Figure 11) such as risperidone (**14**) (Figure 8) (1994), olanzapine (**21**) (1996), and quetiapine (**22**) (Figure 11) (1997).[13] Risperidone (**14**) was developed using the chemical structure of haloperidol (**5**) (Figure 1) as a starting point,[74] while the chemical structures of olanzapine (**21**) and quetiapine (**22**) were derived from clozapine (**8**).[13]

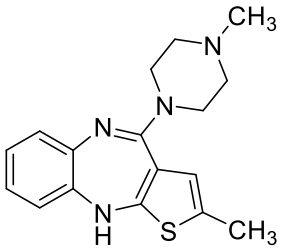

Olanzapine (**21**)

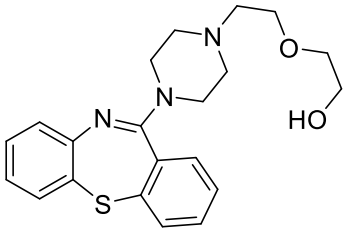

Quetiapine (**22**)

Figure 11. Examples of atypical antipsychotic agents.

Antipsychotic therapy has come a long way from the serendipitous discovery of the antipsychotic effects of CPZ (**2**) to a more precise receptor-targeted approach for the synthesis of newer antipsychotics.[13] There has been a paradigm shift in the design of antipsychotic agents from drugs that solely target the dopaminergic system to a more multi-target approach with newer drugs targeting multiple neurotransmitter systems that include, but are not limited to, 5-HT, GLU, and cholinergic systems.[13]

b. Classification

Antipsychotics can be classified into two main groups: first-generation or "typical" antipsychotics/"neuroleptics" and second-generation or "atypical" antipsychotics. There is an emerging class of atypical antipsychotic agents that are also commonly referred to as third-generation antipsychotic agents.[77] The terminology, and classification of antipsychotics have been a subject of considerable debate until the early 1970s, and terms such as "neuroleptic", "tranquilizer" and "ataraxic" have been used to refer to "typical" antipsychotic agents. The terms tranquilizer, and ataractics were popular until the 1960s, while the term neuroleptic was a more lasting term. These terms have been replaced by the term antipsychotic, and it now is the most popular term used to describe both typical and atypical agents.[78]

Typical antipsychotic agents include drugs such as CPZ (**2**), haloperidol (**5**) (Figure 1), thioridazine (**17**), trifluoperazine (**18**), thiothixene (**19**), and loxapine (**20**) (Figure 10) among others, and are mainly D_2 receptor antagonists.[73,75]

Atypical antipsychotic agents are classified based on their pharmacological action and reflect their affinities for specific receptors.[79] They can be classified into serotonin-dopamine antagonists (SDAs), multi-acting receptor-targeted antipsychotics (MARTAs), and combined D_2/D_3 receptor antagonists.[79] The third-generation atypical antipsychotic agents include partial DA receptor agonists such as aripiprazole (**23**) (Figure 12).[79] SDAs are atypical antipsychotic agents that possess a high affinity for 5-HT_{2A} and D_2 receptors and include agents such as risperidone (**14**) (Figure 8), iloperidone (**24**) (Figure 12), and ziprasidone (**25**) (Figure 12).[79] MARTAs include

agents that have high affinities for 5-HT_{2A} receptors, D_2 receptors, and receptors of other neurotransmitter systems such as cholinergic, histaminergic, and other serotonin receptors such as 5-HT_{1A} and 5-HT_{2C}, some representative examples include agents such as clozapine (**8**) (Figure 2), quetiapine (**22**), and olanzapine (**21**) (Figure 11).[67] Agents such as amisulpride (**26**) and remoxipride (**27**) (Figure 12) are combined D_2/D_3 receptor antagonists.[79]

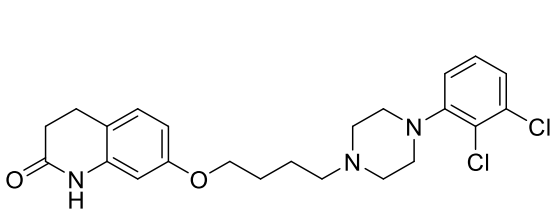

Aripiprazole (**23**)

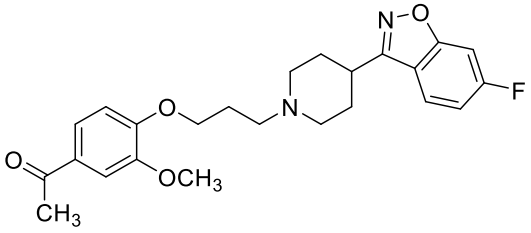

Iloperidone (**24**)

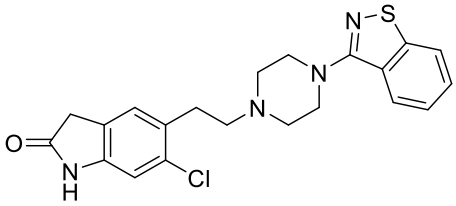

Ziprasidone (**25**)

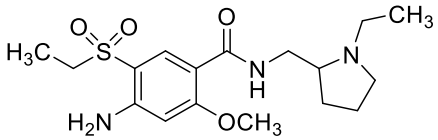

Amisulpride (**26**)

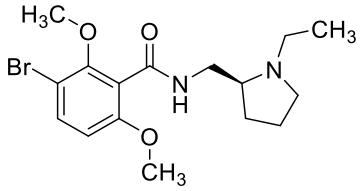

Remoxipride (**27**)

Figure 12. Structures of the partial DA receptor agonist aripiprazole (**23**), the SDAs: iloperidone (**24**), and ziprasidone (**25**), and the combined D_2/D_3 receptor antagonists: amisulpride (**26**) and remoxipride (**27**).

c. Typical versus atypical antipsychotic agents

Typical antipsychotic agents, effective against only the positive symptoms of schizophrenia, are known to cause multiple side effects.[7] The side effect profiles for different chemical classes vary, however, the most prominent side effects that are common to conventional (i.e., typical) antipsychotics are EPS and hyperprolactinemia.[7] Neuroleptic malignant syndrome can occur at higher doses.[7]

Atypical antipsychotic agents have a broader spectrum of clinical efficacy and ameliorate the positive symptoms, negative symptoms, and cognitive deficits of schizophrenia.[79] They are more sparing in their side effects and have a reduced propensity to cause EPS and hyperprolactinemia, the side effects that are commonly associated with the use of typical antipsychotic agents.[79] Even though atypical antipsychotic agents have their own adverse effects such as metabolic side effects, they have an overall better safety profile and are associated with a lower risk of suicide, higher rate of responders and an improved quality of life.[79]

Studies have suggested that atypical antipsychotic agents are equally effective in the control of positive attributes, and are superior in controlling the negative symptoms, and cognitive deficits of schizophrenia as compared to typical antipsychotic agents.[79,80] However, evidence of their superior efficacy is inconsistent, and several double-blind, randomized, controlled trials have been conducted to compare the clinical efficacy of atypical antipsychotic agents over conventional antipsychotic agents as well as a placebo.[79,80] Meta-analyses of published clinical trials by two groups; Geddes et al.[81] and Leucht et al.[82] have suggested that atypical antipsychotic agents offer

modest clinical efficacy over typical antipsychotic agents. Geddes et al.[81] concluded that the atypical antipsychotic agents were moderately better than conventional antipsychotics. At lower doses of the conventional antipsychotic agent; haloperidol (**5**) (Figure 1), there was no difference in terms of efficacy and overall tolerability over atypical agents; however, the first-generation antipsychotic agents demonstrated a liability for EPS even at low doses. A meta-analysis study of published clinical trials using low-potency conventional antipsychotics by Leucht et al.[82] was in agreement with the study by Geddes et al.[81] and suggested that the benefits of atypical agents over typical agents with the exception of clozapine (**8**) (Figure 2) were only moderate. These studies were limited by the lack of available data to evaluate other dimensions such as suicide risk, and quality of life. Contrary to the studies by Geddes et al.[81] and Leucht et al.[82] the meta-analysis of 124 trials by Davis et al.[83] has suggested that some atypical antipsychotic agents such as clozapine (**8**), risperidone (**14**) (Figure 8), olanzapine (**21**) (Figure 11), and amisulpride (**26**) (Figure 12) were significantly more efficacious than conventional antipsychotics.

The US clinical antipsychotic trials of intervention effectiveness (CATIE) study, in 2005, and the UK cost utility of the latest antipsychotic drugs in schizophrenia study (CUtLASS 1), in 2006, showed no differences in effectiveness and overall quality of life between the first- and second-generation (i.e., typical and atypical) agents.[84]

Atypical antipsychotic agents are a heterogeneous group of agents, and differ in terms of effectiveness and side-effects.[79] It has been suggested that rather than using a dichotomous typical-

atypical antipsychotic agent classification, viewing these agents in a dimensional fashion might be best,[80] and the choice of use of drug should be based on the drug as well as patient profile.[84]

3. Newer concepts

i. Serotonin-dopamine antagonists (SDA)

Clozapine (**8**), the first atypical antipsychotic agent, lacked EPS, a side effect associated with conventional antipsychotic therapy, and is a potent antagonist at multiple receptors with the 5-HT_{2A} receptor being one among the many.[85] Activity at serotonergic pathways that impinge on striatal dopaminergic pathways can reduce DA-mediated activity in these pathways, leading to the hypothesis that EPS could be reduced by the addition of 5-HT_{2A} receptor blockade to D_2 receptor antagonism.[85,86] The addition of ritanserin (**28**) (Figure 13), a selective 5-HT_{2A} receptor antagonist as an adjunctive treatment to conventional antipsychotics in patients with schizophrenia resulted in a significant reduction of EPS, and further bolstered the hypothesis.[87]

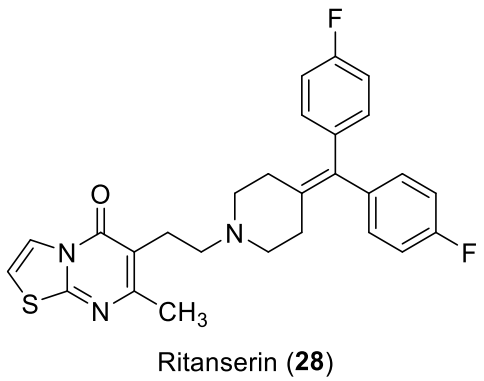

Ritanserin (**28**)

Figure 13. Structure of the 5-HT_{2A} receptor antagonist ritanserin (**28**).

Medicinal chemistry efforts to synthesize agents that combined D_2 receptor and 5-HT_{2A} receptor antagonism in one molecule have resulted in several drugs, with risperidone (**14**) (Figure 8) being

the first marketed SDA. As opposed to conventional antipsychotic agents that are more potent D_2 rather than 5-HT_2 receptor antagonists, SDAs have a higher affinity for 5-HT_{2A} receptors as compared to D_2 receptors.[85] The 5-HT_{2A}/ D_2 receptor binding affinity ratio has been defined by Meltzer et al.[45] and most atypical antipsychotic agents have a 5-HT_{2A}/D_2 receptor binding affinity ratio $\geq$ 1.12. Disinhibition of dopaminergic neurotransmission in the nigrostriatal pathway by 5-HT_{2A} receptor blockade resulting in the release of DA in the striatum by offsetting the D_2 receptor blockade may be a potential mechanism by which SDAs can reduce the expression of EPS. SDAs shift the EPS dose-response curve to the right while the antipsychotic dose response curve remains unchanged, resulting in a reduced propensity to cause EPS.[85] These agents not only produce lower incidence of EPS, but might also be effective against the negative symptoms of schizophrenia and have pro-cognitive effects. The antiserotonergic component of SDAs may increase dopaminergic activity in the frontal cortex leading to an amelioration of negative symptoms of schizophrenia.[45]

Rather than using the term SDAs, a better term to describe these agents is 5-HT spectrum dopamine modulators (SSDMs), since most of these agents have a wide spectrum of activity at 5-HT receptors that includes 5-HT_{2A} receptor antagonism, direct or indirect 5-HT_{1A} receptor agonism, and/or 5-HT_{2C}, 5-HT_6, and 5-HT_7 receptor antagonism, and could be either antagonists or partial agonists at D_2/D_3 receptors. The spectrum of action at 5-HT receptors differs among various members of this class of agents resulting in differences in efficacy and tolerability among the different SSDMs.[88]

ii. Role of inverse agonists in antipsychotic activity

The ability of active conformations of receptors to produce a response in the absence of an agonist is known as constitutive activity, and ligands that decrease constitutive activity are known as inverse agonists. Most ligands (>80% of classical GPCR ligands) that were initially classified as antagonists are inverse agonists.[89,90] 5-HT_{2A} and 5-HT_{2C} receptors modulate the release of DA in the brain.[90] 5-HT_{2A} receptor inverse agonists such as M100907 (**29**) (Figure 14) increase the release of DA in the mesocortical and mesolimbic brain regions,[90,91] whereas 5-HT_{2C} receptor inverse agonists such as SB206553 (**30**) (Figure 14) increase the release of DA in the nucleus accumbens.[90,92] The activity of atypical antipsychotic agents at 5-HT_{2A}, 5-HT_{2C}, and 5-HT_{1A} receptors increases the release of DA in the prefrontal cortex.[90] Most atypical antipsychotic agents such as clozapine (**8**) (Figure 2), risperidone (**14)** (Figure 8), and olanzapine (**21**) (Figure 11) are 5-HT_{2A} and 5-HT_{2C} receptor inverse agonists, and it has been hypothesized that inverse agonist action at these receptors might be responsible for the ability of atypical antipsychotic agents to ameliorate the negative attributes and cognitive deficits of schizophrenia.[90,93] An effective therapeutic strategy to treat the positive symptoms of schizophrenia might be the use of 5-$HT_{2A/2C}$ receptor inverse agonists to indirectly modulate DA levels. Pimavanserin (**31**) (Figure 14), a selective 5-HT_{2A} receptor inverse agonist was found to have antipsychotic activity as well as a better side effect profile than the other atypical and conventional agents in animal models predictive of antipsychotic activity.[94] Although clinical trials with pimavanserin (**31**) monotherapy were disappointing, it is currently available for treating secondary psychosis associated with Parkinsonism.[90,95] The therapeutic potential of 5-HT_2 receptor inverse agonists in treating psychosis associated with Alzheimer's disease is also being evaluated.[96]

Even though targeting a single receptor subtype may not be effective in treating disorders with multiple etiologies such as schizophrenia, understanding the role of 5-HT receptor inverse agonism might pave the way for development of novel agents.[90]

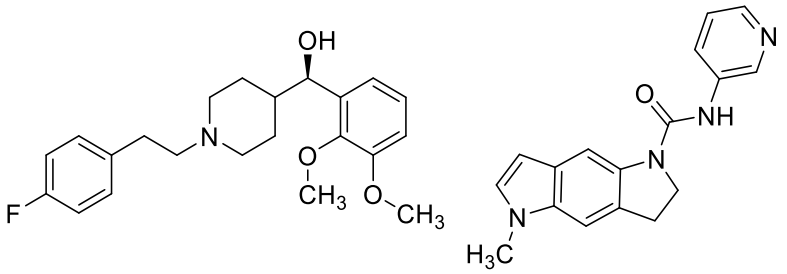

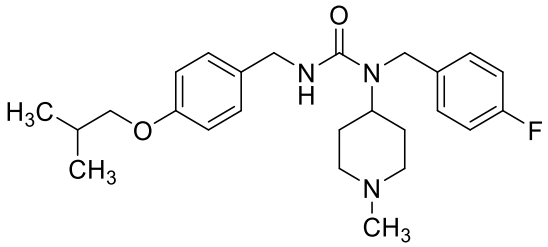

Figure 14. 5-HT_{2A} receptor inverse agonists: M100907 (**29**) and pimavanserin (**31**), and the 5-HT_{2C} receptor inverse agonist: SB206553 (**30**).

iii. Dopamine stabilizing agents

DA stabilizing drugs are a novel therapeutic approach to reduce the side effects associated with conventional antipsychotic agents.[97] D_2 receptor partial agonists represent one class of "DA stabilizers", and can reduce hyperdopaminergia in the mesolimbic area without producing a state of hypodopaminergia in the nigrostriatal DA pathway, thus avoiding EPS, a troublesome side effect that is associated with the first-generation antipsychotic agents that are D_2 receptor

antagonists.[98] Aripiprazole (**23**) (Figure 12), a prototypical DA stabilizing agent that was approved by the US FDA in the early 2000s for the treatment of schizophrenia, is a D_2 receptor partial agonist.[77,99] It can reduce the hyperactivity of the dopaminergic system in a manner that is dependent not only on its intrinsic efficacy but also on systems downstream of DA receptors, and can also enhance dopaminergic activity in the mesocortical circuit, and improve the negative and cognitive symptoms of schizophrenia.[97,98] Besides D_2 receptor partial agonist action, another feature that makes aripiprazole (**23**) (Figure 12) unique, is its functional selectivity at the D_2 receptor: it inhibits accumulation of cAMP and affects the release of arachidonic acid to a much greater extent as compared to its ability to activate mitogen-activated protein kinases (MAPK).[98–101] Aripiprazole (**23**) regulates dopaminergic function based on the hypoactivity or hyperactivity of the system, and based on the cellular environment of the receptor.[98,99] An advantage of using D_2 receptor partial agonists is that they do not up-regulate the D_2 receptors, a phenomenon that is observed with long-term treatment with DA receptor antagonists[99] Aripiprazole (**23**) also binds to 5-HT receptors (5-HT_{1A} receptor partial agonist, 5-HT_{2A} receptor antagonist), and this combined with D_2 receptor partial agonist action may be responsible for its therapeutic efficacy in schizophrenia.[99] Brexpiprazole (**32**) (Figure 15) is another D_2, and 5-HT_{1A} receptor partial agonist, and a potent antagonist at 5-HT_{2A}, α_{2A}, and α_{2c} receptors that was approved by the US FDA in 2015 for the treatment of schizophrenia.[102]

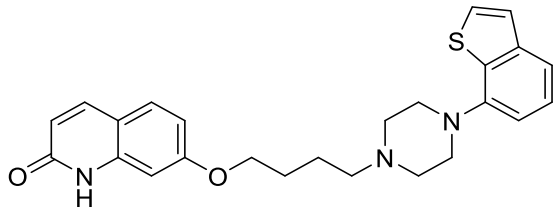

Brexpiprazole (**32**)

Figure 15. Structure of the DA stabilizing agent brexpiprazole (**32**).

D_2 receptor partial agonists such as aripiprazole (**23**) (Figure 12) are as efficacious as first-and second-generation antipsychotic agents in terms of antipsychotic action, with the added advantages of lower incidence of EPS, and reduced side effects such as hyperprolactinemia and weight gain.[98]

4. Serotonin receptors

Gaddum and Picarelli[103] had initially classified the 5-HT receptors into two groups, the 'D'- type that was responsible for the contraction of smooth muscles, and the 'M'- type that mediated cholinergic nerve depolarization. The effects of 5-HT at the 5-HT-D receptor subtype could be blocked by an irreversible antagonist phenoxybenzamine (**33**) (Figure 16) whereas the effects of 5-HT at the 5-HT-M receptor subtype could be blocked by morphine (**34**) or cocaine (**35**) (Figure 16).

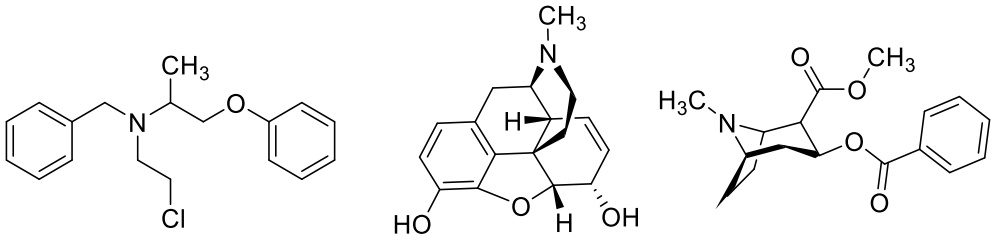

Phenoxybenzamine (**33**) Morphine (**34**) Cocaine (**35**)

Figure 16. Structures of phenoxybenzamine (**33**), morphine (**34**), and cocaine (**35**).

In 1979, Peroutka and Snyder[104] identified two distinct brain 5-HT binding sites and named them 5-HT_1 and 5-HT_2 receptors. 5-HT-D, and 5-HT-M receptors were renamed as 5-HT_2 and 5-HT_3 receptors, respectively. By the early 1990s, several 5-HT receptor sub-populations had been identified, and cloned, and currently 5-HT receptors are classified into seven different families, 5-HT_1 through 5-$HT_{7;}$ except for the 5-HT_3 receptor, which is a ligand-gated ion channel receptor, all the others are type A or rhodopsin-like GPCRs. These receptors are further divided into sub-populations, and a total of 14 different 5-HT receptor sub-types have been described (Table 1).[39]

Table 1. Classification of 5-HT receptors (adapted from Glennon and Dukat[39]).

Populations and subpopulations (Currently accepted name)	**Second messenger system***	**Comments**
5-HT_1		
5-HT_{1A} (5-HT_{1A})	AC(-)	Cloned and pharmacological 5-HT_{1A} receptors.
5-HT_{1B} (5-HT_{1B})	AC(-)	Rodent homolog of h5-HT_{1B} receptors
5-$HT_{1B\beta}$		A mouse homolog of 5-HT_{1B} receptors
5-HT_{1D}		
5-$HT_{1D\alpha}$	AC(-)	A cloned human 5-HT_{1D} subpopulation

(h5-HT_{1D})		
5-$HT_{1D\beta}$ (h5-HT_{1B})	AC(-)	A second cloned human 5-HT_{1D} subpopulation; human counterpart of rat 5-HT_{1B}
5-HT_{1E}	AC(-)	
5-$HT_{1E\alpha}$		An alternate name that has been used for cloned human 5-HT_{1E} receptors
5-$HT_{1E\beta}$	AC(-)	A cloned mouse homolog of 5-HT_{1F} receptors
(5-$HT1_F$) 5-HT_{1F}		A cloned human 5-HT_1 receptor population
5-HT_2		
5-HT_2 (5-HT_{2A})	PI	Original "5-HT_2" (sometimes called 5-$HT_{2\alpha}$) receptors
5-HT_{2F} (5-HT_{2B})	PI	5-HT_2-like receptors originally found in rat fundus
5-HT_{1C} (5-HT_{2C})	PI	Originally described as 5-HT_{1C} (5-$HT_{2\beta}$) receptors
5-HT_3	Ion channel	An ion channel receptor
5-HT_4	AC (+)	
5-HT_{4s}		Short form of cloned 5-HT_4 receptors
5-HT_{4L}		Long form of cloned 5-HT_4 receptors
5-$HT_{4(b)-4(d)}$		Recently identified human 5-HT_4 receptor isoforms
5-HT_5	AC (-)[105]	
5-HT_{5A}		Cloned mouse, rat, and human 5-HT_5 receptors
5-HT_{5B} (5-HT_{5A})		Cloned mouse, and rat 5-HT_{5A}-like receptor
5-HT_6	AC (+)	Cloned rat and human 5-HT receptor
5-HT_7	AC (+)	Cloned rat, mouse, guinea pig, and human 5-HT receptors

*AC: adenylate cyclase; (-): negatively coupled; (+) positively coupled; PI: phospholipase coupled.

a. 5-HT$_{2A}$ Receptors

Branchek et al[106] cloned the human 5-HT$_{2A}$ receptor in 1990. The 5-HT$_{2A}$ receptor plays a role in maintaining normal physiological function, and is widely distributed in the CNS. The 5-HT$_{2A}$ receptor has been mapped by receptor binding, autoradiography using radioligands such as [^{3}H]ketanserin (**36**), [^{3}H]spiperone (**37**), [^{125}I]1-(2,5-dimethoxy-4-iodophenyl)-2-aminopropane (DOI) (**38**) (Figure 17), and [^{3}H]M100907 (**29**) (Figure 14), in situ hybridization, and immunocytochemistry. High densities of 5-HT$_{2A}$ receptors have been identified in forebrain regions that include cortical areas such as the neocortex, claustrum, entorhinal and pyriform cortex, and the olfactory tubercle, nucleus accumbens, caudate nucleus and hippocampus.[107] The 5-HT$_{2A}$ receptor is also expressed in C-fibers and dorsal root ganglia of the spinal cord, activation of these receptors produces analgesia. Peripherally, 5-HT$_{2A}$ receptors have been identified on cardiovascular-related tissues, where they modulate functions such as arterial vasoconstriction and proliferation of arterial fibroblasts.[105]

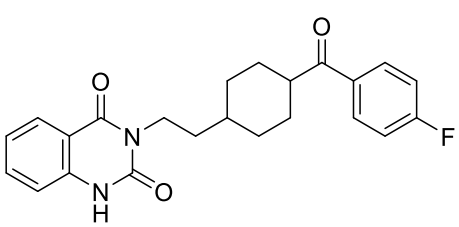

Ketanserin (**36**)

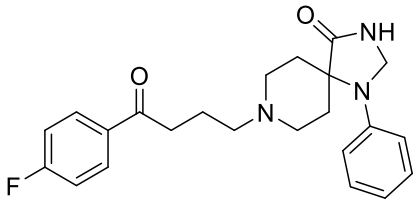

Spiperone (**37**)

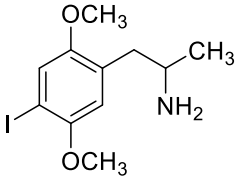

1-(2,5-Dimethoxy-4-iodophenyl)2-aminopropane (DOI; **38**)

Figure 17. Examples of radioligands used to label the 5-HT$_{2A}$ receptor.

The 5-HT_{2A} receptor is a class A GPCR that has seven transmembrane-spanning helices, an intracellular C-terminus, and an extracellular N-terminus. The transmembrane (TM) domains are connected via extracellular and intracellular loops. The intracellular loop between TM5 and TM6 is associated with coupling to second messenger systems (Figure 18). The orthosteric binding site is located in the TM domain, and involves an aspartate moiety in TM3.[39]

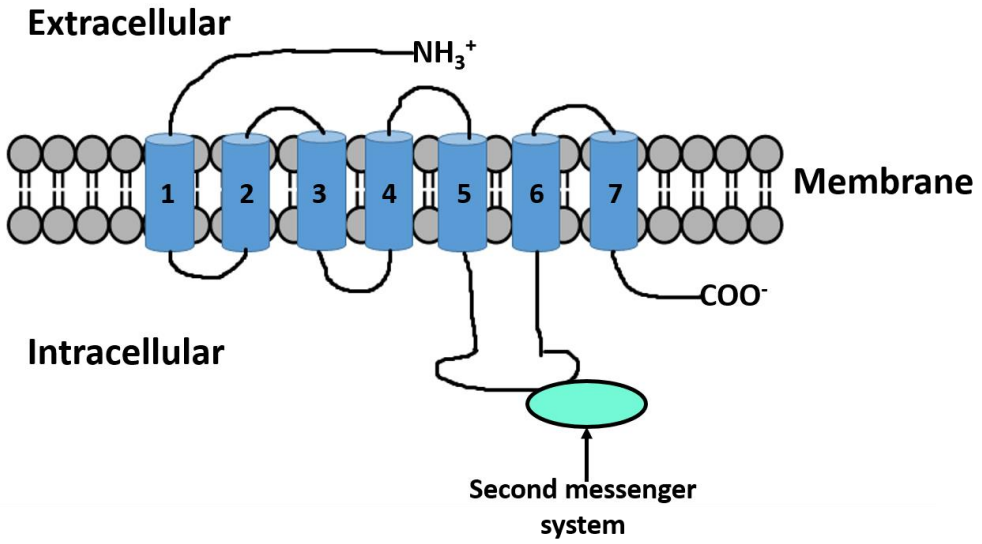

Figure 18. Schematic representation of the 5-HT_{2A} receptor. Transmembrane (TM) spanning helices are numbered as TM1 to TM7 (adapted from Glennon and Dukat[39]).

5-HT_{2A} receptors are coupled to $G_{\alpha q}$, and activation of the receptor leads to hydrolysis of membrane phosphoinositides by the activation of phospholipase C (PLC) resulting in diacyl glycerol (DAG) and inositol phosphates; DAG activates other downstream effectors such as protein kinase C, whereas inositol phosphates can result in an increase in intracellular Ca^{2+} levels, which then activates inwardly rectifying chloride channels.[39,105,107,108] Activation of the rho signaling pathway regulates structural changes in cells.[105]

Agonist action at 5-HT_2 receptors might be involved in the action of classical hallucinogens such as LSD (**7**) (Figure 2), and DOI (**38**) (Figure 17).[109] There is a close correlation between the human hallucinogenic potency of these agents and 5-HT_{2A} receptor affinity, and 5-HT_{2A} receptors might play an important role in the behavioral effects of hallucinogenic agents.[39,110] The 5-HT_{2A} receptor is an important target for antipsychotics, antidepressants, and anxiolytics.[108] The role of 5-HT_{2A} receptors in antipsychotic drug action has evoked considerable interest based on the relationship between 5-HT_{2A} receptors, and hallucinogens, and the high affinity of atypical antipsychotic agents such as clozapine (**8**) (Figure 2), olanzapine (**21**) (Figure 11), and risperidone (**14**) (Figure 8) for 5-HT_{2A} receptors.[107,108]

5. Metabotropic glutamate receptors (mGluRs)

mGlu Receptors are class C GPCRs.[111] There are eight different mGluR subtypes that are divided into three groups, group I through group III, based on sequence homology, pharmacology, and coupling mechanism.[111] Group I consists of $mGlu_1$ and $mGlu_5$ receptors, group II includes $mGlu_2$ and $mGlu_3$ receptors, and Group III consists of $mGlu_4$, $mGlu_6$, $mGlu_7$ and $mGlu_8$ receptor subtypes.[111] Group I receptors couple to $G_{q/11}$ and activate phosphoinositide hydrolysis, while group II and III couple to $G_{i/o}$ and inhibit adenylyl cyclase.[112] The sequence identity between groups is ~45%, while the sequence identity among members of a group is ~70%. [113]

Class C GPCRs differ from class A GPCRs in having a large extracellular N-terminal domain, termed the *venus flytrap domain* that houses the orthosteric binding site.[111,113] The venus flytrap

domain is a clam-shaped structure composed of two lobes with the orthosteric binding site located in between the two lobes.[111,113] The extracellular domain is connected to the heptahelical transmembrane domain via a cysteine rich domain.[111,113] The cysteine-rich domain transmits signals from the venus flytrap domain to the heptahelical transmembrane domain[111,113] (Figure 19). $mGlu_{2/5}$ receptor PAMs, Group II orthosteric agonists have demonstrated antipsychotic activity in preclinical models, and some have advanced into clinical trials.[54,112]

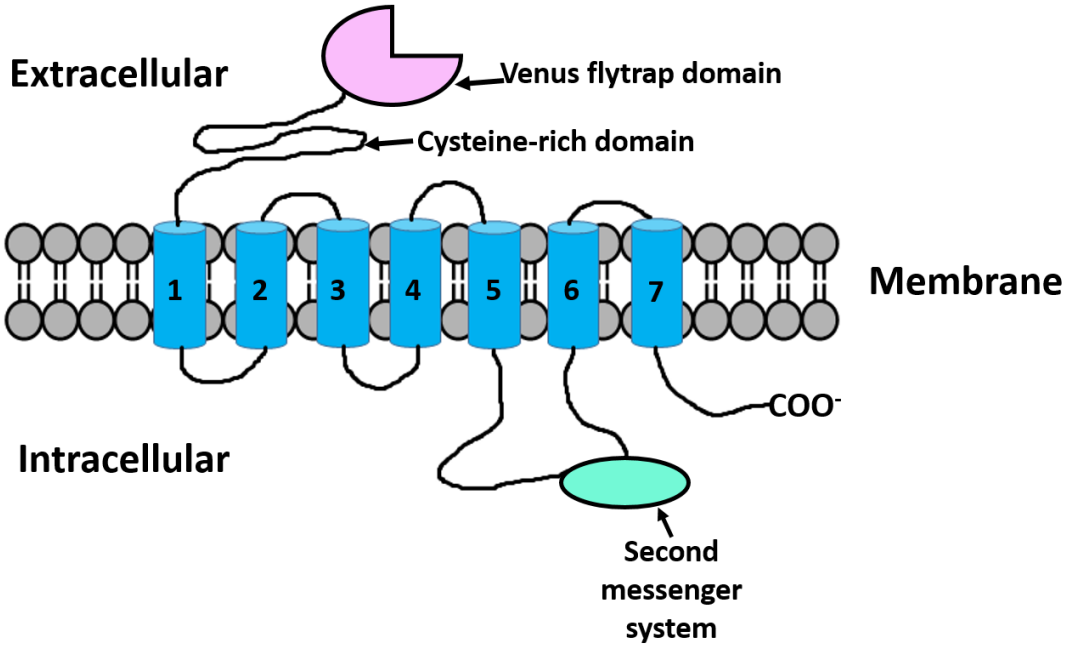

Figure 19. Schematic representation of an mGlu receptor. Transmembrane (TM) spanning helices are numbered as TM1 to TM7 (adapted from Conn et al.[113]).

a. Group II mGlu receptors: $mGlu_2$ and $mGlu_3$ receptors

Group II mGlu receptors are widely expressed in the CNS with higher expression levels in brain regions such as the prefrontal cortex, the thalamus, the hippocampus, the amygdala, and dorsal and ventral striatum.[23] These regions of the brain have been shown to be involved in cognition and

emotional states, and the distribution of the $mGlu_3$ receptor is more dispersed than that of the $mGlu_2$ receptor.[23] $mGlu_2$ receptors are found both presynaptically and postsynaptically while $mGlu_3$ receptors are mainly presynaptic.[23] The $mGlu_2$ receptors can function as autoreceptors that serve as a negative feedback mechanism and suppress the excessive release of GLU, thus maintaining homeostasis.[23] Group II mGluRs can also modulate the release of other neurotransmitters such as GABA, DA, 5-HT, and norepinephrine.[114] They are coupled to $G_{i/o}$ proteins and mediate downstream effects via inhibition of adenylyl cyclase and modulation of voltage-gated ion channels.[23] They might also activate phosphoinositide-3 kinase (pI3K) and MAPK pathways.[23]

There is a large body of evidence suggesting that activation of group II mGlu receptors, specifically the $mGlu_2$ receptor, might be a novel and promising approach to treat anxiety and schizophrenia.[23,115] Preclinical data with orthosteric group II mGlu receptor agonists has been promising, and agents such as LY354740 (**39**), LY404039 (**40**), LY379268 (**41**) (Figure 20) have been shown to possess antipsychotic action in animal models of schizophrenia.[23] LY2140023 (**42**) (Figure 20), an oral prodrug of the Group II mGlu2/3 orthosteric agonist LY404039 (**40**), entered clinical trials; however, it was found to be no more efficacious than placebo in multiple studies.[23,116,117]

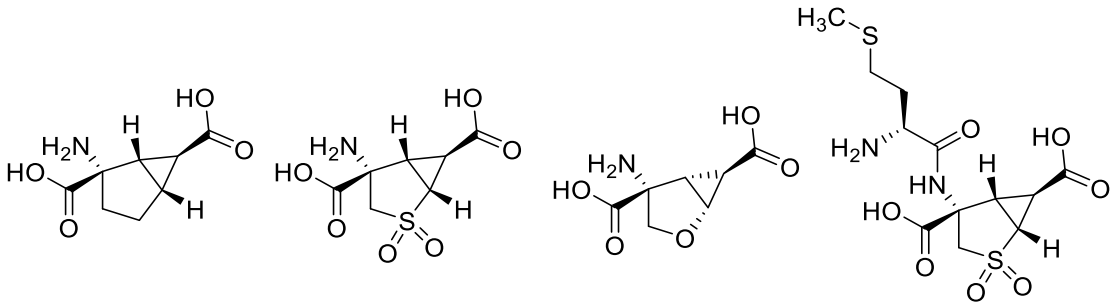

Figure 20. Group II mGlu receptor orthosteric agonists.

Studies with $mGlu_2$- and $mGlu_3$-receptor knock-out mice have suggested that the antipsychotic effects mediated by group II mGlu orthosteric agonists might be due to its action at the $mGlu_2$ receptors, rather than $mGlu_3$ receptors.[118] However, due to similarity and high homology between the orthosteric binding sites of the $mGlu_2$ receptor and $mGlu_3$ receptor, there are no agents that are selective for either subtype thus far.[115] Orthosteric agonists have the disadvantages of non-selectivity and development of tolerance. $mGlu_2$ receptor PAMS are an alternative strategy.[112] Several mGlu receptor PAMs such as BINA (**43**), LY487379 (**44**), JNJ-40411813 (**45**), JNJ-40068782 (**46**), CBiPES (**47**), and AZD8529 (**48**) (Figure 21) have demonstrated antipsychotic activity in preclinical trials, with some of them such as JNJ-40411813 (**45**)[119] and AZD8529 (**48**)[120] having advanced into clinical trials.[23]

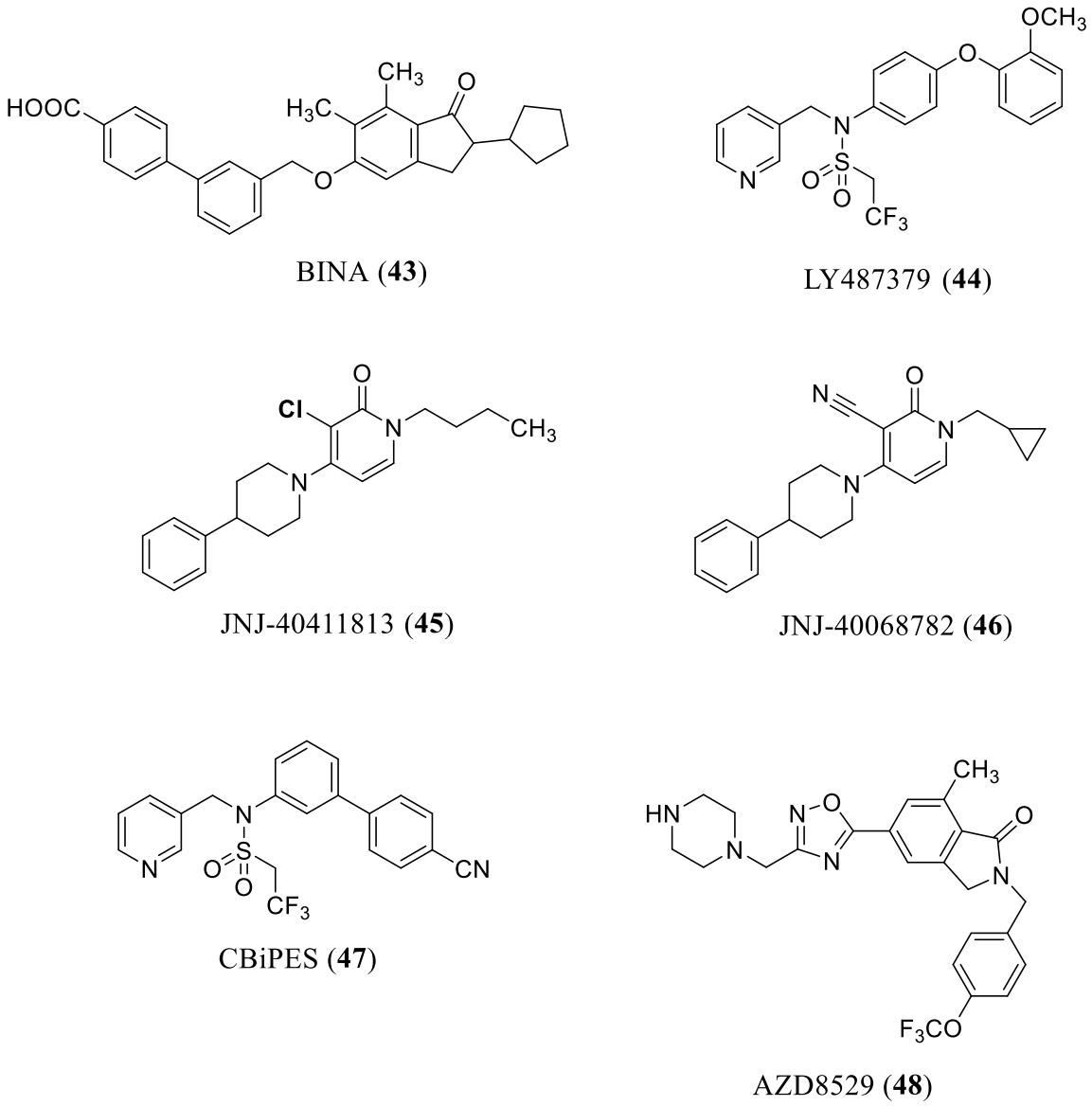

Figure 21. $mGlu_2$ receptor-selective PAMs.

6. Role of the 5-HT_{2A}-$mGlu_2$ receptor heteromer

Roles for the 5-HT_{2A} receptor and the $mGlu_2$ receptor in the pathophysiology of schizophrenia have been well established.[23,88] Several lines of evidence point towards the formation of a functional 5-HT_{2A}-$mGlu_2$ receptor heterocomplex,[18–21] that has been implicated in the mechanism of action of both antipsychotic agents[22] as well as hallucinogenic agents.[20,121] Gonzalez-Maeso et

al.[18] and Moreno et al.[20,121] have validated the necessity of a 5-HT_{2A}/$mGlu_2$ receptor heterocomplex for the behavioral effects of hallucinogenic agents such as LSD (**7**) (Figure 2) and DOI (**38**) (Figure 17). Additionally, Moreno et al.[20] have also identified that three amino acid residues Ala677, Ala681, and Ala685, located at the intracellular end of the TM4 of the $mGlu_2$ receptor are important for formation of the heteromer. Fribourg et al.[22] have demonstrated that the high affinity 5-HT_{2A} receptor atypical antipsychotic agents clozapine (**8**) (Figure 2) and risperidone (**14**) (Figure 8) mediate their effects by binding to the 5-HT_{2A}/$mGlu_2$ receptor heteromer, which then balances $G_{i/o}$ and $G_{q/11}$ signaling. Gonzalez-Maeso et al.[18] have demonstrated that the 5-HT_{2A} receptor is upregulated and the $mGlu_2$ receptor is downregulated in postmortem brain samples of untreated schizophrenic patients. These changes suggest that the 5-HT_{2A}/$mGlu_2$ receptor heteromer may be involved in the altered cortical processes in schizophrenia, and represents an attractive novel target for the treatment of schizophrenia.[18]

III. SPECIFIC AIMS

In pursuit of new antipsychotic agents that cause reduced incidence of EPS than haloperidol (**5**) (Figure 1), Dr. Paul Janssen, as reviewed by Awouters and Lewi,[74] designed more compounds, and based on their pharmacological properties and clinical information selected agents that were better than haloperidol (**5**) (Figure 1). The goal was to synthesize an antipsychotic agent that had an additional effect that could complement DA blocking activity.[74] Central 5-HT_{2A} receptor blockade has been found to rectify and complement central D_2 receptor antagonism, leading to development of molecules such as risperidone (**14**) (Figure 8) that combine 5-HT_{2A} and D_2 receptor antagonism in one molecule.[15,122] Some of the earlier butyrophenone analogs such as pipamperone (**49**) (Figure 22) did possess serotonin activity (strong tryptamine antagonism),[74,123] however, this effect was overlooked since the clinical implications of serotonin in schizophrenia were not clear at that time.[74] Pipamperone (**49**) had efficacy in treating the negative symptoms of schizophrenia, and had resocializing effects.[74,124] However, the relationship between 5-HT antagonism and amelioration of negative symptoms of schizophrenia had not been established at that time.[74] The pharmacological and clinical profiles of pipamperone (**49**) were quite distinctly different from that of haloperidol (**5**) (Figure 1).[74,122,125] Risperidone (**14**) (Figure 8), a prototypical SDA, was found to have a pharmacological profile very similar to that of pipamperone (**49**) (K_i = 1 nM (5-HT_{2A} receptor), K_i = 98 nM (D_2 receptor)), with serotonin receptor antagonism preceding D_2 receptor occupancy,[14] and with risperidone (**14**) (Figure 8) (K_i = 0.16 nM (5-HT_{2A} receptor), K_i

= 3.1 nM (D_2 receptor) being more potent.[15] Risperidone (**14**) is effective in treating the positive and negative symptoms of schizophrenia, and has a lower propensity to cause EPS.[14] Moderate D_2 receptor occupancy, predominantly 5-HT_{2A} receptor occupancy, and the avoidance of D_2 receptor over blockade, might be the mechanism for its effectiveness against the positive, and negative symptoms of schizophrenia, with reduced side effects.[14] There has been marked progress from pipamperone (**49**) to risperidone (**14**), with a hundred-fold reduction in dosing.[74]

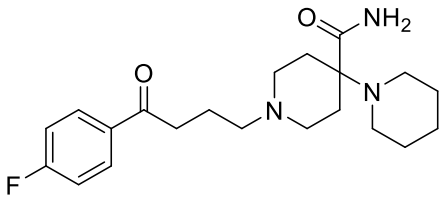

Pipamperone (**49**)

Figure 22. Structure of the butyrophenone analog pipamperone **(49)**.

The pharmacological differences between haloperidol (**5**) (Figure 1) and pipamperone (**49**), and the chemical structures of benperidol (**50**) and lenperone (**51**) (Figure 23), led to the development of risperidone (**14**) (Figure 23).[15]

Benperidol (**50**) and lenperone (**51**) are butyrophenone analogs that bind to D_2 receptors.[15] The butyrophenone moiety is common to both molecules, and since they both bind to D_2 receptors (Table 2), it was hypothesized that the benzimidazolone fragment of benperidol (**50**) and the benzoyl fragment of lenperone (**51**) had pharmacophoric similarity.[15] Lenperone (**51**) can be considered to be an almost symmetrical molecule that has two aromatic regions at a distance of four carbon atoms from the central nitrogen atom, with the only difference being the cyclic form

of the chain in the 4-benzoylpiperidine fragment.[15] Hence the open form of the benzimidiazolone fragment of benperidol (**50**) might have potential activity like the open form of the 4-benzoylpiperidine fragment (butyrophenone fragment) of lenperone (**51**).[15] Declenperone (**52**) and milenperone (**53**) (Figure 23) were a result of combining fragments of benperidol (**50**) and lenperone (**51**).[15] Declenperone (**52**) and milenperone (**53**) were both centrally active and potent DA antagonists, and weak 5-HT antagonists, (Table 2) with milenperone (**53**) being more potent than declenperone (**52**).[15] However, milenperone (**53**) was no more efficacious than haloperidol (**5**) (Figure 1) in clinical trials.[15]

Expansion of the five membered imidazolone ring to a larger ring system that retained the urea moiety, and four atoms between the aromatic ring and central nitrogen atom, resulted in ketanserin (**36**) (Figure 23), a molecule that possessed 100-fold higher affinity for 5-HT_{2A} receptors as compared to D_2 receptors.[15] Ketanserin (**36**) is a potent peripheral 5-HT_{2A} receptor antagonist, and an α_1-adrenoceptor antagonist at higher doses.[15] Ketanserin (**36**) is therapeutically useful as an antihypertensive agent.[15]

Chemical modification of the quinazolinedione ring of ketanserin (**36**) led to pirenperone (**54**) and setoperone (**55**) (Figure 23).[15] Both these agents were centrally active D_2 receptor, and 5-HT_{2A} receptor antagonists with a higher affinity for 5-HT_{2A} receptors (Table 2).[15] Setoperone (**55**) showed antipsychotic potential in preclinical studies,[126] however, it had limited bioavailability due to enzymatic reduction of the keto functionality to an inactive alcohol, and hence was not pursued further.[15] Bioisosteric replacement (to avoid metabolism) of the 4-fluorobenzoyl moiety with 6-

fluorobenzisoxazole resulted in risperidone (**14**) (Figure 23).[15] Risperidone (**14**) was a potent and centrally active D_2 and 5-HT_{2A} receptor antagonist, with higher affinity for 5-HT_{2A} receptors (Table 2), and good bioavailability.[15] Risperidone (**14**) also antagonizes the α_1-adrenoceptors (K_i = 2.4 nM), and histamine H_1 receptors.(K_i = 2.1 nM).[15,127] Paliperidone (**56**) (Figure 23), an active metabolite of risperidone, has a pharmacological profile (Table 2) similar to that of risperidone (**14**).[15,128–130]

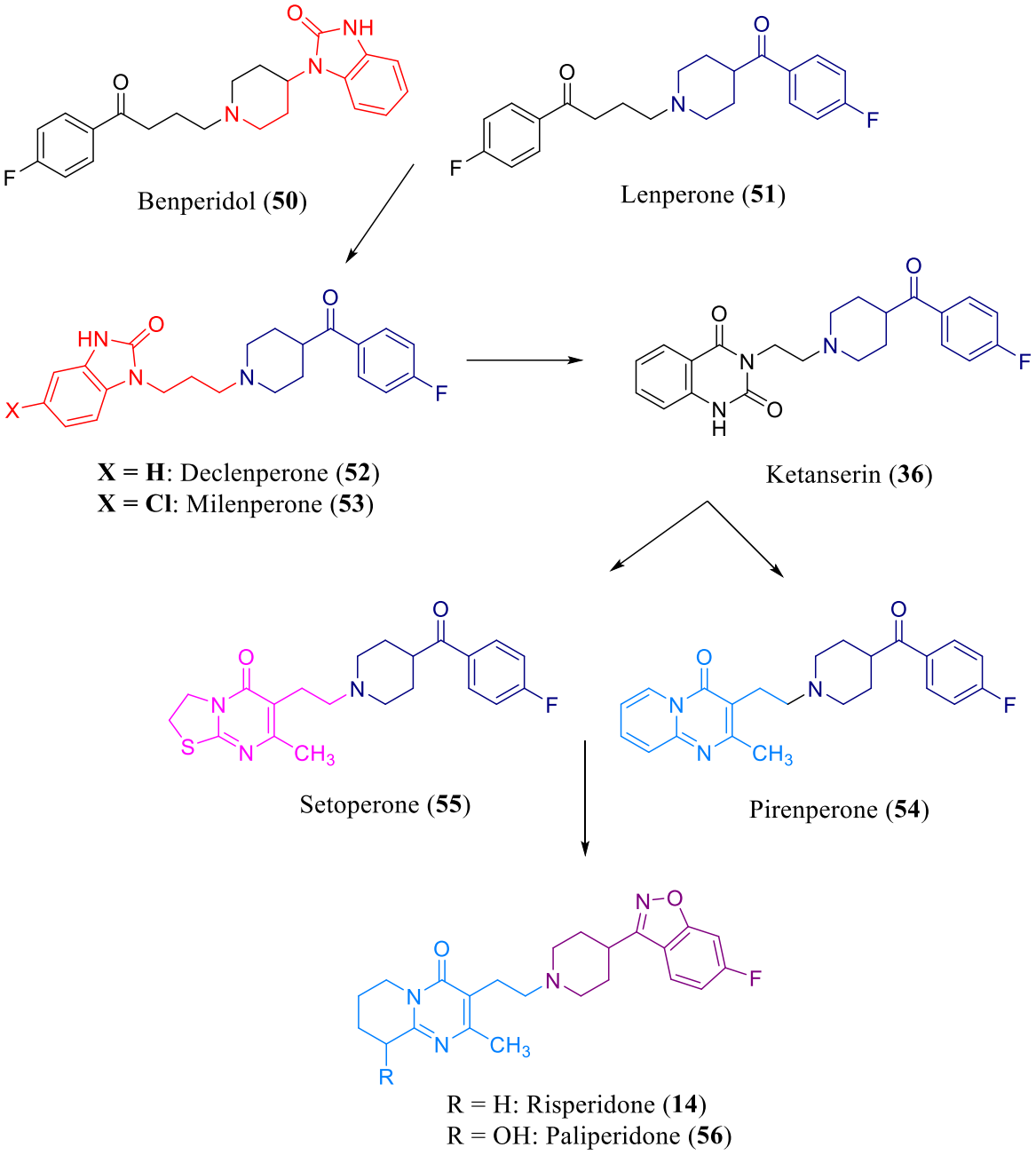

Figure 23. Development of risperidone.[15]

Table 2. Activity profile of risperidone and other analogs (adapted from Megens and Kennis[15]).

Compound	Binding affinity* K_i (nM)		Functional activity** ED_{50} (mg/kg)	
	D_2	5-HT_{2A}	Apomorphine	Tryptamine
Benperidol (**50**)	0.35	6.6	0.0093	0.29
Lenperone (**51**)	4.6	Not tested	0.085	0.39
Declenperone (**52**)	9.3	2.4	0.44	2.4
Milenperone (**53**)	3.9	9.2	0.025	0.51
Ketanserin (**36**)	220	2.1	> 40	2.4
Pirenperone (**54**)	16	2.1	0.098	0.11
Setoperone (**55**)	24	2.3	0.22	0.11
Risperidone (**14**)	3.1	0.16	0.15	0.13
Paliperidone (**56**)	4.1	0.22	0.39	0.22

*Radioligand: [^{3}H]spiperone (**37**) (Figure 17).
**ED_{50} for antagonism of apomorphine-, and tryptamine-induced behavioral effects in the apomorphine- tryptamine- and norepinephrine-interaction test in rats.

The pharmacological profile of risperidone (**14**) has been compared to that of haloperidol (**5**), a D_2 receptor antagonist, and ritanserin (**28**) a selective 5-HT_{2A} receptor antagonist.[122] Similar to ritanserin (**28**), risperidone (**14**) showed activity in tests related to central and peripheral 5-HT_{2A} receptor antagonism such as a reduction in central serotonergic over activity induced by agents such as 5-hydroxytryptophan, mescaline or tryptamine at doses of 0.014-0.049 mg/kg, and is a more potent 5-HT_{2A} receptor antagonist than ritanserin (**28**).[122] Similar to haloperidol (**5**), risperidone (**14**) inhibits the central and peripheral expression of hyperdopaminergia.[122] It inhibits behavioral reactions linked to normal dopaminergic function such as conditioned responses, and

ICS; additionally, it inhibits central hyperdopamaninergia produced by dopaminomimetic agents such as amphetamine, cocaine, and apomorphine at doses of 0.016-0.16 mg/kg.[122]

Ritanserin (**28**) when given as an additional therapy with a typical antipsychotic agent can help decrease EPS, and cause an improvement in the negative and affective symptoms of schizophrenia.[122,131,132] The effects of haloperidol (**5**) include antimanic, antihallucinatory, and antidelusional actions, with the possibility of EPS at higher doses.[122] Hence, since risperidone is an SDA, it should be able to produce clinical effects of both ritanserin (**28**) and haloperidol (**5**) (Figure 1).[122] However, the haloperidol-like antidopaminergic effects can be modified with greater 5-HT_{2A} receptor blockade.[122] Induction of catalepsy and inhibition of locomotor activity by haloperidol (**5**) was seen at the doses used to inhibit evoked responses, while much larger doses of risperidone were required to inhibit locomotor activity and induce catalepsy.[122] Risperidone differs from haloperidol (**5**) and ritanserin (**28**) in being able to antagonize LSD in drug discrimination studies, an effect that is common to SDAs, and thought to be a result of simultaneous 5-HT_2 and D_2 receptor antagonism.[122] Ritanserin (**28**) (Figure 13) is a poor blocker of the LSD cue,[133,134] while haloperidol (**5**) reduces response rates without affecting the discriminative stimulus.[122] Hence, in spite of being able to antagonize 5-HT_{2A} and D_2 receptors, it has a pharmacological profile that is different from that of ritanserin (**28**) and the typical antipsychotic agent haloperidol (**5**).

Studies have suggested that risperidone (**14**) is an inverse agonist at 5-HT_{2A} receptors.[135,136] Risperidone has structural features that make it unique and distinguish it from structurally-related compounds such as ketanserin (**36**) (Figure 17).

Risperidone is used as monotherapy for schizophrenia, as well as an adjunct therapy to lithium or valproate to treat acute manic episodes, and for the maintenance treatment of bipolar disorder I.[16] Even though risperidone has a much lower tendency to cause EPS than typical antipsychotic agents, therapy with risperidone is associated with side effects such as hyperprolactinemia, weight gain, and metabolic disorders such as glucose dysregulation,[13,16,17] and there is a need for newer antipsychotic agents with fewer side effects.

Goals of this project are to study the structural features of risperidone (**14**) (Figure 8), and determine the minimal structural features required for 5-HT_{2A} receptor antagonist activity, and to identify an $mGlu_2$ receptor PAM from known $mGlu_2$ receptor PAMs, that will contribute towards the long-term goal of synthesizing a bivalent molecule that can target the $mGlu_2$/5-HT_{2A} receptor heteromer.

The specific aims of the current project are:

1. **Deconstruction of risperidone to determine the minimal structural features responsible for its 5-HT_{2A} receptor antagonist activity**

2. **Elaboration of risperidone to investigate the role of the two halves of risperidone in its 5-HT$_{2A}$ receptor antagonist activity**

    a. Investigation of the potential role of the two halves of risperidone in its activity by examination of structural hybrids of risperidone and ketanserin.

    b. Investigation of the potential role of the "right half "(i.e., the 6-fluoro-3-(4-piperidinyl)-1,2-benz[*d*]isoxazole portion) of risperidone in its activity by making the right half of risperidone similar to serotonin.

    c. Aromatization of the "left half" (i.e., the 2-methyl-6,7,8,9-tetrahydro-4*H*-pyrido[1,2-*a*]pyrimidin-4-one portion) of risperidone.

    d. Investigation of the role of the "left half" (i.e., the 2-methyl-6,7,8,9-tetrahydro-4*H*-pyrido[1,2-*a*]pyrimidin-4-one portion) of risperidone by making the "left half" of risperidone similar to other antipsychotic agents such as iloperidone.

3. **Molecular modeling studies of risperidone and its deconstructed and elaborated analogs at 5-HT$_{2A}$ receptors to study their binding mode**

4. **mGlu$_2$ receptor PAMs**

    a. Molecular modeling studies of the allosteric site of the mGlu$_2$ receptor to determine whether structurally diverse PAMs of the mGlu$_2$ bind in a similar manner and in the same binding pocket.

    b. Synthesis of the mGlu$_2$ receptor PAM JNJ-40411813.

5. Redefining a pharmacophore for 5-HT_{2A} receptor antagonists.

IV. APPROACH, RESULTS AND DISCUSSION

A. Specific Aim 1: Deconstruction of risperidone to determine the minimal structural features responsible for its 5-HT_{2A} receptor antagonist activity

1. Approach

To study the structure-activity relationships (SAR) of risperidone at 5-HT_{2A} receptors and to possibly identify a 5-HT_{2A} receptor antagonist pharmacophore a "deconstruction-reconstruction-elaboration" approach was used.[137] The "deconstruction-reconstruction-elaboration" approach involves assigning an arbitrary core to a given agent, and removing one structural feature at a time.[137] Biological activity of the deconstructed analogs will enable us to "reconstruct" analogs incorporating only those structural features contributing to activity.[137] The "elaboration" phase involves further exploration of various substituents and functional groups.[137]

Risperidone (**14**) (Figure 24) can be divided into two halves consisting of the 2-methyl-6,7,8,9-tetrahydro-4*H*-pyrido[1,2-*a*]pyrimidin-4-one portion (hereafter referred to as the "left half") and the 6-fluoro-3-(4-piperidinyl)-1,2-benz[*d*]isoxazole portion (hereafter referred to as the "right half") connected by an ethyl linker.

Risperidone (**14**) (Figure 24) was systematically deconstructed into truncated analogs **57-68** (Figure 24) to study the structural features necessary to retain 5-HT_{2A} receptor affinity and (where applicable) antagonist activity.

Analogs **57-59** represent deconstructed analogs where the benz[*d*]isoxazole portion of risperidone (**14**) (the "right half") was removed and the "left half" of risperidone (**14**) was further deconstructed. Analogs **60-63** will examine the "right half" of risperidone (**14**), whereas analogs **64-68** will help examine other whole-molecule features.

A "deconstruction-reconstruction-elaboration" approach was used by our group[138] to study the SAR of ketanserin (**36**) (Figure 25), a molecule that bears structural resemblance to risperidone (**14**) (Figure 25), at 5-HT_{2A} and 5-HT_{2C} receptors. The structural analogs of ketanserin (**36**) were tested for binding affinity at 5-HT_{2A} and 5-HT_{2C} receptors in frontal brain cortical regions of Sprague-Dawley rats using ^{3}[H]ketanserin as the radioligand.[138] Figures 25 and 26 illustrate a comparison of the deconstruction of risperidone (**14**) with the deconstruction of ketanserin (**36**)

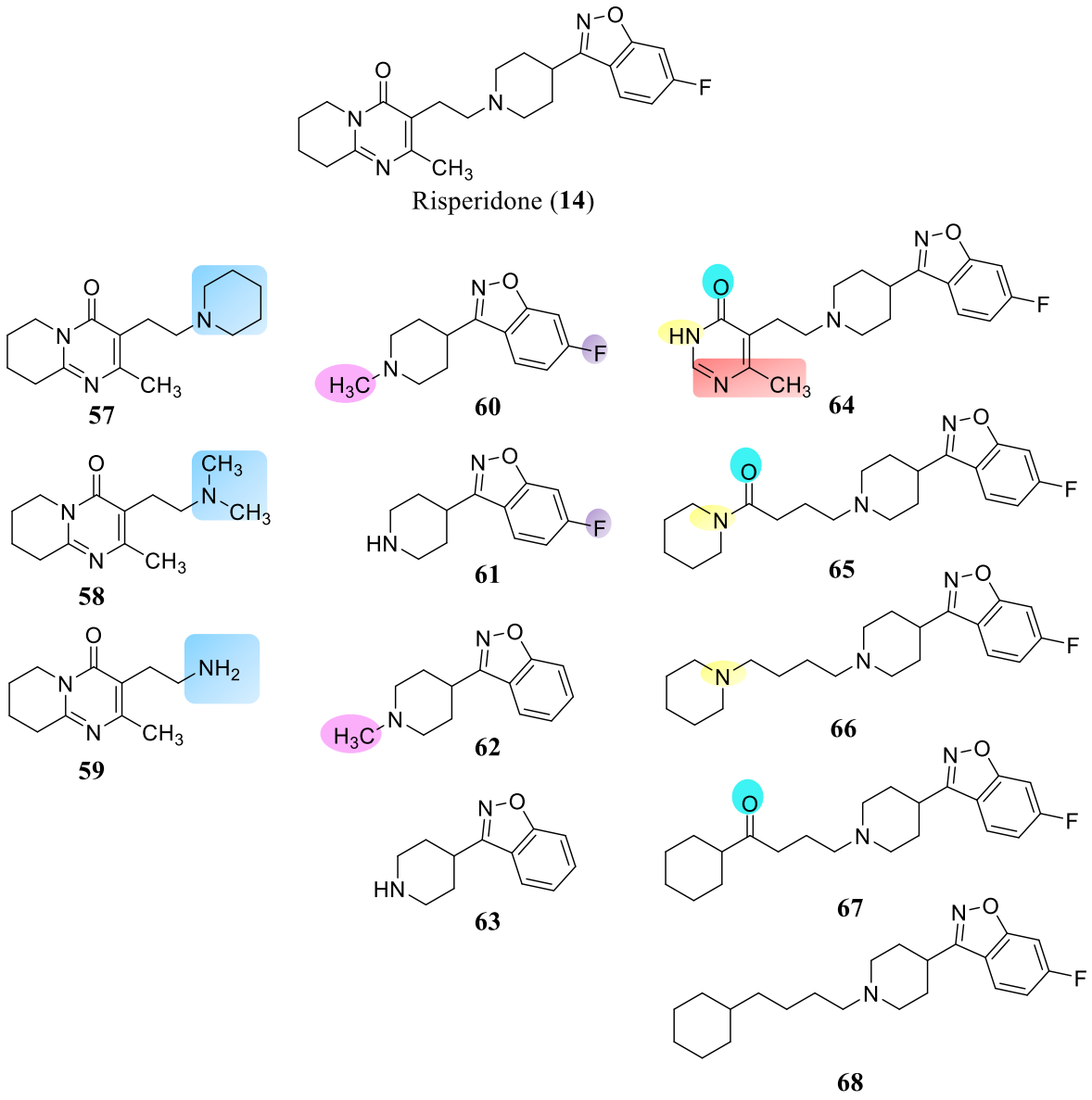

Figure 24. Deconstructed analogs of risperidone (**14**).

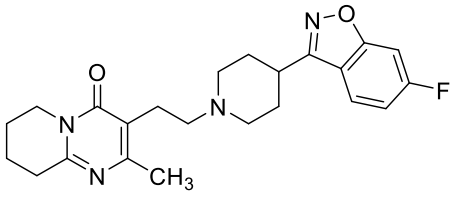

Risperidone (**14**)

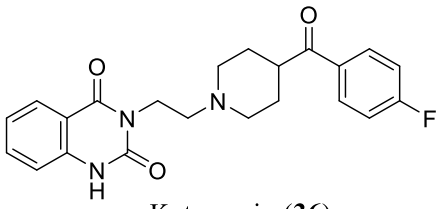

Ketanserin (**36**)

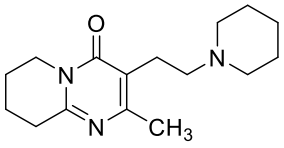

57

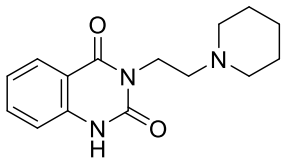

69

K_i = > 10,000 nM

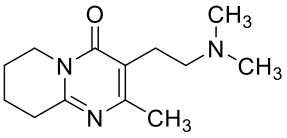

58

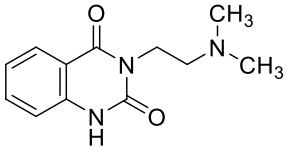

70

K_i = > 10,000 nM

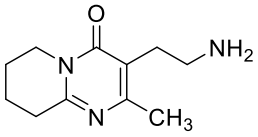

59

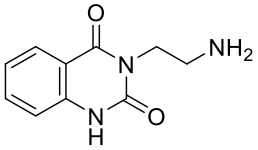

71

K_i = > 10,000 nM

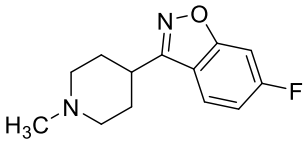

60

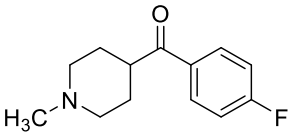

72

K_i = 125 nM

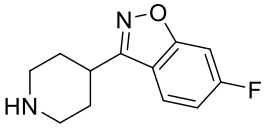

61

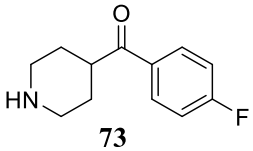

73

K_i = 430 nM

Figure 25. A comparison of the deconstruction of risperidone (**14**) with the deconstruction of ketanserin (**36**). Data for ketanserin analogs are from Herndon et al.[138]

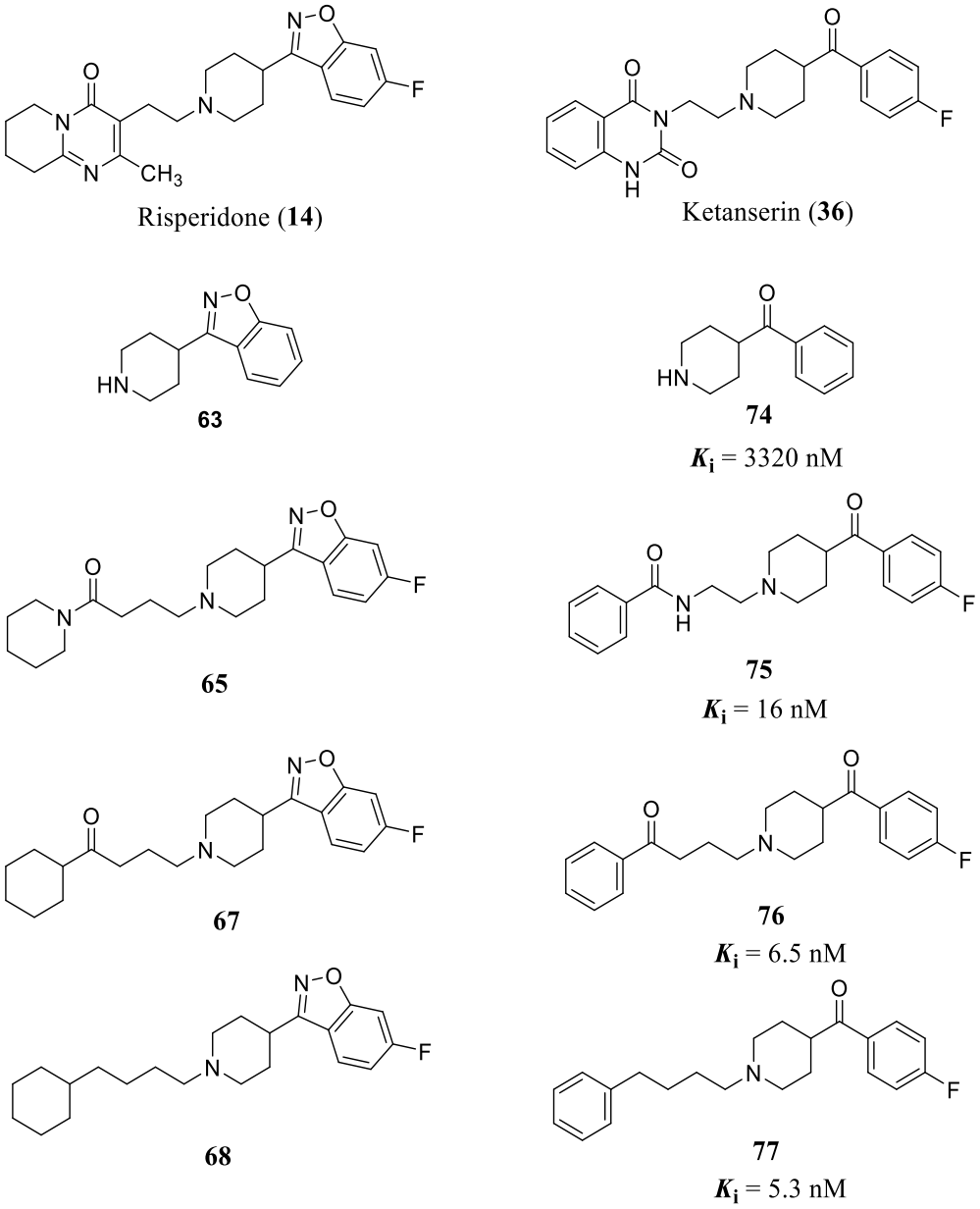

Figure 26. A comparison of the deconstruction of risperidone (**14**) with the deconstruction of ketanserin (**36**). Data for ketanserin analogs are from Herndon et al.[138]

Analog **57** (Figure 24) lacks the 6-fluoro-1,2-benz[*d*]isoxazole portion (the "right half") and will help establish the contribution of the "left half" of risperidone (**14**) towards 5-HT_{2A} receptor affinity and antagonist activity of risperidone (**14**). In analogs **58** and **59** (Figure 24), the piperidine

ring has been deconstructed into a simpler tertiary amine and then an even simpler primary amine, and will additionally help ascertain the role of the piperidine ring, as well as the nature of the amine in binding. A comparison of analog **57** with **58** will additionally help understand the importance of a constrained ring system. Analog **59** represents the "left half" of risperidone with the linker and the amine portion of the "right half". The amine has been retained because the protonated amine of orthosteric agonists and antagonists of the 5-HT_{2A} receptor is involved in a crucial ionic interaction with an aspartate moiety (Asp 155) in TM3.[139] Herndon et al.[138] had deconstructed ketanserin in an analogous manner (analogs **69-71)** and the deconstructed analogs lacked affinity for 5-HT_{2A} receptors. If analogs **57-59** bind in a manner similar to analogs **69-71**, they should also lack affinity for 5-HT_{2A} receptors. If they bind with higher affinity it will indicate that the "left half" of risperidone (**14**) contributes to a greater extent to its binding affinity as compared to the "left half" of ketanserin (**36**).

Analog **60** (Figure 24) represents the "right half" of risperidone (**14**) and retains a part of the linker in the form of a methyl group, and will help study the importance of the "right half" of risperidone in its 5-HT_{2A} receptor affinity and antagonist activity. Deconstructed analog **61** (Figure 24) represents the desmethyl analog of **60**, whereas analogs **62** and **63** (Figure 24) represent the desfluoro analogs of **60** and **61**, respectively. Analog **61** has been shown to be a 5-HT_{2A} receptor antagonist previously by our laboratory.[140] In the prior study, the radioligand binding assay was performed in rat brain homogenates using [^{3}H]ketanserin as the radioligand and analog **61** was found to bind at 5-HT_{2A} receptors with only 16 fold lower affinity than risperidone (**14**). It was shown to be a potent 5-HT_{2A} receptor antagonist in an in vitro assay that measures serotonin

induced inositol phosphate production, as well as in an in vivo assay. The in vivo assay was performed in rats that could discriminate 1-(2,5-dimethoxy-4-methylphenyl)-2-aminopropane (a 5-HT_2 receptor agonist) from vehicle. Our laboratory has recently reported that analogs **60** (K_i = 12.27 nM) and **61** (K_i = 71.41 nM**)** both bind to 5-HT_{2A} receptors and are 5-HT_{2A} receptor antagonists (discussed in the results section).[141] In fact, analog **60** (K_i = 12.27 nM) binds with only ~ 2 fold lower affinity than risperidone (**14**; K_i = 5.29 nM).[141] Herndon et al.[138] had tested the "right halves" of ketanserin (analogs **72** and **73**) and they demonstrated a decrease in affinity for the 5-HT_{2A} receptors as compared to ketanserin (**36**).[138] Analogs **62** and **63** will help establish the importance of the fluoro group for 5-HT_{2A} receptor affinity and antagonism.

Deconstructed analog **64** (Figure 24) retains only the 6-methyl-3*H*-pyrimidin-4-one portion of the "left half" of risperidone (**14**), whereas in abbreviated analogs **65-68** (Figure 24) the 6-methyl-3*H*-pyrimidin-4-one ring system has been deconstructed and will help ascertain the role of the "left half" of risperidone (**14**) in its 5-HT_{2A} receptor antagonist activity. Analog **65** retains the amide portion of the 6-methylpyrimidin-4(3*H*)-one ring system. In analog **66** the carbonyl group present in analog **65** has been removed, whereas in analog **67** the amide nitrogen of **65** has been replaced by a methylene group. Deconstructed analog **68** represents the descarbonyl analog of **67**. Analogous deconstruction of ketanserin (**36**) resulted in molecules (**75-77**) that bind to 5-HT_{2A} receptors with high affinity.[138] Our laboratory has recently reported that analogs **65** (K_i = 39.81 nM) and **66** (K_i = 34.83 nM) bind with high affinity to 5-HT_{2A} receptors and are 5-HT_{2A} receptor antagonists (discussed in the results section).[141]

2. Results

A. Chemistry

The synthesis of compound **57** was initially attempted as outlined in Scheme 1 via a nucleophilic substitution reaction. Piperidine was alkylated with the primary alkyl halide **78** in DMF in the presence of K_2CO_3. K_2CO_3 was added to neutralize the HCl that is formed as a by-product of the reaction. However, the reaction did not progress, and analog **57** was ultimately synthesized using a Finkelstein reaction (Scheme 1- ii and iii). The Finkelstein reaction is a nucleophilic substitution reaction. A small amount of KI is added to the reaction mixture to facilitate halide exchange between the chloride of the alkyl chloride and the iodide of the KI. Synthesis of compound **57** was attempted in two solvents- DMF and MeCN. When MeCN was used as a solvent for the reaction, the yield was comparatively higher (yield: 20%) as compared to when DMF was used as a solvent (yield: 12%). Reported literature suggests that solvents such as *i*-PrOH and MeCN work better than DMF.[142] Compound **57** was unknown and was characterized by NMR and elemental analysis for C, H and N.

Scheme 1. Synthesis of compound **57**.[a]

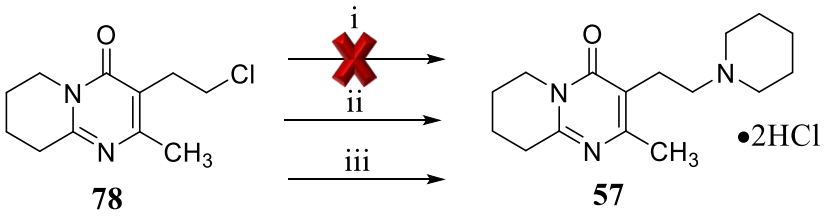

[a]Reagents and conditions: (i) piperidine, K_2CO_3, DMF, reflux, 17 h; (ii) (a) piperidine, K_2CO_3, KI, DMF, reflux, 17 h; (b) EtOH, HCl/EtOH; (iii) (a) piperidine, K_2CO_3, KI, MeCN, reflux, 17 h; (b) EtOH, HCl/ EtOH.

Compound **58** was synthesized in a manner analogous to compound **57**, and the synthesis is outlined in Scheme 2. Analog **58** was synthesized by a Finkelstein reaction between 3-(2-chloroethyl)-2-methyl-6,7,8,9-tetrahydro-4*H*-pyrido[1,2-*a*]pyrimidin-4-one (**78**) and dimethylamine in the presence of K_2CO_3 and KI (catalytic amount) in MeCN. Compound **58** was unknown and was characterized by NMR and elemental analysis for C, H and N.

Scheme 2. Synthesis of compound **58**.[a]

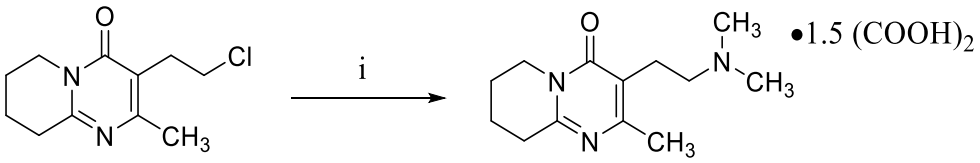

78 **58**

[a]Reagents and conditions: (i) (a) *N*,*N*-dimethylamine (2 M solution in MeOH), K_2CO_3, KI, MeCN, reflux, 30 h; (b) $CHCl_3$, $(COOH)_2/Et_2O$.

Compound **59** was synthesized using a Gabriel synthesis reaction (Scheme 3). The Gabriel synthesis is a nucleophilic substitution reaction that utilizes potassium phthalimide as an -NH_2 synthon. The primary alky halide **78** was allowed to react with potassium phthalimide to yield intermediate **79** that was subsequently converted to compound **59** by hydrazine hydrate. Compound **59** was unknown and was characterized by NMR and elemental analysis for C, H and N.

Scheme 3. Synthesis of compound **59**.[a]

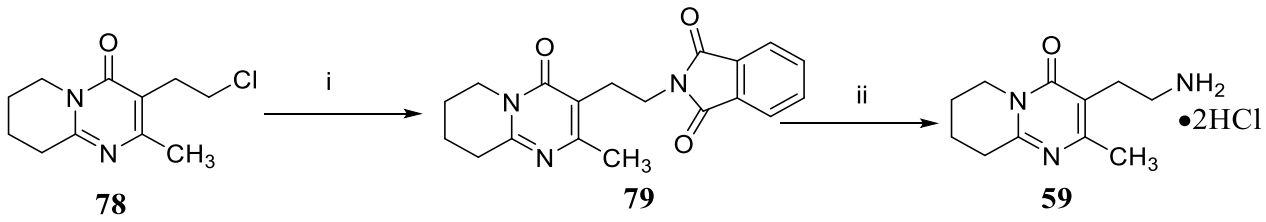

[a]Reagents and conditions: (i) Potassium phthalimide, DMF, 22h, reflux; (ii) (a) hydrazine hydrate, EtOH, reflux, 4h; (b) 1 N HCl, reflux, 5 min; (c) EtOH, HCl/EtOH.

The Gabriel synthesis was used to synthesize analog **59** as opposed to the direct alkylation of ammonia, since alkylation of ammonia is often unselective with poor yields, and can result in a mixture of primary, secondary, tertiary, and quarternary amines.

Compounds **60-63** were synthesized by Dr. Supriya A. Gaitonde, who was a graduate student in the Dukat and Glennon laboratory, and their syntheses are outlined in Schemes 4 (**60, 61**) and 5 (**62, 63**).[143]

Scheme 4. Synthesis of compounds **60** and **61**.[a]

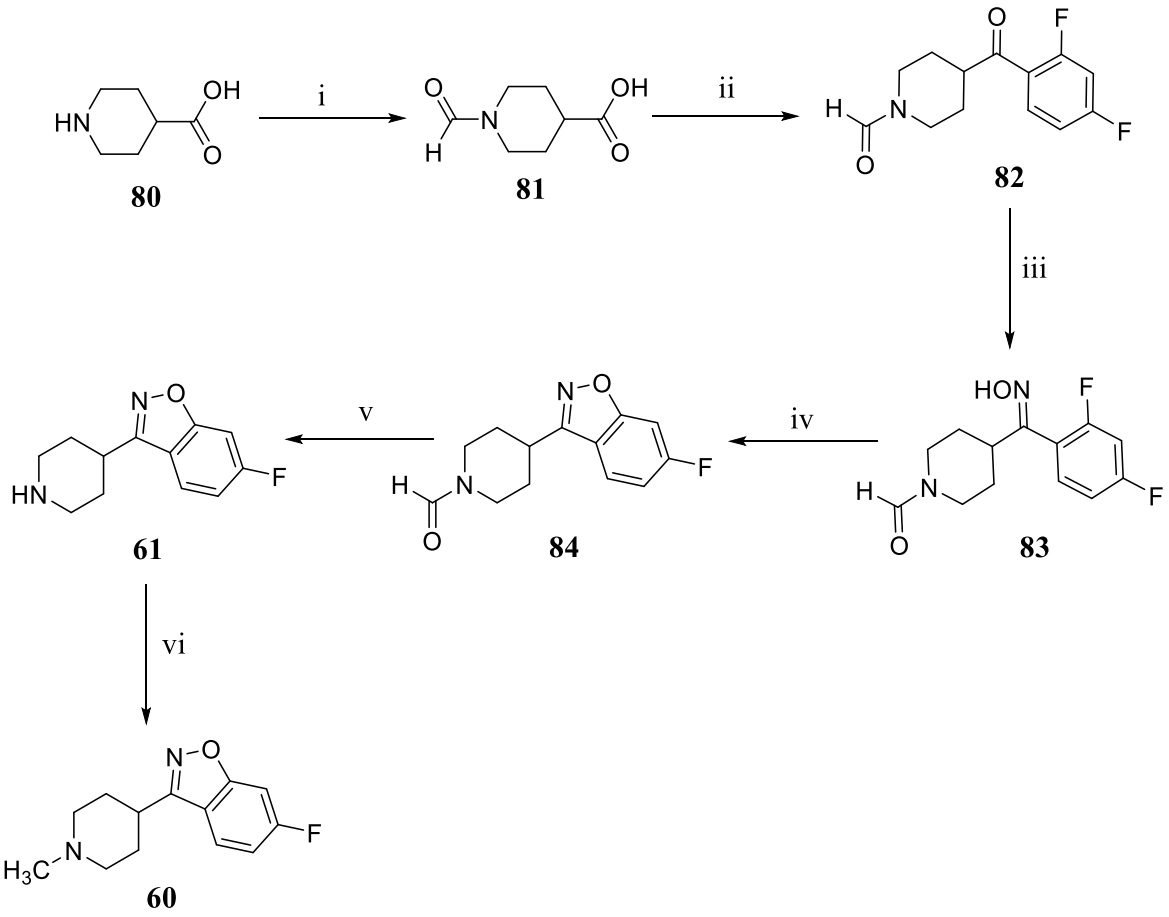

[a]Reagents and conditions: (i) (a)HCOOH, Ac_2O, 65 ºC, 1 h; (b) room temperature, 16 h; (ii) $SOCl_2$, DMF, room temperature, 6 h; (b) 1,3-difluorobenzene, $AlCl_3$, reflux, 45 h; (iii) NH_2OH•HCl, NaOH/H_2O, EtOH, reflux, 96 h; (iv) (a) NaH, DMF, room temperature, 48 h; (v) (a) conc. HCl, EtOH, reflux 3 h; (b) room temperature, 48 h; (vi) (a) HCOOH, HCHO, reflux, 10 h; (b) HCl/Et_2O.

Scheme 5. Synthesis of compounds **62** and **63**.[a]

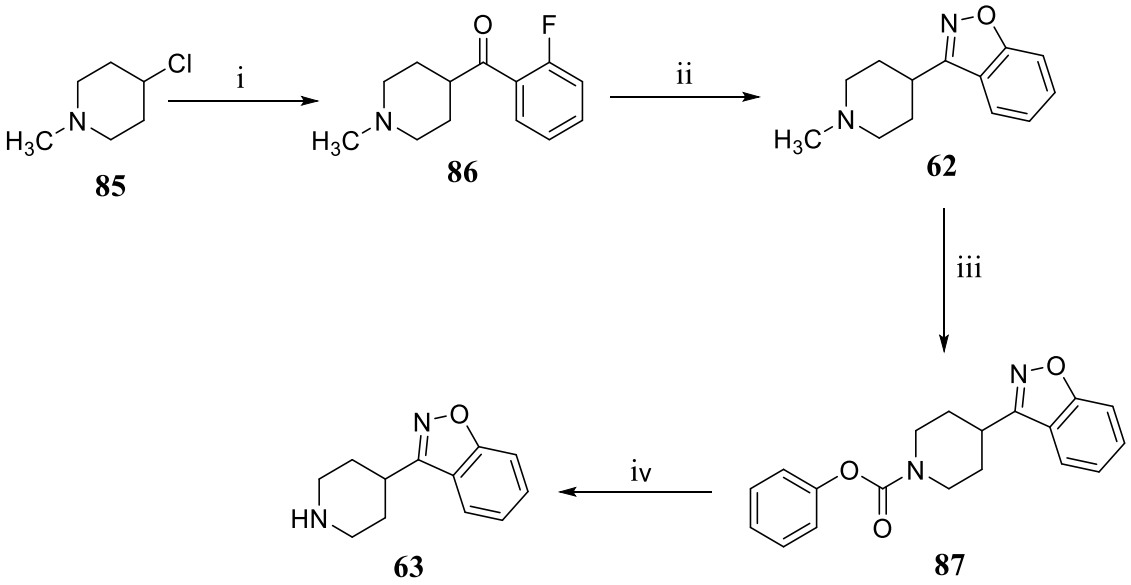

[a]Reagents and conditions: (i) (a) 4-Chloro-*N*-methylpiperidine, THF, Mg, bromoethane, reflux, 1h; (b) room temperature, 2-fluorobenzonitrile, reflux, 3 h; (c) room temperature, 36 h; (d) NH_4Cl, 50 ºC, 2 h; (e) HCl/Et_2O; (ii) (a) KOH (85%), hydroxylamine hydrochloride, ethoxyethanol, reflux, 6 h; (b) HCl/Et_2O (iii) (a) NaOH, toluene, phenyl chloroformate, reflux, 24 h; (b) petroleum ether; (iv) (a) KOH (85%), EtOH, reflux, 48 h; (b) HCl/Et_2O.

The synthesis of analog **64** is outlined in Scheme 6.

Scheme 6. Synthesis of compound **64**.[a]

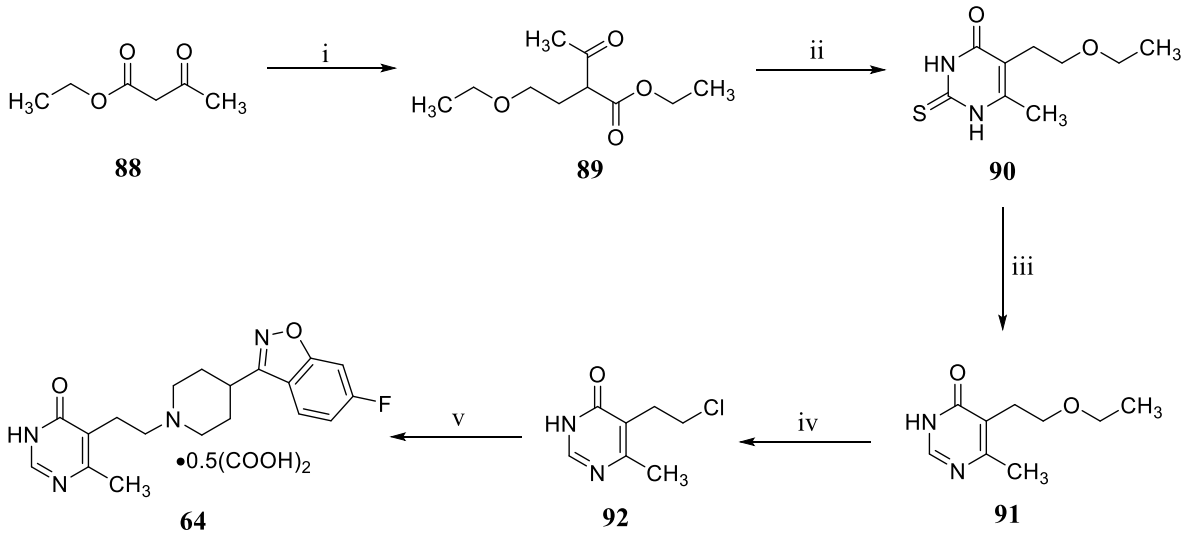

[a]Reagents and conditions. (i) (a) EtONa, EtOH, room temperature, 0.5 h; (b) 2-bromoethyl ether, reflux, 18 h; (ii) thiourea, EtONa, EtOH, reflux, 4 h. (iii) $NiCl_2$, $NaBH_4$, MeOH, room temperature, 0.5 h; (iv) conc. HCl, 150 ºC, 3 h; (v) (a) 6-fluoro-3-(4-piperidinyl)benz[*d*]isoxazole, K_2CO_3, KI, DMF, 134 °C, 18 h; (b) $CHCl_3$, $(COOH)_2/Et_2O$.

Intermediate **89** was synthesized from ethyl acetoacetate (**88**). Intermediate **89** has been reported in the literature,[144] however, the procedure was modified. The literature procedure generates sodium ethoxide in situ from sodium metal and EtOH. For the purpose of this reaction, commercially available sodium ethoxide, available in the laboratory, was used instead. Ethyl acetoacetate (**88**) was allowed to stir with sodium ethoxide for 0.5 h to generate a carbanion, and was followed by the addition of 2-bromoethyl ether to ultimately yield intermediate **89**. Intermediate **89** was cyclized with thiourea to yield intermediate **90**. Intermediate **90** is a known compound;[145] however, here, it was synthesized using a literature procedure for a similar compound[146] so as to avoid the in situ generation of sodim ethoxide. Reductive desulfurization of intermediate **90** yielded the substituted pyrimidone **91.** Intermediate **91** has been reported in the literature,[145] however, the procedure necessitates the use of reagents such as lead acetate, hydrogen

peroxide as well as hydrogen sulfide that are potentially toxic. Hence, a different procedure that has been reported for the synthesis of quinazolin-4(3*H*)-ones and 2,3-dihydro-4(1*H*)-quinazolinones,[147] that are structurally similar to intermediate **91**, was used and resulted in good yields. The reaction uses relatively milder conditions, has higher selectivity, and is relatively cleaner.[147] The reaction involves the slow addition of sodium borohydride to a solution of intermediate **90** and nickel chloride that results in the in situ generation of nickel boride.[147] Nickel boride is responsible for the reductive desulfurization reaction.[147] It has been hypothesized by Khurana and Kukreja,[147] that the reaction mechanism might involve hydrogenolysis of the CH-SH bond that has been obtained from the reduction of the C=S bond, and that there is no formation of colloidal sulfur. The nickel boride needs to be formed in situ since preformed nickel boride loses its activity.[147] However, the reaction could potentially result in a mixture of intermediate **91** and its reduced form **93** (Figure 27) (a second product was noted on TLC but was not isolated), and this was circumvented by optimizing the conditions and using a specific molar ratio of substrate: nickel chloride: sodium borohydride. The use of a 1:3:9 molar ratio of substrate: nickel chloride: sodium borohydride[147] yielded only intermediate **91**, and the time was optimized to 0.5 h. However, the work-up presented a problem due to low solubility of product **91**, in multiple solvents such as dichloromethane, chloroform, and ethyl acetate, and a modified work-up procedure was explored. Intermediate **92** was synthesized according to a literature procedure[145] by heating intermediate **91** in a sealed tube with conc. HCl. The hydrochloride salt of intermediate **92** is known,[145] however, it was extremely hygroscopic and, hence, the free base was synthesized. Analog **64** was synthesized using a Finkelstein reaction. The yields of the reaction were poor (5%)

but most of the unreacted starting material was recovered and could be re-used. Compound **64** was unknown and was characterized by NMR and elemental analysis for C, H and N.

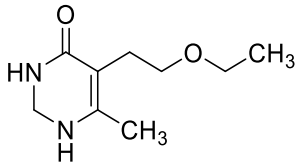

93

Figure 27. Reduced form of intermediate **91**.

Compounds **65** and **66** were synthesized by Dr. Supriya A. Gaitonde, and it might be noted that we, both, were working on similar projects, to a common goal, and the synthesis is illustrated in Scheme 7.[143]

Scheme 7. Synthesis of compounds **65** and **66**.[a]

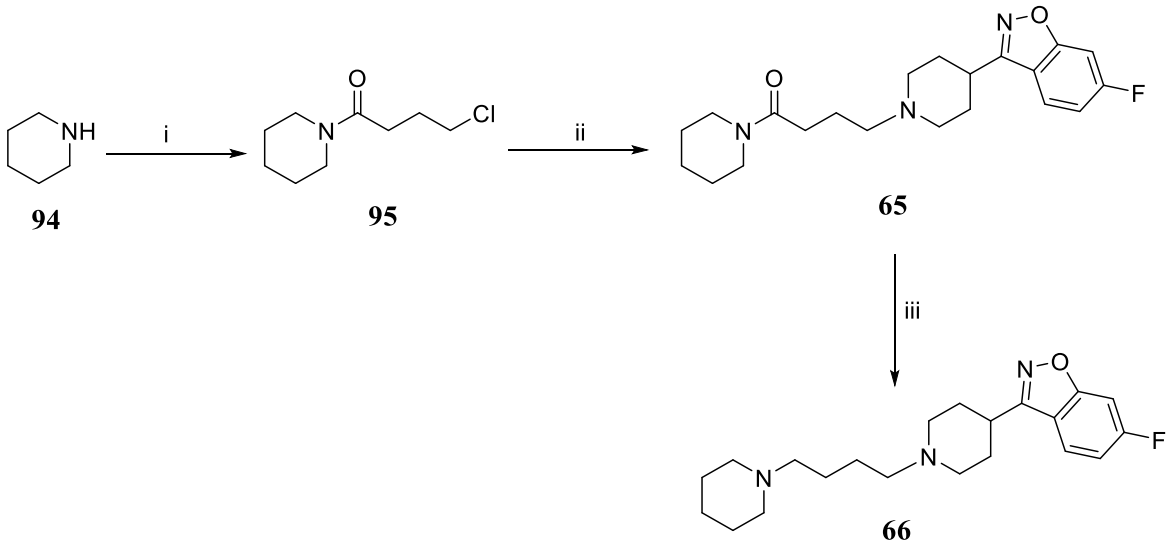

[a]Reagents and conditions. (i) 4-Chlorobutyryl chloride, Et_3N, CH_2Cl_2, room temperature, 75 h; (ii) 6-fluoro-3-(4-piperidinyl)benz[*d*]isoxazole, K_2CO_3, KI, MeCN, 88 ºC, 16 h; (iii) (a) BH_3.THF, reflux, 2 h; (b) 6N HCl, reflux, 1 h.

The synthesis of analogs **67** and **68** is described in Scheme 8. The synthesis of analog **67** and **68** was initially attempted via common intermediate **98**. Intermediate **97** was synthesized using a Grignard reaction. The Grignard reagent was synthesized in situ by reacting freshly distilled cyclohexylbromide with magnesium, and was subsequently reacted with cyclobutanone. Intermediate **97** is known and was synthesized using a literature procedure.[148,149] Intermediate **98** is also known and was synthesized by a literature procedure.[150] Phenyliodine diacetate might be playing a role by forming a complex with intermediate **97**, leading to C-C bond cleavage and the generation of a cation, followed by nucleophilic addition of H_2O.[150] The purpose of the 1,1,1,3,3,3-hexafluoro-2-propanol is to stabilize the cationic intermediate.[150] Intermediate **99** was synthesized by tosylating intermediate **98.** Synthesis of analog **67** was attempted via a nucleophilic substitution reaction, however the reaction led to multiple side-products and analog **67** could not be isolated. The synthesis of analog **67** was abandoned.

The carbonyl group of intermediate **98** was reduced using a Wolff-Kishner reduction to yield intermediate **100**. Intermediate **100** was also synthesized via the reduction of 4-cyclohexylbutanoic acid (**101**) using $LiAlH_4$. Intermediate **100** was known[151] and was synthesized via a procedure for a similar compound.[152] Tosylation of **100** resulted in known intermediate **102**,[151] and, subsequently, analog **68** was synthesized via a nucleophilic substitution reaction between **102** and 6-fluoro-3-(4-piperidinyl)benz[*d*]isoxazole (**61**). Compound **68** was unknown and was characterized by NMR and elemental analysis for C, H and N.

Scheme 8. Synthesis of compounds **67** and **68**.[a]

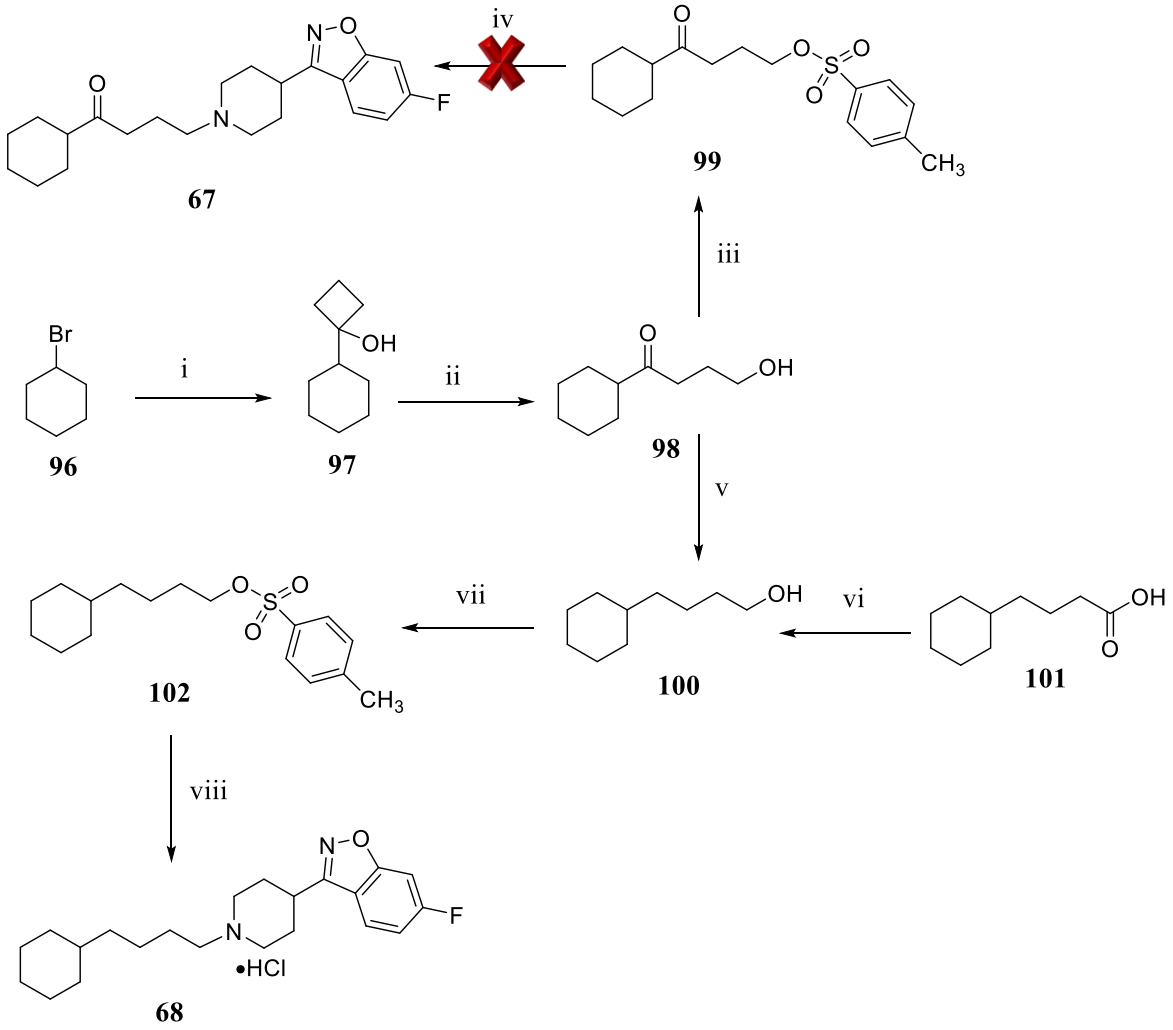

[a]Reagents and conditions: (i) (a) Magnesium turnings, iodine, Et_2O, 40 °C, 2h; (b) cyclobutanone, room temperature, 4 h; (ii) phenyliodine diacetate, 1,1,1,3,3,3-hexafluoro-2-propanol, H_2O, room temperature, 15 min; (iii) tosyl chloride, Et_3N, CH_2Cl_2, room temperature, 48 h; (iv) 6-fluoro-3-(4-piperidinyl)benz[*d*]isoxazole, K_2CO_3, MeCN, 80 ºC, 18 h; (v) (a) Hydrazine hydrate, KOH, diethylene glycol, 135 °C, 2 h; (b) 200 ºC, 6 h; (vi) $LiAlH_4$, THF, room temperature, 6 h; (vii) tosyl chloride, Et_3N, CH_2Cl_2, room temperature, 48 h; (viii) (a) 6-fluoro-3-(4-piperidinyl)benz[*d*]isoxazole , K_2CO_3, MeCN, 80 ºC, 96 h; (b) EtOH, HCl/EtOH.

B. Radioligand binding studies

Radioligand binding studies of the compounds were performed in HEK 293 cells expressing 5-HT_{2A} receptors. [^{3}H]Ketanserin ([^{3}H]**36**) (Figure 17) was used as the radioligand, and non-specific

binding was determined in the presence of methysergide. Competition curves were generated and analyzed by nonlinear regression to determine the binding affinities (K_i values) of the compounds.

The binding affinities of risperidone (**14**) and the compounds **57**, **60**, **61**, **62, 63, 65**, and **66** for 5-HT_{2A} receptors were found to be 5.29 nM (log K_i = -8.27 ± 0.06), 2732 nM (n = 1, performed in duplicate), 12.27 nM (log K_i = -7.91 ± 0.1), 71.41 nM (log K_i = -7.14 ± 0.09), 307.7 nM (n = 1; performed in duplicate), 198.9 nM (n = 1; performed in duplicate), 39.81 (log K_i = -7.40± 0.11), 34.83 nM (log K_i = -7.45 ± 0.12), respectively. The displacement curves for compounds **57**, **62** and **63** are shown in Figure 28.

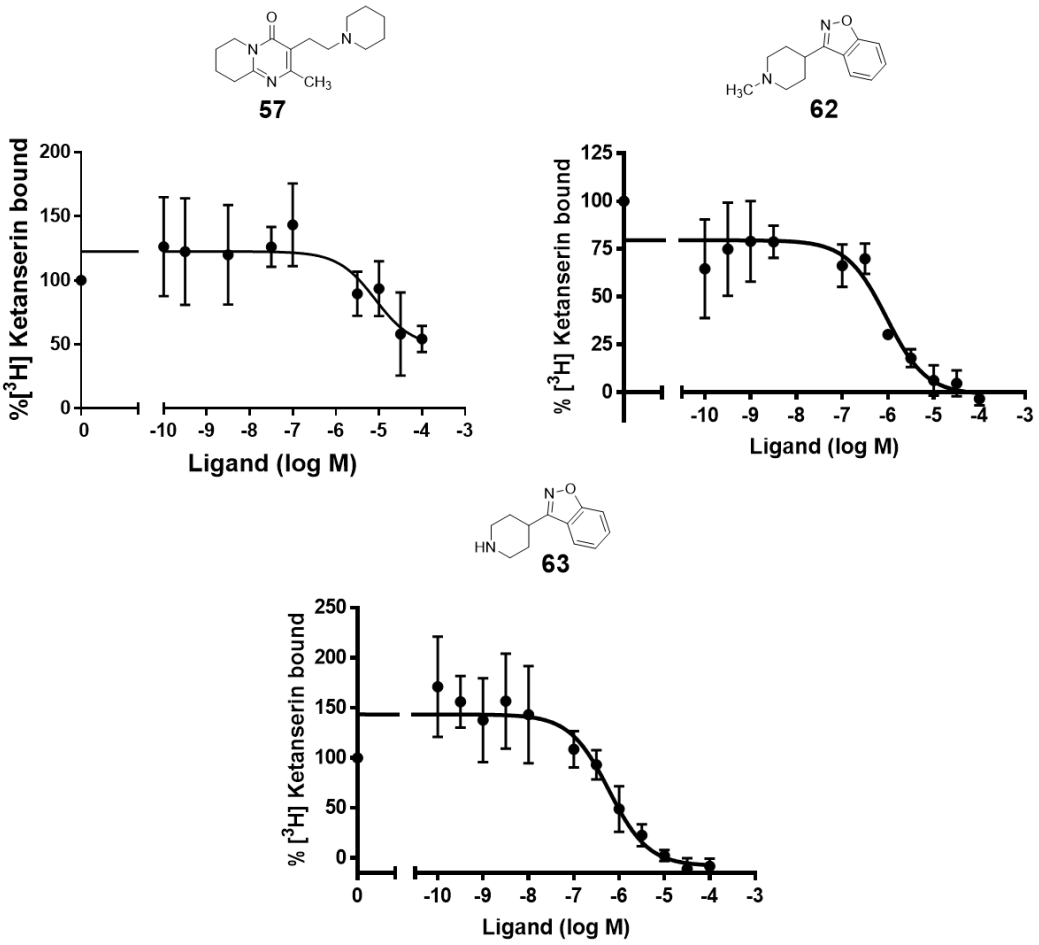

Figure 28. Ketanserin competition binding curves of deconstructed analogs **57**, **62**, and **63** in HEK 293 cell membrane preparations expressing 5-HT_{2A} receptors (*n* = 1, performed in duplicate).

C. Functional activity studies

Functional activity studies of risperidone (**14**), and the deconstructed analogs **60**, **61**, **65**, and **66** were conducted in Dr. Diomedes Logothetis's laboratory and have already been published.[141]

Risperidone (**14**), and compounds **60**, **61**, **65**, and **66**, were initially tested in a two-electrode voltage-clamp (TEVC) electrophysiological assay that utilized a *Xenopus laevis* oocyte heterologous expression system that expresses 5-HT_{2A} receptors and the G protein-gated inwardly

rectifying K^+ channel (GIRK4*) that serves as a sensitive reporter for GPCR activity.[141] However, the ability of the compounds to directly inhibit the GIRK4* channel at higher concentrations (10 µM) for analogs **60**, **61**, and **65** limited their full characterization.[141] Analog **66** inhibited the GIRK4* channel at concentrations as low as 5 µM, and its actions could not be characterized.[141] The assay indicated that analogs **60**, **61** and **65** are 5-HT_{2A} receptor antagonists, however, to fully characterize them, a complementary epifluorescence assay in HEK 293 cells expressing 5-HT_{2A} receptors that utilizes the Fura-2 dye to detect changes in intracellular Ca^{2+} concentrations was used.[141] The IC_{50} values in order of decreasing potency were as follows: risperidone (**14**) (IC_{50} = 5.59 ± 1.41 µM), analog **60** (IC_{50} = 7.40 ± 1.45 µM), analog **65** (IC_{50} = 16.65 ± 1.39 µM), analog **61** (IC_{50} = 20.12 ± 2.24 µM), and analog **66** (IC_{50} 43.88 ± 1.47 µM).[141]

Additionally, analog **61** was able to crosstalk at the 5-HT_{2A}/$mGlu_2$ heteromer (Figure 29), whereas analogs **60**, **65**, and **66** were unable to exert this effect.

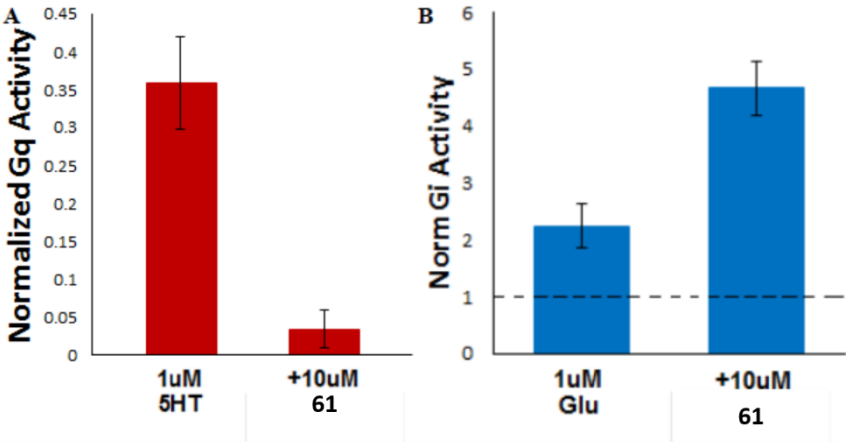

Figure 29. The crosstalk exhibited by analog **61** in the 5-HT_{2A}/$mGlu_2$ heteromeric receptor system (figure provided by Jason Younkin).

3. Discussion

Deconstruction studies of risperidone (**14**) suggest that the entire structure of risperidone (**14**) is not needed for 5-HT_{2A} receptor affinity or antagonist activity. Analog **60**, that bears only half the structural features of risperidone (**14**), binds with only ~2-fold lower affinity than risperidone (**14**) and is nearly equipotent as a 5-HT_{2A} receptor antagonist as compared to risperidone (**14**). Additionally, the other structurally abbreviated analogs (**61**, **62**, **63**, **65**, and **66**) of risperidone (**14**), bind with nanomolar affinity and retain 5-HT_{2A} receptor antagonist activity.

Analog **61**, the desmethyl analog of **60**, binds with ~6-fold lower affinity at 5-HT_{2A} receptors than analog **60**, suggesting that the methyl group makes additional interactions at the receptor.

Analogs **62** and **63** represent desfluoro analogs of **60** and **61**, respectively. Preliminary data suggest that analogs **62** and **63** bind with ~24- and ~3-fold lower affinity than analogs **60** and **61**, indicating additional interactions by the fluoro group at the receptor. Analog **63** binds with similar affinity as analog **62**, suggesting that the methyl group might not be making favorable interactions at the receptor, and that analogs **60** and **61** might be binding differently as compared to analogs **62** and **63**. However, additional replications are required to confirm the present results.

Analog **66** is the descarbonyl analog of **65**. Both bind with comparable affinities at 5-HT_{2A} receptors, suggesting that the carbonyl group may not be an important structural requirement for binding affinity. However, the descarbonyl analog is ~2.5-fold less potent as a 5-HT_{2A} receptor antagonist as compared to analog **65**, suggesting that the carbonyl group might be contributing.

Even though this difference is very small it is statistically significant. (Unpaired t test; P- value = 0.0027; $\alpha = 0.05$).

The "right half" of risperidone (**14**) seems be important for high binding affinity, since the "right half" of risperidone (**14**) i.e. analog **61** binds with ~13-fold lower affinity than risperidone (**14**), whereas, the "left half" of risperidone (**14**) i.e. analog **57** binds with ~500-fold lower affinity than risperidone (**14**). These and other studies previously conducted in our laboratory on analog **61**,[140] suggest that the "right-half" portion of risperidone (**14**) is more important than the "left-half" portion of risperidone (**14**). However, the "left-half" portion of risperidone (**14**) seems to contribute to binding.

B. Specific Aim 2: Elaboration of risperidone to investigate the role of the two halves of risperidone in its 5-HT$_{2A}$ receptor antagonist activity

1. Approach

Elaboration is a part of the "deconstruction-reconstruction-elaboration" approach that is commonly used to study SAR.[137] It involves modifying certain structural features one at a time. In this study, elaboration was used to investigate the roles of the "right" (i.e., the 6-fluoro-3-(4-piperidinyl)-1,2-benz[*d*]isoxazole portion) and "left" (i.e., the 2-methyl-6,7,8,9-tetrahydro-4*H*-pyrido[1,2-*a*]pyrimidin-4-one portion) halves of risperidone in their contribution to its 5-HT$_{2A}$ receptor affinity and/or antagonist activity.

a. Investigation of the potential role of the two halves of risperidone in its activity by examination of structural hybrids of risperidone and ketanserin

Ketanserin (**36**) (Figure 30) is a prototypical, and the first identified, 5-HT$_{2A}$ receptor antagonist that has high affinity for 5-HT$_{2A}$ receptors (K_i = 19 nM). The structure of ketanserin (**36**) (Figure 30) can be divided into two halves in a manner analogous to that of risperidone (**14**) (Figure 30; see also, Figure 25), consisting of the 4-(4-fluorobenzoyl)piperidine ring system (right half) and the 2,4-(1*H*,3*H*)-quinazolinedione ring ("left half") connected by an ethyl linker.

The structures of ketanserin (**36**) and risperidone (**14**) possess some structural similarities as well as some structural differences. In fact, the "right halves" of ketanserin (**36**), [4-(4-fluorobenzoyl)piperidine], and risperidone (**14**), [6-fluoro-3-(4-piperidinyl)-1,2-benz[d]isoxazole, are considered as being bioisosteres.[153] Previous studies by our laboratory have shown that the

right halves of ketanserin (**36**), analogs **72** and **73** (K_i = 125 nM and 430 nM, respectively) bind to 5-HT_{2A} receptors with ~35- and ~123-fold lower affinity than ketanserin (**36**) (K_i = 3.5 nM) (Figure 25).[138] Deconstructed analogs **60** and **61** (K_i = 12.27 and 71.41 nM) bind with only 2- and 13-fold lower affinity than risperidone (**14**) (K_i = 5.29 nM) while retaining 5-HT_{2A} receptor antagonist action,[141] suggesting that the right half of risperidone (**14**) might contribute to binding affinity to a greater degree as compared to the right half of ketanserin (**36**).

As a part of this study, two structural hybrids of risperidone (**14**) and ketanserin (**36**), Ris/Ket (**103**) and Ket/Ris (**104**) (Figure 30), were synthesized to study the contribution of the "left" and "right" halves of risperidone (**14**), and to determine if risperidone (**14**) and ketanserin (**36**) bind in a similar manner. Analog **104** was synthesized by Dr. Supriya A. Gaitonde of our laboratory, but its synthetic details are provided here.[143]

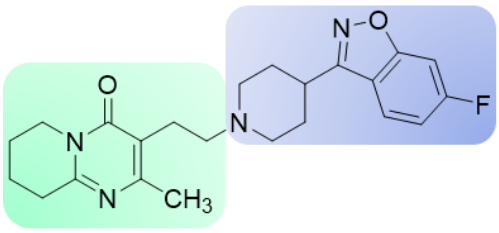

Risperidone (**14**)

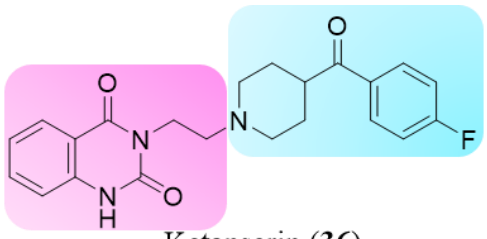

Ketanserin (**36**)

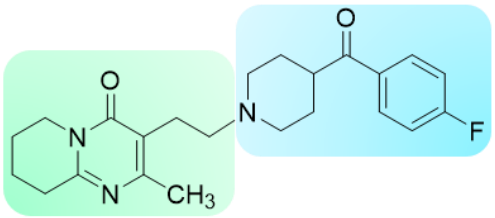

Ris/Ket (**103**)

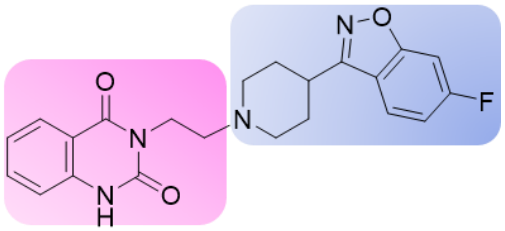

Ket/Ris (**104**)

Figure 30. Compounds **103** and **104** represent structural hybrids of risperidone (**14**) and ketanserin (**36**). Compound **103** has been termed Ris/Ket, and **104** has been termed Ket/Ris.

Hypothesis

*If the right half of risperidone (**14**) is important for binding affinity and functional activity, Ket/Ris (***104***) will have a higher binding affinity and/or activity than Ris/Ket (**103**), and vice versa.*

If ketanserin (**36**) *and risperidone* (**14**) *bind in a common manner, hybrid ligands bearing features of both should bind with high affinity.*

In hybrid molecule **103**, the "right half" of risperidone (**14**) was replaced with the "right half" of ketanserin (**36**), whereas in hybrid molecule **104,** the "left half" of risperidone (**14**) was replaced by the "left half" of ketanserin (**36**). If Ris/Ket (**103**) retains high 5-HT_{2A} receptor affinity, it might indicate that the "right half" of risperidone (**14**) is not important or that the "left half" is important for binding affinity. Conversely, if Ket/Ris (**104**) retains high affinity for 5-HT_{2A} receptors, it might indicate that either the "left half" of risperidone (**14**) is not crucial or that the "right half" of risperidone (**14**) is important for 5-HT_{2A} receptor antagonism and binding affinity. If both the hybrids bind with equally high affinity it might suggest that risperidone (**14**) and ketanserin (**36**) bind in a similar manner.

b. Investigation of the potential role of the "right half" (i.e., the 6-fluoro-3-(4-piperidinyl)-1,2-benz[*d*]isoxazole portion) of risperidone in its binding by making the "right half" of risperidone similar to serotonin

The "right half" of risperidone (**14**) was substituted with moieties found in agonists [i.e.; the tryptamine portion of 5-HT (**6**)] such as compounds **105-108** (Figure 31) to give compounds **109-**

112 (Figure 31), respectively. Compounds **105**, and **107** are known to bind to 5-HT_{2A} receptors and are partial agonists.[154] Binding affinities were measured in COS-1 cells expressing 5-HT_{2A} receptors using [^{3}H]ketanserin as the radioligand.[154] Analogs **105**, and **107** bind with affinities of 960 nM and 509 nM, respectively.[154] Functional activities of analogs **105** (EC_{50} = 2647 nM, E_{max} = 0.43) and **107** (EC_{50} = 1736 nM, E_{max} = 0.12) were determined in HEK 293 cells that stably express 5-HT_{2A} receptors in an assay that measures accumulation of [^{3}H] inositol phosphates.[154] Compound **106** is 5-HT_{2A} receptor agonist in an in vitro calcium mobilization assay in HEK 293 cells that over-express 5-HT_{2A} receptors. (EC_{50} = 4.56; E_{max} = 101).[155]

Hypothesis

*If the right half of risperidone (**14**), and the tryptamine portion of 5-HT (**6**) bind in a similar manner then analogs bearing the tryptamine portion of 5-HT should bind.*

If analogs **109-112** retain high binding affinity, it will indicate that the indole ring binds in a manner similar to the benz[*d*]isoxazole ring of risperidone (**14**). If compounds **109-112** retain antagonist activity, it will be in accordance with the Ariens hypothesis of conversion of agonists to antagonists by addition of bulky substituents on amines. Lack of antagonist activity would indicate that the "left half" of risperidone (**14**) might not be contributing or that the "right half" of risperidone (**14**) is important for 5-HT_{2A} receptor antagonist activity. Additionally, **109** and **110** are secondary amines, whereas **111** and **112** retain the tertiary amine nature of risperidone (**14**), and will help ascertain the importance of the nature of the amine. Also, analogs **109** and **111** lack

the fluoro group and comparing them to analogs **110** and **112** will help investigate the role of the fluoro group.

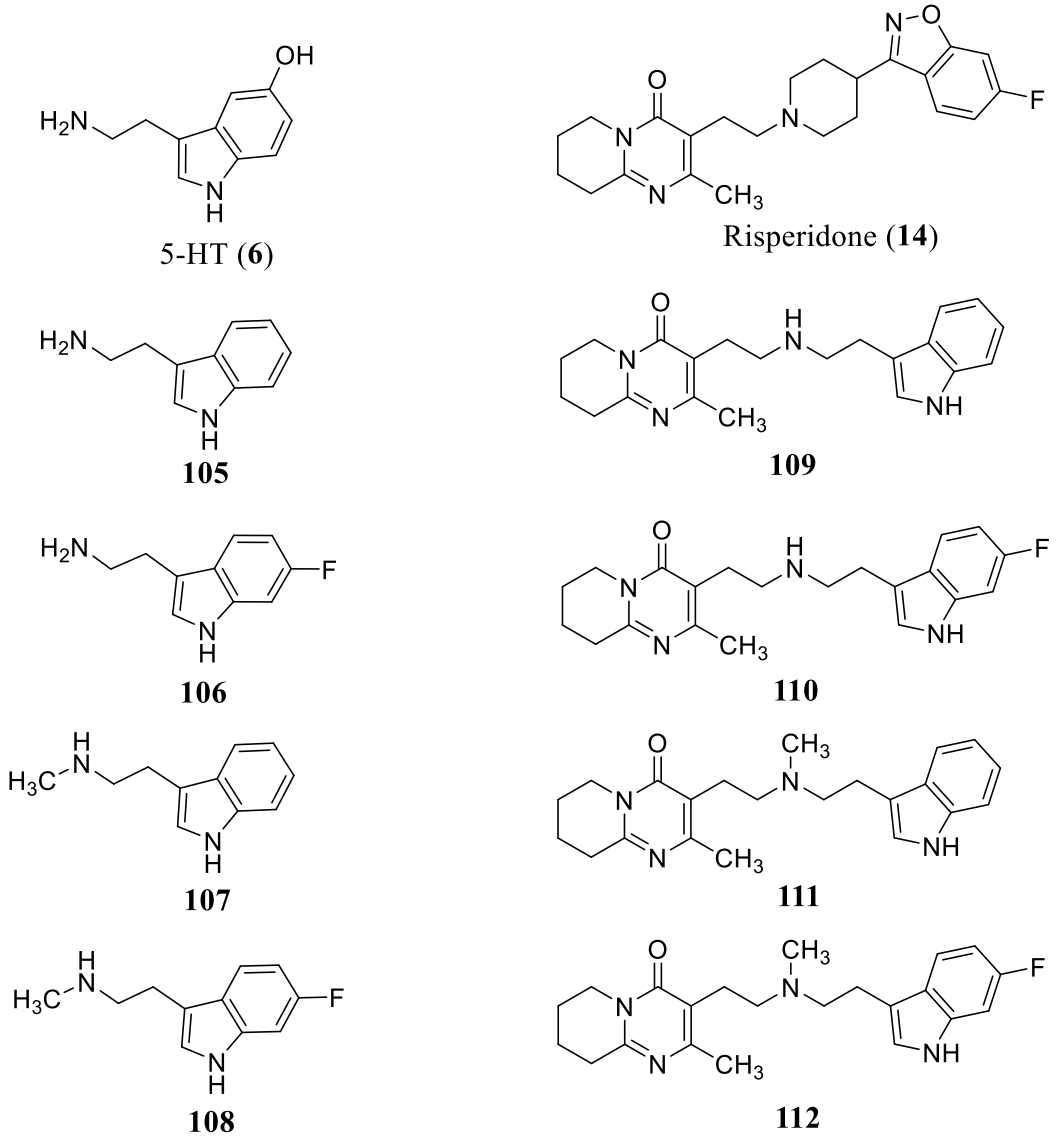

Figure 31. Elaboration of risperidone (**14**) by substituting the "right half" of risperidone with tryptamines.

c. Aromatization of the "left half" (i.e., the 2-methyl-6,7,8,9-tetrahydro-4*H*-pyrido[1,2-*a*]pyrimidin-4-one portion) of risperidone

Several different, but relatively similar, pharmacophores for 5-HT_{2A} receptor antagonists exist, and they all imply that multiple binding modes might exist for these antagonists.[156–159] The pharmacophore consists of a basic amine and two hydrophobic/aromatic portions.[156–159] The distances of the hydrophobic moieties from each other and from the basic amine vary among the different pharmacophores[156–159] (discussed in detail in specific aim 5). These pharmacophores suggest that aromatization of the left-hand portion of risperidone (**14**) should result in enhanced binding affinity. Hence, we prepared analog **113** (Fgure 32), wherein the "left half" of risperidone (**14**) (Fgure 32) was aromatized.

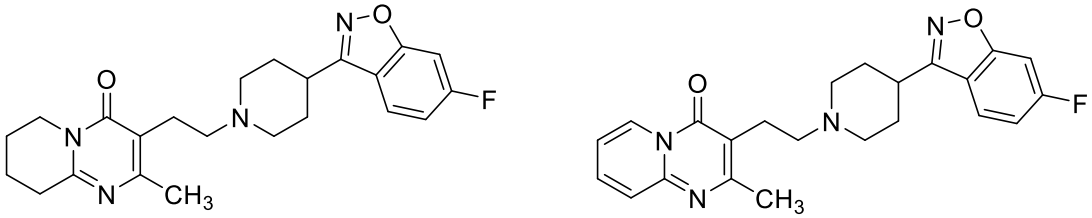

Risperidone (**14**) **113**

Figure 32. Aromatization of the "left half" of risperidone (**14**).

d. Investigation of the role of the "left half" (i.e., the 2-methyl-6,7,8,9-tetrahydro-4*H*-pyrido[1,2-*a*]pyrimidin-4-one portion) of risperidone by making the "left half" of risperidone similar to other antipsychotic agents such as iloperidone

Iloperidone (**24**) (Figure 33) is an atypical antipsychotic agent that has high affinity for 5-HT_{2A} receptors (K_i = 5.6 nM).[160,161] Risperidone (**14**) and iloperidone (**24**) both have the same "right half" consisting of the 6-fluoro-3-(4-piperidinyl)-1,2-benz[*d*]isoxazole moiety. We synthesized analogs **114** and **115** (Figure 33), wherein the "left half" of risperidone was made similar to the left half of iloperidone (**24**). Also, our laboratory has previously shown that deconstructed analogs **76** and **77** (Figure 33) of ketanserin (**36**) that have the same "left half" as that of analogs **114** and **115** respectively, retained 5-HT_{2A} receptor antagonist activity and bind with only ~2 fold lower affinity than ketanserin (**36**).[138] Since the 4-(4-fluorobenzoyl)piperidine moiety present in analogs **76** and **77** and the 6-fluoro-3-(4-piperidinyl)-1,2-benz[*d*]isoxazole moiety present in analogs **114** and **115** are bioisosteric,[153] we might expect analogs **114** and **115** to bind with at least equally high affinity.

In analogs **116** and **117** (Figure 33) we extended the chain connecting the phenyl ring and the piperidinyl nitrogen by one carbon atom to investigate the influence of chain length on 5-HT_{2A} receptor binding affinity and activity.

If analogs **114-117** retain high affinity for 5-HT_{2A} receptors and 5-HT_{2A} receptor antagonism, it might indicate that either the entire "left half" of risperidone (**14**) is not crucial for activity and affinity or that the "right half" of risperidone (**14**) is important for 5-HT_{2A} receptor activity and affinity.

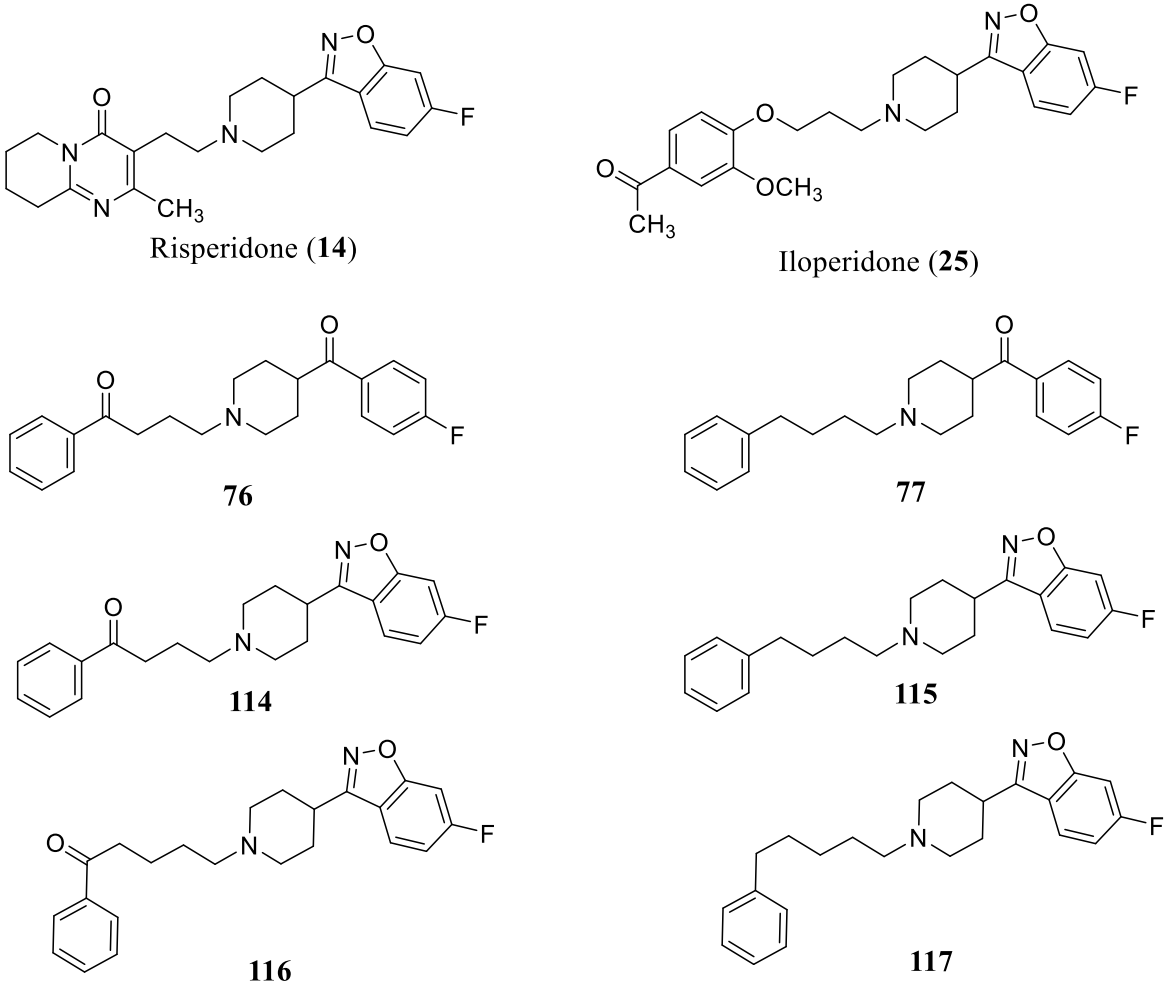

Figure 33. Elaboration of risperidone (**14**) by making the "left half" of risperidone similar to iloperidone (**25**).

2. Results

A Chemistry

a. Investigation of the potential role of the two halves of risperidone in its activity by examination of structural hybrids of risperidone and ketanserin

Hybrid molecule **103** was synthesized using a Finkelstein alkylation reaction between the primary alkyl chloride **78** and 4-(4-fluorobenzoyl)piperidine. The synthesis is outlined in Scheme 9. The reaction was carried out in the presence of KI as a catalyst and 2 equivalents of K_2CO_3 (since the hydrochloride salt of 4-(4-fluorobenzoyl)piperidine was used) in MeCN as the solvent. Analog **103** was unknown and was characterized by NMR and elemental analysis for C, H, and N atoms.

Scheme 9. Synthesis of compound **103**.[a]

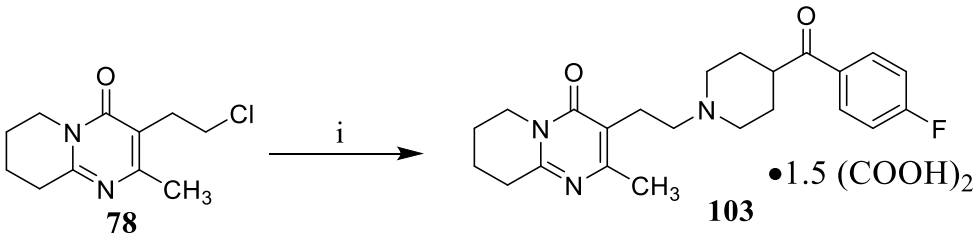

[a]Reagents and conditions. (i) (a) 4-(4-fluorobenzoyl)piperidine hydrochloride, K_2CO_3, KI, MeCN, reflux 24 h; (b) $CHCl_3$, $(COOH)_2/Et_2O$.

Hybrid molecule **104** was synthesized by Dr. Supriya A. Gaitonde and its synthesis is outlined in Scheme 10.[143]

Scheme 10. Synthesis of compound **104**.[a]

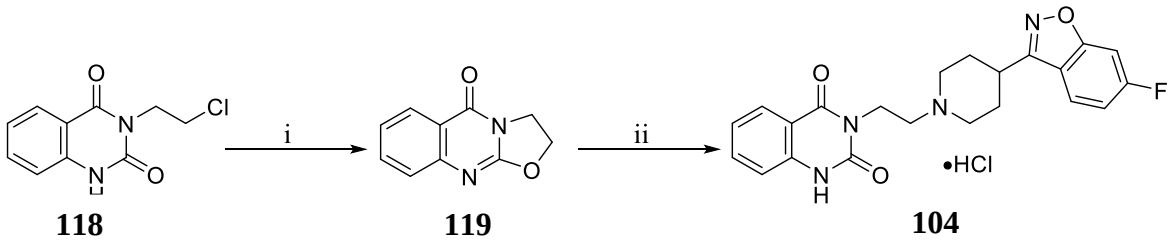

[a]Reagents and conditions. (i) K_2CO_3, acetone, reflux, 2 h; (ii) (a) 6-fluoro-3-(4-piperidinyl)-1,2-benz[*d*]isoxazole, toluene, sealed tube, 100 °C, 44 h (b) 12 N HCl.

b. Investigation of the potential role of the "right half "(i.e., the 6-fluoro-3-(4-piperidinyl)-1,2-benz[*d*]isoxazole portion) of risperidone in its activity by making the "right half" of risperidone similar to serotonin

Compound **106** was successfully synthesized after attempting several synthetic routes. The synthesis of compound **106** is illustrated in Scheme 11. The first synthetic route attempted to synthesize 6-fluorotryptamine (**106**) was the Speeter-Anthony synthesis of tryptamines.[162] The method involves reacting an indole with oxalyl chloride to yield the corresponding 3-indoleglyoxyl chloride, that is subsequently converted to the corresponding glyoxylamide. Reduction of the gyloxylamide should yield the corresponding tryptamine.[162] Glyoxyl chloride intermediate **121** is known, and a literature procedure was followed for its synthesis.[163] Intermediate **121** was synthesized from 6-fluoroindole (**120**) by treating it with with oxalyl chloride, and was subsequently reacted with ammonium hydroxide to afford the glyoxylamide **122**. However, the product could not be isolated. Hence the synthetic route was changed. Intermediate **122** is unknown and a literature procedure that has been reported for the synthesis of 3-indolylglyoxylamide was used instead.[164] The alternative synthetic route utilized a modified Henry reaction, and involved reacting 6-fluoroindole (**120**) with 1-dimethylamino-2-nitroethylene in the

presence of trifluoroacetic acid to yield intermediate **123**. The reduction of intermediate **123** should yield compound **106**. Intermediate **123** is known[165,166] and was synthesized using a procedure for the same compound.[165] The reduction of intermediate **123** was initially attempted using $NaBH_4$ and boron trifluoride etherate as the reducing agent (using a procedure for a similar compound[167]), however, product **106** was difficult to isolate.

Hence, a similar model reaction was tried using indole (**124**), to synthesize tryptamine (**105**), and is outlined in Scheme 12. Indole (**124**) was treated with 1-dimethylamino-2-nitroethylene in the presence of trifluoroacetic acid to yield intermediate **125**, that was subsequently reduced using two different reducing agents- one with $NaBH_4$, boron trifluoride etherate complex (yield: 40%) using a procedure for a similar compound,[167] and another method utilizing $LiAlH_4$ (yield: 80%) using a procedure for the same compound.[168]

Compound **105**[168] is known and was characterized by melting point. Both these methods yielded tryptamine (**105**), however the yields with $LiAlH_4$ as a reducing agent were much better.

Based on the model reaction for the synthesis of tryptamine (**105**), $LiAlH_4$ was chosen as the reagent of the choice for the reduction of intermediate **123** to 6-fluorotryptamine (**106**). For the synthesis of tryptamine (**105**), 20 equivalents of $LiAlH_4$ were used. However, the number of equivalents of $LiAlH_4$ that could be used for the synthesis of compound **106** was limited by the fact that it could potentially defluorinate the compound. Several different reaction conditions were evaluated (Scheme 11 v-viii). A literature procedure for the same compound was used for the

reduction, wherein 6 equivalents of $LiAlH_4$ were used, and the reaction was carried out in THF at room temperature for 36 h (Scheme 11 v).[166] However, the reaction yielded multiple products and **106** could not be isolated. We next utilized conditions reported in a patent,[165] wherein 5 equivalents of $LiAlH_4$ were used and the reaction was carried out in THF at 60 ºC for 1 h. (Scheme 11 vi). The reaction was relatively cleaner and purification using Kugelrohr distillation was attempted, a hydrochloride salt was made. However, the yield was low and the salt was hygroscopic. The reaction was next carried out using the same conditions (Scheme 11 vii), however the work-up procedure was modified. A short column using $CHCl_3$, MeOH and NH_4OH (90:10:1) as eluents, was used to separate **106** from the side products and an oxalate salt was made. The yield was low and hence the reaction conditions were further optimized. We altered the solvent used for the reaction and used a mixture of THF and Et_2O, as opposed to only using THF, keeping all the other reaction conditions constant (Scheme 11 viii). The reaction was much cleaner, and the oxalate salt was made. The oxalate salt was purified by reflux in MeCN for 0.5 h to remove impurities, and was subsequently recrystallized from acetone/H_2O to yield compound **106**. The oxalate salt of compound **106** was unknown, and was characterized by NMR and elemental analysis for C, H, and N atoms.

Scheme 11. Synthesis of compound **106**.[a]

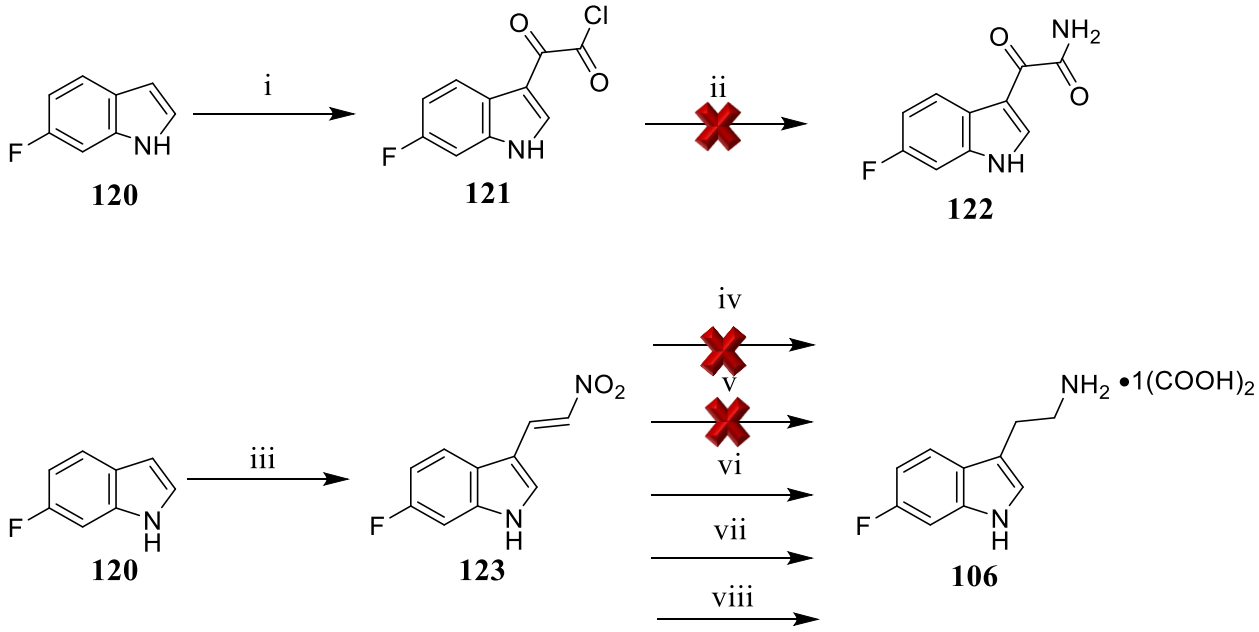

[a]Reagents and conditions. (i) Oxalyl chloride, Et_2O, room temperature, 3.5 h; (ii) NH_4OH, THF, room temperature, 48 h; (iii) 1-dimethylamino-2-nitroethylene, trifluoroacetic acid, room temperature, 1 h; (iv) (a) $NaBH_4$, $BF_3{\cdot}Et_2O$, THF, reflux 2 h; (b) 1N HCl, 85 ºC, 2h; (c) Et_2O, HCl/Et_2O; (v) $LiAlH_4$ (6 equivalents), THF, room temperature, 36 h; (vi) (a) $LiAlH_4$ (5 equivalents), THF, 60 ºC, 1 h; (b) Et_2O, HCl/Et_2O; (vii) (a) $LiAlH_4$ (5 equivalents), THF, 60 ºC , 1 h; (b) Et_2O, $(COOH)_2/Et_2O$ (viii) (a) $LiAlH_4$ (5 equivalents), THF, Et_2O, 60 ºC, 1 h; (b) Et_2O, $(COOH)_2/Et_2O$.

Scheme 12. Synthesis of compound **105**.[a]

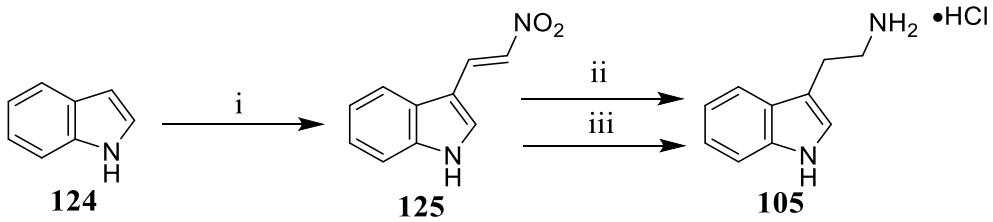

[a]Reagents and conditions. (i) 1-dimethylamino-2-nitroethylene, trifluoroacetic acid, room temperature, 1 h; (ii) (a) $NaBH_4$, $BF_3{\bullet}Et_2O$, THF, reflux 2 h; (b) 1N HCl, 85 ºC, 2h; (c) Et_2O, HCl/Et_2O; (iii) (a) $LiAlH_4$ (20 equivalents), THF, Et_2O, reflux; (1) 3 h, reflux; (2) 12 h, room temperature; (b) Et_2O, HCl/Et_2O.

The synthesis of compound **108** is illustrated in Scheme 13. The initial synthetic route attempted was the Speeter-Anthony synthesis of tryptamines.[162] 6-Fluoroindole (**120**) was converted to the gyloxyl chloride intermediate **121** as previously described,[163] and was followed by conversion to the corresponding glyoxylamide **126**. Reduction of intermediate **126** was attempted using $LiAlH_4$. Intermediate **126** is unknown, and a procedure for a similar compound was followed.[163] However, the reaction for the reduction was not clean and multiple products were formed that were difficult to isolate.

A model reaction was attempted to synthesize *N*-methyltryptamine (**107**), and the synthesis is outlined in Scheme 14. Indole (**124**) was allowed to react in a similar manner to yield the corresponding glyoxylamide **129** via the gyloxyl chloride intermediate **128**. Intermediate **128** has been reported in the literature and was synthesized using the same procedure.[169] Intemediate **129** is known[170] and was synthesized using a general procedure. The reaction for the reduction of the glyoxylamide intermediate **129** to the tryptamine was cleaner,[163] and we observed that rather than getting the tryptamine (**107)** we obtained a side product that was characterized by melting point and found to be **130**,[171] and hence utilized a different synthetic route. The reaction of **105** with ethyl chloroformate yielded intermediate **131** that was subsequently converted to the tryptamine **107** by $LiAlH_4$. Intermediates **131**,[172] and compound **107**,[172,173] have been reported in the literature and were synthesized using the procedures reported by Ignatenko et al.[172] Analog **107** is known and was characterized by melting point and NMR. Tryptamine **108** was synthesized in an analogous manner from tryptamine **106** (synthesized as previously described), and the synthesis is illustrated in Scheme 13 (v-viii). Compound **108** was unknown and was synthesized from **106**

using the procedures for the synthesis of **107** that have been reported in the literature by Ignatenko et al.[172] Compound **108** was characterized by NMR and elemental analysis for C, H, and N atoms.

Scheme 13. Synthesis of compound **108**.[a]

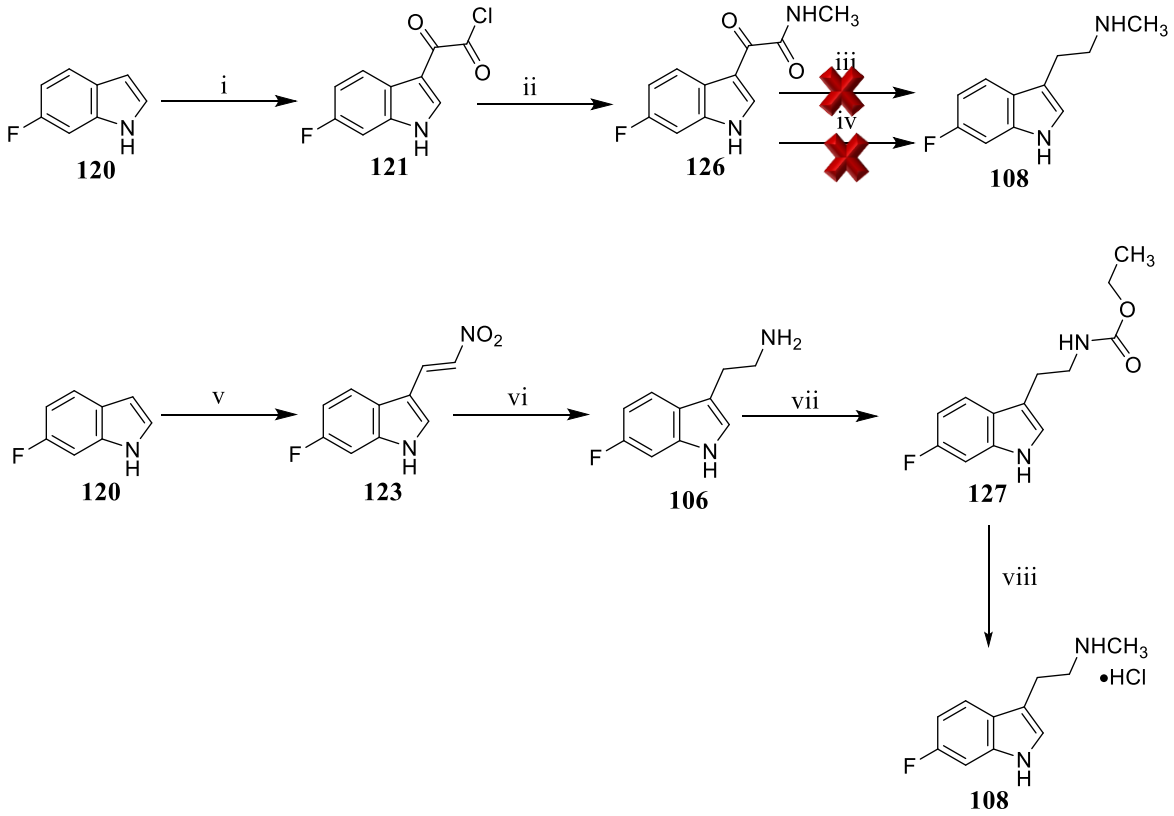

[a]Reagents and conditions. (i) Oxalyl chloride, Et_2O, room temperature, 3.5 h; (ii) methylamine in water (40%), THF, room temperature, 48 h; (iii) $LiAlH_4$ (5 equivalents), THF, reflux, 8 h; (iv) $LiAlH_4$ (1.2 equivalents), THF, reflux, 20 h (v) 1-dimethylamino-2-nitroethylene, trifluoroacetic acid, room temperature, 2 h; (vi) $LiAlH_4$ (5 equivalents), THF, Et_2O, 60 ˚C, 1 h; (vii) ethyl chloroformate, Et_3N, CH_2Cl_2, room temperature, 3 h. (viii) (a) $LiAlH_4$ (3 equivalents), THF, reflux, 1.5 h; (b) Et_2O, HCl/Et_2O.

Scheme 14. Synthesis of compound **107**.[a]

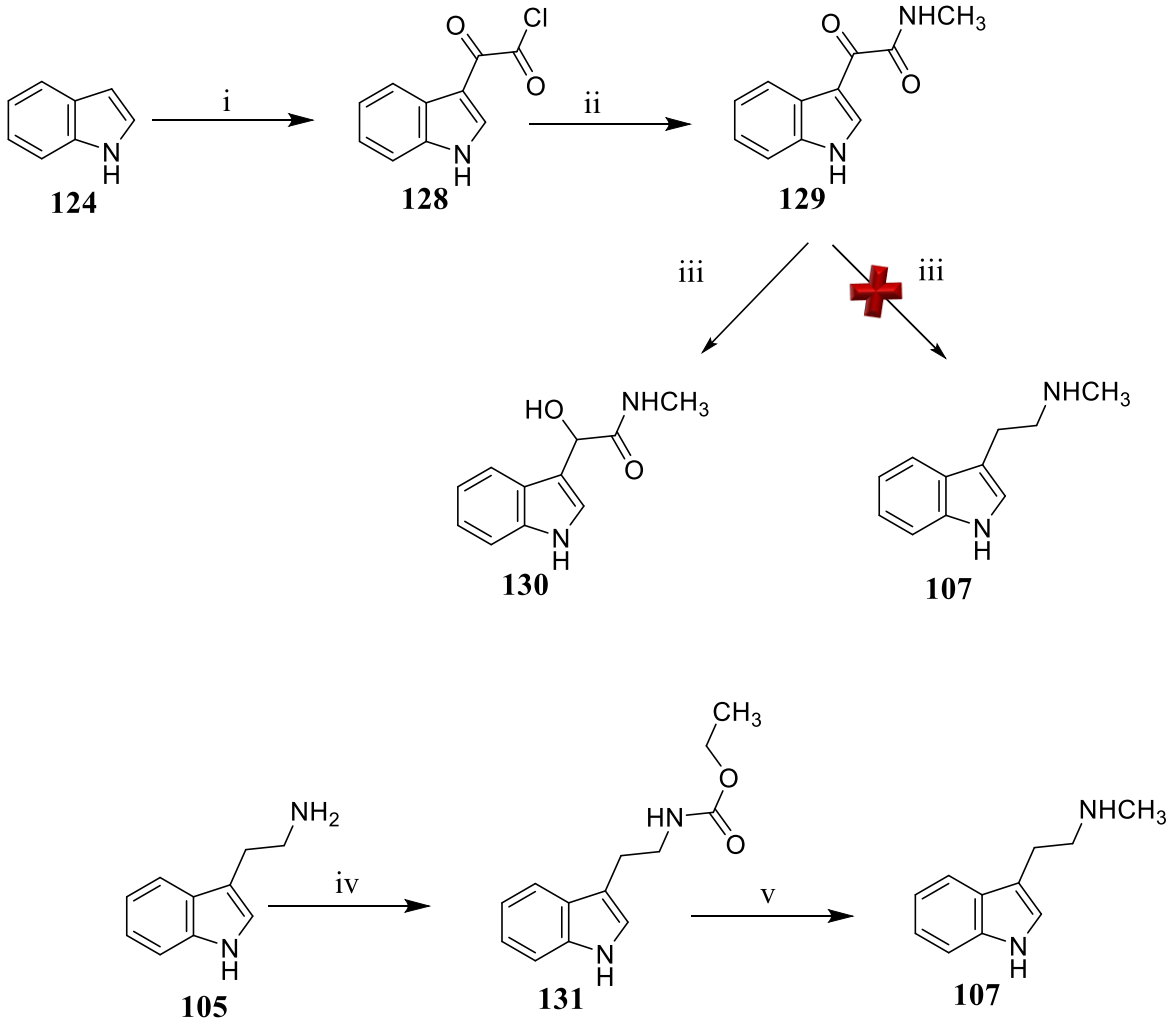

[a]Reagents and conditions. (i) Oxalyl chloride, Et_2O;(a) 0 ºC, 3 h; (b) room temperature, 1 h; (ii) methylamine in water (40%), THF, room temperature, 24 h; (iii) $LiAlH_4$ (5 equivalents), THF, reflux, 8 h; (iv) ethyl chloroformate, Et_3N, CH_2Cl_2, room temperature, 3 h; (v) (a) $LiAlH_4$ (3 equivalents), THF, reflux, 1.5 h.

Compound **109** was synthesized after modifying several reaction conditions (Schemes 15 a-d), and the synthesis is outlined in Scheme 15 c xiii. The synthesis of **109** was initially attempted using a Finkelstein alkylation reaction, wherein an attempt was made to alkylate **105** with the primary alkyl chloride **78,** in the presence of KI as a catalyst and K_2CO_3 as the base in DMF as the solvent.

The reaction mixture was heated at 80 ºC for 48 h. DMF was used as the solvent as opposed to MeCN, since **105** had limited solubilty in MeCN at room temperature. The reaction was not clean and it was impossible to isolate the product. We next used MeCN as the solvent. The tryptamine was solubilized by heating. Keeping the other conditions constant we gradually increased the temperature from room temperature (5 h- no reaction) to 60 ºC (18 h- no change), to finally 85 ºC for 48 h. A mixture of products was obtained that could not be characterized. We next carried out the reaction in a sealed tube at 80 ºC for 5 days using MeCN as the solvent. The reaction was cleaner with one spot being more prominent than the others on TLC, however, the desired product could not be separated. Keeping the other conditions constant we varied the solvent (toluene), to study whether the solvent was playing any role, and subsequently changed the base to Et_3N instead of K_2CO_3 to evaluate if the base was negatively affecting the reaction. However, both attempts were fruitless. Further, to reduce the reaction time, the solvent MeCN was reduced to $1/3^{rd}$ while keeping all the other reaction conditions constant (KI, K_2CO_3). The reaction gave multiple spots, however, there was one prominent spot that could be separated from the others by column chromatography. Characterization by NMR and mass spectrometry suggested that the product could be **132** (Figure 34), which indicates that the primary alkyl chloride **78** initially reacts with **105** to yield product **109** that undergoes further *N*-alkylation to potentially yield **132**. This was quite unexpected because we would not have expected an amine having a bulky substituent to react a second time. However, it is not unlikely since the secondary amine **109** would be more basic than the primary amine **105.** The formation of **132** could be prevented in multiple ways (i) by increasing the dilution, so as to keep the reactants apart; (ii) by eliminating KI; (iii) by increasing

the equivalents of tryptamine (**105**) (not very feasible since the starting material had to be synthesized); and/or (iv) protecting the amine of the tryptamine.

We first tried to dilute the reaction mixture (Scheme 15 b) and modified the amount of solvent keeping all other conditions constant, However, we still observed the formation of the side product **132.** We simultaneously also evaluated reaction conditions wherein we increased the equivalents of tryptamine **(105)** from 1 equivalent to 2 equivalents, and utilized K_2CO_3 as the base, KI as the catalyst, in MeCN (dilution: 1X) (Scheme 15 c). However, we still observed the side product **132.** We next increased the dilution factor to 2X, and utilized 2 equivalents of **105**, keeping all other conditions constant, and at the same time also tried to evaluate a different synthetic route (Scheme 15 d). The alternate synthetic route involved protecting the amine terminal using an *N*-benzyl group and was achieved by a reductive amination reaction. The reaction of the protected tryptamine **133** yielded unknown intermediate **134** that was characterized by NMR, however, it was extremely hygroscopic and the HCl salt seemed to degrade.

We seemed to have reduced the amount of side product that was being formed when the conditions as outlined in scheme 15 c were used. Hence, to further optimize the reaction conditions we eliminated KI. These conditions seemed to yield relatively lower amounts of the side product **132**, and we were able to isolate and purify **109** by column chromatography and recrystallization techniques. Compound **109** was unknown and was characterized by NMR and elemental analysis for C, H and N atoms.

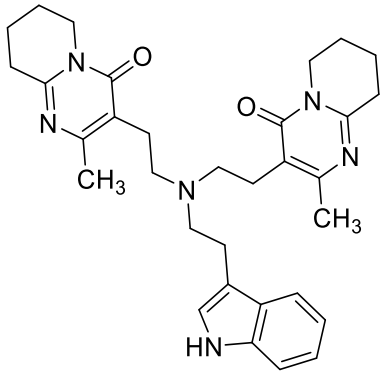

132

Figure 34. A side product of the Finkelstein alkylation reaction.

Scheme 15 a. Synthesis of compound **109**.[a]

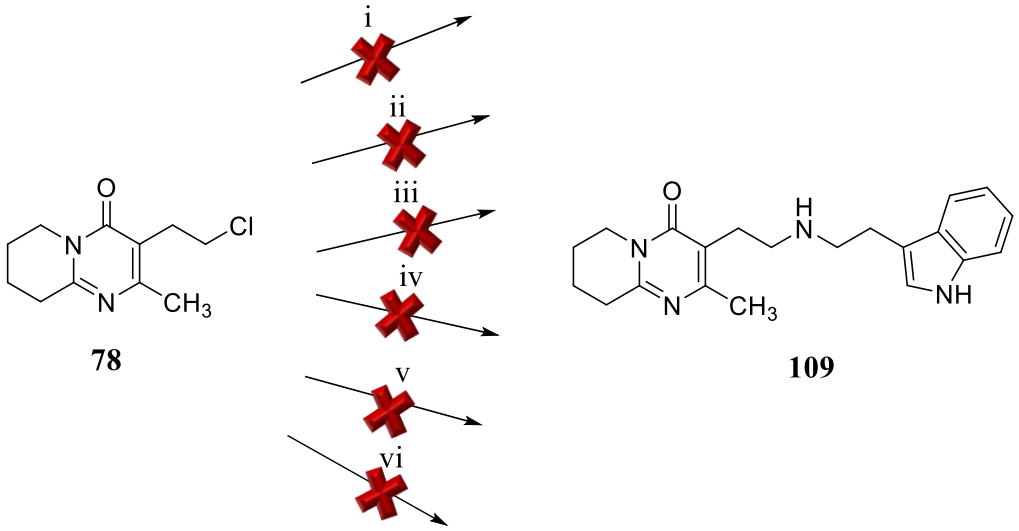

[a]Reagents and conditions. (i) Tryptamine (**105**), K_2CO_3, KI, DMF, 80 °C, 48 h; (ii) Tryptamine (**105**), K_2CO_3, KI, MeCN; (a) room temperature, 5h; (b) 60 °C, 18 h; (c) 85 °C, 48 h; (iii) Tryptamine (**105**), K_2CO_3, KI, MeCN (dilution- 1X), sealed tube, 80 °C, 5 days; (v) Tryptamine (**105**), K_2CO_3, KI, toluene, sealed tube, 80 °C, 5 days; (vi) Tryptamine (**105**), Et_3N, KI, MeCN (dilution- 1X), sealed tube, 80 °C, 5 days; (iv) Tryptamine (**105**), K_2CO_3, KI, MeCN (dilution- X/3), sealed tube, 80 °C, 5 days.

Scheme 15 b. Synthesis of compound **109**.[a]

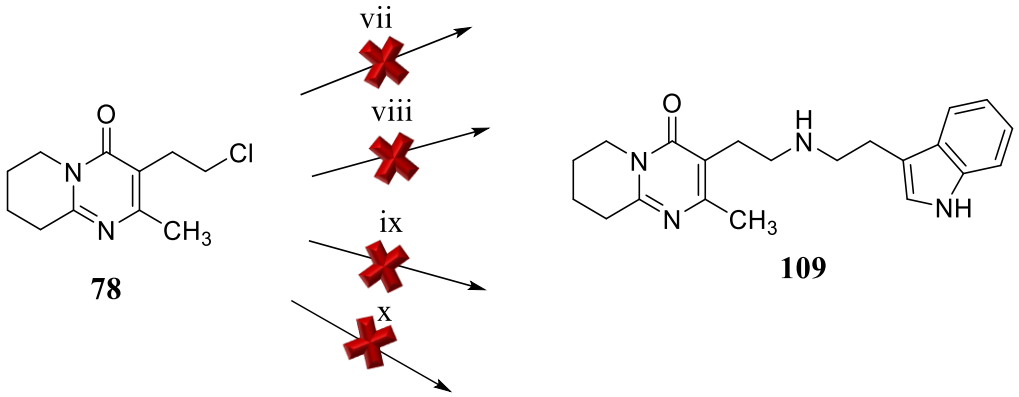

[a]Reagents and conditions. (vii) Tryptamine (**105**), K_2CO_3, KI, MeCN (dilution - 2X), reflux, 18 h; (viii) Tryptamine (**105**), K_2CO_3, KI, MeCN (dilution - 10X), reflux, 18 h;(ix) Tryptamine (**105**), K_2CO_3, KI, MeCN (dilution - 20X), reflux, 18 h; (x) Tryptamine (**105**), K_2CO_3, KI, MeCN (dilution - 1.8X), reflux, 18 h.

Scheme 15 c. Synthesis of compound **109**.[a]

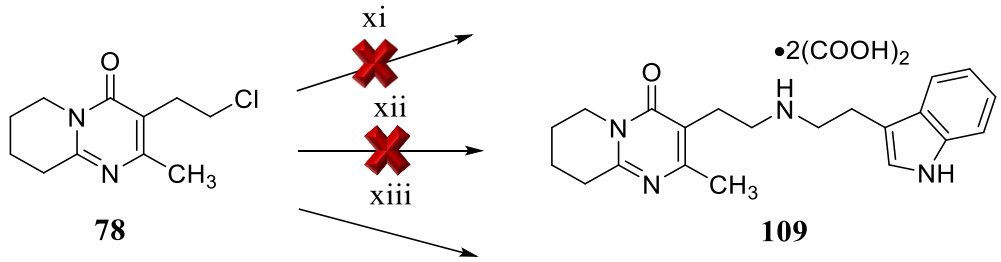

[a]Reagents and conditions. (xi) Tryptamine (**105**) (2 equivalents), K_2CO_3, KI, MeCN (dilution - 1X), reflux, 18 h; (xii) Tryptamine (**105**) (2 equivalents), K_2CO_3, KI, MeCN (dilution - 2X), reflux, 18 h; (xiii) (a) Tryptamine (**105**) (2 equivalents), K_2CO_3, MeCN (dilution - 2X), reflux, 17 h; (b) $CHCl_3$, $(COOH)_2/Et_2O$.

Scheme 15 d. Synthesis of compound **109**.[a]

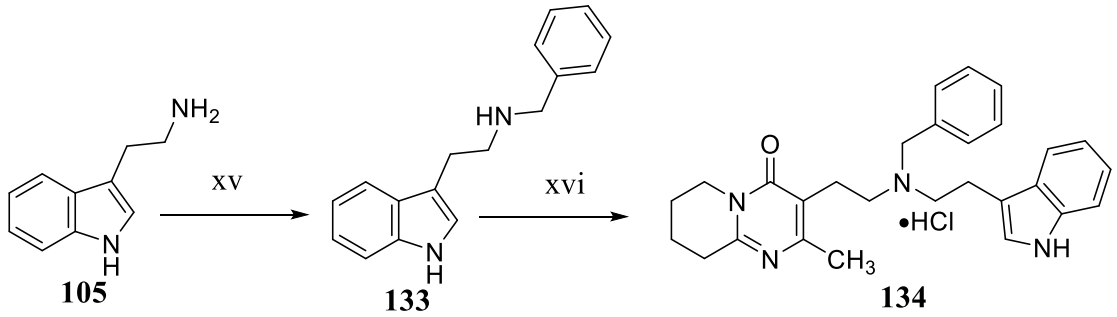

[a]Reagents and conditions. (i) (a) Benzaldehyde, $MgSO_4$, EtOH, 60 °C, 1 h; (b) $NaBH_4$, room temperature, 1.5 h; (ii) 3-(2-Chloroethyl)-2-methyl-6,7,8,9-tetrahydro-4*H*-pyrido[1,2-*a*]pyrimidin-4-one (**78**), KI, K_2CO_3, MeCN, reflux, 48 h. (b) CH_2Cl_2, HCl/EtOH.

The synthesis of compound **110** is outlined in Scheme 16. The conditions that we had optimized for the synthesis of **109** were used to synthesize compound **110**. The tryptamine **106**, was *N*-alkylated by compound **78** to yield compound **110**. We observed a mixture of compound **135** (Figure 35) and compound **110**. Column chromatography and recrystallization techniques were used to separate them. Compound **110** was unknown and was characterized by NMR and elemental analysis for C, H and N atoms.

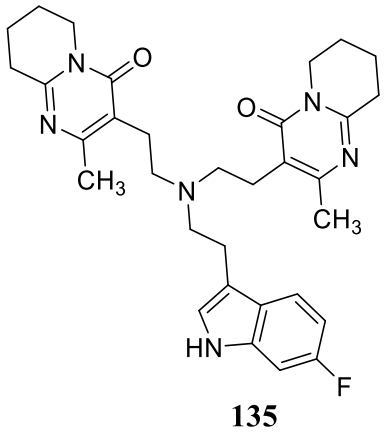

Figure 35. A side product of the Finkelstein alkylation reaction.

Scheme 16. Synthesis of compound **110**.[a]

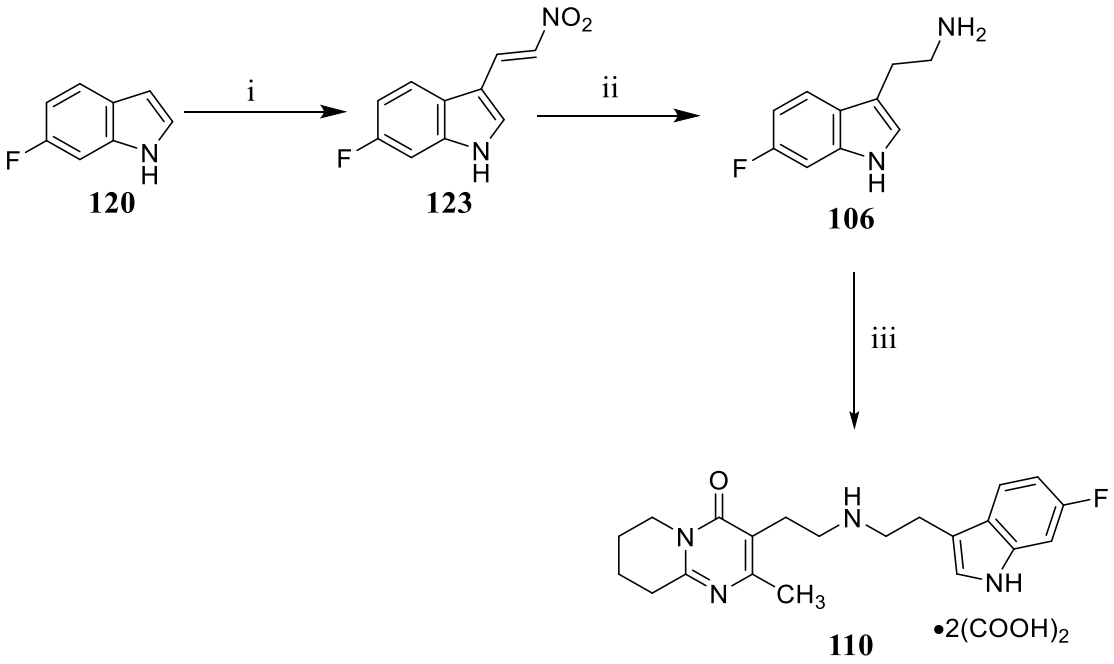

[a]Reagents and conditions. (i) 1-Dimethylamino-2-nitroethylene, trifluoroacetic acid, room temperature, 2 h; (ii) $LiAlH_4$ (5 equivalents), THF, Et_2O, 60 ºC, 1 h; (iii) (a) 3-(2-Chloroethyl)-2-methyl-6,7,8,9-tetrahydro-4*H*-pyrido[1,2-*a*]pyrimidin-4-one (**78**), K_2CO_3, MeCN, reflux, 17 h; (b) $CHCl_3$, $(COOH)_2/Et_2O$.

The synthesis of compounds **111** and **112** are outlined in Scheme 17 and 18, respectively. Compounds **107** and **108** were synthesized as previously described in Schemes 14 and 13, respectively. Finkelstein alkylation reactions between compounds **107**, **108** with compound **78** in MeCN yielded compounds **111** and **112**, respectively. Compounds **111** and **112** were unknown and were characterized by NMR and elemental analysis for C, H and N atoms.

Scheme 17. Synthesis of compound **111**.[a]

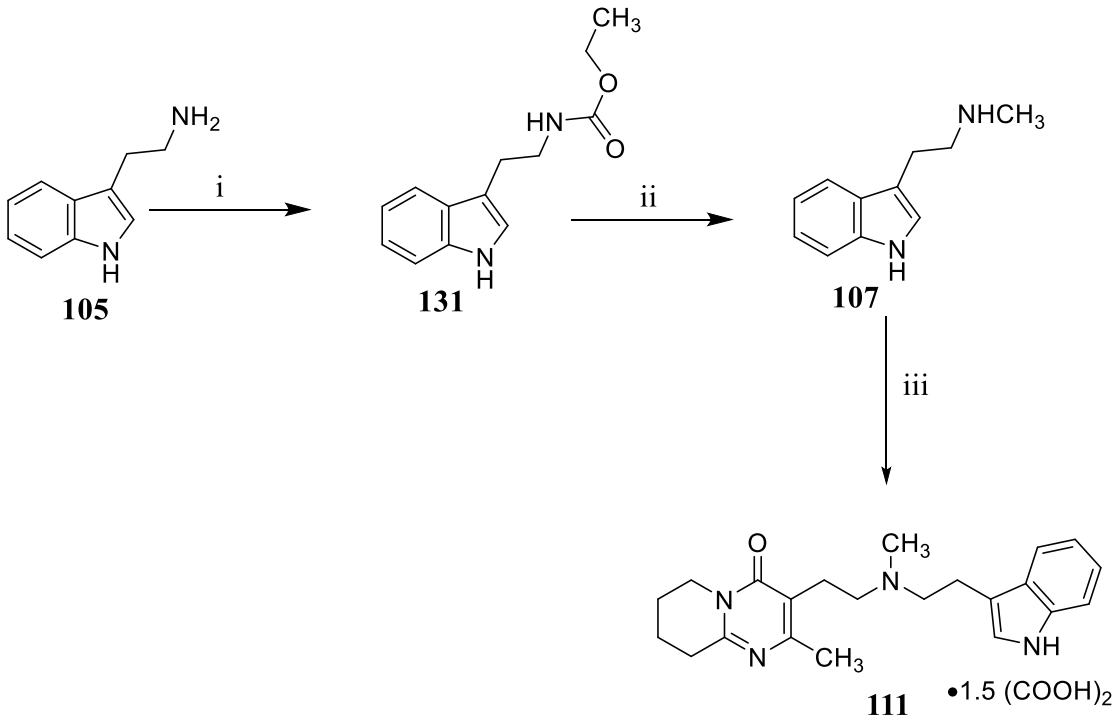

Reagents and conditions. (i) Ethyl chloroformate, Et_3N, CH_2Cl_2, room temperature, 3 h; (ii) (a) $LiAlH_4$ (3 equivalents), THF, reflux, 1.5 h; (iii) (a) 3-(2-Chloroethyl)-2-methyl-6,7,8,9-tetrahydro-4*H*-pyrido[1,2-*a*]pyrimidin-4-one (**78)**, K_2CO_3, KI, MeCN. Reflux, 48 h; (b) CH_2Cl_2, $(COOH)_2/Et_2O$.

Scheme 18. Synthesis of compound **112**.[a]

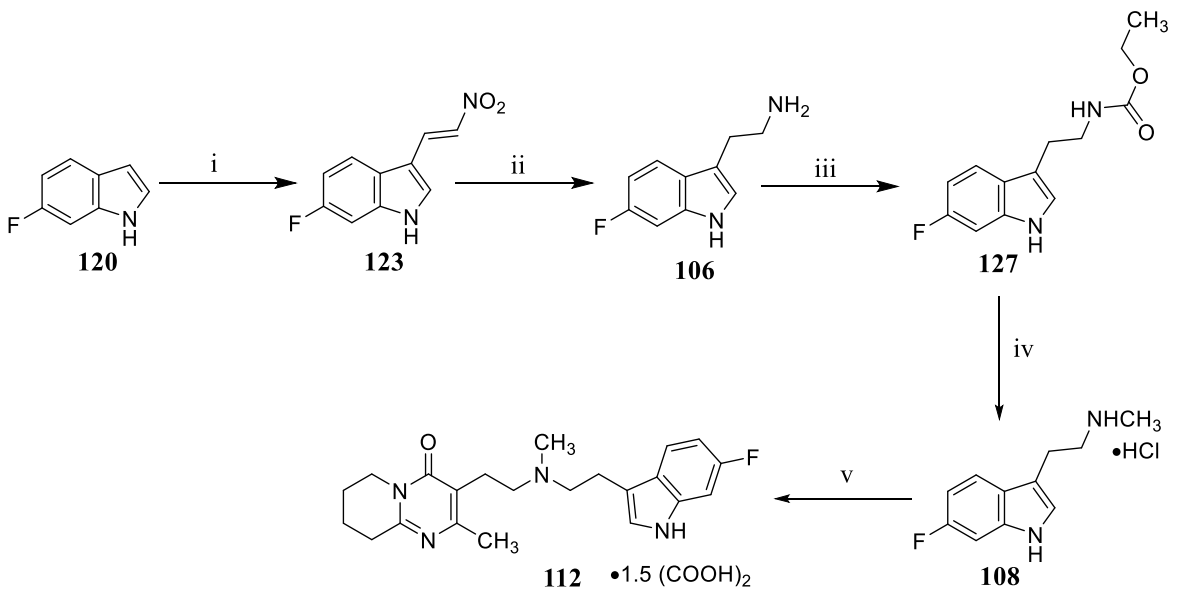

[a]Reagents and conditions: (i) 1-Dimethylamino-2-nitroethylene, trifluoroacetic acid, room temperature, 2 h; (ii) $LiAlH_4$ (5 equivalents), THF, Et_2O, 60 ˚C, 1 h; (iii) ethyl chloroformate, Et_3N, CH_2Cl_2, room temperature, 3 h; (iv) (a) $LiAlH_4$ (3 equivalents), THF, reflux, 1.5 h; (b) Et_2O, HCl/Et_2O; (v) (a) 3-(2-Chloroethyl)-2-methyl-6,7,8,9-tetrahydro-4*H*-pyrido[1,2-*a*]pyrimidin-4-one (**78**), K_2CO_3, KI, MeCN, reflux, 48 h; (b) CH_2Cl_2, $(COOH)_2/Et_2O$.

c. Aromatization of the "left half" (i.e., the 2-methyl-6,7,8,9-tetrahydro-4*H*-pyrido[1,2-*a*]pyrimidin-4-one portion) of risperidone

Scheme 19 outlines the synthesis of compound **113.** A Finkelstein alkylation reaction between 6-fluoro-3-(4-piperidinyl)benz[*d*]isoxazole (**61**) and **136** in MeCN, yielded compound **113.** The free base of compound **113** is known.[174] The oxalate salt of compound **113** was unknown and was characterized by NMR and elemental analysis for C, H and N atoms.

Scheme 19 Synthesis of compound **113**.[a]

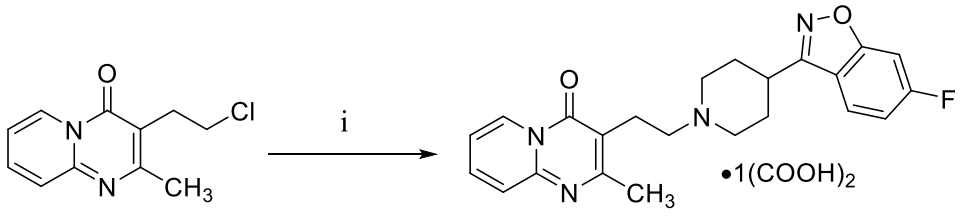

136 **113**

[a]Reagents and conditions. (i) (a) 6-Fluoro-3-(4-piperidinyl)benz[*d*]isoxazole (**61**), KI, K_2CO_3, MeCN, reflux, 20 h; (b) CH_2Cl_2, $COOH_2/Et_2O$.

d. Investigation of the role of the "left half" (i.e., the 2-methyl-6,7,8,9-tetrahydro-4*H*-pyrido[1,2-*a*]pyrimidin-4-one portion) of risperidone by making the "left half" of risperidone similar to other antipsychotic agents such as iloperidone

Scheme 20 illustrates the synthesis of compounds **114** and **115**. A Finkelstein alkylation reaction between **137**, **138** with 6-fluoro-3-(4-piperidinyl)benz[*d*]isoxazole (**61**) in MeCN, yielded compounds **114** and **115** respectively. Compounds **114** and **115** were unknown and were characterized by NMR and elemental analysis for C, H and N atoms.

Scheme 20. Synthesis of compound **114** and **115**.[a]

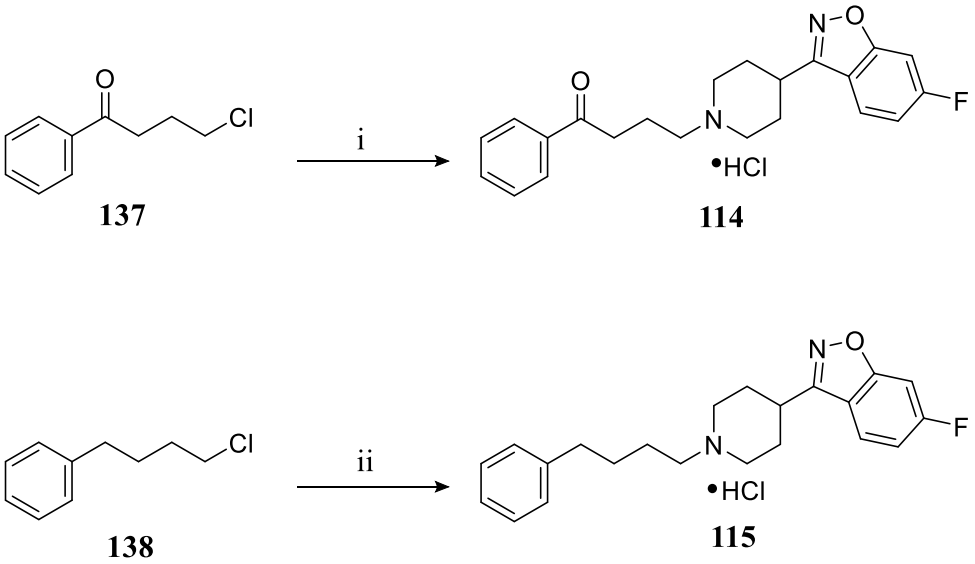

[a]Reagents and conditions. (i) (a) 6-Fluoro-3-(4-piperidinyl)benz[*d*]isoxazole (**61**), KI, K_2CO_3, MeCN, reflux, 20 h; (b) 1 M HCl; (ii) (a) 6-fluoro-3-(4-piperidinyl)benz[*d*]isoxazole (**61**), KI, K_2CO_3, MeCN, reflux, 36 h; (b) EtOAc, HCl/EtOAc.

The synthesis of compound **116** is illustrated in Scheme 21. Compounds **140**[175] and **141**[176] are known and were synthesized by procedures for the same compounds. 5-Chlorovaleroyl chloride **(140)** was synthesized by the reaction of 5-chlorovaleric acid **(139)** with thionyl chloride. A Friedel-Crafts acylation reaction between **140** and benzene yielded intermediate **141.** Several side products were obtained (potentially the Freidel-Crafts alkylation product), and **141** was separated from the side-products by recrystallization and column chromatography. A Finkelstein alkylation reaction between **141** and 6-fluoro-3-(4-piperidinyl)benz[*d*]isoxazole (**61**) in MeCN yielded compound **116**. Compound **116** was unknown and was characterized by NMR and elemental analysis for C, H and N atoms.

Scheme 21. Synthesis of compound **116**.[a]

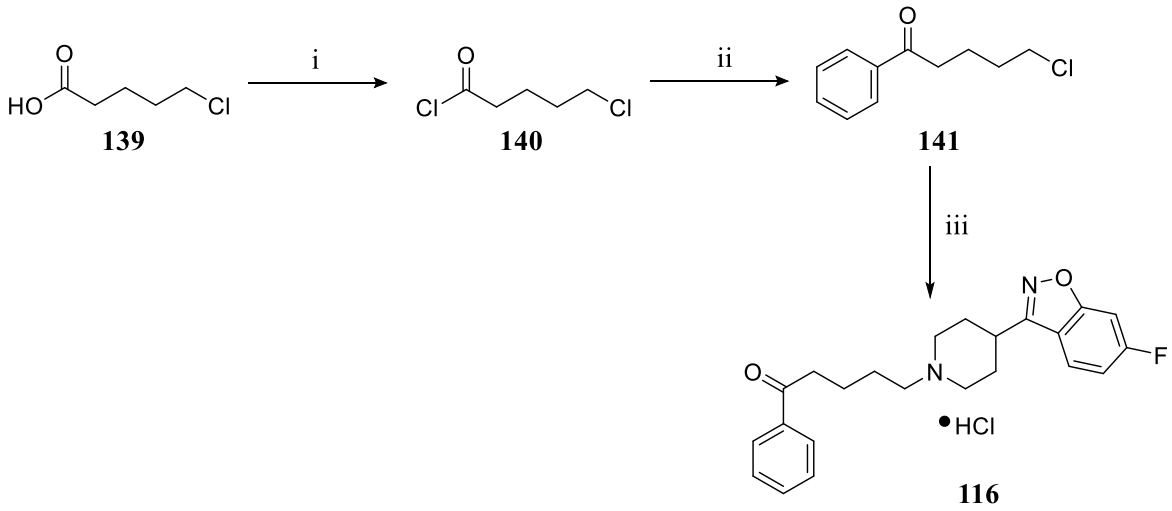

[a]Reagents and conditions: (i) $SOCl_2$, reflux, 3 h; (ii) $AlCl_3$, benzene; (a) 0 ºC, 1 h; (b) room temperature, 1 h; (iii) 6-fluoro-3-(4-piperidinyl)benz[*d*]isoxazole (**61**), K_2CO_3, KI, sealed tube, 80 ºC, 48 h; (b) EtOH, HCl/EtOH.

The Finkelstein alkylation of 6-fluoro-3-(4-piperidinyl)benz[*d*]isoxazole (**61**) with **142** yielded compound **117**, and the synthesis is outlined in Scheme 22. Compound **117** was unknown and was characterized by NMR and elemental analysis for C, H and N atoms.

Scheme 22. Synthesis of compound **117**.[a]

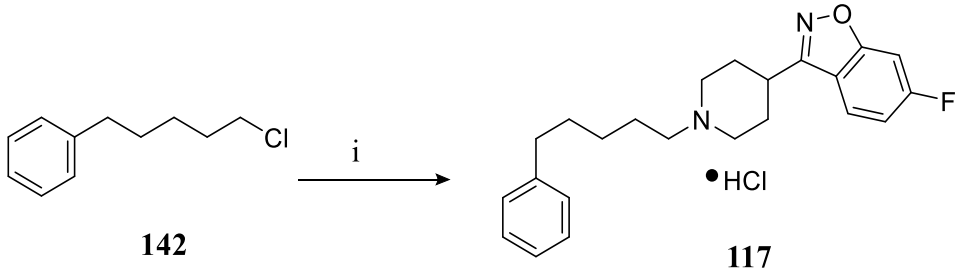

Reagents and conditions: (i) (a) 6-Fluoro-3-(4-piperidinyl)benz[*d*]isoxazole (**61**), KI, K_2CO_3, MeCN, sealed tube, 80 ºC, 96 h; (b) MeOH, HCl/EtOH.

B. Radioligand binding studies

Radioligand binding studies of the compounds were performed in HEK 293 cells expressing 5-HT_{2A} receptors. [^{3}H]Ketanserin (**36**) was used as the radioligand, and non-specific binding was determined in the presence of methysergide. Competition curves were generated and analyzed by nonlinear regression to determine the binding affinities of the compounds (K_i values).

Binding affinities of risperidone (**14**), ketanserin (**36**) and their structural hybrids Ris/Ket (**103)** and Ket/Ris (**104)** were determined. The displacement curves for risperidone (**14**), ketanserin (**36**), **103** and **104** are shown in Figure 36.

Ketanserin (**36**) and risperidone (**14**) bound with affinities of 18.55 nM (log K_i = -7.7 ± 0.1), and 5.29 nM (log K_i = -8.27 ± 0.06). Both the structural hybrids Ris/Ket (**103)** (K_i = 12.74 nM; log K_i = -7.8 ± 0.15) and Ket/Ris (**104)** (K_i = 0.96 nM; log K_i = -9.0 ± 0.12) bound with high affinity to 5-HT_{2A} receptors.

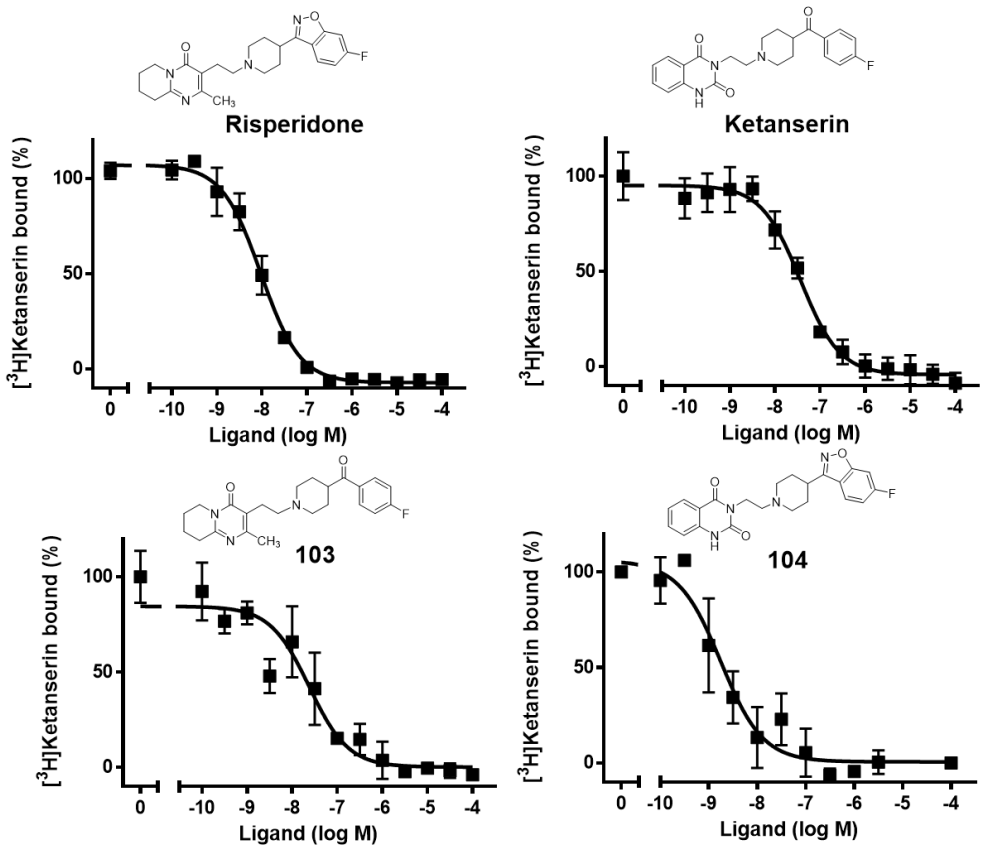

Figure 36. [^{3}H] Ketanserin competition binding curves for risperidone (**14**), ketanserin (**36**), and their hybrids **103** (Ris/Ket) and **104** (Ket/Ris) in HEK 293 cell membrane preparations expressing 5-HT_{2A} receptors (for analogs **103** and **104**: $n = 2$, performed in duplicate; figures provided by Dr. Jose Moreno).

Preliminary competition curves for elaborated analogs **111** and **112** are shown in Figure 37. Analogs **111** and **112** exhibited high affinity for 5-HT_{2A} receptors and bound with affinities of 285 nM ($n = 1$; performed in duplicate), and 4.82 nM ($n = 1$, performed in duplicate), respectively.

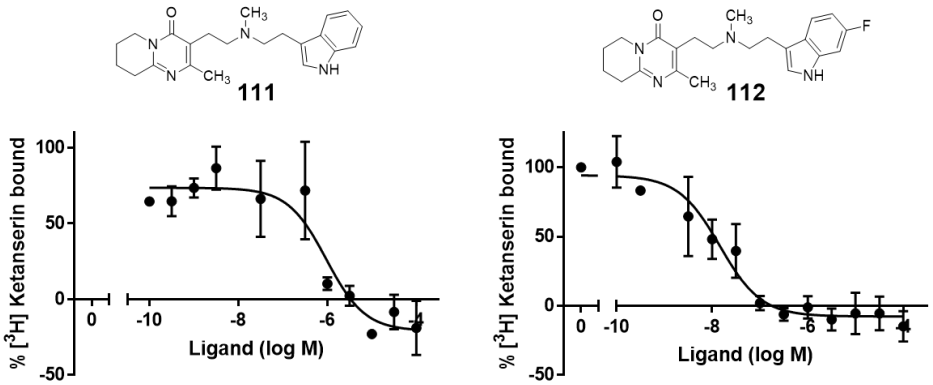

Figure 37. [^{3}H] Ketanserin competition binding curves for elaborated analogs **111** and **112** in HEK 293 cell membrane preparations expressing 5-HT$_{2A}$ receptors (n = 1, performed in duplicate).

C. Functional activity studies

Risperidone (**14**), ketanserin (**36**) and their structural hybrids were tested in a TEVC electrophysiological assay that utilizes the *Xenopus laevis* heterologous expression system as previously described.

The $G_{\alpha q}$ mediated activity of 1 µM 5-HT was antagonized by 10 µM of risperidone (**14**), ketanserin (**36**), and the structural hybrid Ris/Ket (**103**), and reduced the activity to ~20, 15 and 21 % respectively. (Figure 38) Analog **104** did not reduce the activity of 5-HT. When ketanserin (**36**) (a 5-HT$_{2A}$ receptor antagonist) and **104** were tested in the absence of 5-HT, both showed activities of ~45 and 20% as compared to 5-HT suggesting potential partial agonist activity (Figure 39). This positive efficacy might be attributed to its direct effects on the GIRK4* channel or other effects and needs to be investigated further.

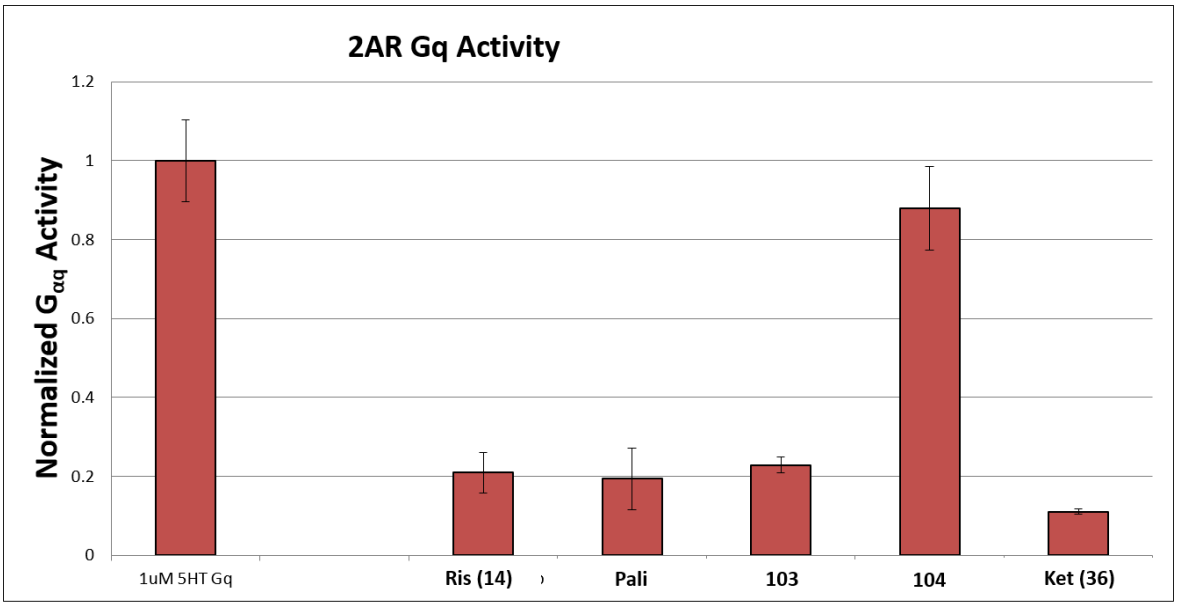

Figure 38. Functional activity of risperidone (**14**), paliperidone (pali, **56**), ketanserin (**36**), and hybrids **103** and **104** in the presence of 5-HT.

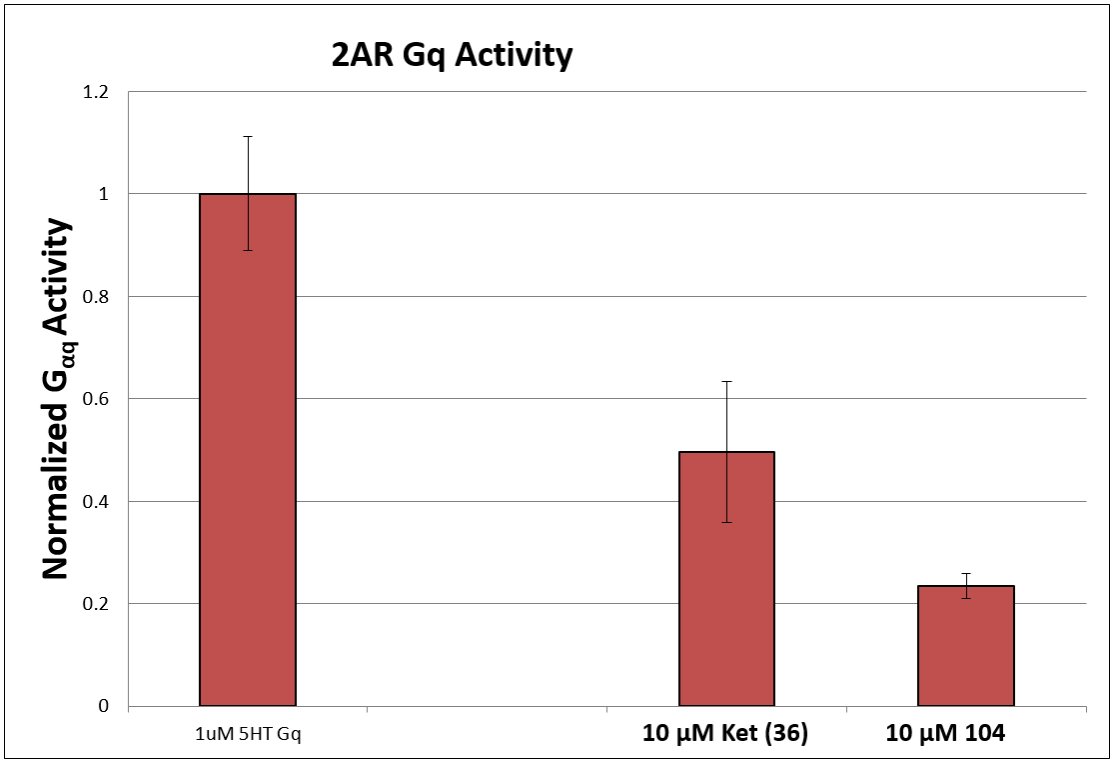

Figure 39. Functional activity of ketanserin (**36**) and hybrid **104** in the absence of 5-HT.

3. Discussion

The structural hybrids of risperidone (**14**) and ketanserin (**36**) i.e. Ris/Ket (**103**) and Ket/Ris (**104**) both retain high affinity for 5-HT_{2A} receptors. Ris/Ket (**103**) (K_i = 12.7 nM) binds with ~ 2-fold lower affinity than risperidone (K_i = 5.3 nM), and ~1.5-fold higher affinity than ketanserin (**36**) This suggests that the "right half" of risperidone (**14**) might be contributing more to binding affinity as compared to the "right half" of ketanserin (**36**). Ket/Ris (**104**) (K_i = 0.96 nM) binds with ~5.5- and ~19- fold higher affinity than risperidone (**14**) (K_i = 5.29 nM), and ketanserin (**36**) (K_i = 18.6 nM), respectively, suggesting that the "left half" of ketanserin (**36**) might be contributing to the binding affinity at 5-HT_{2A} receptor to a greater extent as compared to the "left half" of risperidone (**14**). Hence, consistent with our results from deconstruction of risperidone (**14**) studies, the "right half" of risperidone (**14**) seems to be contributing to its binding affinity to a greater extent as compared to its "left half".

The hybrid molecules seem to have different functional activities at the 5-HT_{2A} receptor. In the presence of 5-HT, risperidone (**14**), ketanserin (**36**) and Ris/Ket (**103**) were antagonists, whereas Ket/Ris (**104**) appeared to have partial agonist activity. In the absence of 5-HT, both ketanserin (a known neutral 5-HT_{2A} receptor antagonist) as well as analog **104** exhibited partial agonist activity. This could be due to their direct effects at the GIRK4* channel or due to other effects. However, to determine if analog **104** is a partial agonist, further investigation is needed.

Analogs **111** and **112** both retain high affinity for 5-HT_{2A} receptors. Analog **112** binds with nanomolar affinity that is comparable to the binding affinity of risperidone. Analog **111** binds with ~57-fold lower affinity than analog **112** and risperidone (**14**). Analog **111** represents the desfluoro analog of **112** and indicates that the fluoro group might be making additional interactions with the 5-HT_{2A} receptors that enhances the binding affinity of analog **112** as compared to analog **111**. Since analog **112** and risperidone (**14**) bind with comparable affinity, it might indicate that the benz[*d*]isoxazole ring of risperidone (**14**), and the indole ring of analog **112** might be interacting in a similar manner at 5-HT_{2A} receptors.

C. Specific Aim 3. Molecular modeling studies of risperidone and its deconstructed and elaborated analogs at the 5-HT$_{2A}$ receptor to study their binding modes

1. Approach

Molecular modeling studies at 5-HT$_{2A}$ receptors were conducted to compare the binding modes of risperidone (**14**) (Figure 8) and its deconstructed and elaborated analogs, and to study receptor-ligand interactions at a molecular level. Studying receptor-ligand interactions will help put into perspective the importance of different structural features. We also wanted to compare the binding modes of risperidone (**14**) to the prototypical 5-HT$_{2A}$ receptor antagonist ketanserin (**36**) (Figure 17) to gain insight into the similarities and differences in their interactions at the 5-HT$_{2A}$ receptor.

The 5-HT$_{2A}$ receptor has not been crystallized; hence, 3-dimensional homology models of 5-HT$_{2A}$ receptors were generated for the purpose of the study, and risperidone (**14**), ketanserin (**36**) and deconstructed and elaborated analogs of risperidone (**14**) were docked in the homology models. The homology models were already available in our laboratory, and were used for these studies;[143] their construction is briefly described below.

a. Template, alignment and generation of homology models of 5-HT$_{2A}$ receptors

The 5-HT$_2$ subfamily of receptors share ~70% homology with each other.[39] The crystal structure of the human (h)5-HT$_{2B}$ receptor (PDB ID: 4IB4; resolution: 2.7 Å) in complex with the agonist ergotamine that was solved by Wacker et al.[177] in 2013 was used as a template to construct homology models of h5-HT$_{2A}$ receptors.[143] The software CLUSTALX 2.1[178] was used to generate the multiple sequence alignment between 5-HT$_{2A}$ and 5-HT$_{2B}$ receptors.[143] Homology models

were constructed using MODELLER 9.1[179] and were further processed to add hydrogen atoms and build disulfide bonds using SYBYL-X 2.1.[143]

b. Validation of homology models, docking studies, and HINT analysis

The models were validated by docking ketanserin (**36**) and comparing the results to those that have been reported in published homology models of 5-HT_{2A} receptors as well as by site-directed mutagenesis data.[143]

Homology models reported in the literature, and site-directed mutagenesis studies, have implicated a number of residues in TM3, TM5, TM6, and TM7 to be important for binding of orthosteric agents to 5-HT_{2A} receptors, and include Trp151,[180] D155,[139,180,181] S159 (TM3),[182] S239 (TM5),[183] S242 (TM5),[183] W336,[180] F339,[184] F340 (TM6),[184–186] and Y370 (TM7).[184]

Ketanserin (**36**), risperidone (**14**), and deconstructed, and elaborated analogs of risperidone were docked using GOLD Suite 5.2, GOLD Suite 5.3, or GOLD Suite 5.4[187] depending on the version available at the time the docking studies were performed. Risperidone (**14**), an orthosteric 5-HT_{2A} receptor antagonist/inverse agonist, binds at the same site as 5-HT (**6**).[127] The amino acid residue Asp155 was used to define the binding site (radius: 10 Å) as this residue has been shown to be important and necessary for the binding both of orthosteric agonists such as 5-HT, as well as orthosteric antagonists such as ketanserin (**36**), by site-directed mutagenesis.[139,181] Asp155, anchors the terminal amine moiety of 5-HT via an ionic interaction.[181] The docked solutions were clustered (using a script provided by Dr. Philip D. Mosier). Solutions in the same cluster have a

similar docking pose, and the intra-cluster RMSD is less than 2 Å. Models were chosen based on ChemPLP scores (the higher the score, the better the interactions), cluster size, and the ability of the protonated amines of the compounds to form an ionic interaction with Asp155. The selected models were energy minimized in SYBYL-X 2.1 and the interactions were quantified by Hydropathic INTeraction (HINT) analysis.[188] The HINT score is the sum of interactions between two molecules and accounts both for favorable and unfavorable interactions. A positive HINT score indicates overall favorable interactions.[188] In our study, the HINT score indicates the sum of the interactions between the 5-HT_{2A} receptor and the docked ligand. The HINT scores for the receptor-ligand complexes can be converted into free energy values and ~515 HINT score units correspond to 1 kcal/mol.[189,190]

2. Results and discussion

Risperidone (**14**) showed two docking/binding modes at 5-HT_{2A} receptors (Figures 40 and 41). In one binding mode, the fluorine atom was oriented towards TM5 and is shown in Figure 40 (docking mode 1). In the other mode, the fluorine atom was oriented towards TM7 and is shown in Figure 41 (docking mode 2). The second docking mode is consistent with what has been previously reported in the literature for risperidone.[191]

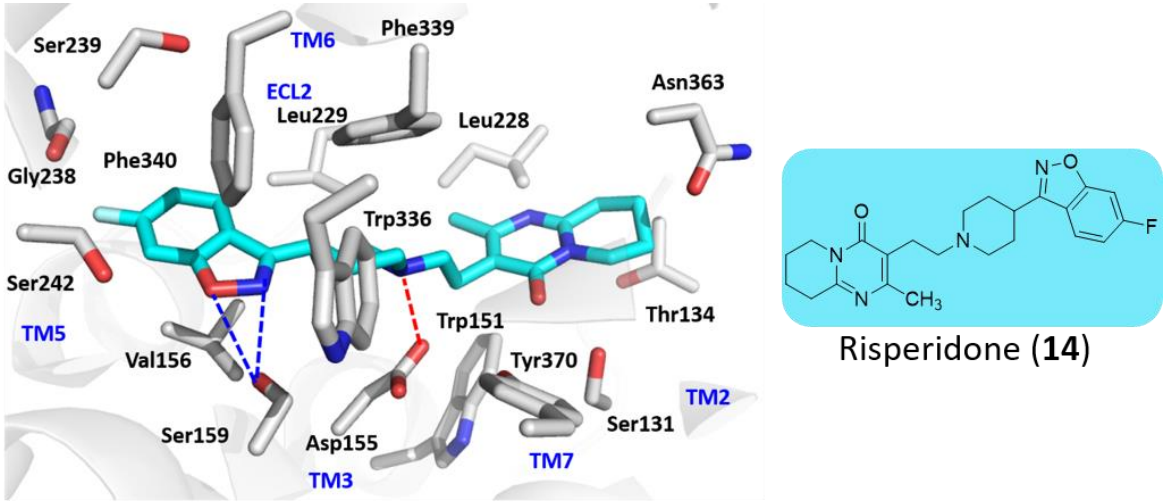

Figure 40. Docking mode 1 of risperidone (**14**) (cyan) at the 5-HT_{2A} receptor with the fluorine atom oriented toward TM5. The red dashed lines indicate ionic interactions and the blue dashed lines indicate hydrogen bonds.

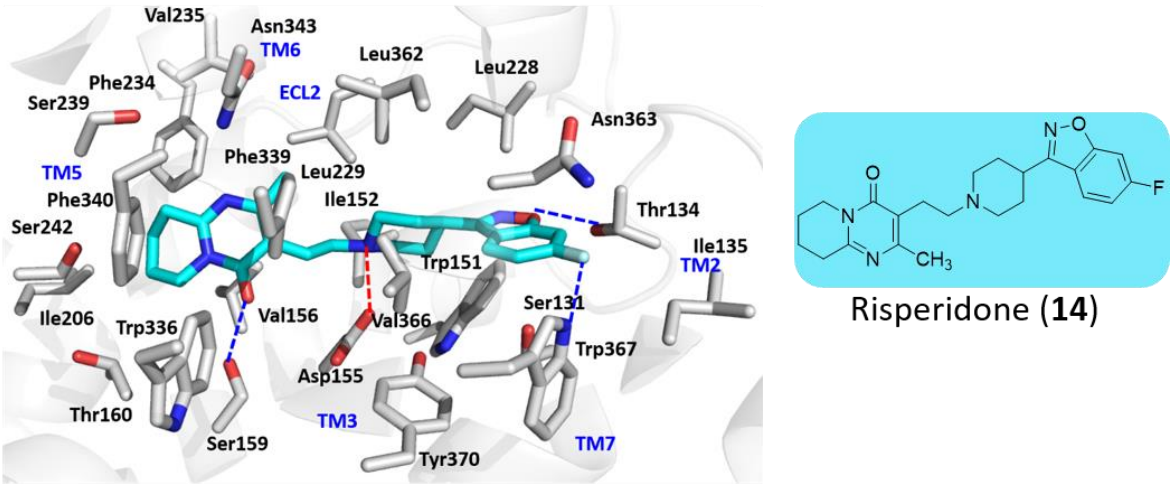

Figure 41. Docking mode 2 of risperidone (**14**) (cyan) at the 5-HT_{2A} receptor with the fluorine atom oriented toward TM7. The red dashed lines indicate ionic interactions and the blue dashed lines indicate hydrogen bonds.

Risperidone (**14**) formed strong hydrophobic and polar interactions at the receptor. In docking mode 1, the 6-fluoro-(3-piperidinyl)benz[*d*]isoxazole moiety ("right half") of risperidone (**14**) predominantly formed polar interactions whereas the 6,7,8,9-tetrahydro-4*H*-pyrido[1,2-

a]pyrimidin-4-one ring system ("left half") of risperidone (**14**) appeared to predominantly form hydrophobic interactions. On the other hand, in mode 2, while the "right half" formed predominantly polar interactions, the "left half" seemed to form polar as well as hydrophobic interactions. In both modes, the indispensable ionic interaction between the protonated amine of the piperidine ring and Asp155 (TM3) was present. In mode 1, the nitrogen and oxygen atoms of the benz[*d*]isoxazale ring formed a bifurcated hydrogen bond with Ser159. In mode 2, the oxygen atom of the 6,7,8,9-tetrahydro-4*H*-pyrido[1,2-*a*]pyrimidin-4-one ring system formed a hydrogen bond with Ser159, whereas the fluorine atom and the oxygen atom of the benz[*d*]isoxazole ring formed hydrogen bonds with Trp367 and Thr134, respectively. Additionally, hydrophobic interactions with Trp151, Leu228, Leu229, Trp336, Phe339, Phe340, Trp367 and Tyr370 were observed for both binding modes.

Both binding modes of risperidone at 5-HT_{2A} receptors seem possible; however, mode 1 (HINT score = 1204) has a higher total HINT score as compared to mode 2 (HINT score = 1001), indicating more overall favorable interactions at the receptor (Table 3). However, the differences in the total HINT scores do not appear to be substantial. The binding and functional activity data available so far suggest that the fluorine atom is important for enhancing binding affinity, and that the carbonyl group of the 6,7,8,9-tetrahydro-4*H*-pyrido[1,2-*a*]pyrimidin-4-one ring system might be important for functional activity (albeit to a very small extent). In mode 2 the carbonyl oxygen and fluorine atom both formed hydrogen bonds with Ser159 and Trp367 making this mode more likely. However, both binding modes might exist, or be in equilibrium.

Table 3. Summary of HINT scores of the two binding modes of risperidone (**14**).

Binding mode	Polar	Hydrophobic	Total HINT score*
Mode 1	1523	1225	1204
Mode 2	1475	1280	1001

*Other terms, e.g., hydrophobic-polar, acid-acid and base-base are reflected in this total.

a. Molecular modeling studies of the deconstructed analogs at 5-HT$_{2A}$ receptors

Figure 42 shows docking modes of truncated analogs **57**, **58** and **59** relative to risperidone (**14**). They docked at the 5-HT$_{2A}$ receptor in a manner similar to docking mode 2 of risperidone (**14**). Analogs **57-59** predominantly show only one binding mode.

For analogs **57-59**, the 6,7,8,9-tetrahydro-4*H*-pyrido[1,2-*a*]pyrimidin-4-one ring system is flipped by ~180 ° about the horizontal axis. (Figure 42).

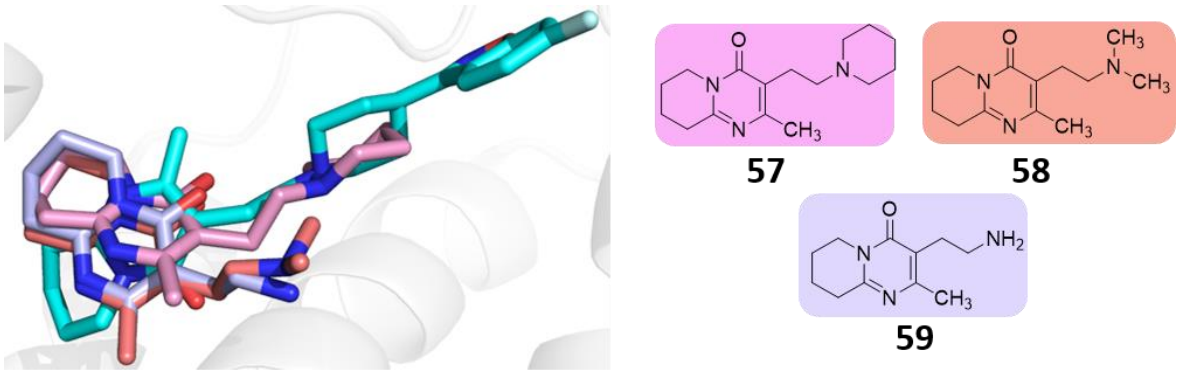

Figure 42. Docking modes of deconstructed analogs **57** (light pink), **58** (salmon), and **59** (violet) at the 5-HT$_{2A}$ receptor relative to risperidone (**14**) (cyan).

Figure 43 illustrates the interactions that analogs **57-59** make with the 5-HT$_{2A}$ receptor. The protonated amines of analogs **57**, **58** and **59** made the crucial ionic interaction with Asp155. The

protonated amine of **59** also formed a hydrogen bond with Tyr370. Analogs **57**, **58** and **59** showed hydrophobic interactions with the residues: Leu229, Phe234, Val235, Trp336, Phe339, and Phe340. Analog **57** made an additional hydrophobic interaction with Val366.

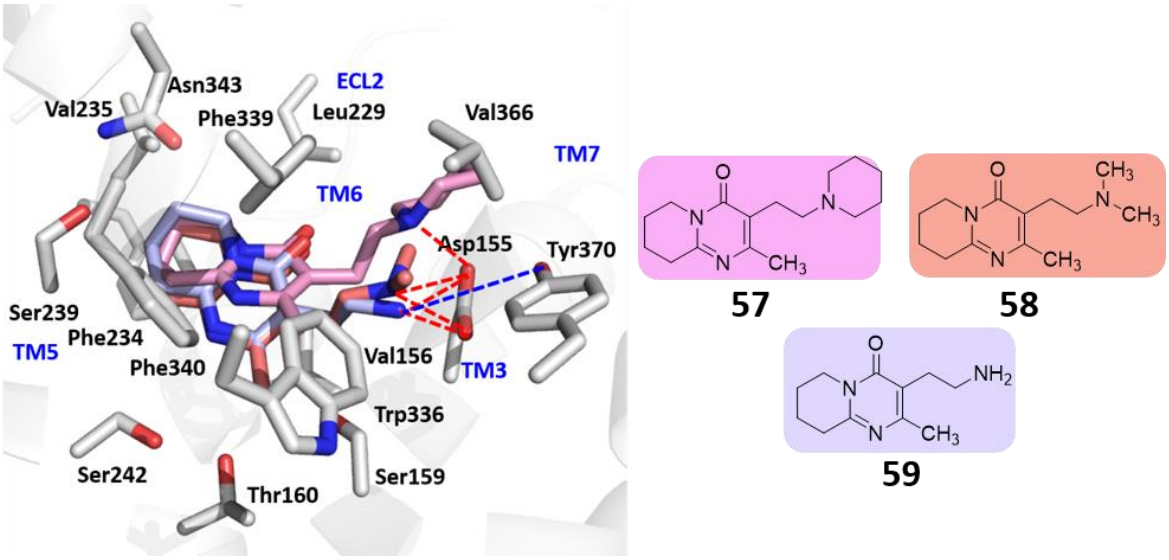

Figure 43. Docking modes of deconstructed analogs **57** (light pink), **58** (salmon), and **59** (violet) at the 5-HT_{2A} receptor. The red dashed lines indicate ionic interactions and the blue dashed lines indicate hydrogen bonds.

HINT scores for analogs **57**, **58** and **59** are shown in Table 4.

Table 4. Summary of HINT scores for risperidone (**14**) and analogs **57**, **58** and **59**.

Binding mode	Polar	Hydrophobic	Total HINT score*
Risperidone (**14**); Mode 1	1523	1225	1204
Risperidone (**14**); Mode 2	1475	1280	1001
57	1103	1037	670
58	1194	988	309
59	2793	734	1851

*Other terms, e.g., hydrophobic-polar, acid-acid and base-base are reflected in this total.

The total HINT scores for analogs **57** and **58** are lower than that for risperidone (**14**) (Table 4), and suggest that risperidone (**14**) makes overall more favorable interactions with 5-HT_{2A} receptors as compared to analogs **57** and **58**. The binding affinity of analog **57** (K_i = ~2732 nM) is ~500-fold lower than the binding affinity of risperidone (K_i = 5.29 nM), and the "right half" of risperidone (**14**) seems to be more important for retaining binding affinity since analogs **60** (K_i = 12.27 nM and **61 (**K_i = 71.41 nM) bind with only ~2 and ~14 fold lower affinity than risperidone (**14**) (K_i = 5.29 nM) The total HINT score for analog **59** is higher than that for risperidone (**14**) suggesting that it makes overall more favorable interactions at the 5-HT_{2A} receptor as compared to risperidone (**14**). However, preliminary binding data suggests that analog **59** might have a very low binding affinity for 5-HT_{2A} receptors [(K_i > 10,000 nM]. The binding affinity might reflect the hydrophobic interactions (Table 4) since analog **59** has a lower score for total favorable hydrophobic interactions as compared to risperidone and analog **57**.

Molecular modeling studies for analogs **60**-**63**, **65**, and **66** have been reported previously.[143]

Analogs **64** and **68** (Figure 44 and 45) have two binding modes that closely resemble docking modes 1 and 2 of risperidone (**14**). Figures 44 and 45 illustrate the interactions that the deconstructed analogs **64**, **68**, and risperidone (**14**) make with the 5-HT_{2A} receptor in docking modes 1 and 2, respectively.

In binding mode 1 (Figure 44), analogs **64** and **68** docked in a manner similar to risperidone (**14**) and formed the interactions that were previously described for binding mode 1 of risperidone (**14**). In addition to those interactions, the pyrimidone oxygen of deconstructed analog **64** formed a hydrogen bond with Ser131.

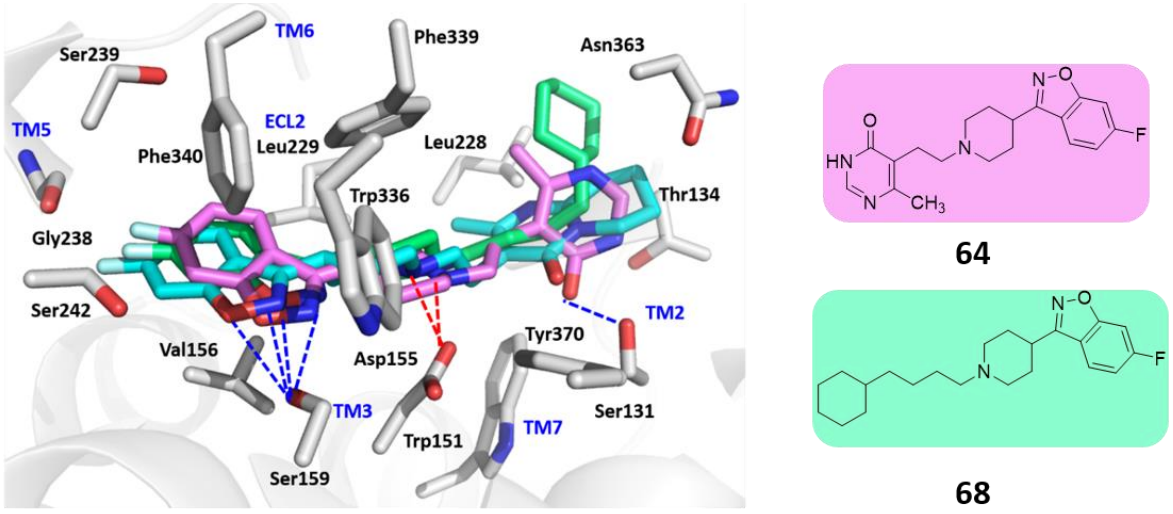

Figure 44. Docking modes of risperidone (**14**) (cyan), and analogs **64** (magenta) and **68** (green) at the 5-HT_{2A} receptor (docking mode 1). The red dashed lines indicate ionic interactions and the blue dashed lines indicate hydrogen bonds.

In binding mode 2 (Figure 45), the molecules **64** and **68** docked in a manner similar to binding mode 2 of risperidone (**14**), and formed interactions that were consistent with what was previously described for binding mode 2 of risperidone (**14**). The pyrimidone oxygen of deconstructed analog **64** formed a hydrogen bond with Ser159 whereas analog **68** lacks the carbonyl group that is present in risperidone (**14**), and hence lacks the hydrogen bond with Ser159.

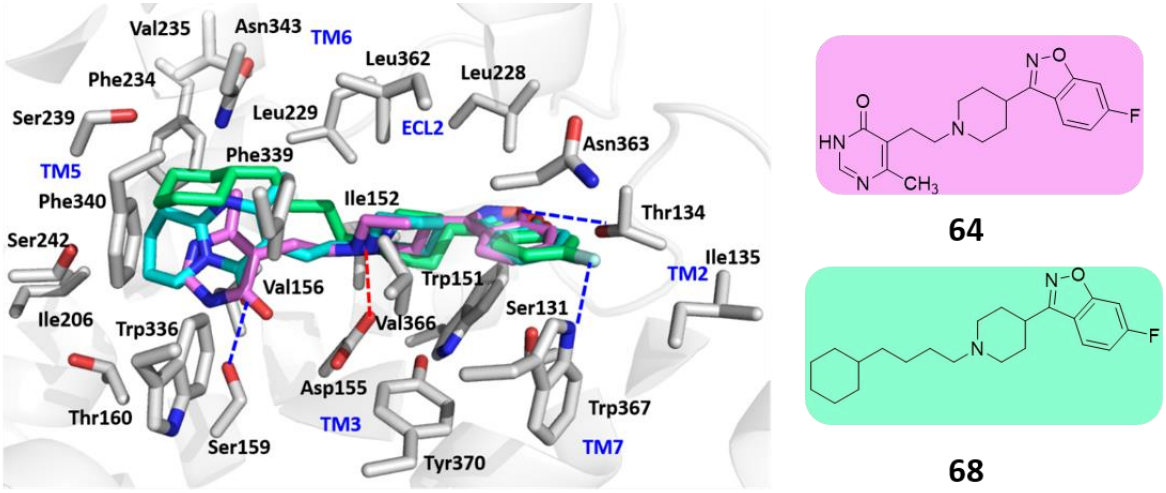

Figure 45. Docking modes of risperidone (**14**) (cyan), and analogs **64** (magenta) and **68** (green) at the 5-HT_{2A} receptor (docking mode 2). The red dashed lines indicate ionic interactions and the blue dashed lines indicate hydrogen bonds.

As seen previously with risperidone (**14**), both binding modes seem possible. HINT scores for both analogs are summarized in Table 5. Total HINT scores for analogs **64** and **68** in binding mode 1 were higher than that for binding mode 2 suggesting that it makes more overall favorable interactions in binding mode 1 with the receptor. However, the differences in HINT scores do not appear to be substantial.

Table 5. Summary of HINT scores for binding modes 1 and 2 of risperidone (**14**) and analogs **64** and **68**.

Binding mode	Polar	Hydrophobic	Total HINT score*
Risperidone (**14**); Mode 1	1523	1225	1204
Risperidone (**14**); Mode 2	1475	1280	1001
64; Mode 1	1936	810	847
64; Mode 2	1538	811	616
68; Mode 1	1464	1036	1166
68; Mode 2	1156	1111	1057

*Other terms, e.g., hydrophobic-polar, acid-acid and base-base are reflected in this total.

b. Molecular modeling studies of elaborated analogs of risperidone

Figures 46-49 show risperidone (**14**), ketanserin (**36**) and their structural hybrids (**103** and **104**) docked in homology models of the 5-HT_{2A} receptor.

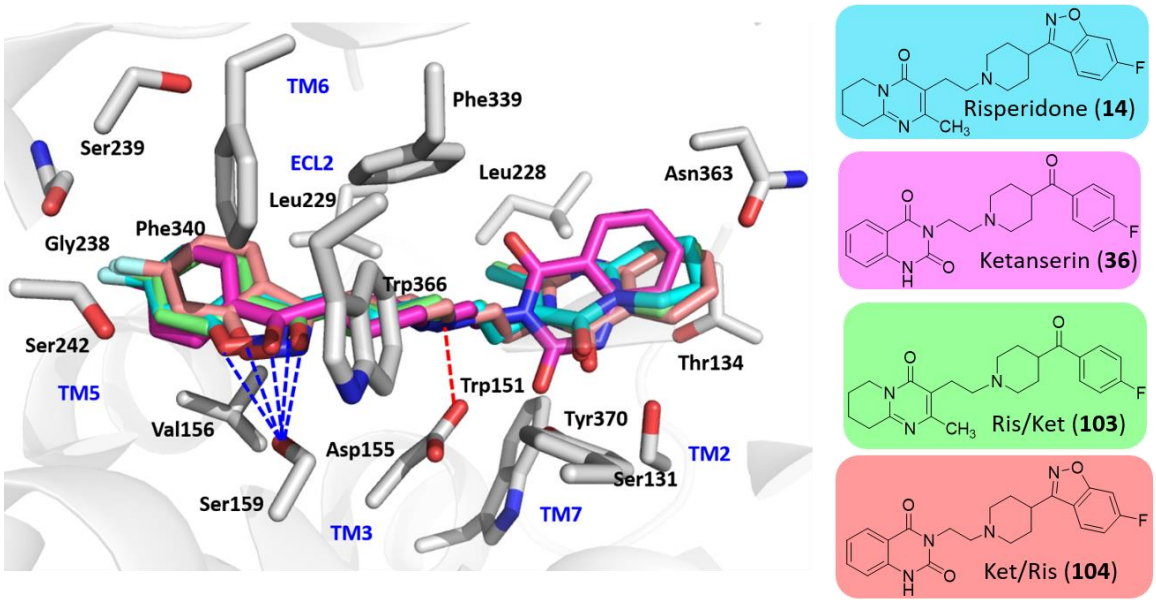

Figure 46. Docking modes of risperidone (**14**) (cyan), ketanserin (magenta), analogs **103** (green) and **104** (salmon) at the 5-HT_{2A} receptor (docking mode 1). The red dashed lines indicate ionic interactions and the blue dashed lines indicate hydrogen bonds.

Figure 46 shows Ris/Ket (**103)** and Ket/Ris (**104**), as well as ketanserin (**36**), docked in a manner that is consistent with binding mode 1 of risperidone (**14**). The protonated amines of all analogs formed the crucial ionic interaction with Asp155. Ketanserin (**36**) interacts with the 5-HT_{2A} receptor in a manner similar to that described previously for binding mode 1 of risperidone (**14**). The oxygen atom of the carbonyl group of the 4-fluorobenzoyl piperidine ring ("right half" of ketanserin) is engaged in a hydrogen bond with Ser159. Ris/Ket (**103**) has the "left half" of risperidone (**14**) and the "right half" of ketanserin (**36**). The "left half" of Ris/Ket (**103**) aligned well with the "left half" of risperidone (**14**) whereas the "right half" of Ris/Ket (**103**) aligned well the "right half" of ketanserin (**36**). The "left half" of Ris/Ket (**103**) interacts with the receptor in a manner similar to the binding mode 1 of risperidone (**14**), whereas the "right half" interacts in a manner that has been described for the "right half" of ketanserin (**36**). Ket/Ris (**104**) has the "left half" of ketanserin (**36**) and the "right half" of risperidone (**14**). Despite having the "left half" of

ketanserin (**36**) i.e. the quinazolinedione ring, the molecule docked in a manner such that the quinazolinedione ring was flipped by ~180 ° about the horizontal axis [when compared to the docking solution for ketanserin (**36**)] (Figure 47 A), and seemed to align better with the "left half" of risperidone (**14**) (Figure 47 B). The "right half" of Ket/Ris (**104**) overlapped well with the "right half" of risperidone (**14**) and showed the same interactions at the 5-HT_{2A} receptor as were previously described for docking mode 1 of risperidone (**14**).

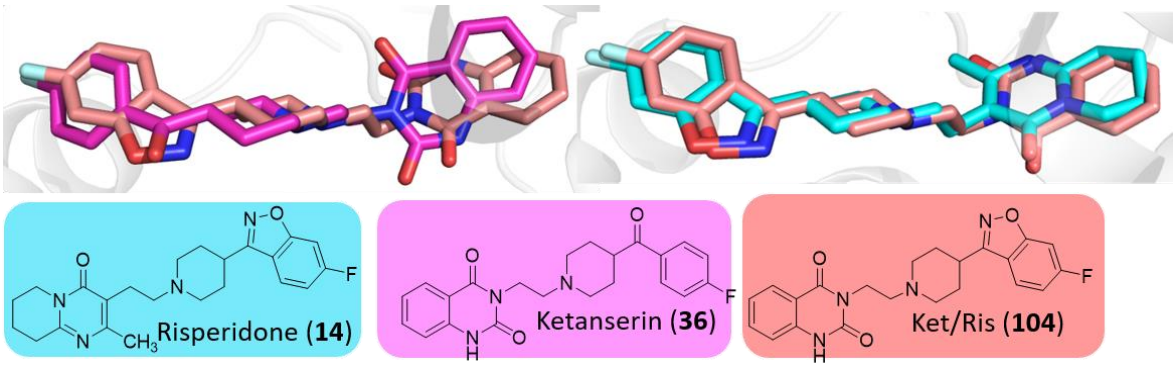

Figure 47. A comparison between (A) binding modes of Ket/Ris (**104**) (salmon) and ketanserin (**36**) (magenta); (B) binding modes of Ket/Ris (**104**) (salmon) and risperidone (**14**) (cyan).

Figure 48 shows a comparison of the Ris/Ket (**103**) and the Ket/Ris (**104**) hybrid with risperidone (**14**) and ketanserin (**36**) at the 5-HT_{2A} receptor when oriented in docking mode 2. The "left half" of Ris/Ket (**103**) docked in a manner similar to risperidone (**14**) (Figure 48 B), whereas the "right half" was flipped by ~180 º about the horizontal axis as compared to the "right half" of ketanserin (**36**) (Figure 48 A). The "left half" of Ket/Ris (**104**) was flipped by ~180 º about the horizontal axis as compared to the "left half" of ketanserin (**36**) (Figure 48 C), and aligned better with the "left half" of risperidone (**14**) as opposed to the "left half" of ketanserin (**36**) (Figure 48 D) whereas

the “right half” of Ket/Ris (**104)** docked in a manner similar to the “right half” of risperidone (**14**) (Figure 48 D).

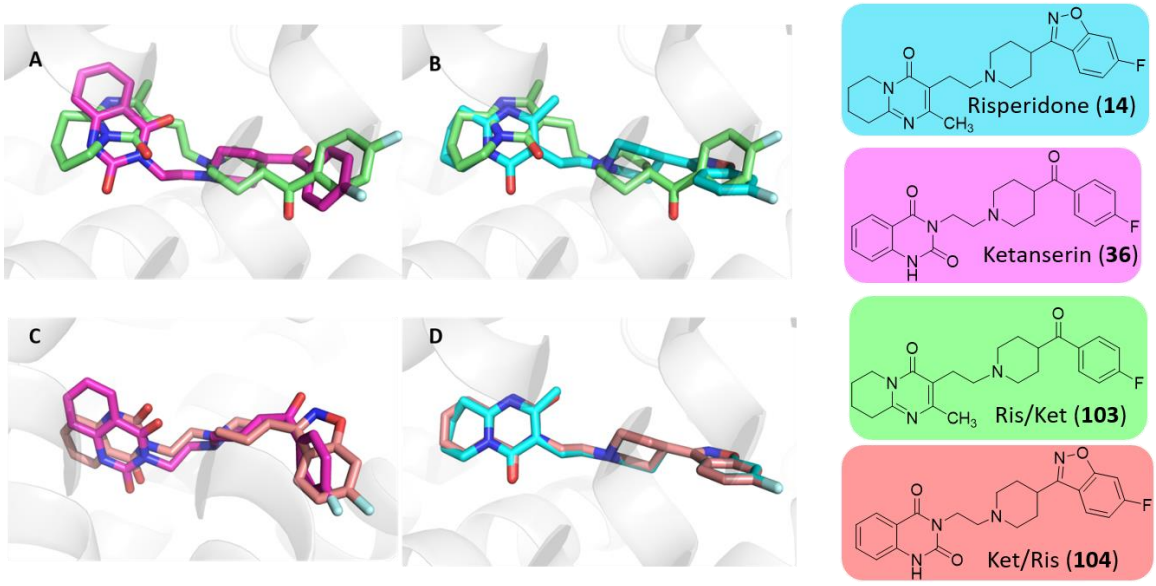

Figure 48. A comparison between (A) binding modes of Ris/Ket (**103**) (green) and ketanserin (**36**) (magenta); (B) binding modes of Ris/Ket (**103**) (green) and risperidone (**14**) (cyan); (C) binding modes of Ket/Ris (**104**) (salmon) and ketanserin (**36**) (magenta); (D) binding modes of Ket/Ris (**104**) (salmon) and risperidone (**14**) (cyan).

Figure 49 shows Ris/Ket (**103**), Ket/Ris (**104**) and ketanserin (**36**) docked in a manner that was consistent with binding mode 2 of risperidone (**14**). Risperidone (**14**) interacts with the 5-HT_{2A} receptor in a manner previously described for binding mode 2 of risperidone (**14**). The protonated amines of ketanserin (**36**) and the two structural hybrids **103** and **104** formed an ionic salt-bridge interaction with Asp155. The carbonyl oxygen atom of Ris/Ket (**103**) formed a hydrogen bond with Ser131. The O2 and O1 oxygen atoms of the quinazolinedione rings of the Ket/Ris hybrid (**104**) and ketanserin (**36**), respectively, and the oxygen atom of the 6,7,8,9-tetrahydro-4*H*-pyrido[1,2-*a*]pyrimidin-4-one ring of risperidone (**14**) formed a hydrogen bond with Ser159. The

fluorine atoms of risperidone (**14**), ketanserin **(36**) and the Ket/Ris hybrid (**104**) formed a hydrogen bond with Trp367. The oxygen atoms of the benz[*d*]isoxazole rings of risperidone (**14**), and the Ket/Ris hybrid (**104**) formed a hydrogen bond with Thr134. Additionally, hydrophobic interactions with Trp151, Leu228, Leu229, Trp336, Phe339, Phe340, Trp367, and Tyr370 were observed for hybrid molecules **103** and **104**, risperidone (**14**) and ketanserin (**36**).

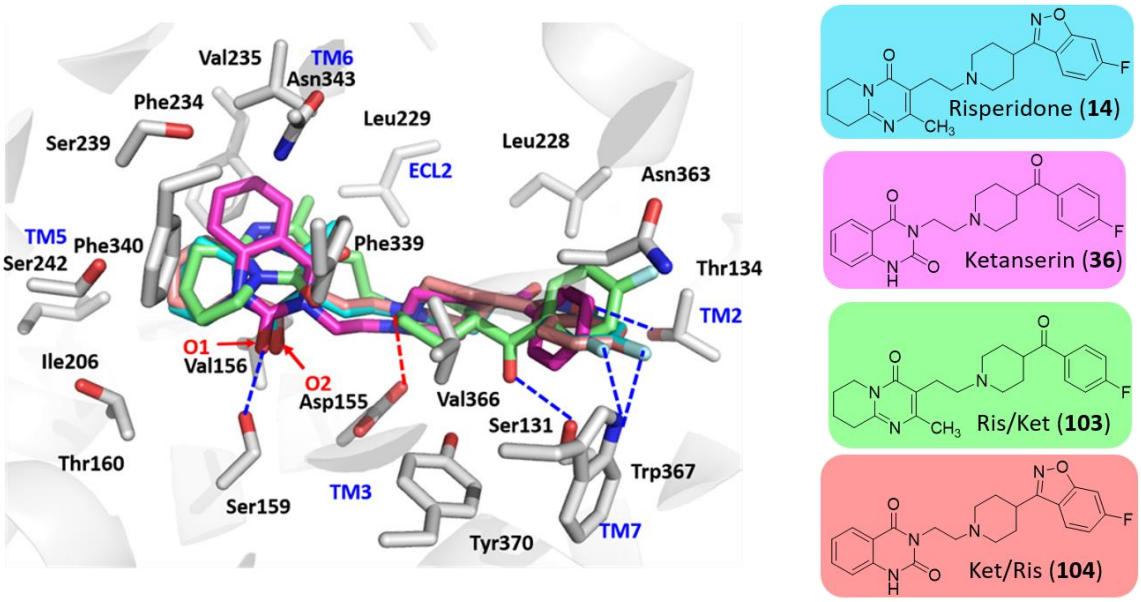

Figure 49. Docking modes of risperidone (**14**) (cyan), ketanserin (magenta), analogs **103** (green) and **104** (salmon) at the 5-HT_{2A} receptor (docking mode 2). The red dashed lines indicate ionic interactions and the blue dashed lines indicate hydrogen bonds.

Total HINT scores for risperidone (**14**), ketanserin (**36**), and their structural hybrids are summarized in Table 6. Both binding modes seem possible for risperidone (**14**) and the Ris/Ket (**103**), and Ket/Ris (**104**) hybrid. However, our molecular modeling studies suggest that binding mode 1 appears to be more likely for ketanserin (**36**) (total HINT score for binding mode 1 is 2-fold higher than total HINT score for binding mode 2), and hence, risperidone (**14**) and ketanserin

(**36**) might not be binding in a similar manner at the 5-HT_{2A} receptor. This could potentially explain the differences in binding affinities of the hybrids. Also the Ket/Ris (**104**) hybrid binds in a manner similar to risperidone (**14**), and this is supported by binding data since Ket/Ris (**104**) (K_i = 0.96 nM) had a binding affinity similar to that of risperidone (**14**) (K_i = 5.29 nM).

Ris/Ket (**103**) (K_i = 12.74 nM) binds with ~ 2-fold lower affinity than risperidone (K_i = 5.29 nM) and ~1.5-fold higher affinity than ketanserin (**36**). This suggests that the "right half" of risperidone (**14**) makes stronger interactions as compared to the "right half" of ketanserin (**36**). Ket/Ris (**104**) (K_i = 0.96 nM) binds with ~5.5- and ~19-fold higher affinity than risperidone (**14**) (K_i = 5.29 nM), and ketanserin (**36**) (K_i = 18.55 nM), respectively, suggesting that the "left half" of ketanserin (**36**) makes stronger interactions at the 5-HT_{2A} receptor as compared to the "left half" of risperidone (**14**). The high binding affinity of the Ket/Ris hybrid might be attributed to the quinazolinedione ring of the Ket/Ris hybrid (**104**) aligning/superimposing better with the 6,7,8,9-tetrahydro-4*H*-pyrido[1,2-*a*]pyrimidin-4-one ring of risperidone (**14**) as opposed to the quinazolinedione ring of ketanserin (**36**).

Table 6. Summary of HINT scores for binding modes 1 and 2 of risperidone (**14**), ketanserin (**36**), and analogs **103** and **104**.

Binding mode	Polar	Hydrophobic	Total HINT score*
Risperidone (**14**); Mode 1	1523	1225	1204
Risperidone (**14**); Mode 2	1475	1280	1001
Ketanserin (**36**); Mode 1	1658	900	1112
Ketanserin (**36**); Mode 2	1649	872	556
Ris/Ket (**103**); Mode 1	1387	1054	1044
Ris/Ket (**103**); Mode 2	1429	1357	992
Ket/Ris (**104**); Mode 1	1547	870	1121
Ket/Ris (**104**); Mode 2	1699	872	848

*Other terms, e.g., hydrophobic-polar, acid-acid and base-base are reflected in this total.

Figure 50 shows analogs **109** and **110** docked at the 5-HT_{2A} receptor. It can be compared to docking mode 1 of risperidone (**14**), however, the 6,7,8,9-tetrahydro-4*H*-pyrido[1,2-*a*]pyrimidin-4-one ring system ring system was displaced, and the fluorine atom of analog **110** is oriented differently as compared to the fluorine atom of risperidone (**14**) (Figure 50).

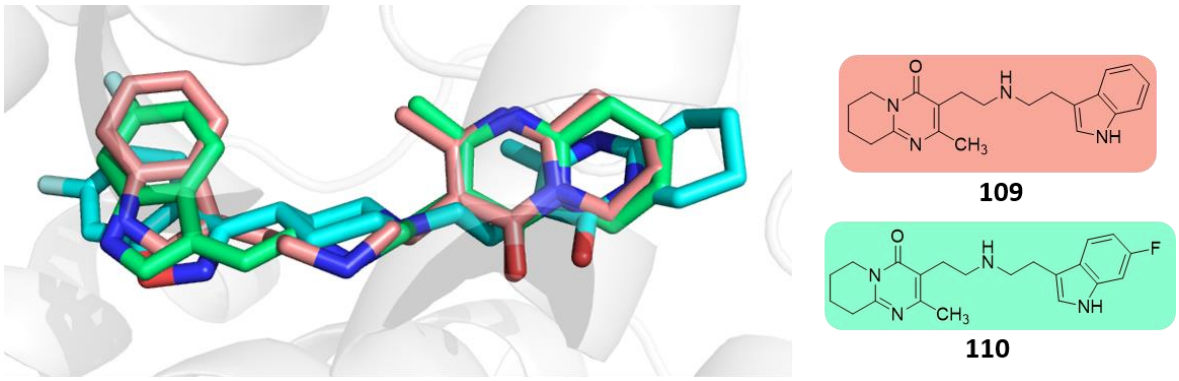

Figure 50. A comparison of the docking modes of analogs **109** (salmon) and **110** (green) with risperidone (**14**) (cyan) (docking mode 1).

Figure 51 shows the receptor-ligand interactions that analogs **109** and **110** make with the 5-HT_{2A} receptor in docking mode 1. A bidentate ionic interaction between the protonated amines of analogs **109** and **110** and Asp155 as well as a hydrogen bond between the oxygen atom of the 6,7,8,9-tetrahydro-4*H*-pyrido[1,2-*a*]pyrimidin-4-one ring system and Tyr370 was observed. Hydrophobic interactions with the amino acids Thr134, Ile152, Val156, Leu228, Phe234, Val235, Phe339, Phe340, Leu362, Trp336, Trp367, and Tyr370 were observed for analogs **109** and **110**. Analog **109** had a total HINT score of 1065, whereas analog **110** had a HINT score of 881 (Table 7), suggesting that analog **109** makes overall more favorable interactions in docking mode 1 at the 5-HT_{2A} receptor. However, the difference in total HINT scores does not appear to be substantial.

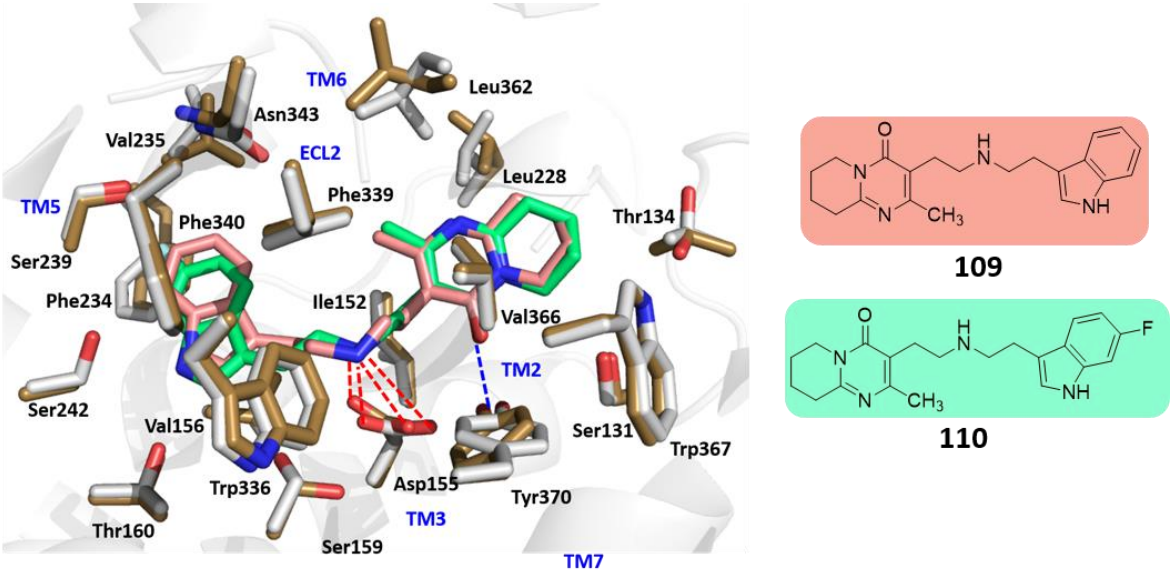

Figure 51. Docking modes of analogs **109** (salmon) and **110** (green) at the 5-HT_{2A} receptor (docking mode 1). The red dashed lines indicate ionic interactions and the blue dashed lines indicate hydrogen bonds.

Figure 52 shows analogs **109** and **110** docked at the 5-HT_{2A} receptor. It can be compared to docking mode 2 of risperidone (**14**), however, the 6,7,8,9-tetrahydro-4*H*-pyrido[1,2-*a*]pyrimidin-4-one ring system ring system was flipped by ~180 º along the horizontal axis, and the fluorine atom of analog **110** was oriented differently as compared to the fluorine atom of risperidone (**14**) (Figure 52).

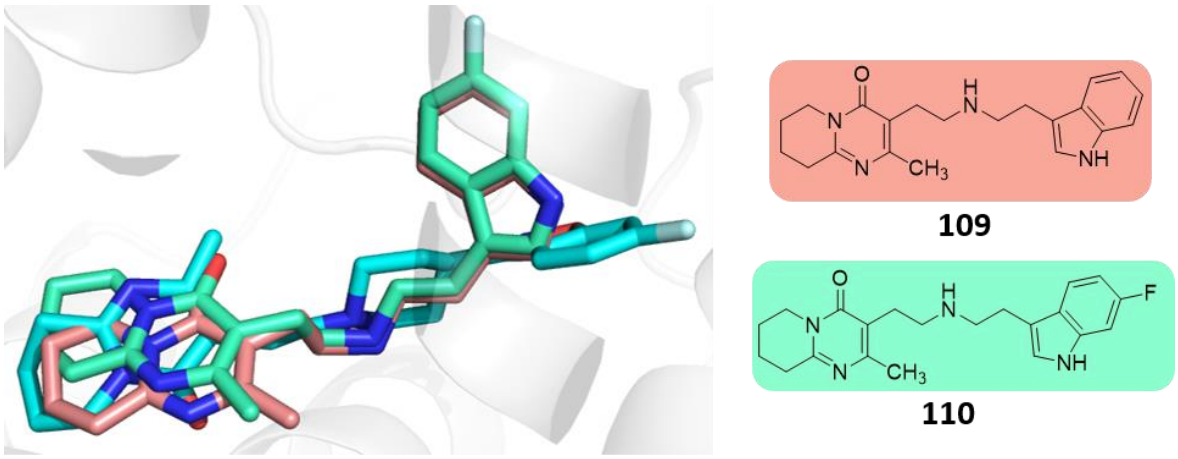

Figure 52. A comparison of the docking modes of analogs **109** (salmon) and **110** (green) with risperidone (**14**) (cyan) (docking mode 2).

Figure 53 depicts the receptor-ligand interactions that analogs **109** and **110** make with the 5-HT_{2A} receptor in docking mode 2. The nitrogen atoms of the indole rings of analogs **109** and **110** formed a hydrogen bond with Asn363. An ionic interaction between the protonated amines and Asp155 as well as a hydrogen bond between the N1 nitrogen atom of the 6,7,8,9-tetrahydro-4*H*-pyrido[1,2-*a*]pyrimidin-4-one ring system and Ser159 was observed. Hydrophobic interactions with the amino acids Thr134, Trp151, Ile206, Leu228, Leu229, Ile236, Phe234, Phe339, Phe340, and Tyr370 were observed for analogs **109** and **110**. The fluorine atom of analog **110** was involved in a hydrophobic interaction with Leu362. Analog **109** had a total HINT score of 1083, whereas analog **110** had a HINT score of 1297 (Table 7), suggesting that analog **110** makes overall more favorable interactions at the 5-HT_{2A} receptor in docking mode 2. However, the difference in total HINT scores does not appear to be substantial.

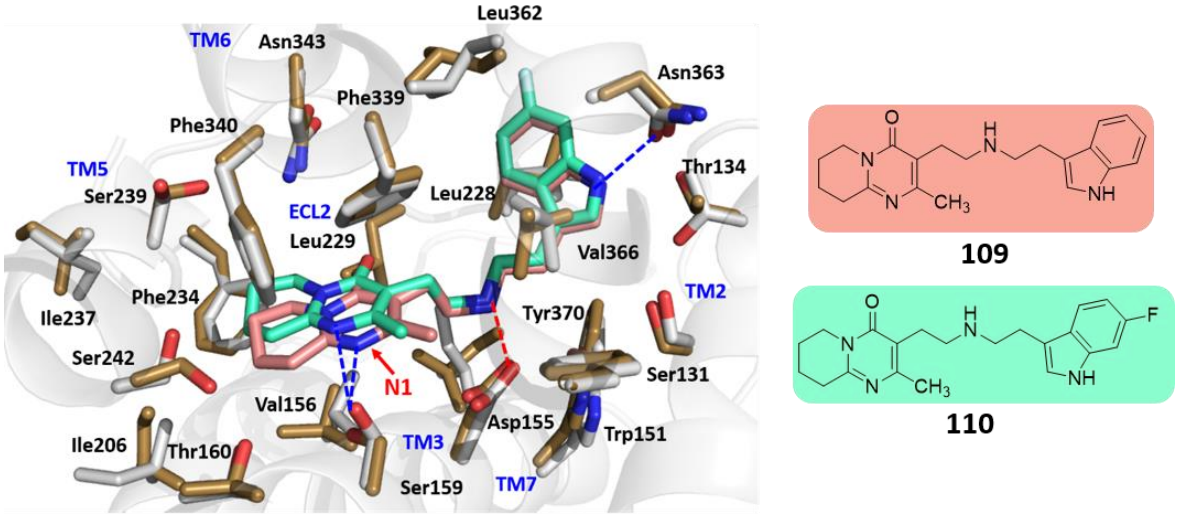

Figure 53. Docking modes of analogs **109** (salmon) and **110** (green) at the 5-HT_{2A} receptor (docking mode 2). The red dashed lines indicate ionic interactions and the blue dashed lines indicate hydrogen bonds.

Based on the total HINT scores both binding modes might exist for analog **109**, whereas binding mode 2 seems to be more likely for analog **110**.

Table 7. Summary of HINT scores for binding modes 1 and 2 of risperidone (**14**) and analogs **109** and **110.**

Binding mode	Polar	Hydrophobic	Total HINT score*
Risperidone (**14**) Mode 1	1523	1225	1204
Risperidone (**14**) Mode 1	1475	1280	1001
109; Mode 1	2038	952	1065
109; Mode 2	2175	1026	1083
110; Mode 1	2010	890	881
110; Mode 2	2160	1091	1297

*Other terms, e.g., hydrophobic-polar, acid-acid and base-base are reflected in this total.

Analogs **111** and **112** showed two docking modes at the 5-HT_{2A} receptor (Figures 54, 55 and 56).

Figure 54 shows analogs **111** and **112** docked at the 5-HT_{2A} receptor. The binding mode was consistent with binding mode 1 of risperidone (**14**), however, the 2-methyl-6,7,8,9-tetrahydro-4*H*-pyrido[1,2-*a*]pyrimidin-4-one ring system ("left half") of analogs **111** and **112** was oriented differently. Both analogs formed the essential ionic interaction with Asp155. The nitrogen atoms of the indole rings of both analogs formed a hydrogen bond with Ser159. Hydrophobic interactions with amino acid residues Trp151, Val156, Leu228, Leu229, Ile236, Trp336, Phe339, Phe340, and Tyr370 were observed for both analogs.

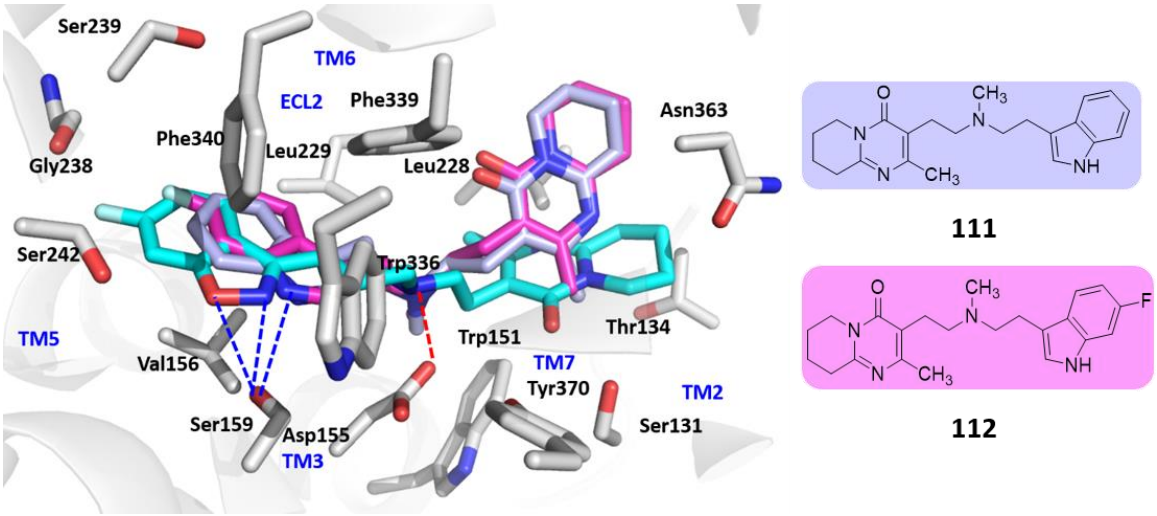

Figure 54. Docking modes of risperidone (**14**) (cyan), and analogs **111** (violet) and **112** (magenta) at the 5-HT_{2A} receptor (docking mode 1). The red dashed lines indicate ionic interactions and the blue dashed lines indicate hydrogen bonds.

In the second binding pose, analogs **111** and **112** were positioned in a manner similar to binding mode 2 of risperidone (**14**) at 5-HT_{2A} receptors (Figure 55). However, the 6,7,8,9-tetrahydro-4*H*-

pyrido[1,2-*a*]pyrimidin-4-one ring system ("left half") of analogs **111** and **112** was flipped by ~180º about the horizontal axis when compared to the "left half" of risperidone (**14**).

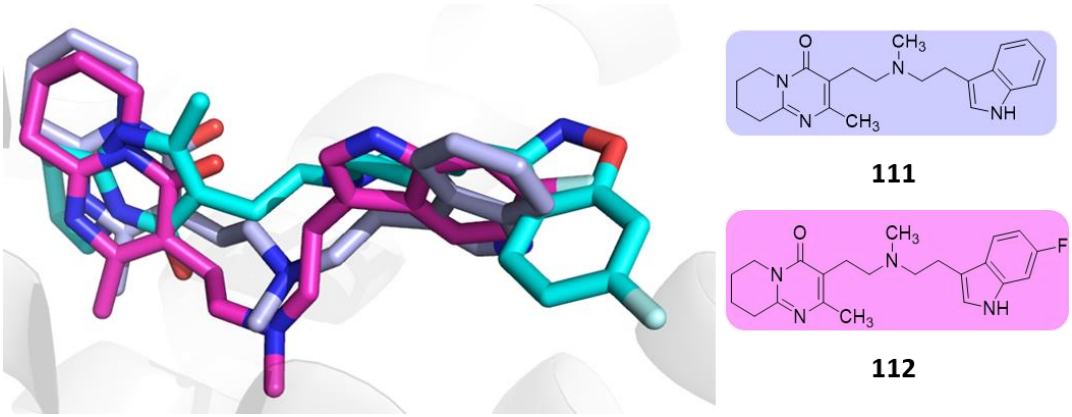

Figure 55. A comparison of docking modes of analogs **111** (violet) and **112** (magenta) with the docking mode 2 of risperidone (**14**) (cyan) at 5-HT_{2A} receptors.

The receptor-ligand interactions that analogs **111** and **112** make with the 5-HT_{2A} receptor in docking mode 2 are illustrated in Figure 56. The "left halves" of analogs **111** and **112** superimposed well, and were predominantly involved in hydrophobic interactions. The "right halves" of analogs **111** and **112** are comprised of an indole ring system and were oriented differently with respect to each other as well as with respect to the "right half" (benz[*d*]isoxazole ring) of risperidone (**14**). The protonated amines of both analogs formed a bidentate ionic interaction with the amino acid residue Asp155, and a hydrogen bond with Tyr370. The fluorine atom of analog **112** formed a hydrogen bond with Thr134. Additional hydrophobic interactions with amino acid residues Ile163, Trp151, Val156, Thr160, Leu228, Leu229, leu362, Trp336, Phe340, Val366 and Tyr370 were observed.

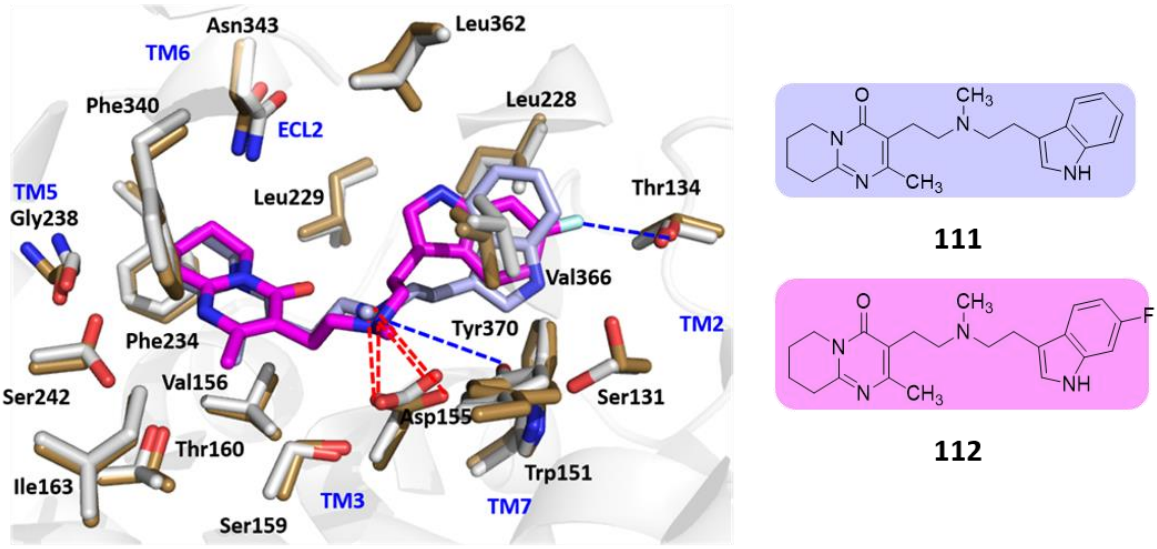

Figure 56. Docking modes of analogs **111** (violet) and **112** (magenta) at the 5-HT_{2A} receptor (docking mode 2). The red dashed lines indicate ionic interactions and the blue dashed lines indicate hydrogen bonds.

Modeling studies suggest that both binding modes are equally possible. Total HINT scores for analogs **111** and **112** are summarized in Table 8. Binding mode 2 seemed to have an overall higher HINT score as compared to the HINT score for binding mode 1 for analogs **111** and **112**, and suggested more favorable interactions at 5-HT_{2A} receptors in binding mode 2. However, the differences in the total HINT scores do not appear to be substantial. Analog **111** represents the desfluoro analog of compound **112.** Preliminary biological data indicate that analog **111** (K_i ~ 285 nM) binds with ~57-fold lower affinity than analog **112** (K_i ~ 5 nM) , suggesting that the fluoro group of analog **112** is playing a role in enhancing its binding affinity. In binding mode 1 for analog **112**, the fluorine atom did not seem to be making any significant contributions whereas in binding mode 2 the fluorine atom of analog **112** formed a hydrogen bond with Thr134. Hence, analogs **111** and **112** might be binding at the receptor in a manner that is consistent with binding

mode 2. The binding affinity of analog **112** is similar to the binding affinity of risperidone (**14**) suggesting that they might bind in a similar manner. However, the nitrogen atom of the indole ring of **112** is a hydrogen bond donor whereas the nitrogen and oxygen atoms of the benz[d]isoxazole ring of risperidone (**14**) are hydrogen bond acceptors and the nature of the hydrogen bonds they make with the receptor are different. This also suggests that the bifurcated hydrogen bond may not be crucial for binding affinity, and that risperidone (**14**) might be binding in a manner that is consistent with binding mode 2, even though both modes might exist.

Table 8. Summary of HINT scores for binding modes 1 and 2 of risperidone (**14**) and analogs **111** and **112**.

Binding mode	Polar	Hydrophobic	Total HINT score*
Risperidone (**14**), Mode 1	1523	1225	1204
Risperidone (**14**), Mode 2	1475	1280	1001
111 ; Mode 1	1316	1161	629
111; Mode 2	1495	1163	648
112; Mode 1	1263	1217	666
112; Mode 2	1411	1238	782

*Other terms, e.g., hydrophobic-polar, acid-acid and base-base are reflected in this total.

Analog **113** showed two docking modes at 5-HT_{2A} receptors (Figures 57 and 58).

Figure 57 depicts analog **113** docked at the 5-HT_{2A} receptor in a manner similar to docking mode 1 of risperidone (**14**). Analog **113** interacted with the 5-HT_{2A} receptor in a manner that has been

previously described for risperidone (**14**). The 2-methyl-4*H*-pyrido[1,2-*a*]pyrimidin-4-one ring system ("left half") of analog **113** is oriented differently as compared to the 2-methyl-6,7,8,9-tetrahydro-4*H*-pyrido[1,2-*a*]pyrimidin-4-one ring system ("left half") of risperidone (**14**), and makes an additional hydrophobic interaction with Leu362.

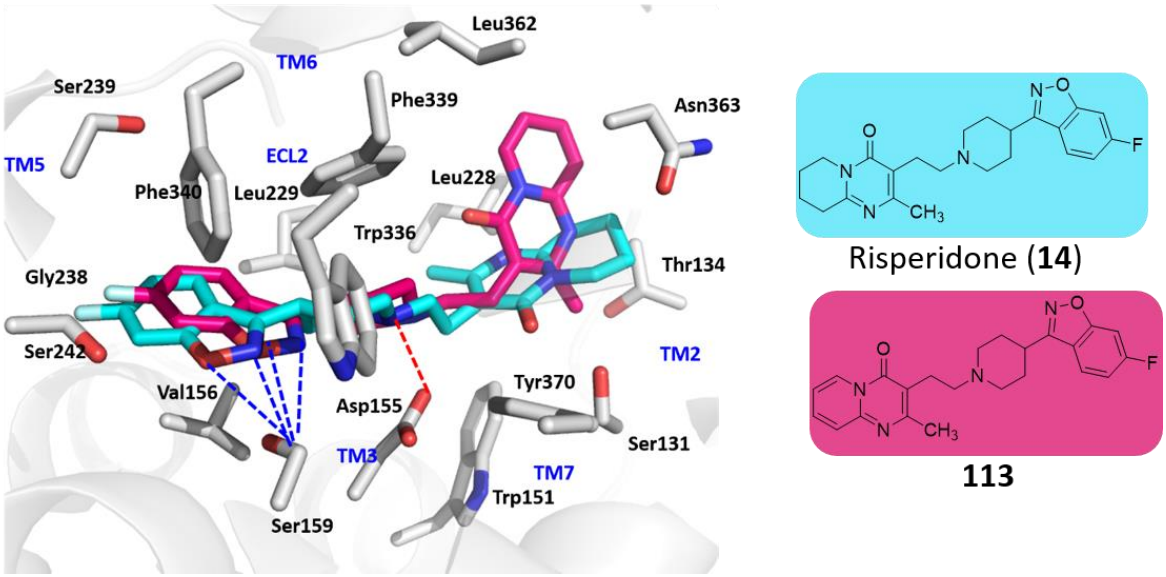

Figure 57. Docking modes of risperidone (**14**) (cyan) and analog **113** (pink) at the 5-HT$_{2A}$ receptor (docking mode 1). The red dashed lines indicate ionic interactions and the blue dashed lines indicate hydrogen bonds.

Figure 58 shows analog **113** docked at the 5-HT$_{2A}$ receptor in a manner similar to docking mode 2 of risperidone (**14**). Analog **113** interacts with the 5-HT$_{2A}$ receptor in a manner that has been previously described for docking mode 2 of risperidone (**14**).

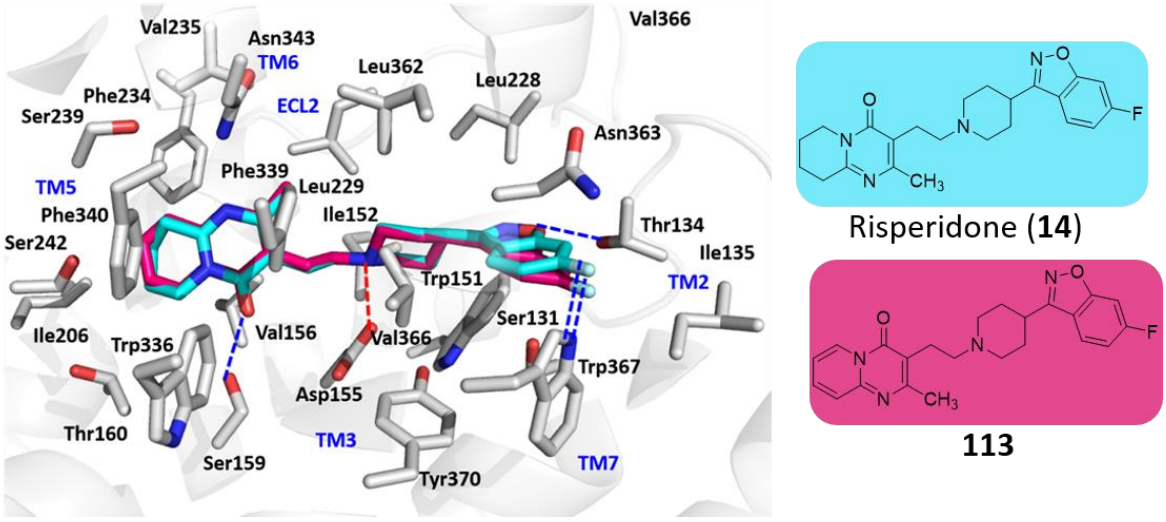

Figure 58. Docking modes of risperidone (**14**) (cyan) and analog **113** (pink) at the 5-HT_{2A} receptor (docking mode 2). The red dashed lines indicate ionic interactions and the blue dashed lines indicate hydrogen bonds.

Table 9 summarizes the HINT scores for docking modes 1 and 2 of analog **113**. Both modes seem possible, and there does not appear to be a substantial difference in the total HINT scores of risperidone (**14**) and analog **113**.

Table 9. Summary of HINT scores for binding modes 1 and 2 of risperidone (**14**), and analog **113**.

Binding mode	Polar	Hydrophobic	Total HINT score*
Risperidone (**14**); Mode 1	1523	1225	1204
Risperidone (**14**); Mode 2	1475	1280	1001
113; Mode 1	1654	1131	904
113; Mode 2	1575	1008	1102

*Other terms, e.g., hydrophobic-polar, acid-acid and base-base are reflected in this total.

Analogs **114**, **115**, **116** and **117** showed two docking modes at the 5-HT_{2A} receptor (Figures 59, 60, 61 and 62).

Figure 59 shows analogs **114-117** docked at the receptor in a pose that is analogous to docking mode 1 of risperidone (**14**). The benz[*d*]isoxazole rings ("right half") of all four analogs (**114**, **115**, **116** and **117**) were oriented in a manner similar to risperidone (**14**), the nitrogen and oxygen atoms of the benz[*d*]isoxazole rings form a bifurcated hydrogen bond with Ser159. The "left halves" of the molecules were oriented differently with respect to each other as well as risperidone (**14**). Hydrophobic interactions with amino acid residues Trp151, Val156, Thr134, Leu228, Leu229, Trp336, Phe339, Phe340 and Tyr370 were observed for all analogs. The phenyl rings of analogs **115** and analogs **117** formed additional hydrophobic interactions with Leu362 and Asn363. Analog **116** and **118** formed additional hydrophobic interactions with Leu362 and Trp141, respectively.

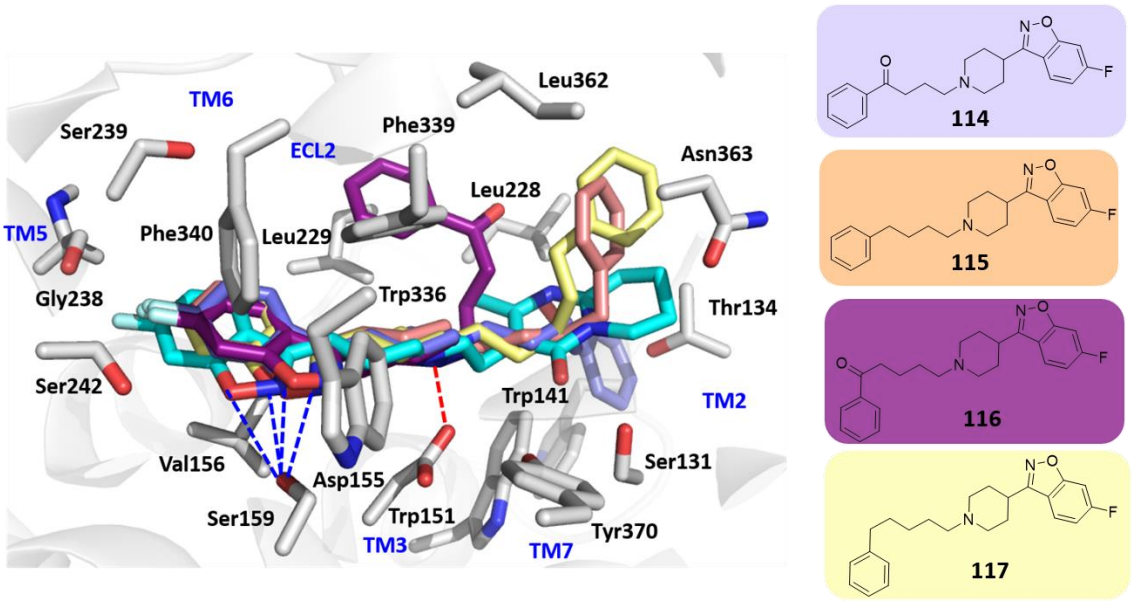

Figure 59. Docking modes of risperidone (**14**), and analogs **114** (violet), **115** (light orange), **116** (purple), and **117** (pale yellow) at the 5-HT_{2A} receptor (docking mode 1). The red dashed lines indicate ionic interactions and the blue dashed lines indicate hydrogen bonds.

Figure 60 shows analogs **114** and **116** docked at the 5-HT_{2A} receptor. The orientation can be compared to docking mode 2 of risperidone (**14**) at the 5-HT_{2A} receptor.

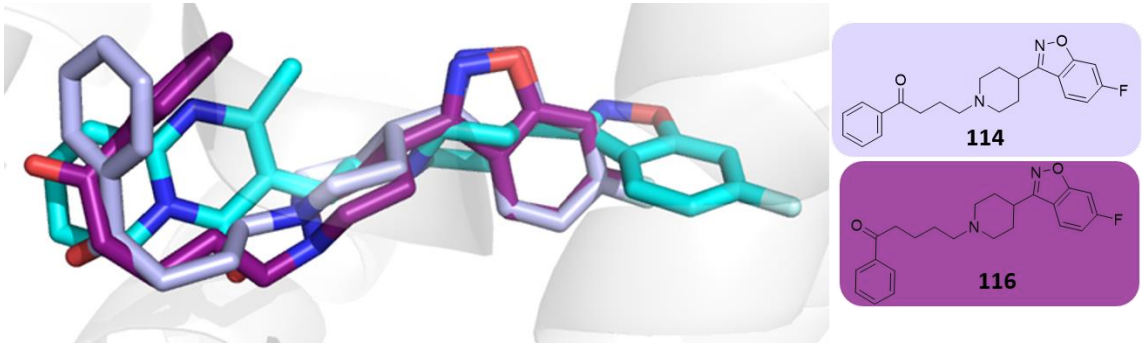

Figure 60. A comparison of the docking modes of risperidone (**14**), and analogs **114** (violet) and **116** (purple), at the 5-HT_{2A} receptor.

The receptor-ligand interactions that analogs **114** and **116** make with the 5-HT_{2A} receptor are depicted in Figure 61. The protonated amines of analogs **114** and **116** formed an ionic interaction

with the amino acid residue Asp155, and a hydrogen bond with Tyr370. The carbonyl oxygen atoms of both the molecules formed a hydrogen bond with Ser242, the carbonyl oxygen atom of analog **114** formed an additional hydrogen bond with Thr160. Additional hydrophobic interactions with Thr134, Ile206, Leu228, Leu229, Val235, Trp336, Phe339, Phe340, Asn343, and Val366 were observed for both analogs.

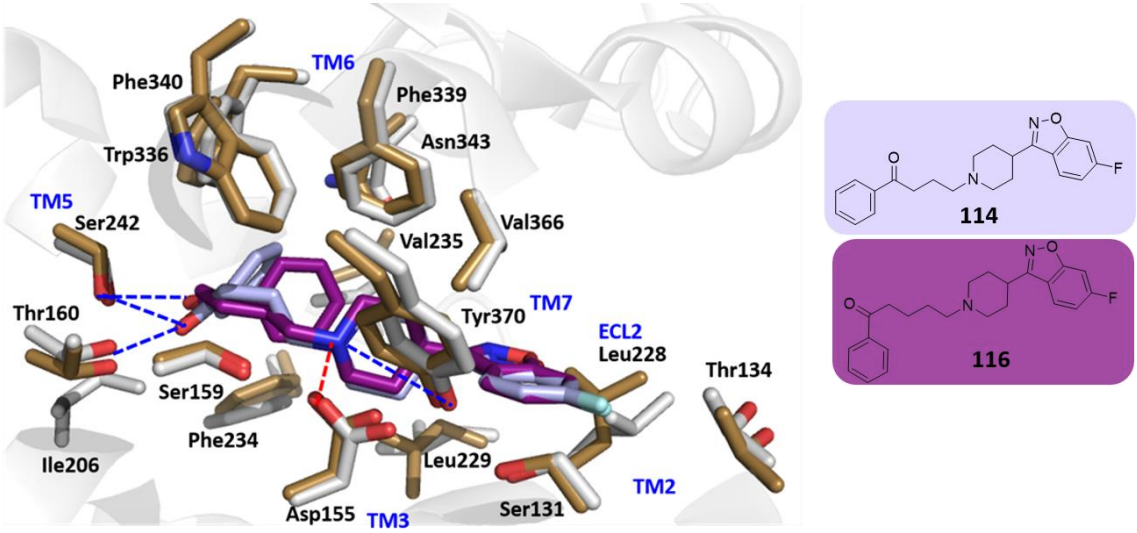

Figure 61. Docking modes of analogs **114** (violet) and **116** (purple) at the 5-HT_{2A} receptor (docking mode 2). The red dashed lines indicate ionic interactions and the blue dashed lines indicate hydrogen bonds.

Figure 62 shows analogs **115** and **117** docked at the 5-HT_{2A} receptor in an orientation similar to the docking mode 2 of risperidone (**14**). The benz[*d*]isoxazole rings ("right half") of both analogs aligned with the benz[*d*]isoxazole ring of risperidone (**14**), and the oxygen and fluorine atoms of benz[*d*]isoxazole rings of the analogs formed hydrogen bonds with Thr134 and Trp151, respectively. Additionally, hydrophobic interactions with Ile135, Trp151, Ile152, Leu228, Leu229, Phe234, Leu362, Trp336, Phe339, Phe340, Val 366, Trp367 and Tyr370 were observed.

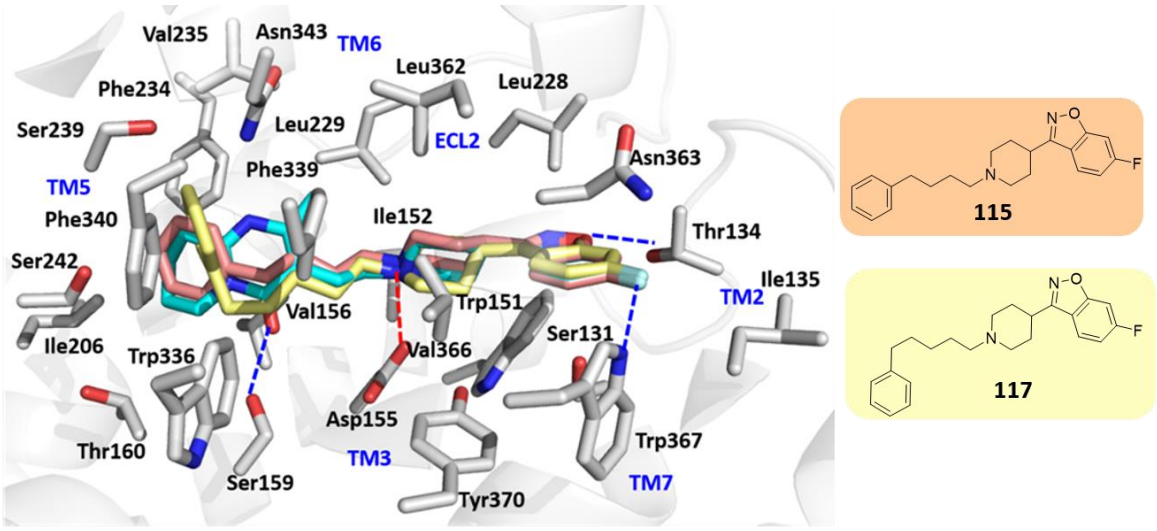

Figure 62. Docking modes of risperidone (**14**) (cyan), and analogs **115** (salmon) and **117** (pale yellow) at the 5-HT_{2A} receptor (docking mode 2). The red dashed lines indicate ionic interactions and the blue dashed lines indicate hydrogen bonds.

The HINT scores for analogs **114**, **115**, **116,** and **117** are summarized in Table 10.

Table 10. Summary of HINT scores for binding modes 1 and 2 of risperidone (**14**) and analogs **114**, **115**, **116** and **117**.

Binding mode	Polar	Hydrophobic	Total HINT score*
Risperidone (**14**); Mode 1	1523	1225	1204
Risperidone (**14**); Mode 2	1475	1280	1001
114; Mode 1	1510	838	992
114; Mode 2	1701	763	927
115; Mode 1	1344	931	1004
115; Mode 2	1285	897	1199
116; Mode 1	1669	784	769
116; Mode 2	1609	931	853
117; Mode 1	1548	984	1274
117; Mode 2	1287	807	996

*Other terms, e.g., hydrophobic-polar, acid-acid and base-base are reflected in this total.

Modeling studies suggest that both binding modes are possible for analogs **114**, **115**, **116** and **117**. The total HINT scores for the analogs do not appear to be substantially different.

3. Summary

Modeling studies suggest that risperidone (**14**) might bind in two different modes that might be equally feasible. However, biological data suggests that a fluorine atom enhances binding affinity, and that the carbonyl oxygen group might contribute towards enhancing 5-HT_{2A} receptor antagonist activity, albeit to a very small extent. This suggests that binding mode 2 of risperidone

(**14**) might be the preferred orientation, since both the fluoro group and the carbonyl group make interactions with the receptor in binding mode 2. Additionally, modeling studies suggest that ketanserin might be utilizing binding mode 1 suggesting that risperidone (**14**) and ketanserin (**36**) might have different orientations at the 5-HT_{2A} receptor.

The different scenarios for preferred binding modes of risperidone (**14**) and its analogs are summarized in Table 11.

Table 11. A summary of the preferred binding modes of risperidone (**14**) and its deconstructed and elaborated analogs.

Binding modes	**Analogs**
Mode 1 = Mode 2	Risperidone (**14**), **64**, **68**, **103**, **104**, **111**, **112**, **113**, **114**, **115**, **116**, **117**
Mode 1 > Mode 2	Ketanserin (**36**)
Mode 1 < Mode 2	**110**
No mode 1, only mode 2	**57**, **58**, **59**

D. Specific Aim 4. $mGlu_2$ receptor PAMs

a. Molecular modeling studies of the allosteric site of the $mGlu_2$ receptor to determine whether structurally diverse PAMs of the $mGlu_2$ receptor bind in a similar manner and in the same binding pocket

1. Approach

The $mGlu_2$ receptor allosteric site is in the TMD.[192] Molecular modeling studies of the TMD of the $mGlu_2$ receptor were conducted to study the allosteric binding site, and also to determine how structurally diverse $mGlu_2$ receptor PAMs bind relative to one another and whether they bind in the same binding pocket.

At the time the modeling studies were conducted there was limited mutagenesis data available, and the PAM binding pocket was not well defined. Schaffhauser et al.[192] have identified that Ser688 (TM4), Gly689 (TM4), and Asn735 (TM5) are important for positive allosteric modulation of the $mGlu_2$ receptor. They identified that either Ser688 or Gly689 in combination with Asn735 or a combination of all three residues together forms the binding pocket of the PAM LY487379 (**44**) (Figure 21).[192] Hemstapat et al.[193] subsequently reported mutagenesis data for LY487379 (**44**) (Figure 21) binding that was consistent with previous studies by Schaffhauser et al.[192] They additionally reported that binding of the structurally diverse PAM BINA (**43**) (Figure 21) is also affected by Ser 688 (TM4), Gly 689 (TM4) and Asn735 (TM5) mutants, and potentially binds in the same binding pocket as LY487379 (**44**). LY487379 (**44**) and BINA(**43**) are selective for the $mGlu_2$ receptor over the $mGlu_3$ receptor.[192,193] Hempstapat et al.[193] have demonstrated that the negative allosteric modulator (NAM) MNI-135 is not affected by mutations of Ser688, Gly689

and Asn735, and does not show any selectivity for the $mGlu_2$ receptor over the $mGlu_3$ receptor, suggesting that the $mGlu_2$ receptor might have multiple allosteric binding sites. Conversely, Lundström et al.[194] have reported that Asn 735 mutants do affect the activity of NAMs, albeit to a lower extent than that of PAMs. However, they were not able to find any direct interactions between NAMs and Asn735 and they have hypothesized that Asn735 might be important for receptor stabilization. Additionally, Lundström et al.[194] demonstrated that NAMs: RO4988546 and RO5488608 can completely displace the [^{3}H] PAM- [^{3}H]-2,2,2-TEMPS, suggesting that NAMs and PAMs of the $mGlu_2$ receptor might occupy overlapping sites.

A cavity search was performed using the MOLCAD function in SYBYL-X 2.1. Five cavities were detected. (Figure 63 A). Ser688, Gly689 and Asn735 were not a part of the same cavity. Asn735 was located close to a larger and more well defined pocket (Figure 63 B). Based on the cavity search, and site-directed mutagenesis studies, we defined the PAM binding pocket as being within a 10 Å radius of the amino acid residue Asn735 (TM5) for our docking studies. Figure 64 illustrates the PAM JNJ-40411813 (**45**) docked in our homology model of the TMD of the $mGlu_2$ receptor.

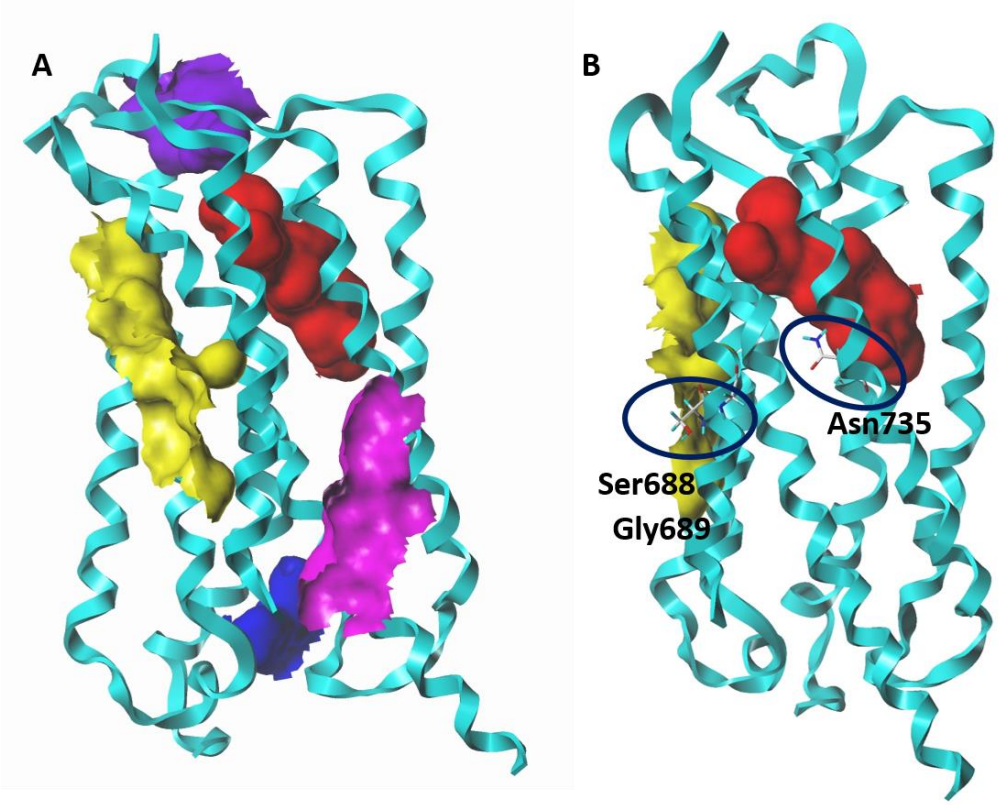

Figure 63. (A) Potential binding pockets in the TMD of the $mGlu_2$ receptor; (B) binding pockets located close to residues Ser688, Gly689 and Asn735.

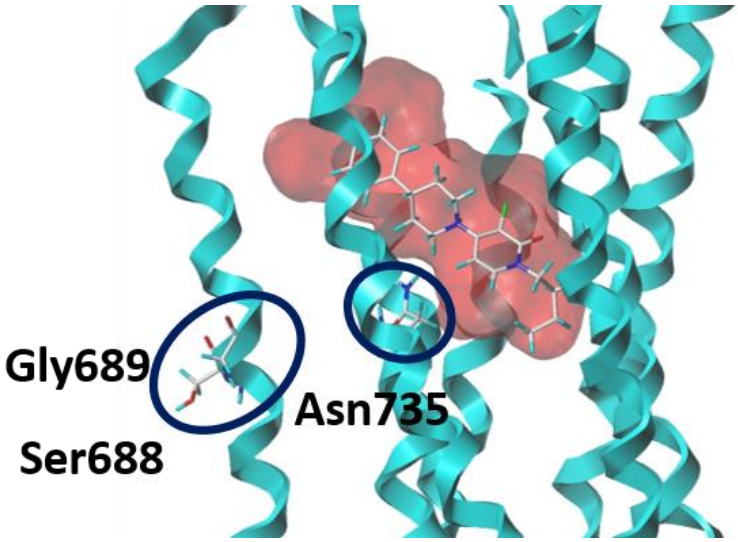

Figure 64. JNJ-40411813 (**45**) docked in our $mGlu_2$ receptor homology model.

Four known $mGlu_2$ receptor PAMs: BINA (**43**), LY487379 (**44**), JNJ-40411813 (**45**), and JNJ-40068782 (**46)** (Figure 21) were selected for our docking studies.

The $mGlu_2$ receptor is composed of 872 amino acids and is about 96 kDa. [Universal Protein Resource (UniProt) database; accession code: Q11416]. The extracellular domain of the $mGlu_2$ receptor has been crystallized and houses the orthosteric binding site.[195] Since the crystal structure of the TMD of the $mGlu_2$ receptor has not yet been solved, three-dimensional homology models of the TMD of the $mGlu_2$ receptor were constructed.

2. Results and discussion

a. Template, alignment and generation of homology models

The metabotropic glutamate receptor type 5 ($mGlu_5$) shares high sequence identity (~50%) with the $mGlu_2$ receptor. The crystal structure of the TMD of $mGlu_5$ receptor co-crystallized with the

NAM mavoglurant has been solved (PDB ID:4OO9; resolution: 2.6 Å),[196] and served as a template for building homology models of the $mGlu_2$ receptor. One major disadvantage of using this template is that it is the crystal structure of the inactive form of the receptor. The X-ray crystal structure of the $mGlu_5$ receptor suggests that Lys665 in TM3 forms a salt-bridge interaction (ionic-lock) with Glu770 in TM6, and also interacts with Ser 613 in intracellular loop 1 (ICL1).[196] Arg668 in TM3 forms a H-bond with Ser614 in ICL1, and constitutes a secondary lock tethering TM3 to TM6 via a secondary lock (Figure 65).[196] Lys665, Glu770 and Ser613 are highly conserved across most class C GPCRs, and this ionic-lock can be considered a hallmark feature of the inactive state of the receptor.[196] However, the mechanism of activation still lacks understanding and a likely active state is still unknown.

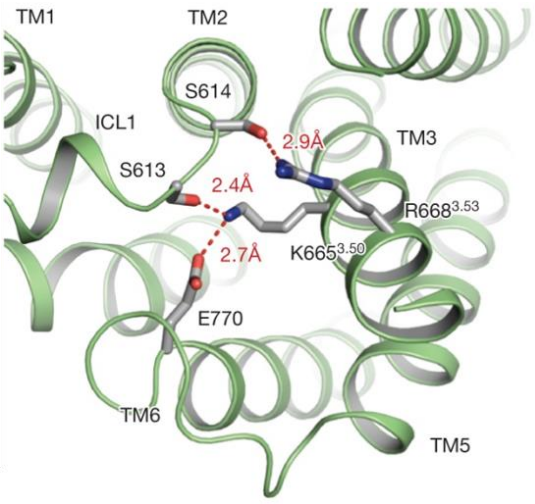

Figure 65. Ionic lock mechanism for maintenance of the inactive state of the $mGlu_5$ receptor.[196]

The $mGlu_2$ receptor TMD sequence was obtained in the form of a FASTA file from the Universal Protein Resource (UniProt) database (UniProt accession code: Q14416), whereas the FASTA file for the sequence of the template was obtained from the Protein Databank (PDB ID: 4OO9). The

$mGlu_2$ receptor TMD amino acid sequence was aligned with the amino acid sequence of the TMD of the $mGlu_5$ receptor using CLUSTAL X 2.1.[178] Since the sequence identity between the $mGlu_2$ receptor and the $mGlu_5$ receptor is high (~50%) the sequences aligned well. (Figure 66)

```
4009_A|PDBID|CHAIN|SEQUENCE     AASPVQYLRWGDPAPIAAVVFACLGLLATLFVTVVFIIYRDTPVVKSSSR
sp|Q14416|GRM2_HUMAN            ----QEYIRWGDAWAVGPVTIACLGALATLFVLGVFVRHNATPVVKASGR
                                     :*:****. .:..*.:**** ******  **: :. *****:*.*
                                                          TM1
4009_A|PDBID|CHAIN|SEQUENCE     ELCYIILAGICLGYLCTFCLIAKPKQIYCYLQRIGIGLSPAMSYSALVTK
sp|Q14416|GRM2_HUMAN            ELCYILLGGVFLCYCMTFIFIAKPSTAVCTLRRLGLGTAFSVCYSALLTK
                                *****:*.*: * *  ** :****.   * *:*:*:* : ::.****:**
                                         TM2                                TM3
4009_A|PDBID|CHAIN|SEQUENCE     TYRAARILAMSKKKICTKKPRFMSACAQLVIAFILICIQLGIIVALFIME
sp|Q14416|GRM2_HUMAN            TNRIARIFGGAREG--AQRPRFISPASQVAICLALISGQLLIVVAWLVVE
                                * * ***:. :::   :::***:*..:*:.*.: **. ** *:** :::*
                                TM3                                TM4
4009_A|PDBID|CHAIN|SEQUENCE     PPDIMHDYPSIR--EVYLICNTTNLGVVAPLGYNGLLILACTFYAFKTRN
sp|Q14416|GRM2_HUMAN            APGTGKETAPERREVVTLRCNHRDASMLGSLAYNVLLIALCTLYAFKTRK
                                .*.  :: .. *   * * **  : .:::.*.** ***  **:******:
                                                       TM5
4009_A|PDBID|CHAIN|SEQUENCE     VPANFNEAKYIAFTMYTTCIIWLAFVPIYFG--SNYKIIT--MCFSVSLS
sp|Q14416|GRM2_HUMAN            CPENFNEAKFIGFTMYTTCIIWLAFLPIFYVTSSDYRVQTTTMCVSVSLS
                                 * ******:*.**************:**::   *:*:: *  **.*****
                                                  TM6                  TM7
4009_A|PDBID|CHAIN|SEQUENCE     ATVALGCMFVPKVYIILAKPERNVRS---------AAAAHHHHHHHHHH-
sp|Q14416|GRM2_HUMAN            GSVVLGCLFAPKLHIILFQPQKNVVSHRAPTSRFGSAAARASSSLGQGSG
                                .:*.***:*.**::*** :*::** *         :***:      :
                                       TM7
4009_A|PDBID|CHAIN|SEQUENCE     ---------------------
sp|Q14416|GRM2_HUMAN            SQFVPTVCNGREVVDSTTSSL
```

Figure 66. Sequence alignment of the $mGlu_5$ receptor (template) with the $mGlu_2$ receptor (to be modeled).
(*) fully conserved residues between the sequences; (:) highly conserved residues between the sequences; (.) weakly conserved residues between the sequences.

Homology models (100) were generated using MODELLER v9.12.[179] Hydrogen atoms were added to the homology models and disulfide bonds were built using SYBYL-X 2.1. Figure 67 illustrates a homology model of the TMD of the $mGlu_2$ receptor that was generated as a part of this study.

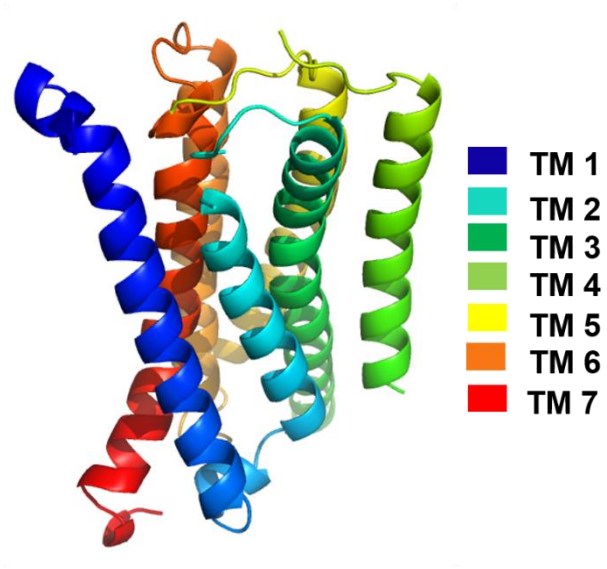

Figure 67. A representative homology model of the TMD of the $mGlu_2$ receptor that was generated as a part of this study.

b. Validation and Docking studies

Ramachandran plots were generated using MolProbity.[197] The plots (Figure 68) indicated that 97.5% (231/237) of the residues were in favored regions, 99.6% (236/237) of the residues were in allowed regions, and there was one outlier (Gln790).

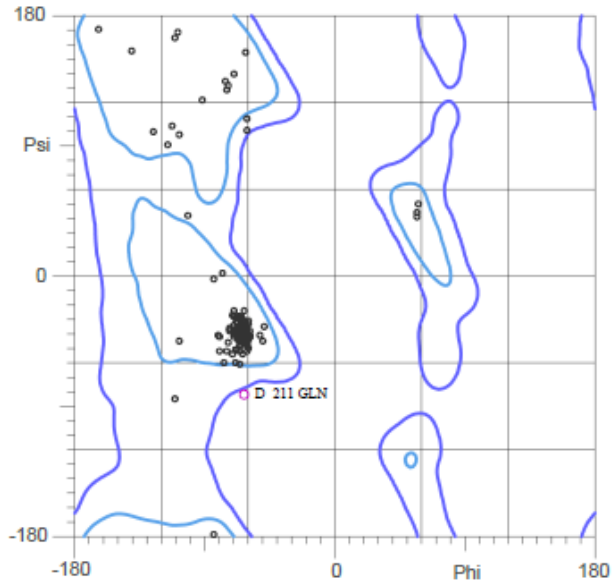

Figure 68. Ramachandran plot for a homology model of the $mGlu_2$ receptor [Gln211 corresponds to Gln790 (amino acids were renumbered after generation of the Ramachandran plot)].

Molecules were sketched using SYBYL-X 2.1, energy-minimized, and docked into the 100 homology models of the $mGlu_2$ receptor using GOLD Suite 5.2,[187] The docking solutions were scored using the ChemPLP function. Docked solutions were divided into clusters using a script provided by Dr. Philip Mosier (Intracluster RMSD $\leq$ 2.0 Å). Top solutions (based on ChemPLP scores and cluster size) were analyzed using SYBYL-X 2.1, and best models were selected. Best models and solutions were merged and energy-minimized. HINT[188] analysis was performed to choose the best models.

Four well characterized PAMs- BINA (**43**), LY487379 (**44**), JNJ-40411813 (**45**), and JNJ-40068782 (**46**) (Figure 21) were docked in our homology models, and all four ligands were found to have a common docking pose and docked in the same binding pocket (Figure 69). Based on our modeling studies we have proposed that the PAM binding pocket is comprised of the following

amino acid residues: Arg635 (ECL2). Leu639, Gly640, Phe643 (TM3), Ser731, Met728, Leu732, Asn735, Val736, Ser737 (TM5), Thr769, Ile772, Trp773 (TM6), Met794, Ser797, Val798 (TM7).

After the completion of our molecular modeling studies conducted to gain insight into the binding mode of PAMs, a study characterizing the binding pocket of PAMs with mutagenesis data and homology modeling of the TMD of the $mGlu_2$ receptor by Farinha et al.[198] and more recently by Lundström et al.[199] was reported. Site-directed mutagenesis data reported in the literature have shown the following residues to be important for the activity of multiple PAMs : Arg635, Leu639, Phe643 (TM3), Ser688, Gly689 (TM4), Leu732 (TM5) and Trp773, Phe776 (TM6), Ser797(TM7),[192,198,199] Trp773, and Asn735 mutants impact the activity and potency of most PAMs to a greater extent as compared to mutants of other amino acid residues.[198]

The binding pocket for PAMs that we characterized is similar to what has now been reported in the literature.[198,199] Of these, the amino acid residues Arg635, Leu639, Phe643, Leu732, Asn735, Trp773, and Ser797 were found important in prior site-directed mutagenesis studies

Ser688 and Gly689 were not located close to the binding pocket of PAMS. It has been suggested that Ser688 and Gly689 might be involved in indirect signaling effects or in receptor dimerization.[198]

The receptor-ligand interactions for PAMs: BINA (**43**), LY487379 (**44**), JNJ-40411813 (**45**), and JNJ-40068782 (**46**) with the mGlu2 receptor are shown in Figure 69.

The oxygen atoms of the indanone ring of BINA (**43**), the sulfonyl group of LY487379 (**44**), and the oxygen atoms of the pyridone rings of JNJ-40411813 (**45**) and JNJ-40068782 (**46**) formed a hydrogen bond with Ser797. The carboxylate group of BINA (**43**) formed an ionic salt-bridge interaction with Arg635. Additionally, the molecules formed hydrophobic interactions with Leu639, Phe643, Leu732, Val736, Ile739, Ile772, Trp773 and Val798. BINA (**43**) makes an additional hydrophobic interaction with Met794. Site-directed mutagenesis data suggests that Asn735 is important for binding of PAMs; however, we did not observe any hydrogen bonds with Asn735 in this docking pose, and as previously suggested for NAMS, Asn735 might be involved in receptor stabilization.[194]

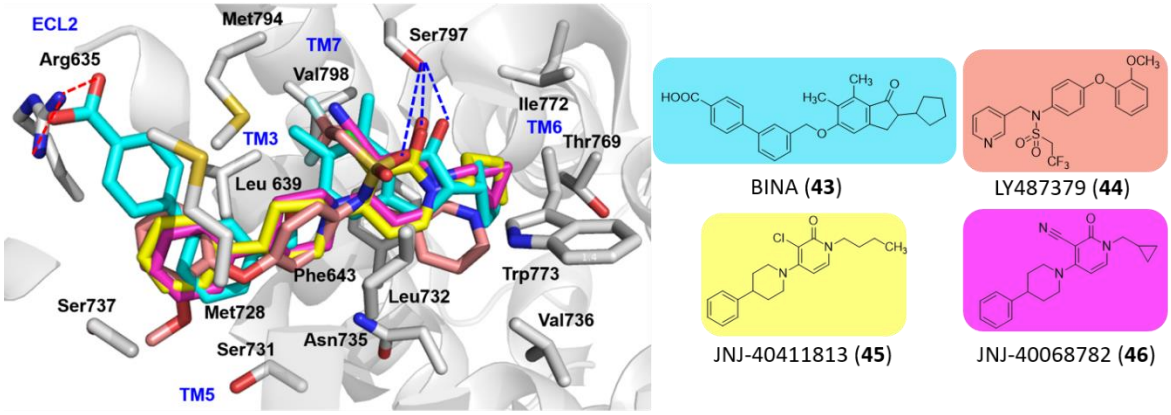

Figure 69. Receptor-ligand interactions of BINA (**43**) (cyan), LY487379 (**44**) (salmon), JNJ-40411813 (**45**) (yellow), and JNJ-40068782 (**46**) (magenta) with the $mGlu_2$ receptor (binding mode 1). The red dashed lines indicate ionic interactions and the blue dashed lines indicate hydrogen bonds.

BINA (**43**) and LY487379 (**44**) also dock in a different orientation where we observed hydrogen bonds with Asn735, and are shown in Figures 70 and 71, respectively.

The receptor-ligand interactions for BINA (**43**) with the $mGlu_2$ receptor (docking mode 2) are shown in Figure 70. The oxygen atom of the indanone ring of BINA (**43**) forms a hydrogen bond with Asn735. Hydrophobic interactions with the amino acid residues Leu639, Leu732, Val736, Phe643, Met728, Trp773, Phe776, Ile 779, Val796, Val798, Thr793, and Leu800 were observed.

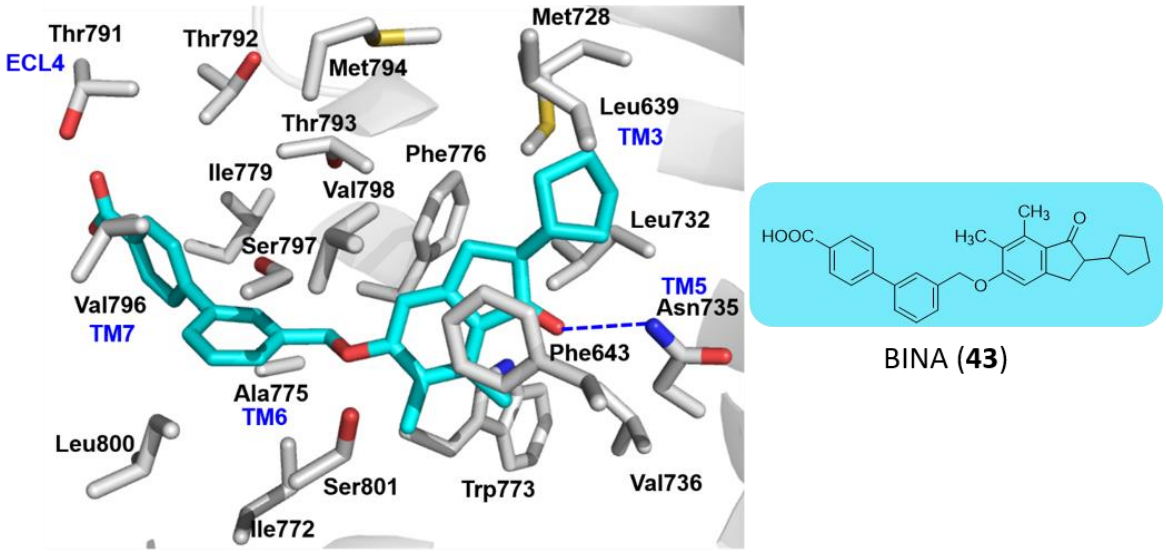

Figure 70. Receptor-ligand interactions for BINA (**43**) with the $mGlu_2$ receptor (docking mode 2). The blue dashed indicate hydrogen bonds.

The receptor-ligand interactions of LY487379 (**44**) with the $mGlu_2$ receptor (docking mode 2) are shown in Figure 71. The sulfonyl oxygen atom of LY487379 (**44**) formed a hydrogen bond with Asn735, while the pyridinyl nitrogen atom formed a hydrogen bond with Ser801. Hydrophobic interactions with several amino acid residues such as His723, Leu639, Leu732, Val736, Val798, Phe643, Phe776, Trp773, Tyr647, Ile739, and Ile772 were observed.

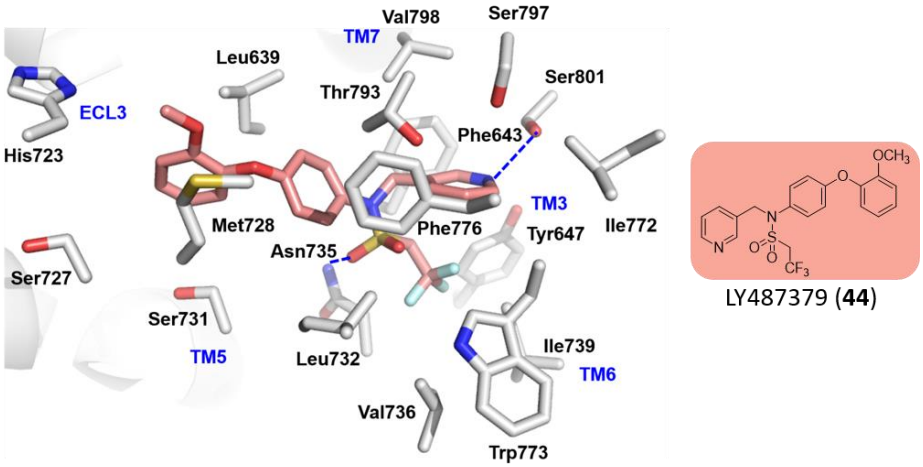

Figure 71. Receptor-ligand interactions for LY487379 (**44**) with the $mGlu_2$ receptor (docking mode 2). The blue dashed lines indicate hydrogen bonds.

HINT scores for PAMs: BINA (**43**), LY487379 (**44**), JNJ-40411813 (**45**), and JNJ-40068782 (**46**) are summarized in Table 12. BINA (**43**) had a higher total HINT score in mode 1 as compared to mode 2, and mode 1 might be the preferred orientation whereas the total HINT score for mode 2 of LY487379 (**44**) was higher as compared to mode 1, and LY487379 (**44**) might bind in a manner that utilizes mode 2.

Table 12. Summary of HINT scores for $mGlu_2$ PAMs: BINA (**43**), LY487379 (**44**), JNJ-40411813 (**45**), and JNJ-40068782 (**46**).

Binding mode	Polar	Hydrophobic	Total HINT score*
BINA (**43**); Mode 1	2232	1941	1124
BINA (**43**); Mode 2	531	2083	554
LY487379 (**44**); Mode 1	881	1482	205
LY487379 (**44**); Mode 2	1645	883	996
JNJ-40411813 (**45**)	2227	1077	517
JNJ-40068782 (**46**)	545	889	113

*Other terms, e.g., hydrophobic-polar, acid-acid and base-base are reflected in this total.

Modeling studies suggest that BINA (**43**), JNJ-40411813 (**45**), and JNJ-40068782 (**46**) might be binding similarly whereas LY487379 (**44**) might bind in a different orientation. Additionally, the HINT scores for all four PAMs seem to be substantially different suggesting that they may have different binding affinities and/or potencies.

b. Synthesis of the $mGlu_2$ receptor PAM JNJ-40411813 (45)

1. Approach

A long-term goal of this project is to synthesize a bivalent ligand where a 5-HT_{2A} receptor antagonist will be tethered to an $mGlu_2$ PAM via a linker. An $mGlu_2$ PAM was chosen over an $mGlu_2$ receptor orthosteric agonist for two main reasons. The allosteric modulatory site is in the TMD as opposed to the orthosteric agonist binding site that is in the extracellular domain of $mGlu_2$ receptors. This is important because the 5-HT_{2A} receptor antagonist binding site is in the TMD,

and it might be easier to connect a PAM that binds to the TMD of the $mGlu_2$ receptor as compared to connecting an orthosteric agonist that binds in the extracellular domain via a linker. Another reason was that $mGlu_2$ receptor PAMS are selective for $mGlu_2$ receptors over $mGlu_3$ receptors, whereas orthosteric $mGlu_2$ agonists are not selective for $mGlu_2$ over $mGlu_3$ receptors.[193]

JNJ-40411813 (**45**) was chosen for several reasons: (i) the SAR of JNJ-40411813 (**45**) at the mGlu2 receptor has been studied previously;[119] (ii) JNJ-40411813 (**45**) has shown antipsychotic potential in preclinical studies;[119] and (iii) the nitrogen atom of the pyridone ring can serve as a potential positon to attach a linker.

Based on SAR studies we know that the nitrogen atom of JNJ-40411813 (**45**) can tolerate longer chain lengths, and our molecular modeling studies suggest that the binding pocket has room to accommodate a longer chain length, making JNJ-40411813 (**45**) an ideal candidate.

The synthesis of JNJ-40411813 (**45**) has been reported by Cid et al,[119] and is outlined in Scheme 23. A drawback of this scheme was that the nitrogen substituent was added in the first step. Our aim was to synthesize multiple compounds, with varying linkers at the nitrogen atom of the pyridine ring, and hence, we decided to utilize a different synthetic route where the linker would be added in the penultimate/final step. This would enable us to synthesize multiple molecules relatively quickly.

Scheme 23. Synthesis of JNJ-40411813 (**45**)[a] (as reported by Cid et al.[119]).

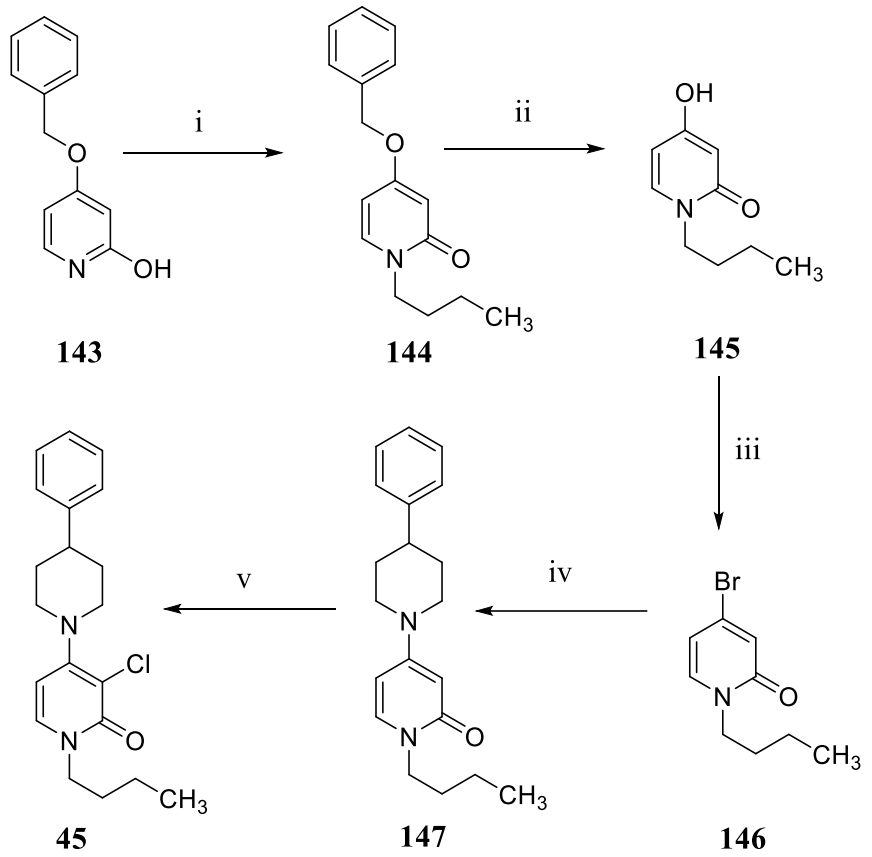

[a]Reagents and Conditions. (i) n-Butyl bromide, K_2CO_3, MeCN, reflux, 16 h; (ii) Hydrogen, Pd/C, EtOH, 2 h, 20 ºC, 760.05 Torr; (iii) phosphorous oxybromide, DMF, 100 °C, 1 h; (iv) 4-phenylpiperidine, palladium diacetate, sodium t-butanoate, BINAP, toluene, sealed tube, 100 ºC, 16 h; (v) *N*-chlorosuccinimide, CH_2Cl_2, 20 °C, 0.17 h.

2. Results and discussion

Scheme 24 outlines a synthetic route that we initially proposed for the synthesis of JNJ-40411813 (**45**). 4-Bromo-2-chloropyridine (**148**) was allowed to react with 4-phenylpiperidine to yield intermediate **149**. The product was characterized by mass spectrometry to ensure that the bromo group, and not the chloro group had been substituted**.** The substitution of the chloro group of intermediate **149** with a hydroxy group was attempted. Intermediate **150** is unknown and

procedures for similar reactions were used. The reaction was carried out using reagents such as potassium hydroxide,[200] sodium hydroxide,[201] and acetic acid[202] (scheme 24 ii-iv). However, the yields were low, and we could isolate most of the starting material. The reactions failed to go to completion, hence, we modified the synthetic route.

Scheme 24. Unsuccessful synthesis of JNJ-40411813 (**45**).[a]

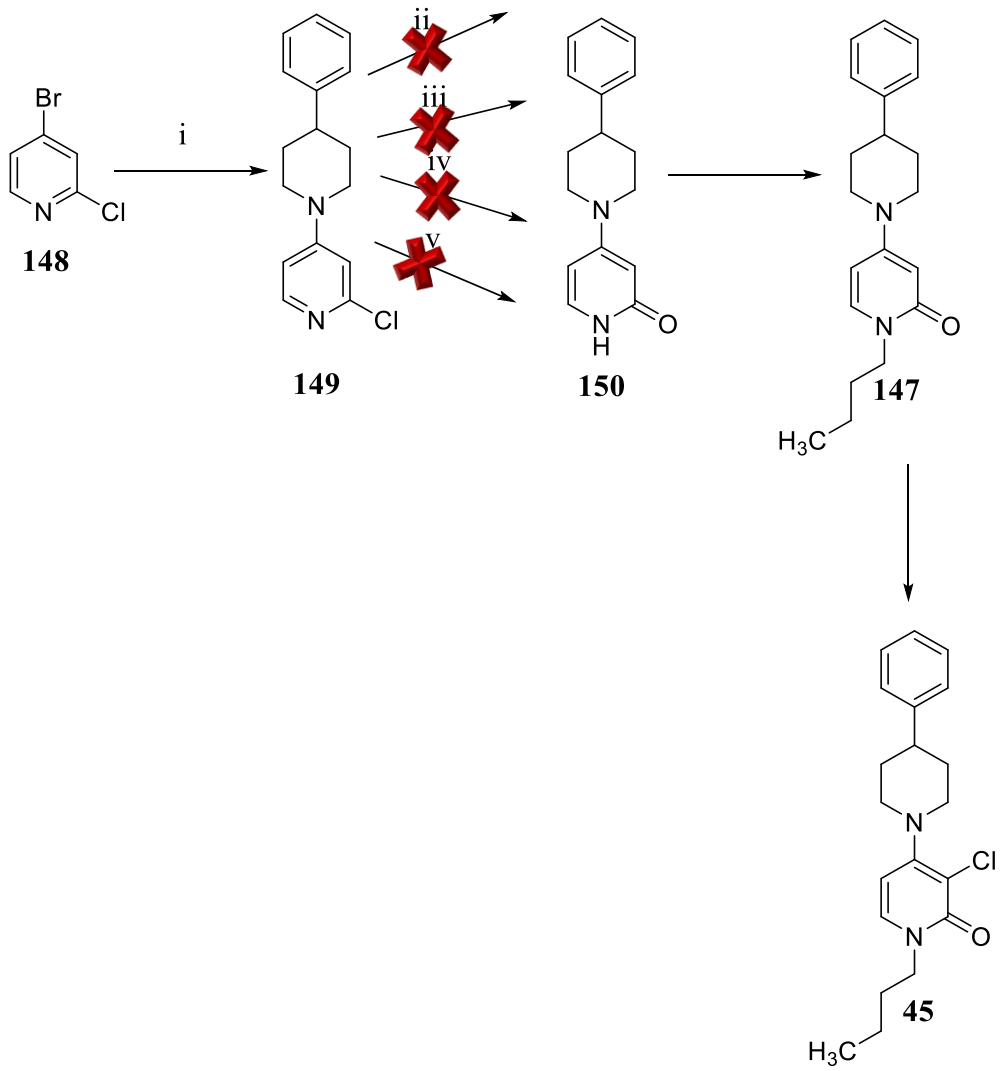

[a]Reagents and Conditions. (i) 4-Phenylpiperidine, K_2CO_3, DMF, 90 ºC, 6 h; (ii) 50% KOH, DMF, (a) 24 h, reflux, 36 h; (iii) NaOH (2M), H_2O, reflux, 30 h; (iv) AcOH, H_2O, reflux, 15 h; (v) KOH (50%), t-BuOH, reflux, 36 h.

The modified synthetic route is outlined in Scheme 25. Intermediate **149** was synthesized as previously described, and we subsequently attempted to substitute the chloro group with a benzyloxy group to yield intermediate **151**, however the reaction did not progress. We next modified the synthetic route further. We substituted the chloro group of **148** with a benzyloxy

group to yield intermediate **152**. Intermediate **152** was known and was synthesized using a procedure for the same compound.[203] The nucleophilic substitution of **152** with 4-phenylpiperidne using K_2CO_3 in DMF as a solvent resulted in very low yields of **151**. Hence, we used a Buchwald-Hartwig reaction to synthesize intermediate **151**. Intermediate **151** was not known and was synthesized by a procedure for a similar compound.[119] Intermediate **150** was synthesized by the debenzylation of intermediate **151** using hydrogen and Pd/C as the catalyst. Intermediate **150** was not known and was synthesized using a procedure for a similar compound.[204] The *N*-alkylation of intermediate **150** was attempted using various methods (Scheme 25 viii-x), however, they all resulted in the formation of the O-alkylated product (**153**) (Figure 72). We further modified the synthetic scheme.

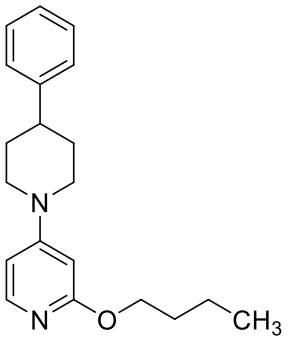

153

Figure 72. O-Alkylated product.

Scheme 25. Proposed synthesis of JNJ-40411813 (**45**).[a]

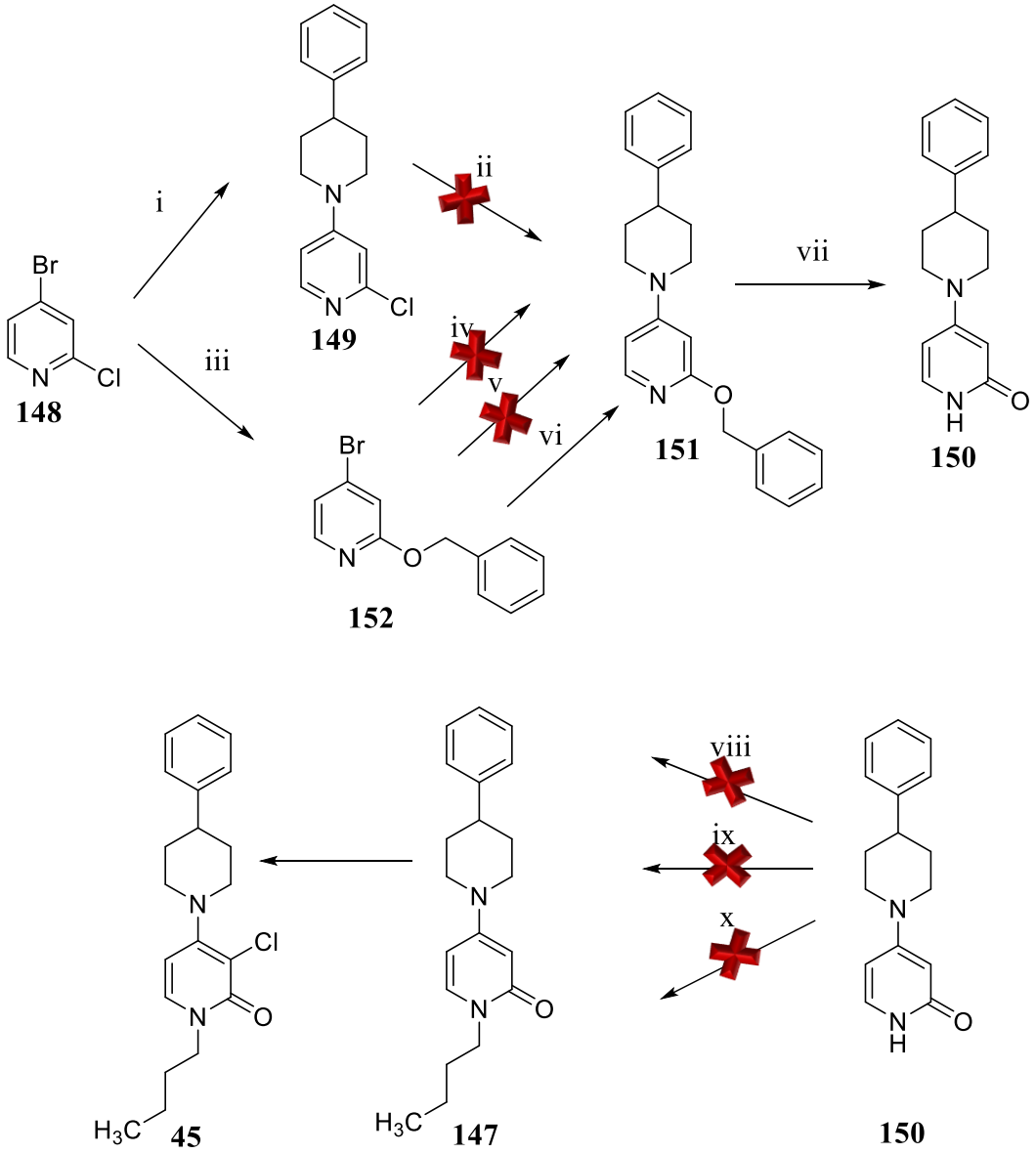

Reagents and conditions (i) 4-Phenylpiperidine, K_2CO_3, DMF, 90 ºC, 6 h; (ii) benzyl alcohol, NaH, THF; (a) room temperature, 48 h; (b) reflux, 24 h; (iii) (a) benzyl alcohol, NaH, THF, room temperature 15 min; (b) **148**, reflux, 3 h; (iv) 4-phenylpiperidine, K_2CO_3, KI, DMF, 90 ºC, 21 h; (v) 4-phenylpiperidine, K_2CO_3, DMF, 110 ºC, 48 h; (vi) 4-phenylpiperidine, palladium diacetate, sodium t-butanoate, BINAP, toluene, sealed tube, 100 ºC, 27 h; (vii) H_2, Pd/C, 30-40 psi, MeOH, EtOAc, room temperature, 2h; (viii) n-butyl bromide KI, K_2CO_3, MeCN, reflux, 20 h; (ix) (a) NaH, DMF, room temperature, 30 minutes; (b) n-butyl bromide, 78 ºC, 4 days (x) (a) NaH, DMF, room temperature, 1 h; (b) n-butyl bromide, 103 ºC, 3 days.

The modified synthetic route is outlined in Scheme 26. Intermediate **150** was synthesized as previously described. Intermediate **150** was chlorinated to yield intermediate **154.** Intermediate **154** was unknown and was synthesized using a procedure for a similar compound.[119] The *N*-alkylation of intermediate **154** was attempted using a procedure for *N*-alkylation of 2-pyridones in water,[205] however the reaction was not clean, and product could not be isolated.

Scheme 26. Proposed synthesis of JNJ-40411813 (**45**).[a]

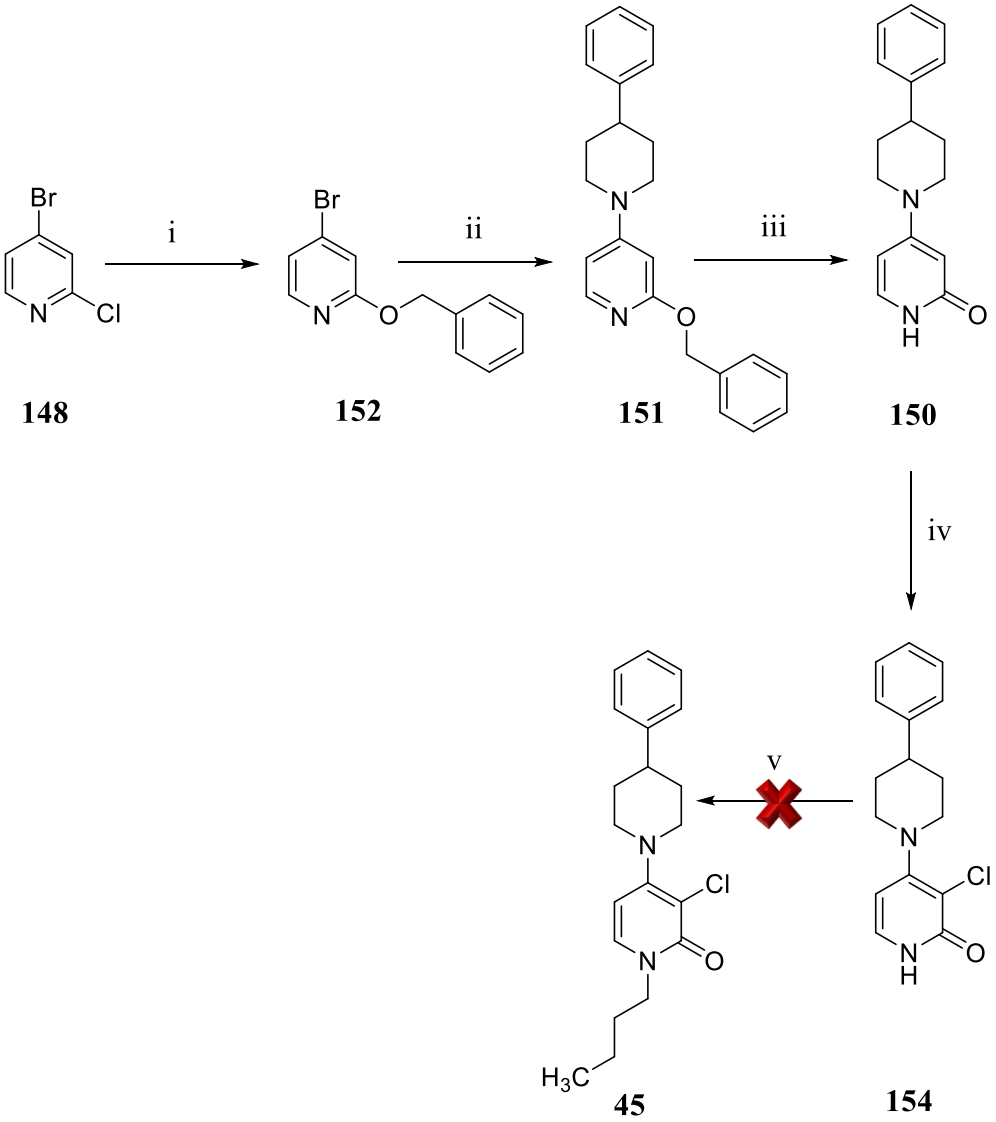

[a]Reagents and conditions. (i) Benzyl alcohol, NaH, THF, reflux, 3 h; (ii) 4-phenylpiperidine, palladium diacetate, sodium t-butanoate, BINAP, toluene, sealed tube, 100 ºC, 27 h; (iii) H_2, Pd/C, 30-40 psi, MeOH, EtOAc, room temperature, 2h.; (iv) *N*-chlorosuccinimide, CH_2Cl_2, room temperature, 10 min; (v) n-butyl bromide, tween 20, K_2CO_3, 70 ºC, 22 h.

We came within one step of our desired synthetic goal (Scheme 26). But we were ultimately unable to synthesize JNJ-40411813 (**45**) using a modified procedure where the linker would be added in the penultimate/ultimate step. Either an entirely new synthetic route will need to be devised, or the

scheme that was originally reported in the literature might be used to add the linker in the very first step since *N*-alkylation of the compound at a later stage did not yield the desired product.

In any event, such studies are beyond the scope of the present work, and further pursuit of a novel method of preparation of JNJ-40411813 (**45**) was abandoned.

E. Specific Aim 5. Redefining a pharmacophore for 5-HT$_{2A}$ receptor antagonists

1. Approach

5-HT$_{2A}$ Receptor antagonists belong to diverse chemical classes and a number of pharmacophore models have been proposed to explain the receptor-ligand interactions. [156–159,206,207] Reported pharmacophore models for 5-HT$_{2A}$ receptor antagonists include *two* aromatic/hydrophobic regions and a protonated basic amine (Figure 73), and suggest that these agents might have multiple binding modes.[156–159] When a central ring is flanked by two other ring systems, the fold angle between the rings seems to play a role as well.[208]

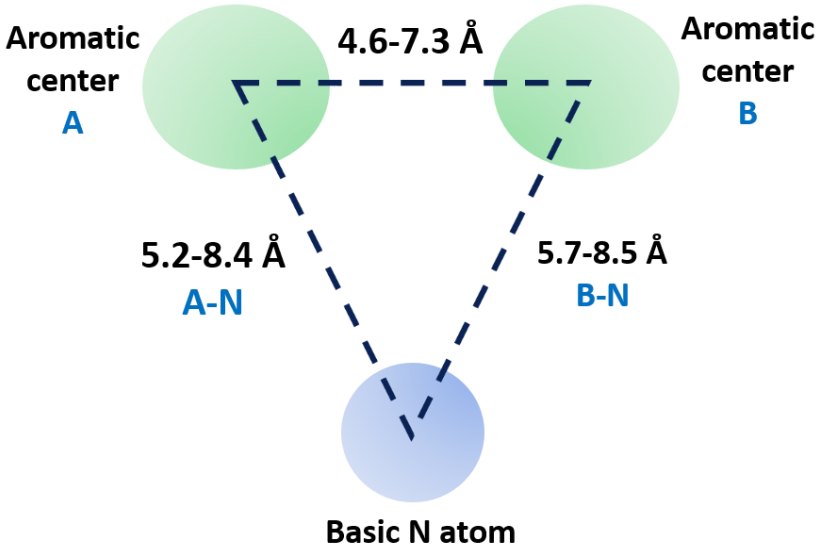

Figure 73. A representative pharmacophore for 5-HT$_{2A}$ receptor antagonists (data from references 156-159).

Risperidone (**14**) (Figure 8) has been studied in two pharmacophoric studies. A study by Sekhar et al.[209] has identified pharmacophoric features essential for atypical antipsychotic action (SDAs) (Figure 74). However, the investigation did not specifically address 5-HT_{2A} receptor binding, only SDA action in general. Hence, it is not particularly relevant to the studies at hand. Another study by Awadallah[210] identified multiple pharmacophoric features for 5-HT_{2A} receptor antagonist activity (Figure 75).

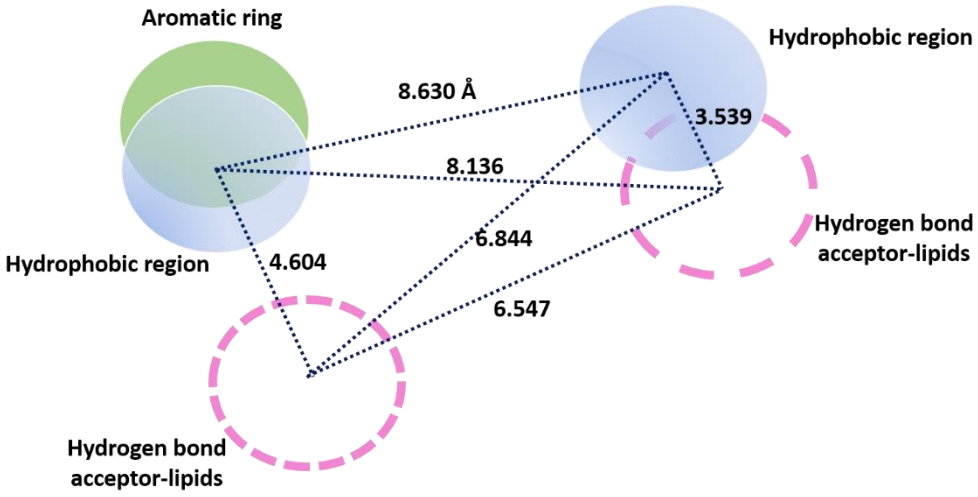

Figure 74. A pharmacophore for 5-HT_{2A} receptor antagonist action (adapted from Sekhar et al.[209]).

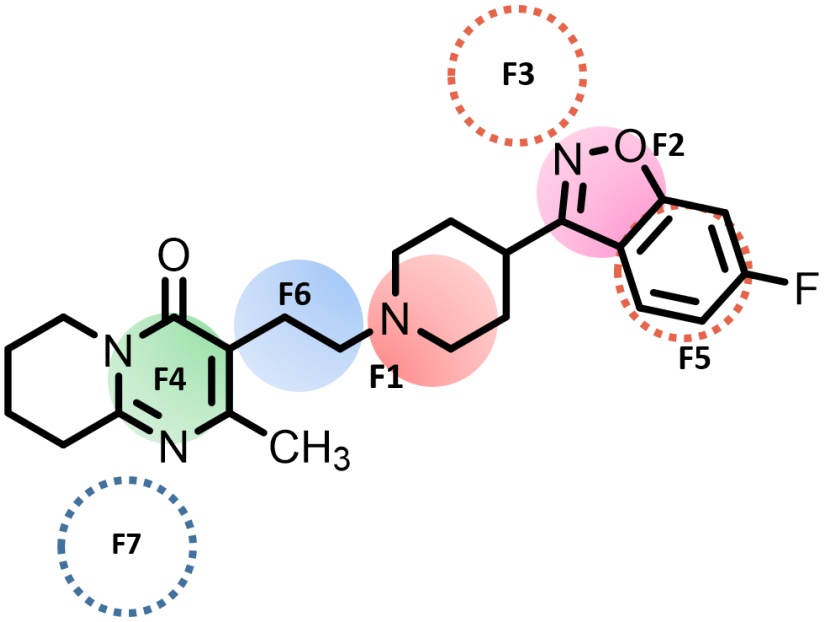

Figure 75. A representative pharmacophore for SDAs **F1**: H-bond acceptor center; **F2**: aromatic or hydrophobic center; **F3** and **F5**: Pi orbital accommodation; **F4**: aromatic center with a H-bond donor group; **F6**: hydrophobic center; **F7**: H-bond acceptor center (adapted from Awadallah[210]).

The SAR of risperidone (**14**) at 5-HT_{2A} receptors has not been studied extensively. Deconstruction studies were conducted in our laboratory to determine the minimal structural requirements for risperidone (**14**) to retain 5-HT_{2A} receptor affinity and antagonism (described previously). We have shown that analog **61** (K_i = 71.41 nM) (Figure 24) that has only half the structural features of risperidone (**14**) (K_i = 5.29 nM) binds with ~ 14 fold lower affinity than risperidone (**14**) and retains 5-HT_{2A} receptor antagonism.[141] Furthermore, the N-methyl analog of **61** (analog **60**, K_i = 12.27 nM) binds with even higher affinity and retains antagonist activity. This suggests that the entire structure of risperidone (**14**) is not necessary for 5-HT_{2A} receptor affinity and antagonism. Analog **61** has only *one* aromatic region and a basic protonated amine, as opposed to the previously reported 5-HT_{2A} receptor antagonist pharmacophores[156–159] that consist of *two* aromatic regions and a basic protonated amine (Figure 73), and lacks many of the features shown in Figures 74 and

75. To define a revised pharmacophore, analog **155** was proposed (Figure 76) for synthesis and evaluation. In analog **155** the nitrogen atom of the piperidine ring is located at a shorter distance from the aromatic center (benzene-ring centroid; Table 13; see also Appendix A) as compared to the distance for the same in analog **61** (6.81 Å) (in its lowest energy conformation), and will help evaluate the effect of this distance on 5-HT_{2A} receptor affinity and antagonism. For 5-HT (**6**), the distance of the aromatic center from the terminal nitrogen atom is 6.51 Å, and lies in-between the distances of the aromatic center from the nitrogen atoms for analogs **61** and **155**. Analog **63** (Figure 76) will help evaluate the contribution to binding of the fluoro group.

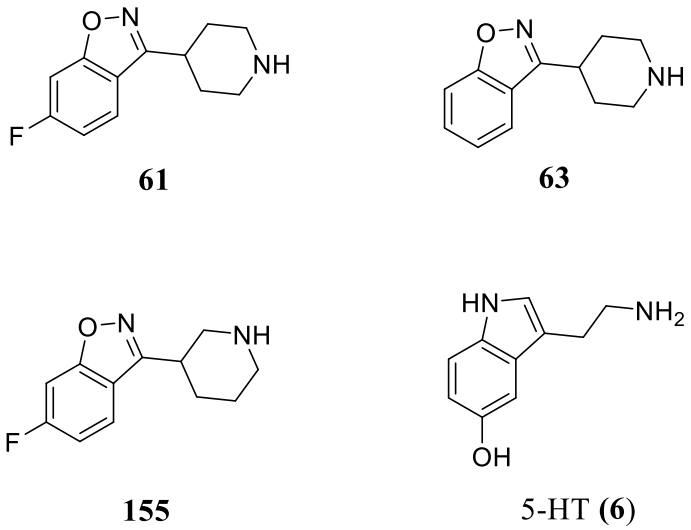

Figure 76. Analogs proposed to define a 5-HT_{2A} receptor antagonist pharmacophore as compared to the structure of 5-HT (**6**).

Table 13. Distances of the aromatic centroid from the N atom and the energy of the lowest energy conformer (CNF_#) for the different isomers of analog **155** (see Appendix A).

Isomer	Distance (Å)	Energy (kcal/mol)
S equatorial* **155** (CNF_15)	5.75	15.56
R axial** **155** (CNF_1)	5.75	15.22
R equatorial* **155** (CNF_1)	6.45	15.56
S axial** **155** (CNF_1)	5.85	15.94

*Equatorial indicates that the benz[*d*]isoxazole ring is an equatorial substituent. **Axial indicates that the benz[*d*]isoxazole ring is an axial substituent. Distances of the aromatic (benzene-ring) centroid from the N atom for 5-HT and analog **61** are 6.51 Å and 6.81 Å, respectively.

2. Results

A. Synthesis

The synthesis of analog **155** is outlined in Scheme 27. The amine of nipecotic acid (**156**) was protected using a formyl group. Formic acid and acetic anhydride were used to generate formic acetic anhydride in situ, which then acted as a formylating agent to yield intermediate **157**. Intermediate **157** was unknown, and was synthesized using a procedure for a similar compound.[143] The reaction of **157** with thionyl chloride yielded intermediate **158** that was subsequently converted to **159** via a Friedel Crafts acylation reaction with 1,3-difluorobenzene. Intermediates **158** and **159** were unknown and were synthesized using procedures for similar compounds.[153] The Friedel Crafts acylation reaction was sensitive to moisture and it was necessary to use freshly sublimed aluminum chloride for the reaction. The reaction of intermediate **159** with hydroxylamine yielded the *E* and *Z* isomers of the oxime **160**. The oxime intermediate **160** is not known and was synthesized by a procedure for a similar compound.[143] The cyclization of oxime **160** via intramolecular displacement of the 2-fluoro group to intermediate **161** was catalyzed by

sodium hydride. It has been reported in the literature that only the *Z* isomer of the oxime participates in the cyclization reaction for similar compounds.[153] Intermediate **161** was deprotected using conc. HCl to yield analog **155**. Intermediate **161** and analog **155** are unknown and were synthesized using procedures for similar compounds.[153] Analog **155** was characterized by NMR and C, H, N analysis.

Scheme 27. Synthesis of analog **155**.[a]

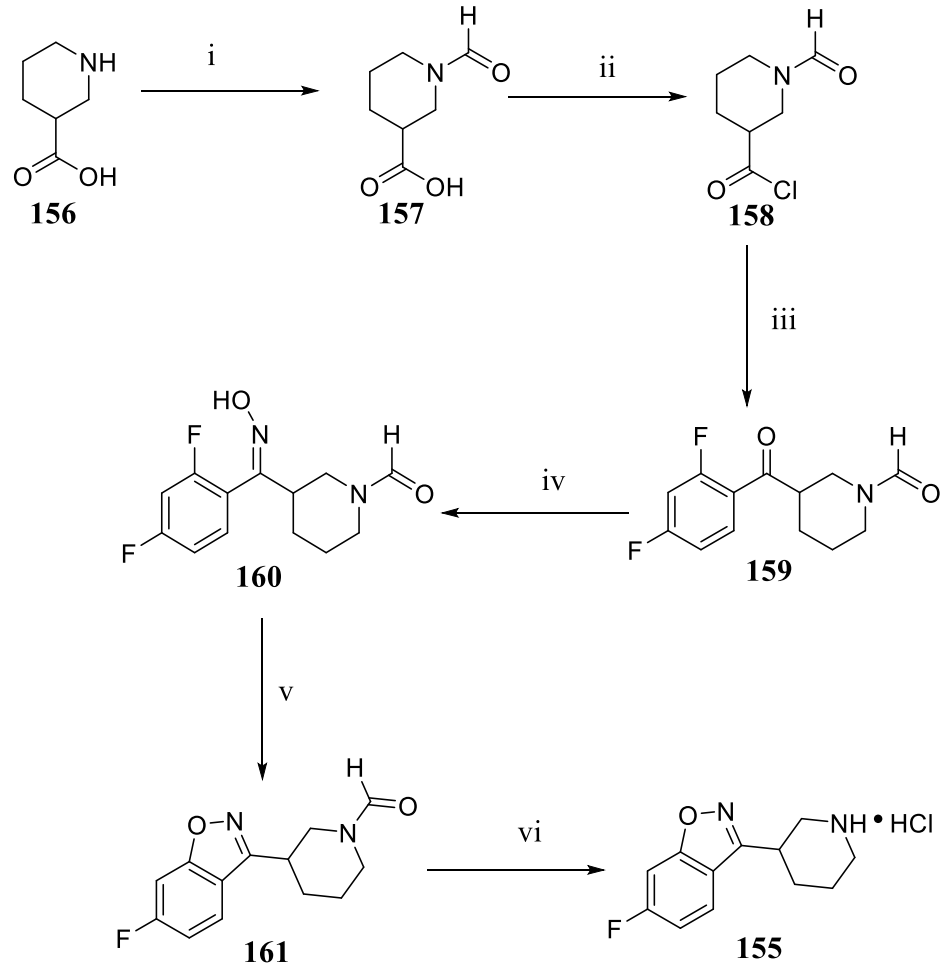

[a]Reagents and conditions: (i) (a) HCOOH, Ac_2O, 65 ºC, 1 h; (b) room temperature, 16 h; (ii) $SOCl_2$, room temperature, 6 h; (iii) 1,3-difluorobenzene, $AlCl_3$, reflux, 22 h; (iv) NH_2OH•HCl, NaOH/H_2O, EtOH, reflux, 96 h; (v) NaH, DMF, THF 75 C, 4h; (vi) HCl (3 N), EtOH, reflux 3 h.

B. Radioligand binding and functional activity studies

Radioligand binding studies were performed in HEK 293 cells expressing 5-HT_{2A} receptors. [^{3}H]Ketanserin ([^{3}H]**36**) was used as the radioligand, and non-specific binding was determined in the presence of methysergide. Competition curves were generated and analyzed by non-linear regression analysis to determine the binding affinities (K_i values) of the compounds.

As previously reported analog **61** has a binding affinity of 71.41 nM (log K_i = -7.14 ± 0.09), and is a 5-HT_{2A} receptor antagonist,[141] whereas analog **63** binds to 5-HT_{2A} receptors with an affinity of ~200 nM (n = 1, performed in duplicate). Analog **155** has a binding affinity of ~256 nM (n = 1, performed in duplicate) (Figure. 77). However, the racemic mixture of analog **155** was used, and if any of the stereoisomers are inactive, the binding affinity of the other sterioisomers might be higher.

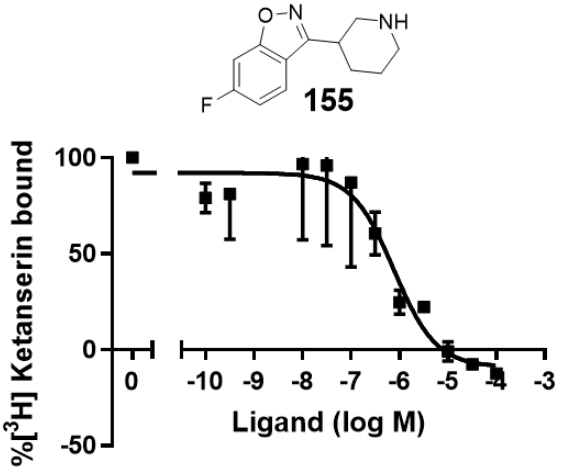

Figure 77. [^{3}H]Ketanserin binding competition curve by compound **155** in HEK 293 cell membrane preparations expressing 5-HT_{2A} receptors (n = 1, performed in duplicate).

C. Molecular modeling studies

Analogs **61**, **63**, and **155** were docked in homology models of 5-HT_{2A} receptors to study the receptor-ligand interactions. The analogs were docked into 100 homology models of the receptor and analyzed as previously described. Analogs **61** and **63** were docked by Dr. Supriya A. Gaitonde.[143]

Figure 78 shows analogs **61**, **63** and the *R* equatorial (CNF_1) and *S* equatorial (CNF_15) (see Appendix A) isomers of analog **155** docked at the 5-HT_{2A} receptor. They all seem to dock in a similar manner, however, their benz[*d*]isoxazole rings are oriented slightly differently and do not overlap, leading to differences in their interactions with the receptor.

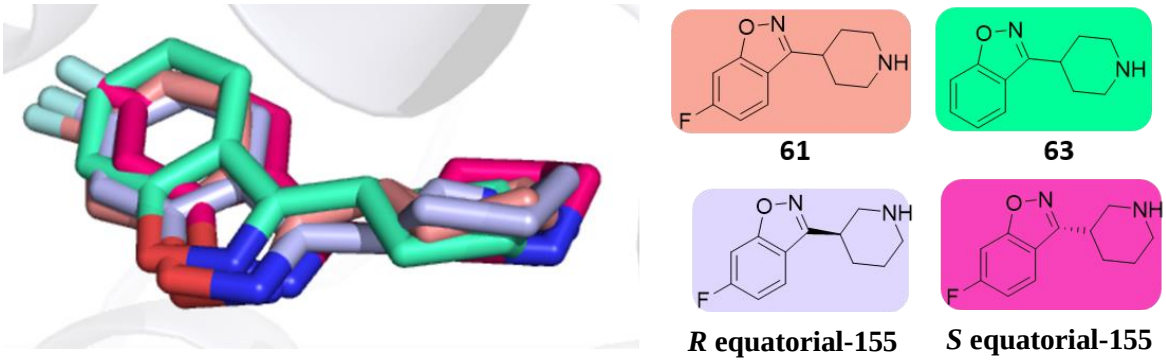

Figure 78. Docking modes of analog **61** (salmon), **63** (green), *R* equatorial-**155** (CNF_1; violet) and *S* equatorial-**155** (CNF_15; pink) at the 5-HT_{2A} receptor.

Figure 79 illustrates the interactions that molecules **61** and **63** made with the 5-HT_{2A} receptor. The nitrogen and oxygen atoms of the benz[*d*]isoxazole rings formed two bifurcated hydrogen bonds with Ser159 and Ser242. Both analogs formed a crucial bidentate ionic interaction with Asp155.

Additionally, the fluorine atom of analog **61** seemed to be making a potential hydrogen bond with Ser239. The analogs made hydrophobic interactions with Phe234, Trp336, Phe339, Phe340, Val156, and Val366.

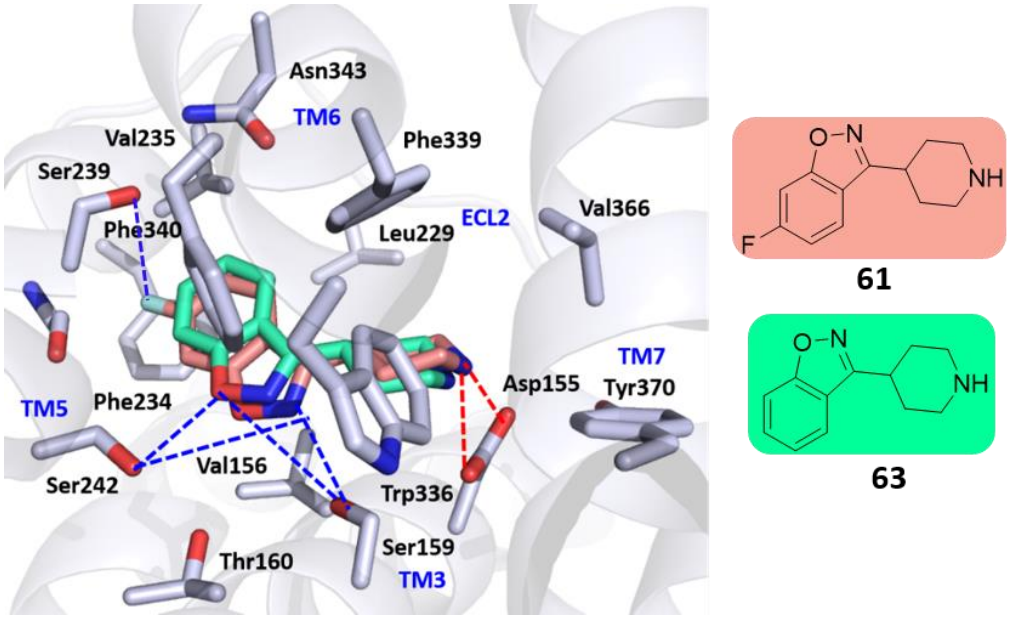

Figure 79. Docking modes of analogs **61** (salmon) and **63** (green) at the 5-HT$_{2A}$ receptor. The red dashed lines indicate ionic interactions and the blue dashed lines indicate hydrogen bonds.

Figure 80 shows the *R* equatorial (CNF_1) and *S* equatorial (CNF_15) isomers of analog **155** docked at the 5-HT$_{2A}$ receptor. Analog **155** interacts with the receptor in a manner that is different from analogs **61** and **63**. The benz[*d*]isoxazole rings of the molecules did not show a bifurcated hydrogen bond. The oxygen atoms of the benz[*d*]isoxazole rings of both isomers formed hydrogen bonds with Thr160 and Ser242, and the fluoro groups formed a hydrogen bond with Ser239. The protonated amine of the *R* equatorial isomer formed a bidentate ionic interaction with Asp155, whereas the protonated amine of the *S* equatorial isomer formed an ionic interaction with the carbonyl oxygen of Asp155, and a hydrogen bond with Tyr370. Additionally, hydrophobic

interactions with Phe234, Trp336, Phe339, Phe340, Val156, and Val366 were observed for both isomers. HINT scores (Table 14) for the *R* equatorial and *S* equatorial isomers of analog **155** are comparable and suggest that they might bind at 5-HT_{2A} receptors with similar affinities.

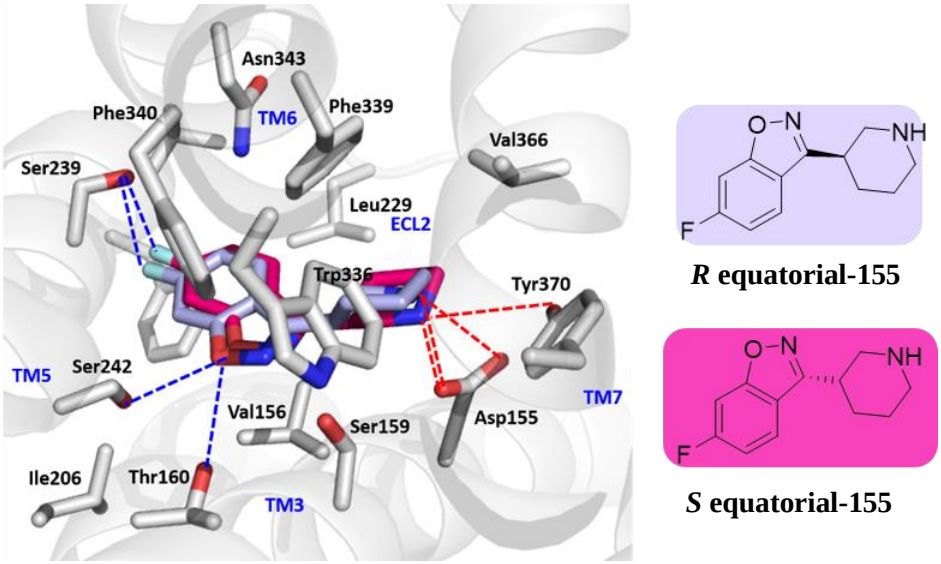

Figure 80. Docking modes of *R* equatorial-**155** (CNF_1; violet) and *S* equatorial-**155** (CNF_15; pink) at the 5-HT_{2A} receptor. The red dashed lines indicate ionic interactions and the blue dashed lines indicate hydrogen bonds.

HINT scores for analogs **61**, **63** and the *R* equatorial (CNF_1) and *S* equatorial (CNF_15) isomers of **155** are shown in Table 14. The HINT scores for all molecules seemed to be comparable. The interactions of the fluorine atoms with Ser239 are quantified in Table 14.

Table 14. Summary of HINT scores for analogs **61**, **63** and **155**.

Binding mode	Polar	Hydrophobic	Total HINT score*	Ser239
61	1593	430	1366	33
63	1862	342	1463	1
R equatorial **155** (CNF_1)	1788	442	1391	17
S equatorial-**155** (CNF_15)	1946	447	1467	14

*Other terms, e.g., hydrophobic-polar, acid-acid and base-base are reflected in this total.

3. Discussion

Based on the preliminary data available so far for analog **155**, the distance of the nitrogen atom from the aromatic center might be playing a role in enhancing the binding affinity of analog **61**, since analog **155** binds with ~3.5-fold lower affinity (if the isomers bind with equal affinity) than analog **61**. The fluorine atom might also be playing a role in enhancing the binding affinity of analog **61** for 5-HT_{2A} receptors, since analog **63** binds with ~3-fold lower affinity than analog **61**. However, functional activity data on analogs **63** and **155** are required to draw any further conclusions. Also, remains to be determined: is it the benz[*d*]isoxazole, the presence of the fluoro group, the aromatic-to-amine distance, or lack of -OH that converts 5-HT to antagonists.

Based on the data available for analog **61**, we propose a new pharmacophore for 5-HT_{2A} receptor antagonists (Figure 81).

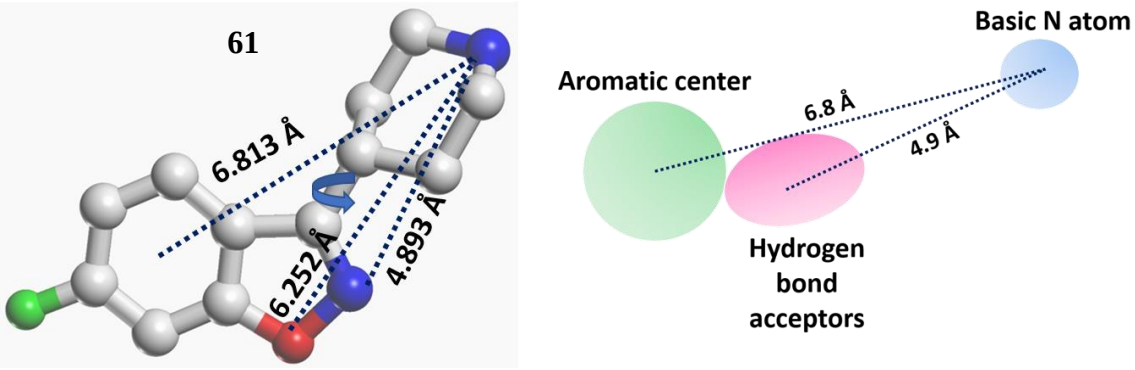

Figure 81. A new pharmacophore for 5-HT_{2A} receptor antagonists based on the structural features of analog **61**.

The proposed pharmacophore consists of only ***one*** aromatic region, as opposed to ***two*** aromatic regions that has been previosly reported, a basic protonated amine, and hydrogn bond acceptors. Interesting is that the centroid-N distance (6.8 Å) is exactly midway between the A-N distance shown in Figure 72 (i.e., 6.8 Å). In addition, preliminary binding data show that although the fluoro group of analog **61** is not required, it adds to affinity.

V. CONCLUSIONS

The 5-HT_{2A}/$mGlu_2$ receptor heteromeric complex has been identified as a novel therapeutic target for the treatment of schizophrenia.[18] A long-term goal of this project is to synthesize a bivalent ligand that will have a 5-HT_{2A} receptor antagonist moiety tethered to an $mGlu_2$ PAM. The atypical antipsychotic agent risperidone (**14**) (Figure 82) is a known 5-HT_{2A} receptor antagonist. However, the SAR of risperidone (**14**) at 5-HT_{2A} receptors has not been extensively studied. The current investigation was conducted to determine the minimal structural requirements for risperidone (**14**) to retain 5-HT_{2A} receptor affinity and antagonist action, and to determine where on the "minimized" structure of risperidone (**14**) an $mGlu_2$ PAM can be introduced. A "deconstruction-reconstruction-elaboration" approach was used to study the SAR of risperidone (**14**) at 5-HT_{2A} receptors. The current investigation was also aimed at identifying where on an $mGlu_2$ PAM a "partial" risperidone structure might be introduced.

The entire structure of risperidone (**14**) does not appear to be necessary for 5-HT_{2A} receptor affinity and antagonism since analog **60** (Figure 82) (K_i = 12.74 nM) that has only half the structural features of risperidone (**14**) binds with only 2-fold lower affinity than risperidone (**14**) K_i = 5.29 nM) and is nearly equipotent as an antagonist. Analog **61** (Figure 82) (K_i = 71.41 nM) represents the "right half" of risperidone (**14**), and binds with ~13-fold lower affinity than risperidone (**14**). Analog **57** (Figure 82) (K_i ~ 2700 nM) represents the "left half" of risperidone (**14**), and binds with

~500-fold lower affinity than risperidone (**14**) suggesting that the "right half" of risperidone (**14**) might be more important for binding affinity at 5-HT_{2A} receptors, however, the "left half" contributes, and might be reinforcing binding affinity. Introduction of amine substituents showed that the affinity of analog **61** can be enhanced. For example, compound **104** (Figure 82) (i.e., Ket/Ris, K_i = 0.96 nM) displayed 75-fold higher affinity than analog **61**, and >5-fold higher affinity than risperidone (**14**) for 5-HT_{2A} receptors. Deconstruction studies have also suggested that the fluorine atom of the benz[*d*]isoxazole ring might be playing a role in enhancing binding affinity since analogs **62** (K_i ~300 nM) and **63** (Figure 82) (K_i ~200 nM) that are desfluoro analog of compounds **60** and **61**, respectively, bound with ~24- and ~3-fold lower affinities, respectively. Analog **61**, the desmethyl analog of **60,** binds with ~6-fold lower affinity at 5-HT_{2A} receptors than analog **60**, suggesting that the methyl group makes additional interactions at the receptor. Analog **63** (Figure 82) binds with similar affinity as analog **62**, suggesting that the methyl group might not be making additional favorable interactions in this case at the receptor, and that analogs **60** and **61** might have different binding modes as compared to analogs **62** and **63**.

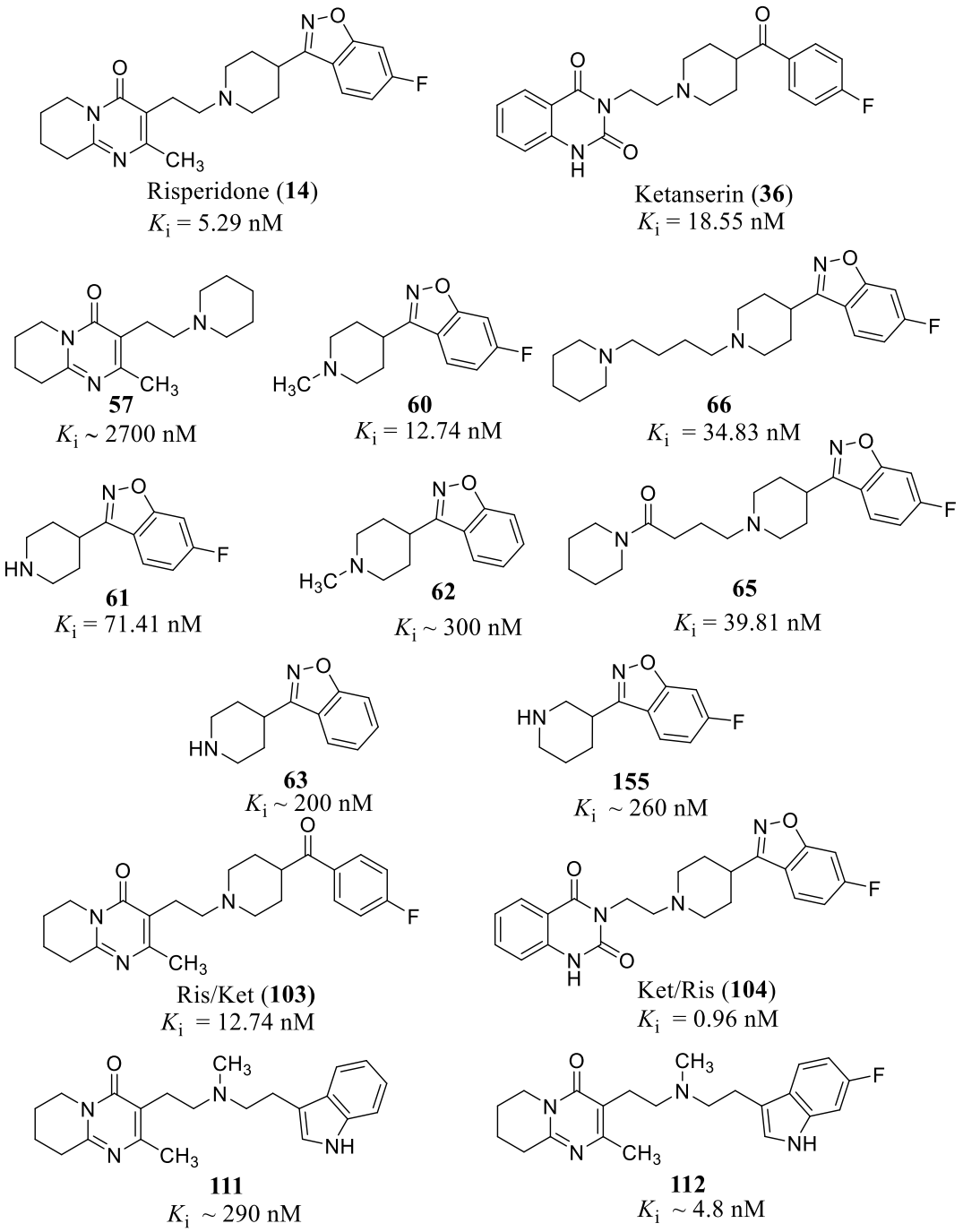

Figure 82. Compounds discussed in the conclusion section.

Analogs **65** and **66** (Figure 82) bind with reduced binding affinity, and are less potent antagonists as compared to risperidone (**14**). However, the carbonyl group might contribute.

Hybrid molecules Ris/Ket (**103**) and Ket/Ris (**104**) (Figure 82) were also examined to study the relative binding modes of risperidone (**14**) and ketanserin (**36**) (Figure 82). The Ket/Ris (**104**) hybrid that has the quinazolinedione ring of ketanserin (**36**) and the benz[*d*]isoxazole ring of risperidone (**14**) bound to 5-HT_{2A} receptors with high affinity (K_i = 0.96 nM), and had a 5-, 13-, and 19-fold higher affinity than risperidone (**14**), the Ris/Ket (**103**) hybrid, and ketanserin (**36**). This suggests that the quinazolinedione ring of the Ket/Ris (**104**) hybrid might be enhancing the binding affinity of the "right half" of risperidone to a greater extent than the 6,7,8,9-tetrahydro-4*H*-pyrido[1,2-*a*]pyrimidin-4-one ring system of risperidone (**14**). The Ris/Ket (K_i = 12.74 nM) hybrid has the "left half" of risperidone (**14**), and binds with ~2-fold lower affinity than risperidone (**14**) suggesting that the "right half" of risperidone (**14**) might be contributing to its binding affinity to a greater extent as compared to the "left half".

Functional activity data obtained from the TEVC assay suggests that the hybrids might have different functional activities at 5-HT_{2A} receptors. Ris/Ket (**103**) blocked the effects of 5-HT in a manner similar to that of risperidone (**14**), and appears to be a 5-HT_{2A} receptor antagonist whereas Ket/Ris (**104**) did not block the effects of 5-HT. When examined in the absence of 5-HT, Ket/Ris (**104)** demonstrated partial agonist activity. However, the observed efficacy of the Ket/Ris (**104**) hybrid might have been due to its direct effects at the GIRK4* channel that might be masking its potential antagonist activity, and this needs to be evaluated further. The "left" and "right" half of

the Ket/Ris (**104**) hybrid is composed of 5-HT_{2A} receptor antagonists ketanserin (**36**), and risperidone (**14**), respectively. The "right half" of risperidone (**14**) is represented by analog **61** that has been shown to be a 5-HT_{2A} receptor antagonist as a part of this investigation as well as in previous studies conducted in our laboratory.[140] The 6-fluoro-(3-piperidinyl)benz[*d*]isoxazole moiety is common to atypical antipsychotic agents such as risperidone (**14**), paliperidone (**56**) (Figure 23), and iloperidone (**24**) (Figure 12), as well as in agents that produce antipsychotic effects such as ADN-1184 (**162**) (Figure 83), a MARTA that is a high affinity 5-HT_{2A} receptor antagonist (K_i = 2 nM),[211] and compound **163** (Figure 83), a 5-HT_{2A}/dopamine D_3 receptor antagonist that has high affinity for 5-HT_{2A} receptors (K_i = 2 nM).[212] Binding affinities (K_i values) for ADN-1184 (**162**)[211] and **163**[212] were determined in HEK 293 cell membrane preparations that utilized [^{3}H] ketanserin as the radioligand.

All of them have diverse "left halves", however, they all retain 5-HT_{2A} receptor affinity and antagonism. Based on literature precedent, Ket/Ris (**104**) should be a 5-HT_{2A} receptor antagonist since it has a 6-fluoro-(3-piperidinyl)benz[*d*]isoxazole moiety that is common to multiple 5-HT_{2A} receptor antagonists. However, we can only speculate until further functional activity studies are conducted.

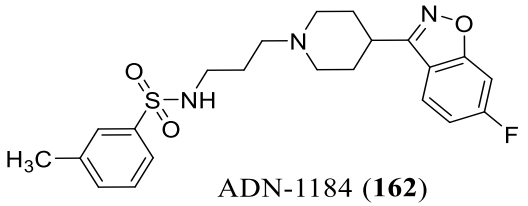

ADN-1184 (**162**)

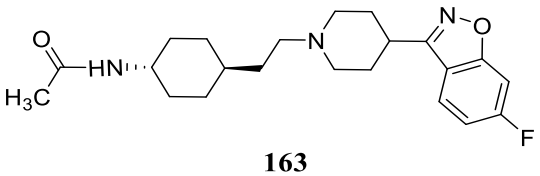

163

Figure 83. Representative agents that show antipsychotic activity.

Analog **60** (K_i = 12.27 nM) and the Ket/Ris (**104**) (K_i = 0.96 nM) hybrid bind with ~6- and ~74-fold higher affinities than analog **61**, respectively. Also, as previously discussed above, analog **61** is common to several high affinity 5-HT_{2A} receptor antagonists that have diverse "left halves". This suggests that adding substituents to the piperidinyl nitrogen atom can enhance binding affinity, and represents a position where a linker might be attached without potentially compromising the molecules 5-HT_{2A} receptor binding affinity. Additionally, studies have shown that analog **61** can also crosstalk at the 5-HT_{2A} receptor/$mGlu_2$ receptor heteromer. This crosstalk has been demonstrated for antipsychotic agents such as clozapine (**8**) and risperidone (**14**).[22] Hence, analog **61** represents the "minimized risperidone" structure that could potentially be used to synthesize the bivalent ligand.

Elaborated analog **112** (Figure 82) (K_i ~4.8 nM) has a 6-fluoro-*N*-methyltryptamine moiety instead of the 6-fluorobenz[*d*]isoxazole ring of risperidone (**14**), and binds with an affinity that is comparable to the binding affinity of risperidone (**14**) (K_i = 5.29 nM) at 5-HT_{2A} receptors. This suggests that the benz[*d*]isoxazole ring of risperidone (**14**) might not be crucial for its binding affinity since it can be replaced by an indole ring. In fact, there are reports in the literature to suggest that indole rings of tryptamines and benz[*d*]isoxazole rings are isosteric, and that they might bind in a similar manner.[213] Analog **111** (Figure 82) represents the desfluoro analog of compound **112,** and binds with ~57-fold lower affinity than analog **112**, again suggesting that the fluoro group might be important for binding affinity.

Molecular modeling studies with deconstructed and elaborated analogs of risperidone (**14**) suggest that the fluorine atom might be involved in a hydrogen bonding interaction with 5-HT_{2A} receptors. The amino acid residue that participates in the hydrogen bond with the fluorine atom varies for different molecules. Additionally, risperidone (**14**) and its analogs might utilize more than one binding mode.

Molecular modeling studies of the $mGlu_2$ receptor suggested that the chemically diverse PAMS: BINA (**43**), LY487379 (**44**), JNJ-40411813 (**45**), and JNJ-40068782 (**46**) (Figure 69) dock in the same binding pocket.

Molecular modeling studies conducted as a part of this study as well as SAR studies reported in the literature[119] suggest that the pyridone nitrogen atom of the PAM JNJ-40411813 (**45**) can tolerate longer chain lengths, and represents a potential position to attach a linker.

Deconstruction of risperidone (**14**) studies suggested that only half the structural features (analog **61**) of risperidone (**14**) are required to retain binding affinity and 5-HT_{2A} receptor antagonism. This is in contrast to previously reported pharmacophores[156–159] for 5-HT_{2A} receptor antagonists in the literature that consist of *two* aromatic regions. Binding data on analogs **61** and **155** (Figure 76) suggests that the distance of the aromatic center from the protonated amine might influence binding affinity, with a distance of ~6.8 Å being optimal. Binding data on analog **63** suggest that the fluorine atom might be important for 5-HT_{2A} receptor affinity. Based on the data available so far, we have proposed a new pharmacophore for 5-HT_{2A} receptor antagonists that is comprised of

only *one* aromatic center, a basic protonated amine and hydrogen bond acceptors. Perhaps this pharmacophore was never previously identified because nearly all of the earlier agents possessed two or more aromatic rings.

Overall we (i) identified a risperidone-like pharmacophore for 5-HT_{2A} receptor antagonist action, (ii) demonstrated that a fluoro group contributes to 5-HT_{2A} receptor affinity, (iii) investigated binding modes of risperidone (**14**) and risperidone analogs revealing that more than one mode of binding might be possible, (iv) identified where on the pharmacophore (i.e, the piperidine amine) substituents might be attached without loss (and, indeed, with enhancement) of 5-HT_{2A} receptor affinity, (v) examined the modes of binding of various $mGlu_2$ PAMs at models of the $mGlu_2$ receptor, (vi) identified, together with known SAR information, a PAM and a potential linker site for eventual construction of bivalent ligands, and (vii) explored potential synthetic routes that might be of value in the synthesis of bivalent ligands.

VI. EXPERIMENTAL

A. Synthesis

Compounds were characterized using proton nuclear magnetic resonance (^{1}H NMR), infrared (IR) spectroscopy (where applicable), mass spectrometry (MS) (where applicable). and by elemental analysis (if unkown) for C, H and N performed by Atlantic Microlab Inc. (Norcross, GA). Compounds were considered pure if the elemental analysis values obtained were within 0.4% of theoretical values. Melting points were measured on Thomas Hoover or MEL TEMP (if melting points were above 200 ºC) melting point apparatuses and are uncorrected. ^{1}H NMR spectra were obtained using a Bruker ARX 400 MHz spectrometer using trimethylsilane (TMS) as an internal standard. The ^{1}H NMR spectra were reported by indicating the peak positions (parts per million, δ), splitting pattern of peaks (s: singlet, d: doublet, t: triplet, q: quartet, dd: doublet of doublets, td: triplet of doublets, m: multiplet), coupling constant (*J*, Hz) and integration values. IR spectra were obtained using Thermo Nicolet iS10 FT-IR. MS was obtained using a Waters Acquity TQD (tandem quadrapole) spectrometer that utilizes electrospray ionization. Reactions were monitored using a combination of thin-layer chromatography (TLC) on silica gel GHLF plates (250 µm, 2.5 x 10 cm; Analtech Inc. Newark, DE) and/ or IR spectroscopy where applicable. Flash chromatography was performed on a CombiFlash Companion/TS (Teledyne Isco Inc. Lincoln, NE) using packed silica gel (Silica Gel 230-400 mesh) columns (RediSep Rf Normal-phase Silica

Flash Column, Teledyne Isco Inc., Lincoln, NE). Hydrochloride or oxalate salts (if the hydrochloride salt was hygroscopic) of compounds were prepared.

2-Methyl-3-(2-(piperidin-1-yl)ethyl)-6,7,8,9-tetrahydro-4*H*-pyrido[1,2-*a*]pyrimidin-4-one Hydrochloride (57)

Method A:

3-(2-Chloroethyl)-2-methyl-6,7,8,9-tetrahydro-4*H*-pyrido[1,2-*a*]pyrimidin-4-one (**78**) (0.10 g, 0.44 mmol) was added to a stirred suspension of piperidine (0.09 g, 0.44 mmol), anhydrous K_2CO_3 (0.06 g, 0.44 mmol) and KI (few crystals) in DMF (9 mL) under an N_2 atmosphere. The stirred reaction mixture was heated at reflux for 17 h. The reaction mixture was allowed to cool to room temperature, diluted with H_2O (~15 mL), and extracted with $CHCl_3$ (3 x 10 mL). The combined organic portion was washed with H_2O (3 x 5 mL), brine (5 mL), dried (Na_2SO_4) and evaporated under reduced pressure to yield 0.04 g of a pale yellow-colored solid. The solid was dissolved in EtOH and cooled to 0 ºC (ice-bath). A saturated solution of gaseous HCl /EtOH was added and the reaction mixture was allowed to stir at room temperature overnight. The precipitate was collected by filtration to yield a yellow-colored solid (0.03 g) which upon recrystallization from MeOH afforded 0.02 g (12%) of compound **57** as a pale yellow solid: mp 262-264 ºC.

Method B:

3-(2-Chloroethyl)-2-methyl-6,7,8,9-tetrahydro-4*H*-pyrido[1,2-*a*]pyrimidin-4-one (**78**) (0.10 g, 0.44 mmol) was added to a stirred suspension of piperidine (0.09 g, 0.44 mmol), anhydrous K_2CO_3 (0.06 g, 0.44 mmol) and KI (few crystals) in MeCN (9 mL) under an N_2 atmosphere. The stirred

reaction mixture was heated at reflux for 17 h. The hot reaction mixture was filtered and the filtrate was evaporated under reduced pressure to give 0.06 g of a pale yellow-colored solid. The solid was dissolved in H_2O, basified with NaOH (3 M to ~pH 12), and extracted with $CHCl_3$ (3 x 5 mL). The combined organic portion was washed with H_2O (3 x 5 mL), brine (5 mL), dried (Na_2SO_4) and evaporated under reduced pressure to yield 0.05 g of a pale yellow-colored solid. The solid was dissolved in EtOH and cooled to 0 ºC (ice-bath). A saturated solution of gaseous HCl /EtOH was added and the reaction mixture was allowed to stir at room temperature overnight. The precipitate was collected by filtration to yield a yellow-colored solid (0.04 g) which upon recrystallization from MeOH afforded 0.03 g (20%) of compound **57** as a pale yellow solid: mp 266-270 ºC.

^{1}H NMR (DMSO-d_6) δ 1.36-1.39 (m, 2H, CH_2), 1.69-1.82 (m, 8H, 4 CH_2), 1.87-1.92 (m, 2H, CH_2), 2.42 (s, 3H, CH_3), 2.91-2.95 (m, 6H, CH_2, CH_3), 3.47-3.51 (d, 2H, CH_2, J = 11.5 Hz), 3.79-3.82 (t, 2H, CH_2, J = 6.1 Hz), 10.59 (br s, 1H, NH^+). Anal. Calcd for ($C_{16}H_{25}N_3O$•2HCl•0.5H_2O•0.5CH_3OH) C, 53.08; H, 8.10; N, 11.26. Found: C, 52.96; H, 7.94; N, 11.45. MS calculated $[M + H]^+$: 276.2070, MS found $[M + H]^+$: 276.2084.

3-(2-(Dimethylamino)ethyl)-2-methyl-6,7,8,9-tetrahydro-4*H*-pyrido[1,2-*a*]pyrimidin-4-one Oxalate (58)

3-(2-Chloroethyl)-2-methyl-6,7,8,9-tetrahydro-4*H*-pyrido[1,2-*a*]pyrimidin-4-one (**78**) (0.50 g, 2.20 mmol) was added to a stirred suspension of *N*,*N*-dimethylamine (2 M solution in MeOH) (1.1 mL, 2.2 mmol), anhydrous K_2CO_3 (0.30 g, 2.20 mmol) and KI (few crystals) in MeCN (45 mL) under an N_2 atmosphere. The stirred reaction mixture was heated at reflux for 30 h. The hot reaction

mixture was filtered and the filtrate was evaporated under reduced pressure to give 0.30 g of a yellow liquid. The liquid was dissolved in H_2O, basified with NaOH (3 M to ~pH 12), and extracted with $CHCl_3$ (5 x 5 mL). The combined organic portion was washed with H_2O (3 x 5 mL), brine (5 mL), dried (Na_2SO_4) and evaporated under reduced pressure to yield 0.21 g of crude free base as a yellow-colored liquid. The liquid was purified using kugelrohr distillation (220 ºC, 0.75 millibar) to yield 0.11 g of a colorless oil which was dissolved in $CHCl_3$, cooled to 0 °C (ice-bath) and treated with a saturated solution of $(COOH)_2$ /Et_2O and then the reaction mixture was allowed to stir at room temperature overnight. The precipitate was collected by filtration to yield a white solid (0.07 g) which upon recrystallization from EtOH afforded 0.05 g (12%) of compound **58** as a white solid: mp 154-156 ºC. ^{1}H NMR (DMSO-d_6) δ 1.76-1.80 (m, 2H, CH_2), 1.84-1.89 (m, 2H, CH_2), 2.24 (s, 3H, CH_3), 2.50-2.52 (m, 10 H, $2CH_2$, $2CH_3$), 3.05-3.09 (t, 2H, CH_2, J = 8.0 Hz), 3.78-3.81 (t, 2H, CH_2, J = 6.2 Hz). Anal. Calcd for ($C_{13}H_{21}N_3O$•1.5 $(COOH)_2$) C, 51.89; H, 6.53; N, 11.34. Found: C, 51.96; H, 6.66; N, 11.37.

3-(2-Aminoethyl)-2-methyl-6,7,8,9-tetrahydro-4*H*-pyrido[1,2-*a*]pyrimidin-4-one Hydrochloride (59)

Compound **59** was synthesized using a literature procedure for a Gabriel synthesis reaction for a different compound.[214] Hydrazine hydrate (0.20 mL, 4.10 mmol) was added to a stirred suspension of **79** (0.52 g, 1.55 mmol) in absolute EtOH (16 mL) under an N_2 atmosphere. The stirred reaction mixture was heated at reflux for 4 h, cooled to room temperature and heated at reflux for 5 min with HCl (1 N, 15.5 mL) until a clear solution was formed. The solid that crystallized on cooling was removed by filtration and washed with H_2O (5 mL). The filtrate was basified with NaOH (3

M to ~pH 12), and extracted with $CHCl_3$ (3 x 5 mL). The combined organic portion was washed with H_2O (3 x 5mL), brine (5 mL), dried (Na_2SO_4) and evaporated under reduced pressure to yield 0.21 g (66%) as a yellow-colored oil. The oil was dissolved in EtOH and cooled to 0 °C (ice-bath). A saturated solution of gaseous HCl/EtOH was added and the reaction mixture was allowed to stir at room temperature overnight, the precipitate was collected by filtration to yield a yellow-colored solid which upon recrystallization from MeOH afforded 0.06 g (20%) of compound **59** as a pale yellow solid: mp 268-270 ºC. ^{1}H NMR (DMSO-d_6) δ 1.79-1.82 (m, 2H, CH_2), 1.90-1.93 (m, 2H, CH_2), 2.4 (s, 3H, CH_3), 2.79 (m, 2H, CH_2), 2.89-2.90 (m, 2H, CH_2), 3.03-3.04 (m, 2H, CH_2), 3.29 (m, 2H, CH_2), 8.07 (br s, 2H, NH_2^+). Anal. Calcd for ($C_{11}H_{17}N_3O$•2HCl) C, 47.15; H, 6.83; N, 14.99. Found: C, 46.93; H, 6.75; N, 14.76.

Compounds **60**-**63** were synthesized by Dr. Supriya A. Gaitonde as previously reported.[143]

5-(2-(4-(6-Fluorobenz[*d*]isoxazol-3-yl)piperidin-1-yl)ethyl)-6-methylpyrimidin-4(3*H*)-one Oxalate (64)

Compound **92** (0.24 g, 1.36 mmol) was added to a stirred suspension of 6-fluoro-3-(4-piperidinyl)benz[*d*]isoxazole (**61**) (0.33 g, 1.50 mmol), anhydrous K_2CO_3 (0.19 g, 1.36 mmol) and KI (few crystals) in DMF (4 mL). The stirred reaction mixture was heated in a sealed tube at 134 ºC for 18 h, and allowed to cool to room temperature. The reaction mixture was diluted with H_2O (~10 mL), and extracted with $CHCl_3$ (3 x 10 mL). The combined organic portion was washed with H_2O (10 mL), brine (10 mL), dried (Na_2SO_4), and evaporated under reduced pressure to yield 0.38 g of an orange-colored oil which was purified by column chromatography (silica gel;

$CHCl_3$/MeOH; 100:0 to 85:15) to afford 0.08 g of a crude, brown sticky solid. The solid was dissolved in $CHCl_3$ (10 mL) and cooled to 0 °C (ice-bath). A saturated solution of $(COOH)_2/Et_2O$ was added and the reaction mixture was allowed to stir at room temperature overnight. The precipitate was collected by filtration to yield a pale brown-colored solid (0.06 g) which upon recrystallization from EtOH afforded 0.03 g (5%) of compound **64** as a white solid: mp 228-230 °C. ^{1}H NMR (DMSO-d_6) δ 1.96-2.04 (m, 2H, CH_2), 2.17-2.24 (m, 2H, CH_2), 2.28 (s, 3H, CH_3), 2.68-2.80 (m, 5H, CH_2), 2.44-2.47 (m, 2H, CH_2), 3.43-3.48 (m, 2H, CH_2), 7.30-7.35 (td, 1H, ArH, J = 2.1, 9.1 Hz), 7.71-7.74 (dd, 1H, ArH, J = 2.1, 9.1 Hz), 8.01-8.07 (m, 2H, ArH) (The -NH of the pyrimdone was not visible). Anal. Calcd for ($C_{19}H_{21}N_4O_2F$•0.5$(COOH)_2$•0.9H_2O) C, 57.52; H, 5.74; N, 13.41. Found C, 57.77; H, 5.47; N, 13.15. MS calculated $[M+H]^+$: 357.1726 MS found $[M+H]^+$: 357.1754.

Compounds **65** and **66** were synthesized by Dr. Supriya A. Gaitonde as previously reported.[143]

3-[1-(4-Cyclohexylbutyl)piperidin-4-yl]-6-fluorobenz[*d*]isoxazole Hydrochloride (68)

Compound **102** (0.28 g, 0.92 mmol) was added to a stirred suspension of 6-fluoro-3-(4-piperidinyl)benz[*d*]isoxazole (**61**) (0.26 g, 1.18 mmol), anhydrous K_2CO_3 (0.25 g, 1.83 mmol) in MeCN (5 mL). The stirred reaction mixture was heated in a sealed tube at 80 °C for 96 h, filtered, and the filtrate was evaporated under reduced pressure to give 0.42 g of a sticky solid. The solid was purified by column chromatography (silica gel; CH_2Cl_2/MeOH; 9.5:0.5) to afford 0.15 g of a sticky, white solid. The solid was dissolved in EtOH (2 mL), and cooled to 0 °C (ice-bath). A saturated solution of gaseous HCl/EtOH was added and the reaction mixture was allowed to stir at

room temperature overnight. The solvent was evaporated under reduced pressure to yield 0.09 g of a white solid which upon recrystallization from *i*-PrOH/H_2O afforded 0.08 g (23%) of compound **68** as a white solid: mp 242-244 °C. ^{1}H NMR (DMSO-d_6) δ 0.86-0.91 (m, 2H, CH_2), 1.11-1.36 (m, 8H, CH_2), 1.61-1.74 (m, 7H, CH_2,CH), 2.23-2.33 (m, 4H, CH_2, *J* = 13.3 Hz) 3.08-3.11 (m, 4H, CH_2) 3.41-3.51 (m, 1H, CH), 3.60-3.63 (d, 2H, CH_2, *J* = 11.5 Hz) 7.33-7.38 (td, 1H, ArH, *J* = 2.2, 9.2 Hz), 7.72-7.75 (dd, 1H, ArH, *J* = 2.0, 9.0 Hz), 8.15-8.22 (m, 1H, ArH), 10.16 (br s, 1H, NH^+). Anal. Calcd for ($C_{22}H_{31}N_2OF$•1 HCl•0.4H_2O) C, 65.70; H, 8.22; N, 6.97. Found C, 65.93; H, 8.21; N, 6.86.

2-(2-(2-Methyl-4-oxo-6,7,8,9-tetrahydro-4*H*-pyrido[1,2-*a*]pyrimidin-3-yl)ethyl)isoindoline-1,3-dione (79)

Compound **79** was synthesized using a literature procedure for a Gabriel synthesis reaction for a different compound.[214] Potassium phthalimide (0.72 g, 3.87 mmol) was added to a stirred suspension of 3-(2-chloroethyl)-2-methyl-6,7,8,9-tetrahydro-4*H*-pyrido[1,2-*a*]pyrimidin-4-one (**78**) (0.80 g, 3.52 mmol) in anhydrous DMF (7.8 mL) under an N_2 atmosphere. The stirred reaction mixture was heated at reflux for 22 h, cooled to room temperature and quenched by the careful addition of ice-cold H_2O (15.5 mL). The precipitate was collected by filtration to yield a pale yellow solid (0.60 g) which upon recrystallization from EtOH afforded 0.54 g (45%) of compound **79** as a yellow-colored solid: mp 164-166 °C. ^{1}H NMR (DMSO-d_6) δ 1.75-1.77 (m, 2H, CH_2), 1.82-1.85 (m, 2H, CH_2),2.13 (s, 3H, CH_3), 2.75-2.76 (m, 4H, CH_2), 3.69-3.73 (t, 4H, CH_2, *J* = 5.7Hz), 7.84-7.85 (d, 4H, ArH, *J* = 2.6 Hz). Compound **79** was used in the preparation of compound **59**.

Ethyl 2-acetyl-4-ethoxybutanoate (89)

Compound **89** was synthesized using a modified literature procedure for the same compound.[144] Sodium ethoxide (1.36 g, 19.99 mmol) was dissolved in EtOH (20 mL) and ethyl acetoacetate (**88**) (2.55 g, 19.59 mmol) was added at 0 °C (ice-bath) and stirred at room temperature for 0.5 h. 2-Bromoethyl ether (3.00 g, 19.61 mmol) was added dropwise when the reaction mixture started refluxing, and the reaction mixture was heated at reflux for 18 h. The reaction mixture was allowed to cool to room temperature, filtered and concentrated under reduced pressure. The residue was diluted with Et_2O and filtered. The filtrate was concentrated under reduced pressure to yield 3.20 g of a crude, yellow oil, which was purified using vacuum distillation (110 °C, 1.33 millibar) to yield 1.57 g (40%) of compound **89** as a colorless oil. ^{1}H NMR (DMSO-d_6) δ 1.08-1.12 (t, 3H, CH_3, J = 7.0 Hz), 1.21-1.24 (t, 3H, CH_3, J = 7.1 Hz), 1.91-2.1 (m, 2H, CH_2), 2.22 (s, 3H, CH_3), 3.34-3.41 (m, 4H, CH_2), 3.67-3.71 (t, 1H, CH, J = 7.0 Hz), 4.12-4.18 (q, 2H, CH_2, J = 7.1 Hz). Compound **89** was used in the preparation of compound **90**.

5-(2-Ethoxyethyl)-6-methyl-2-thioxo-2,3-dihydropyrimidin-4(1*H*)-one (90)

Compound **90** was synthesized using a literature procedure for a similar compound.[146] Thiourea (2.93 g, 38.49 mmol) and a solution of intermediate **89** (1.56 g, 7.71 mmol) in EtOH (22 mL) were added to a stirred solution of sodium ethoxide (3.20 g, 47.03 mmol) in EtOH (25 mL) at 0 ºC (ice-bath). The reaction mixture was heated at reflux for 4 h, allowed to cool to room temperature and concentrated under reduced pressure to yield a crude residue The residue was dissolved in H_2O, acidified with HCl (1 M, ~ pH 4), and filtered to yield 1.70 g of a pale yellow solid which was

purified using column chromatography (silica gel; CH_2Cl_2/MeOH; 100:0 to 90:10) to afford 0.91 g (55%) of compound **90** as a pale yellow solid: mp 196-198 ºC (lit.[145] mp 203-203.5 ºC). ^{1}H NMR (DMSO-d_6) δ 1.10-1.13 (t, 3H, CH_3, J = 7.0 Hz), 2.17 (s, 3H, CH_3), 3.35-3.45 (m, 6H, CH_2), 12.15 (br s, 1H, NH), 12.36 (br s, 1H, NH). Compound **90** was used in the preparation of compound **91**.

5-(2-Ethoxyethyl)-6-methylpyrimidin-4(3*H*)-one (**91**)

Compound **91** was synthesized using a literature procedure for a similar compound**.**[147] $NiCl_2$ (1.62 g, 12.50 mmol) was added to a stirred solution of **90** (0.90 g, 4.20 mmol) in anhydrous MeOH (70 mL). This was followed by the slow addition of $NaBH_4$ (1.43 g, 37.66 mmol) at room temperature. The reaction mixture was allowed to stir at room temperature for 0.5 h and filtered over celite. The filtrate was evaporated under reduced pressure and the residue was washed with $CHCl_3$ (15 mL). The $CHCl_3$ was evaporated under reduced pressure to yield 0.46 g (61%) of compound **91** as a pale green solid: mp 144-148 °C (lit.[145] mp 147.5-148 ºC) ^{1}H NMR (DMSO-d_6) δ 1.10-1.13 (t, 3H, CH_3, J = 7 Hz), 2.27 (s, 3H, CH_3), 2.66-2.70 (t, 2H, CH_2, J = 7.08 Hz), 3.41-3.46 (m, 4H, CH_2), 7.98 (s, 1H, ArH) (-NH of the pyrimidone was not visible). Compound **91** was used in the preparation of compound **92**.

5-(2-Chloroethyl)-6-methylpyrimidin-4(3*H*)-one (**92**)

Compound **92** was synthesized using a literature procedure for the same compound with a modified work-up procedure.[145] Compound **91** (0.46 g, 2.52 mmol) was dissolved in HCl (12 N, 6 mL) and heated in a sealed tube at 150 °C for 3 h, allowed to cool to room temperature, diluted with H_2O (30 mL) and filtered. The filtrate was neutralized to ~pH 7 using a saturated aqueous

$NaHCO_3$ solution and extracted with $CHCl_3$ (3 x 15 mL). The combined organic portion was washed with H_2O (10 mL), brine (10 mL), dried (Na_2SO_4), and evaporated under reduced pressure to yield 0.31 g of a brown-colored oil which was purified by column chromatography (silica gel; $CHCl_3$/MeOH; 100:0 to 90:10) to afford 0.25 g (57%) of compound **92** as an orange-colored oil. ^{1}H NMR (DMSO-d_6) δ 2.37 (s, 3H, CH_3), 3.24-3.28 (t, 2H, CH_2, J = 8.32 Hz), 4.64-4.69 (t, 2H, CH_2, J = 8.7 Hz), 8.46 (s, 1H, ArCH), (-NH of the pyrimidone was not visible). Compound **92** was used in the preparation of compound **64**.

1-Cyclohexylcyclobutan-1-ol (**97)**

Compound **97** was synthesized using a literature procedure for the same compound.[148,149] Iodine (few crystals) and magnesium turnings (0.16 g, 6.41 mmol) were added to a stirred solution of freshly distilled cyclohexyl bromide (**96**) (1.00 g, 6.13 mmol) in anhydrous Et_2O (5 mL) at 0 ºC (ice-bath) under an N_2 atmosphere. The stirred reaction mixture was heated at 40 ºC for 2 h, cooled to 0 ºC (ice-bath), and cyclobutanone (0.43 g, 6.13 mmol) was added dropwise. The reaction mixture was allowed to stir at room temperature for 4 h, cooled to 0 ºC (ice-bath) and quenched by the careful addition of H_2O (~10 mL). The organic portion was separated, and the aqueous portion was extracted with Et_2O (3 x 10 mL). The combined organic portions were washed with H_2O (10 mL), brine (10 mL), dried (Na_2SO_4), and evaporated under reduced pressure to yield 0.31 g of a colorless oil. The oil was purified using Kugelrohr distillation (72-80 ºC, 1.33 millibar) to yield 0.21 g (21%) of compound **97** as a colorless oil ^{1}H NMR (DMSO-d_6) δ 0.96-1.3 (m, 6H, CH_2), 1.38-1.50 (m, 1H, CH), 1.66-1.79 (m, 6H), 1.83-1.90 (m, 2H, CH_2), 2.01-2.08 (m, 2H, CH_2). Compound **97** was used in the preparation of compound **98**.

1-Cyclohexyl-4-hydroxybutan-1-one (**98**)

Intermediate **98** was synthesized using a literature procedure for the same compound.[150] Phenyliodine diacetate (0.43 g, 1.36 mmol) was added to a stirred solution of **97** (0.2 g, 1.30 mmol) in 1,1,1,3,3,3-hexafluoro-2-propanol/H_2O (10 mL, 9/1). The reaction mixture was allowed to stir at room temperature for 15 min, and was quenched using a saturated aqueous $NaHCO_3$ solution (10 mL), and was extracted using EtOAc (3 x 10 mL). The combined organic portion was washed with H_2O (10 mL), brine (10 mL), dried (Na_2SO_4), and evaporated under reduced pressure to yield 0.18 g of a crude colorless oil. The oil was purified by column chromatography (silica gel; hexanes/EtOAc; 3:1) to afford 0.12 g (50%) of compound **98** as a colorless oil. ^{1}H NMR (DMSO-d_6) δ 1.09-1.26 (m, 5H, CH_2), 1.53-1.76 (m, 7H, CH_2), 2.32-2.37 (m, 1H, CH), 2.45-2.49 (t, 2H, CH_2, J = 7.2 Hz), 3.31-3.34 (t, 2H, CH_2, J = 6.5 Hz), 4.40-4.42 (t, 1H, OH, D_2O ex., J = 4.7 Hz). IR (diamond, cm^{-1}) 1700 (-C=O), 3400 (-OH). Compound **98** was used in the preparation of compound **99** and **100**.

4-Cyclohexyl-4-oxobutyl 4-methylbenzenesulfonate (99)

Compound **99** was synthesized using a modified literature procedure for a similar compound.[151] Intermediate **98** (0.11 g, 0.65 mmol) was added to a stirred solution of tosyl chloride (0.19 g, 0.98 mmol) and Et_3N (0.20 g, 1.96 mmol) in CH_2Cl_2 (5 mL). The reaction mixture was allowed to stir at room temperature for 48 h, filtered, and the filtrate was evaporated under reduced pressure to give 0.15 g of a crude residue. The residue was purified by column chromatography (silica gel; hexanes/EtOAc; 8.5:1.5) to afford 0.07 g (33%) of compound **99** as a colorless oil. ^{1}H NMR

(DMSO-d_6) δ 1.07-1.26 (m, 5H, CH_2), 1.56-1.76 (m, 7H, CH_2), 2.26-2.33 (m, 1H, CH), 2.46-2.51 (m, 5H, CH_2, CH_3), 3.98-4.01 (t, 2H, CH_2, J = 6.4 Hz), 7.48-7.50 (d, 2H, ArH, J = 8.0 Hz) 7.77-7.79 (dd, 2H, ArH, J = 1.72 Hz, 6.7 Hz).

4-Cyclohexylbutan-1-ol (100)

Method A:

Compound **100** is known and was synthesized using a literature procedure for a similar compound.[215] KOH (0.09 g, 1.61 mmol) and hydrazine hydrate (0.15 g, 4.68 mmol) were added to a solution of compound **98** (0.06 g, 0.35 mmol) in diethylene glycol (4 mL) at 0 ºC (ice-bath). The stirred reaction mixture was heated at 135 ºC for 2 h, a Dean-Stark apparatus was connected to the flask, and the temperature was increased to 200 ºC. The stirred reaction mixture was heated at 200 ºC for 6 h, diluted with H_2O (~5 mL), and extracted with CH_2Cl_2 (3 x 5 mL). The combined organic portion was washed with H_2O (10 mL), brine (10 mL), dried (Na_2SO_4), and evaporated under reduced pressure to yield 0.03 g (58%) of compound **100** as a colorless oil.

Method B:

Compound **100** was synthesized using a literature procedure for a similar compound.[152] A solution of 4-cyclohexylbutanoic acid (**101**) (1.00 g, 5.87 mmol) in anhydrous THF (5 mL) was added to a stirred suspension of $LiAlH_4$ (0.44 g, 11.74 mmol) in anhydrous THF (10 mL) at 0 ºC (ice-bath) under an N_2 atmosphere The reaction mixture was allowed to stir at room temperature for 6 h, cooled to 0 ºC (ice-bath), quenched by addition of H_2O (0.5 mL), 15% NaOH (0.5 mL) and H_2O (1.5 mL). The suspension was filtered over Celite and the residue was washed with THF. The

aqueous portion was basified with 15% NaOH (pH ~12) and extracted with Et_2O (3 x 10 mL). The combined organic portion was washed with H_2O (10 mL), brine (10 mL), dried (Na_2SO_4), and evaporated under reduced pressure to yield 0.49 g (54%) of compound **100** as a colorless oil. Intermediate **100** was used without further purification in the next step.

IR (diamond, cm^{-1}) 3388 (-OH). ^1H NMR (DMSO-d_6) δ 0.83-0.92 (m, 2H, CH_2), 1.12-1.24 (m, 6H, CH_2), 1.28-1.35 (m, 2H, CH_2) 1.39-1.46 (m, 2H, CH_2), 1.63-1.71 (m, 5H, CH_2, CH), 3.39-3.43 (m, 2H, CH) 4.30-4.33 (t, 1H, OH, J = 5.2 Hz). Compound **100** was used in the preparation of compound **102**.

4-Cyclohexylbutyl 4-methylbenzenesulfonate (102)

Compound **102** was synthesized using a modified literature procedure for the same compound.[151] Compound **100** (0.48 g, 3.08 mmol) was added to a stirred solution of tosyl chloride (0.88 g, 4.62 mmol) and Et_3N (0.94 g, 9.23 mmol) in CH_2Cl_2 (15 mL). The reaction mixture was allowed to stir at room temperature for 48 h, filtered, and the filtrate was evaporated under reduced pressure to give 1.21 g of a crude residue. The residue was purified by column chromatography (silica gel; hexanes/EtOAc; 8.5:1.5) to afford 0.29 g (30%) of compound **102** as a white solid: mp 40-42 ºC. (lit.[151] mp 41.5-42.5 ºC). Intermediate **102** was used without further purification in the next step. Compound **102** was used in the preparation of compound **68**.

3-[2-(4-(4-Fluorobenzoyl)piperidin-1-yl)ethyl]-2-methyl-6,7,8,9-tetrahydro-4*H*-pyrido[1,2-*a*]pyrimidin-4-one Oxalate (103)

3-(2-Chloroethyl)-2-methyl-6,7,8,9-tetrahydro-4*H*-pyrido[1,2-*a*]pyrimidin-4-one (**78**) (0.40 g, 1.76 mmol) was added to a stirred suspension of 4-(4-fluorobenzoyl) piperidine hydrochloride (0.43 g, 1.76 mmol), anhydrous K_2CO_3 (0.49 g, 3.52 mmol) and KI (few crystals) in MeCN (40 mL) under an N_2 atmosphere. The stirred reaction mixture was heated at reflux for 24 h, filtered while hot, and the filtrate was evaporated under reduced pressure to give 0.60 g of a yellow, sticky solid. The sticky solid was dissolved in H_2O, basified with NaOH (3 M to pH ~12), and extracted with $CHCl_3$ (3 x 5 mL). The combined organic portion was washed with H_2O (3 x 5 mL), brine (5 mL), dried (Na_2SO_4) and evaporated under reduced pressure to yield 0.51 g of crude free base as a yellow-colored solid. The free base was purified using a short column (silica gel; $CHCl_3$/MeOH; 90:10) to afford 0.36 g of a yellow-colored solid that was dissolved in $CHCl_3$ (2 mL), cooled to 0 °C (ice-bath) and treated with a saturated solution of $(COOH)_2/Et_2O$ and then the reaction mixture was allowed to stir at room temperature overnight. The precipitate was collected by filtration to yield a white solid (0.40 g) which upon recrystallization from EtOH afforded 0.30 g (27%) of compound **57** as a white solid: mp 194-198 °C. ^{1}H NMR (DMSO-d_6) δ 1.74-1.85 (m, 6H, CH_2), 1.89-2.01 (d, 2H, CH_2, J = 13.2 Hz), 2.23 (s, 3H, CH_3), 2.76-2.8 (m, 4H, CH_2) 2.97-2.99 (m, 4H, CH_2), 3.46-3.51 (m, 2H, CH_2), 3.66-3.68 (m, 1H, CH), 3.78-3.81 (t, 2H, CH_2, J = 6.2 Hz), 7.37-7.41 (t, 2H, ArH, J = 8.8 Hz), 8.07-8.11 (m, 2H, ArH). Anal. Calcd for $(C_{23}H_{28}N_3O_2F•1.5\ (COOH)_2$ C, 58.64; H, 5.87; N, 7.89. Found C, 58.63; H, 6.03; N, 8.10.

Compound **104** was synthesized by Dr. Supriya A. Gaitonde as previously reported.[143]

Tryptamine Hydrochloride (105)

Method A:

Compound **105** was synthesized using a literature procedure for a similar compound.[167] BF_3•Et_2O (0.60 mL, 4.40 mmol) was added to a stirred suspension of $NaBH_4$ (0.14 g, 4.00 mmol) in THF (10 mL) at 0 ºC (ice-bath), and was allowed to stir at room temperature for 15 min. A solution of compound **125** (0.14g, 0.75 mmol) in anhydrous THF (2 mL) was added in a dropwise manner, and the reaction mixture was heated at reflux for 2 h, cooled to room temperature and quenched with addition of ice-H_2O. The reaction mixture was acidified with HCl (1 N, to ~pH 2) and heated at 85 °C for 2 h. The reaction mixture was allowed to cool to room temperature and extracted with Et_2O (3 x 10 mL). The aqueous portion was basified with NaOH (1 N to ~pH 12) and extracted with Et_2O (3 x 10 mL). The combined organic portion was washed with H_2O (10 mL), brine (10 mL), dried (Na_2SO_4), and evaporated under reduced pressure to yield 0.09 g as a brown-colored oil. The oil was dissolved in Et_2O (5 mL) and cooled to 0 °C (ice-bath). A gaseous solution of HCl/Et_2O was added and the reaction mixture was allowed to stir at room temperature for 1 h. The precipitate was filtered to yield a beige-colored solid that was recrystallized from EtOH/Et_2O to yield 0.06 g (40%) of compound **105** as a beige solid: mp 242-244 ºC (lit.[168] mp 248-249 °C).

Method B:

Compound **105** was synthesized using a literature procedure for the same compound.[168] $LiAlH_4$ (0.56 g, 14.75 mmol) was added to a stirred solution of compound **125** (0.14 g, 0.77 mmol) in anhydrous Et_2O (8.4 mL) at 0 °C (ice-bath) under an N_2 atmosphere. The stirred reaction mixture

was heated at reflux for 3 h, allowed to stir at room temperature for 12 h, cooled to 0 °C (ice-bath), and quenched by addition of H_2O (0.6 mL), 15% NaOH (0.6 mL) and H_2O (1.8 mL). The suspension was filtered and the residue was washed with Et_2O. The aqueous portion was extracted with Et_2O (3 x 10 mL). The combined organic portion was washed with water (3 x 10 mL), brine (10 mL), dried (Na_2SO_4), and evaporated under reduced pressure to yield 0.13 g as a brown-colored oil. The oil was dissolved in Et_2O (5 mL) and cooled to 0 °C (ice-bath). A gaseous solution of HCl/Et_2O was added and the reaction mixture was allowed to stir at room temperature for 1 h. The precipitate was filtered to yield a beige-colored solid that was recrystallized from EtOH/Et_2O to yield 0.11 g (80%) of compound **105** as a beige solid: mp 246-248 ºC (lit.[168] mp 248-249 °C).

2-(6-Fluoro-1*H*-indol-3-yl)ethan-1-amine Oxalate (106)

$LiAlH_4$ (0.58 g, 15.33 mmol) was added to a stirred solution of compound **123** (0.63 g, 3.07 mmol) in anhydrous THF (8.5 mL) and anhydrous Et_2O (9.5 mL) at 0 °C (ice-bath) under an N_2 atmosphere. The stirred reaction mixture was heated at 60 °C for 1 h, cooled to 0 °C (ice-bath), quenched by addition of H_2O (0.6 mL), 15% NaOH (0.6 mL) and H_2O (1.8 mL). The suspension was filtered and the residue was washed with THF. The aqueous portion was extracted with Et_2O (3 x 10 mL). The combined organic portion was washed with brine (10 mL), dried (Na_2SO_4), and evaporated under reduced pressure to yield 0.42 g as a brown-colored oil. The oil was dissolved in Et_2O (5 mL) and cooled to 0 °C (ice-bath). A saturated solution of $(COOH)_2$/Et_2O was added and the reaction mixture was allowed to warm to room temperature and stirred for 1 h. The precipitate was filtered to yield a brown-colored solid that was heated at reflux in MeCN for 0.5 h, and recrystallized from acetone/H_2O to yield 0.22 g (27%) of compound **106** as a beige-colored

solid: mp 152-154 ºC. ^{1}H NMR (DMSO-d_6) δ 2.99-3.08 (m, 4H, CH_2), 6.86-6.91 (m, 1H, ArH), 7.14-7.17 (d, 1H, ArH, J = 9.6 Hz) 7.24 (s, 1H, ArH), 7.53-7.57 (t, 1H, ArH, J = 7.1 Hz), 11.08 (s, 1H, NH). Anal. Calcd for ($C_{10}H_{11}N_2F$•1$(COOH)_2$•0.2H_2O•0.1CH_3COCH_3) C, 53.21; H, 5.08; N, 10.09. Found C, 53.03; H, 5.14; N, 9.99.

2-(1*H*-Indol-3-yl)-*N*-methylethanamine (107)

Compound **107** was synthesized using a literature procedure for the same compound.[172] $LiAlH_4$ (0.86 g, 22.75 mmol) was added to a stirred solution of intermediate **131** (1.76 g, 7.59 mmol) in anhydrous THF (16 mL) at 0 ºC (ice-bath) under an N_2 atmosphere. The stirred reaction mixture was heated at reflux for 1.5 h, cooled to 0 °C (ice-bath), and quenched by addition of H_2O (0.9 mL), 15% NaOH (0.9 mL) and H_2O (2.7 mL). The suspension was filtered and the residue was washed with THF. The aqueous portion was extracted with CH_2Cl_2 (3 x 10 mL). The combined organic portion was washed with brine (10 mL), dried (Na_2SO_4), and evaporated under reduced pressure to yield 0.83 g (48%) of compound **107** as a white solid: mp 82-84 °C (lit.[173] mp 80-84 °C).

2-(6-Fluoro-1*H*-indol-3-yl)-*N*-methylethan-1-amine Hydrochloride (108)

$LiAlH_4$ (0.23 g, 6.03 mmol) was added to a stirred solution of **127** (0.50 g, 2.01 mmol) in anhydrous THF (18 mL) at 0 ºC (ice-bath) under an N_2 atmosphere. The stirred reaction mixture was heated at reflux for 1.5 h, cooled to 0 ºC (ice-bath), quenched by addition of H_2O (0.2 mL), 15% NaOH (0.2 mL) and H_2O (0.6 mL). The suspension was filtered and the residue was washed with THF. The aqueous portion was extracted with CH_2Cl_2 (3 x 10 mL). The combined organic portion was

washed with brine (10 mL), dried (Na_2SO_4), and evaporated under reduced pressure to yield 0.28 g of crude free base as an oil. The free base was dissolved in Et_2O (3 mL) and cooled to 0 °C (ice-bath). A saturated solution of gaseous HCl/Et_2O was added and the reaction mixture was allowed to stir at room temperature overnight. The precipitate was collected by filtration to yield a brown-colored solid which upon recrystallization from acetone/H_2O afforded 0.36 g (78%) of compound **108** as a brown-colored solid: mp 216-220 ºC. ^{1}H NMR (DMSO-d_6) δ 2.58-2.61 (t, 3H, CH_3, J = 5.48 Hz), 3.01-3.05 (t, 2H, CH_2, J = 7.28 Hz), 3.13-3.18 (m, 2H, CH_2), 6.87-6.92 (m, 1H, ArH), 7.14-7.17 (dd, 1H, ArH, J = 2.2, 10.16 Hz), 7.24-7.25 (d, 1H, ArH, J = 2.32 Hz), 7.56-7.60 (m, 1H, ArH), 8.58 (s, 1H, NH^+), 11.01 (s, 1H, NH). Anal. Calcd for ($C_{11}H_{13}N_2F$•1HCl) C, 57.77; H, 6.17; N, 12.25. Found C, 57.52; H, 6.15; N, 11.98).

3-[2-((2-(1*H*-Indol-3-yl)ethyl)amino)ethyl]-2-methyl-6,7,8,9-tetrahydro-4*H*-pyrido[1,2-*a*]pyrimidin-4-one Oxalate (109)

3-(2-Chloroethyl)-2-methyl-6,7,8,9-tetrahydro-4*H*-pyrido[1,2-*a*]pyrimidin-4-one (0.20 g, 0.88 mmol) was added to a stirred suspension of tryptamine (**105**) (0.31 g, 1.96 mmol) and anhydrous K_2CO_3 (0.12 g, 0.88 mmol) in MeCN (40 mL) under an N_2 atmosphere. The stirred reaction mixture was heated at reflux for 17 h. The hot reaction mixture was filtered and the filtrate was evaporated under reduced pressure to give 0.32 g of crude free base as a yellow liquid. The free base was purified using a short column (silica gel; CH_2Cl_2/MeOH/NH_4OH; 8.5:1.5:0.1) to yield 0.06 g of a liquid, that was dissolved in $CHCl_3$ (2 mL), cooled to 0 °C (ice-bath). A saturated solution of $(COOH)_2$/Et_2O was added and the reaction mixture was allowed to stir at room temperature overnight. The precipitate was collected by filtration to yield a yellow-colored solid

(0.05 g) which upon recrystallization from MeOH afforded 0.03 g (6%) of compound **109** as a yellow solid: mp 112-114 ºC. ^{1}H NMR (DMSO-d_6) δ 1.75-1.90 (m, 4H, CH_2), 2.24 (s, 3H, CH_3), 2.78-2.82 (m, 4H, CH_2), 3.03-3.07 (t, 4H, CH_2, J = 7.0 Hz), 3.22-3.23 (m, 2H, CH_2), 3.78-3.82 (t, 2H, CH_2, J = 6.2 Hz), 7.00-7.04 (t, 1H, ArH, J = 7.0 Hz), 7.09-7.13 (t, 1H, ArH, J = 7.2 Hz), 7.24 (s, 1H, ArH), 7.37-7.39(d, 1H, ArH, J = 8.1 Hz), 7.58-7.60 (d, 1H, ArH, J = 7.8 Hz), 8.67-8.76 (brs, 1H, NH^+), 11.0 (s, 1H, NH). Anal. Calcd for ($C_{21}H_{26}N_4O$•2$(COOH)_2$•1H_2O•1CH_3OH) C, 53.79; H, 6.25; N, 9.65. Found: C, 53.84; H, 5.95; N, 9.84.

3-(2-((2-(6-Fluoro-1*H*-indol-3-yl)ethyl)amino)ethyl)-2-methyl-6,7,8,9-tetrahydro-4*H*-pyrido[1,2-*a*]pyrimidin-4-one Oxalate (110)

3-(2-Chloroethyl)-2-methyl-6,7,8,9-tetrahydro-4*H*-pyrido[1,2-*a*]pyrimidin-4-one (**78**) (0.22 g, 0.98 mmol) was added to a stirred suspension of compound **106** (0.35 g, 1.96 mmol) and anhydrous K_2CO_3 (0.12 g, 1.98 mmol) in MeCN (40 mL) under an N_2 atmosphere. The stirred reaction mixture was heated at reflux for 17 h. The reaction mixture was allowed to cool and evaporated under reduced pressure to give 0.66 g of a yellow semi-solid. The semi-solid was dissolved in H_2O, basified with NaOH (2 M to ~pH 12) and extracted with CH_2Cl_2 (5 x 5 mL). The combined organic portion was washed with H_2O (3 x 5 mL), brine (5 mL), dried (Na_2SO_4) and evaporated under reduced pressure to yield 0.40 g of crude free base as a yellow-colored liquid. The free base was purified using a short column (silica gel; $CHCl_3$/MeOH/NH_4OH; 9:1:0.1) to afford 0.06 g of a liquid, that was dissolved in $CHCl_3$ (2 mL) and cooled to 0 ºC (ice-bath). A saturated solution of $(COOH)_2$/Et_2O was added and the reaction mixture was allowed to stir at room temperature overnight. The precipitate was collected by filtration to yield a yellow-colored solid (0.05g) which

upon recrystallization from MeOH afforded 0.03 g (17%) of compound **110** as a yellow solid: mp 188-192 ºC. ^{1}H NMR (DMSO-d_6) δ 1.75-1.90 (m, 4H, CH_2), 2.24 (s, 3H, CH_3), 2.78-2.81 (t, 4H, CH_2, J = 6.6 Hz), 3.01-3.05 (m, 4H, CH_2), 3.22-3.23 (m, 2H, CH_2), 3.78-3.81, (t, 2H, CH_2 J = 6.2 Hz), 6.86-6.91 (td, 1H, ArH, J = 2.3 Hz, 7.5 Hz), 7.14-7.17 (dd, 1H, ArH, J = 2.3 Hz, 7.9 Hz), 7.24-7.25 (d, 1H, ArH, J = 1.6 Hz), 7.56-7.59 (m, 1H, ArH), 8.70 (brs, 1H, NH^+) 11.01 (s, 1H, NH). Anal. Calcd for ($C_{21}H_{25}N_4OF$•2$(COOH)_2$) C, 54.74; H, 5.32; N, 10.21. Found: C, 54.87; H, 5.50; N, 10.20.

3-[2-((2-(1*H*-Indol-3-yl)ethyl)(methyl)amino)ethyl]-2-methyl-6,7,8,9-tetrahydro-4*H*-pyrido[1,2-*a*]pyrimidin-4-one Oxalate (111)

3-(2-Chloroethyl)-2-methyl-6,7,8,9-tetrahydro-4*H*-pyrido[1,2-*a*]pyrimidin-4-one (**78**) (0.30 g, 1.32 mmol) was added to a stirred suspension of **107** (0.23 g, 1.32 mmol), anhydrous K_2CO_3 (0.18 g, 1.32 mmol) and KI (few crystals) in MeCN (27 mL) under an N_2 atmosphere. The stirred reaction mixture was heated at reflux for 48 h, and evaporated under reduced pressure to give 0.60 g of a yellow sticky solid. The sticky solid was dissolved in H_2O, basified with NaOH (1 M to ~pH 12), and extracted with CH_2Cl_2 (3 x 10 mL). The combined organic portion was washed with H_2O (5 mL), brine (5 mL), dried (Na_2SO_4) and evaporated under reduced pressure to yield 0.41 g of a crude free base as a yellow-colored solid. The free base was purified using a short column (silica gel; $CHCl_3$/MeOH/NH_4OH; 9:1:0.1) to afford 0.38 g of a solid, that was dissolved in CH_2Cl_2 (2 mL) and cooled to 0 °C (ice-bath). A saturated solution of $(COOH)_2$/Et_2O was added and the reaction mixture was allowed to stir at room temperature overnight. The precipitate was collected by filtration to yield a white solid (0.40 g) which upon recrystallization from EtOH afforded 0.31

g (47%) of compound **111** as a white solid: mp 190-192 ºC. ^{1}H NMR (DMSO-d_6) δ 1.74-1.90 (m, 4H, CH_2), 2.25 (s, 3H, CH_3), 2.77-2.88 (m, 4H, CH_2), 2.95 (s, 3H, CH_3), 3.11-3.18 (m, 4H, CH_2), 3.40-3.44 (m, 2H, CH_2), 3.78-3.81 (t, 2H, CH_2, *J* = 6.2, 12.3 Hz), 7.00-7.04 (m, 1H, ArH,), 7.09-7.13 (m, 1H, ArH), 7.26-7.27 (d, 1H, ArH, *J* = 2.0 Hz), 7.37-7.39 (d, 1H, ArH, *J* = 8.1 Hz), 7.62-7.64 (d, 1H, ArH *J* = 7.8 Hz), 11.00 (s, 1H, NH). Anal. Calcd for ($C_{22}H_{28}N_4O$•1.5$(COOH)_2$) C, 60.10; H, 6.25; N, 11.21. Found C, 59.92; H, 6.24; N, 11.12. MS calculated $[M+H]^+$: 365.2263 MS found $[M+H]^+$: 365.2260.

3-[2-((2-(6-Fluoro-1*H*-indol-3-yl)ethyl)(methyl)amino)ethyl]-2-methyl-6,7,8,9-tetrahydro-4*H*-pyrido[1,2-*a*]pyrimidin-4-one Hydrogen Oxalate (112)

3-(2-Chloroethyl)-2-methyl-6,7,8,9-tetrahydro-4*H*-pyrido[1,2-*a*]pyrimidin-4-one (0.30 g, 1.31 mmol) was added to a stirred suspension of compound **108** (0.30 g, 1.31 mmol), anhydrous K_2CO_3 (0.36 g, 2.62 mmol) and KI (few crystals) in MeCN (20 mL) under an N_2 atmosphere. The stirred reaction mixture was heated at reflux for 48 h. The hot reaction mixture was filtered and the filtrate was evaporated under reduced pressure to give 0.36 g of a yellow liquid. The liquid was dissolved in H_2O, basified with NaOH (2 M to ~pH 12) and extracted with CH_2Cl_2 (5 x 5 mL). The combined organic portion was washed with H_2O (3 x 5 mL), brine (5 mL), dried (Na_2SO_4) and evaporated under reduced pressure to yield 0.22 g of crude free base as a yellow-colored liquid. The free base was purified using a short column (silica gel; CH_2Cl_2/MeOH/NH_4OH; 9:1:0.1) to afford 0.17 g of a liquid that was dissolved in CH_2Cl_2 (2 mL) and cooled to 0 °C (ice-bath). A saturated solution of $(COOH)_2$/Et_2O was added and the reaction mixture was allowed to stir at room temperature overnight. The precipitate was collected by filtration to yield a yellow-colored solid (0.19 g) which

upon recrystallization from EtOH afforded 0.14 g (16%) of compound **112** as a yellow solid: mp 78-82 ºC. ^{1}H NMR (DMSO-d_6) δ 1.76-1.90 (m, 4H, CH_2), 2.25 (s, 3H, CH_3), 2.78-2.87 (m, 4H, CH_2), 2.95 (s, 3H, CH_3), 3.11-3.18 (m, 4H, CH2), 3.40-3.46 (m, 2H, CH_2), 3.78-3.81 (t, 2H, CH_2, *J* = 6.2 Hz), 6.86-6.92 (td, 1H, ArH, *J* = 2.32, 9.84 Hz), 7.14-7.17 (dd, 1H, ArH, *J* = 2.24, 10.12 Hz), 7.27 (s, 1H, ArH), 7.61-7.65 (q, 1H, ArH, *J* = 5.4 Hz), 11.01 (s, 1H, NH). Anal. Calcd for ($C_{22}H_{27}N_4OF$•1.5 $(COOH)_2$ •0.7CH_2Cl_2•0.1 C_2H_5OH) C, 53.49; H, 5.55; N, 9.63. Found: C, 53.46; H, 5.47; N, 9.36). MS calculated $[M+H]^+$: 383.2169 MS found $[M+H]^+$: 383.2244.

3-[2-[4-(6-Fluoro-1,2-benzisoxazol-3-yl)-1-piperidinyl]ethyl]-2-methyl-4*H*-pyrido[1,2-a]pyrimidin-4-one Oxalate (113)

3-(2-Chloroethyl)-2-methyl-4*H*-pyrido[1,2-*a*]pyrimidin-4-one (**136**) (0.20 g, 0.90 mmol) was added to a stirred suspension of 6-fluoro-3-(4-piperidinyl)benz[*d*]isoxazole (0.20 g, 0.90 mmol), anhydrous K_2CO_3 (0.12 g, 0.90 mmol) and KI (few crystals) in MeCN (20 mL) under an N_2 atmosphere. The stirred reaction mixture was heated at reflux for 20 h, cooled to room temperature and filtered. The residue was washed with MeOH (2 x 10 mL) and H_2O to yield 0.18 g of a pink-colored solid: mp 172-174 ºC (lit.[174] mp 170.4 ºC). The solid (0.18 g) was dissolved in CH_2Cl_2 (2 mL) and cooled to 0 °C (ice-bath). A saturated solution of $(COOH)_2$/Et_2O was added and the reaction mixture was allowed to stir at room temperature overnight. The precipitate was collected by filtration to yield a white solid (0.25 g) which upon recrystallization from EtOH/H_2O afforded 0.17 g (5%) of compound **113** as a white solid: mp 198-200 ºC. ^{1}H NMR (DMSO-d_6) δ 1.04-1.07 (t, 3H, CH_3 from EtOH), 2.09-2.33 (m, 4H, CH_2), 3.04-3.17 (m, 6H, CH_2) 3.42-3.48 (m, 3H, CH_2 from EtOH, CH), 3.65 (s, 2H, CH_2), 7.31-7.36 (m, 2H, ArH), 7.62-7.64 (d, 1H, ArH, *J* = 8.8 Hz),

7.73-7.75 (dd, 1H, ArH, *J* = 2.1 Hz, 9.1 Hz), 7.90-7.94 (m, 1H, ArH), 8.07-8.10 (m, 1H, ArH), 8.90-8.92 (d, 1H, ArH, *J* = 6.6 Hz)), (3H are under the DMSO peak, verified by COSY). Anal. Calcd for ($C_{23}H_{23}N_4O_2F{\cdot}1(COOH)_2{\bullet}1C_2H_5OH{\cdot}0.2H_2O$) C, 59.38; H, 5.79; N, 10.26. Found C, 59.11; H, 5.62; N, 10.20. MS calculated $[M+H]^+$: 407.1805 MS found $[M+H]^+$: 407.1883.

4-[4-(6-Fluorobenz[*d*]isoxazol-3-yl)piperidin-1-yl]-1-phenylbutan-1-one Hydrochloride (114)

4-Chlorobutyrophenone (**137**) (1.19 g, 0.82 mmol) was added to a stirred suspension of 6-fluoro-3-(4-piperidinyl)benz[*d*]isoxazole (1.43 g, 0.82 mmol), anhydrous K_2CO_3 (0.90 g, 0.82 mmol) and KI (few crystals) in MeCN (50 mL) under an N_2 atmosphere. The stirred reaction mixture was heated at reflux for 20 h, filtered, and the filtrate was evaporated under reduced pressure to give 1.9 g of a yellow oil. The yellow oil was dissolved in CH_2Cl_2 and 1M HCl (10 mL) was added to afford a precipitate that was insoluble in H_2O. The precipitate was collected by filtration and washed with CH_2Cl_2 (3 x 15 mL) and H_2O (3 x 15 mL) to yield a white solid (1.44 g) which upon recrystallization from EtOH/H_2O afforded 0.42 g (15%) of compound **114** as a white solid: mp 224-228 °C. ^{1}H NMR (DMSO-d_6) δ 2.05-2.15 (m, 2H, CH_2), 2.22-2.25 (d, 2H, CH_2, *J* = 12.4 Hz) 2.33-2.42 (m, 2H, CH_2), 3.11-3.27 (m, 6H, CH_2) 3.47-3.53 (m, 1H, CH), 3.65-3.68 (d, 2H, CH_2, *J* = 11.7 Hz), 7.33-7.38 (m, 1H, ArH), 7.54-7.58 (t, 2H, ArH, *J* = 7.4 Hz), 7.65-7.69 (t, 1H, ArH, *J* = 7.4 Hz), 7.72-7.75 (dd, 1H, ArH, *J* = 2, 9.1 Hz), 8.00-8.02 (m, 2H, ArH), 8.20-8.24 (m, 1H, ArH) 10.58 (br s, 1H, NH^+, D_2O ex). Anal. Calcd for ($C_{22}H_{23}N_2O_2F{\bullet}1HCl$) C, 65.59; H, 6.00; N, 6.95. Found C, 65.29; H, 6.01; N, 6.89.

6-Fluoro-3-[1-(4-phenylbutyl)piperidin-4-yl]benz[*d*]isoxazole Hydrochloride (115)

1-Chloro-4-phenylbutane (**138**) (0.14 g, 0.82 mmol) was added to a stirred suspension of 6-fluoro-3-(4-piperidinyl)benz[*d*]isoxazole (0.18 g, 0.82 mmol), anhydrous K_2CO_3 (0.11 g, 0.82 mmol) and KI (few crystals) in MeCN (15 mL) under an N_2 atmosphere. The stirred reaction mixture was heated at reflux for 36 h, filtered, and the filtrate was evaporated under reduced pressure to give 0.28 g of crude free base as a yellow oil. The free base was unsuccessfully purified using Kugelrohr distillation and was purified by column chromatography (silica gel; CH_2Cl_2/MeOH; 9:1) to afford 0.20 g of a yellow-colored oil, that was dissolved in EtOAc (2 mL), cooled to 0 °C (ice-bath) and treated with a saturated solution of gaseous HCl/EtOAc, and then the reaction mixture was allowed to stir at room temperature overnight. The precipitate was collected by filtration to yield a white solid (0.19 g) which upon recrystallization from EtOH/H_2O afforded 0.13 g (40%) of compound **115** as a white solid: mp 200-204 ºC. ^{1}H NMR (DMSO-d_6) δ 1.62-1.81 (m, 4H, CH_2), 2.21-2.36 (m, 4H, CH_2), 2.63-2.67 (t, 2H, CH_2, J = 7.4 Hz), 3.05-3.17 (m, 4H, CH_2), 3.43-3.51 (m, 1H, CH), 3.59-3.62 (d, 2H, CH_2, J = 12.0 Hz), 7.18-7.38 (m, 6H, ArH), 7.72-7.76 (m, 1H, ArH), 8.17-8.21 (m, 1H, ArH), 10.38 (br s, 1H, NH^+). Anal. Calcd for ($C_{22}H_{25}N_2OF$•1 HCl) C, 67.94; H, 6.74; N, 7.20. Found C, 67.65; H, 6.81; N, 7.11.

4-[4-(6-Fluorobenz[*d*]isoxazol-3-yl)piperidin-1-yl]-1-phenylpentan-1-one Hydrochloride (116)

Compound **141** (0.20 g, 1.01 mmol) was added to a stirred suspension of 6-fluoro-3-(4-piperidinyl)benz[*d*]isoxazole (0.25 g, 1.12 mmol), anhydrous K_2CO_3 (0.15 g, 1.12 mmol) and KI (few crystals) in MeCN (5 mL). The stirred reaction mixture was heated in a sealed tube at 80 ºC

for 48 h, filtered, and the filtrate was evaporated under reduced pressure to give 0.29 g of a sticky solid. The solid was purified by column chromatography (silica gel; CH_2Cl_2/MeOH; 9:1) to yield 0.13 g of a sticky solid. The solid was dissolved in EtOH, cooled to 0 °C (ice-bath) and a saturated solution of gaseous HCl/EtOH was added. The EtOH was removed under reduced pressure to yield a white solid (0.06 g; mp 206-208 ºC) which upon recrystallization from MEOH/H_2O afforded 0.05 g (13%) of compound **116** as a white solid: mp 206-208 ºC. ^{1}H NMR (DMSO-d_6) δ 1.68-1.80 (m, 4H, CH_2), 2.15-2.22.28 (m, 4H, CH_2), 3.07-3.20 (m, 6H, CH_2), 3.49-3.51 (m, 1H, CH), 3.62-3.65 (d, 2H, CH_2, *J* = 11.84 Hz), 7.34-7.39 (td, 1H, ArH, *J* = 2.0, 8.9 Hz), 7.53-7.57 (t, 2H, ArH, *J* = 7.4 Hz), 7.64-7.68 (t, 1H, ArH, *J* = 7.32), 7.74-7.76 (dd, 1H, ArH, *J* = 2.1, 9.1 Hz), 7.97-8.01 (m, 2H, ArH), 8.12-8.15 (m, 1H, ArH), 9.97 (brs, 1H, NH^+). Anal. Calcd for ($C_{23}H_{25}N_2O_2F$•1HCl•0.2CH_3OH•0.7H_2O) C, 63.92; H, 6.52; N, 6.43. Found C, 63.65; H, 6.14; N, 6.40.

6-Fluoro-3-[1-(5-phenylpentyl)piperidin-4-yl]benz[*d*]isoxazole Hydrochloride (117)

1-Chloro-5-phenylpentane (**142**) (0.50 g, 2.73 mmol) was added to a stirred suspension of 6-fluoro-3-(4-piperidinyl)benz[*d*]isoxazole (0.66 g, 2.97 mmol), anhydrous K_2CO_3 (0.41 g, 2.97 mmol) and KI (few crystals) in MeCN (4 mL). The stirred reaction mixture was heated at 80 °C in a sealed tube for 96 h, allowed to cool to room temperature, filtered, and the filtrate was evaporated under reduced pressure to give 0.90 g of a yellow oil. The oil was purified by column chromatography (silica gel; CH_2Cl_2/MeOH; 9.5:0.5) to afford 0.23 g of a sticky white solid. The solid was dissolved in MeOH (2 mL), and cooled to 0 °C (ice-bath). A saturated solution of gaseous HCl/EtOH was added and the reaction mixture was allowed to stir at room temperature overnight.

The solvent was evaporated under reduced pressure to yield a white solid (0.21 g) which upon recrystallization from MeOH/H_2O afforded 0.14 g (12%) of compound **117** as a white solid: mp 166 °C. ^{1}H NMR (DMSO-d_6) δ 1.30-1.38 (m, 2H, CH_2), 1.59-1.66 (m, 2H, CH_2), 1.76-1.84 (m, 2H, CH_2), 2.18-2.21 (d, 2H, CH_2, J = 13.3 Hz), 2.33-2.43 (m, 2H, CH_2), 2.59-2.63 (t, 2H, CH_2, J = 7.7 Hz), 3.04-3.17 (m, 4H, CH_2), 3.40-3.50 (m, 1H, CH), 3.60-3.62 (d, 2H, CH_2, J = 11.8 Hz), 7.16-7.36 (m, 6H, ArCH), 7.71-7.74 (dd, 1H, ArCH, J = 2.0, 9.0 Hz), 8.22-8.25 (m, 1H, ArCH), 10.84 (br s, 1H, NH^+). Anal. Calcd for ($C_{23}H_{27}N_2OF$•1 HCl) C, 68.56; H, 7.00; N, 6.95. Found C, 68.66; H, 7.10; N, 6.93.

6-Fluoro-3-(2-nitrovinyl)-1*H*-indole (123)

Compound **123** was synthesized using a literature procedure for the same compound.[165] Trifluoroacetic acid (3.7 mL) was added to 6-fluoroindole (**120**) (0.5 g, 3.69 mmol) and 1-dimethylamino-2-nitroethylene (0.43 g, 3.71 mmol) under an N_2 atmosphere. The reaction mixture was allowed to stir at room temperature for 1 h, and quenched carefully with a saturated aqueous $NaHCO_3$ solution. The residue was collected by filtration, washed with H_2O and dried to yield 0.65 g (85%) of compound **123** as a yellow solid. mp 172-174 ºC (lit.[166] mp 170-172 ºC). Compound **123** was used in the preparation of compound **106**.

3-(2-Nitrovinyl)-1*H*-indole (125)

Compound **125** was synthesized using a literature procedure for a similar compound.[165] Trifluoroacetic acid (3.7 mL) was added to indole (**124**) (0.43 g, 3.69 mmol) and 1-dimethylamino-2-nitroethylene (0.43 g, 3.71 mmol) under an N_2 atmosphere. The reaction mixture was allowed

to stir at room temperature for 1 h and quenched carefully with a saturated aqueous $NaHCO_3$ solution. The residue was collected by filtration, washed with H_2O and dried to yield 0.56 g (81%) of compound **125** as a yellow solid: mp 164-168 ºC (lit.[168] mp 167-168 ºC). Compound **125** was used in the preparation of compound **105**.

Ethyl (2-(6-fluoro-1*H*-indol-3-yl)ethyl)carbamate (127)

Compound **127** was synthesized using a literature procedure for a similar compound.[172] Ethyl chloroformate (0.37 mL, 3.92 mmol) was added in a dropwise manner at 0 ºC (ice-bath) to a stirred solution of **106** (0.7 g, 3.91 mmol) and Et_3N (0.549 mL, 3.92 mmol) in anhydrous CH_2Cl_2 (13 mL) under an N_2 atmosphere. The reaction mixture was allowed to stir at room temperature for 3 h. The organic portion was washed with H_2O (13 mL), 1M HCl (5 mL), 5% $NaHCO_3$ solution (5 mL), H_2O (5 mL), brine (5 mL), dried (Na_2SO_4), and evaporated under reduced pressure to yield 0.84 g (86%) as an orange-colored oil. An attempt was made to isolate the product using a short column (silica gel; Ethyl acetate /Hexanes; 4:6). 0.50 g (51%) of a mixture of **127** and impurities was isolated as an orange-colored oil and was used without further purification in the next step. IR (diamond, cm^{-1}) 1689 (-NH), 3318 (-C=O). Compound **127** was used in the preparation of compound **108**.

Indolyl-3-glyoxyl chloride (128)

Compound **128** was synthesized using a literature procedure for the same compound.[169] Oxalyl chloride (0.71 mL, 8.17 mmol) was added dropwise to a stirred solution of indole **124** (0.83 g, 7.08 mmol) in anhydrous Et_2O (15 mL) at 0 ºC (ice-bath) under an N_2 atmosphere, and was allowed to

stir at 0 ºC for 3 h, and at room temperature for 1 h. The reaction mixture was filtered, and the residue was washed with cold Et_2O, and dried to yield 1.02 g (73%) of compound **128** as yellow crystals: mp 120-124 ºC (decomposes) (lit.[216] mp 116-117 °C). Compound **128** was used in the preparation of compound **129**.

Indole-3-yl-*N*-methylglyoxalylamide (129)

Compound **129** is known and was synthesized using a literature procedure for the same compound.[217] A solution of compound **128** (0.60 g, 2.89 mmol) in THF was added to methylamine (40% in H_2O, 30 mL) at 0 ºC (ice-bath), and the reaction mixture was allowed stirred at room temperature for 24 h. The solvent was removed under reduced pressure to yield a crude sticky residue that was dried and recrystallized from MeOH to yield 0.4 g (68%) of compound **129** as a beige-colored solid: mp 214-216 ºC (lit.[217] mp 220-222 ºC). Compound **129** was used in the preparation of compound **130**.

Hydroxy-indol-3-yl-acetic acid methylamide (130)

Compound **130** was obtained as a side-product and was synthesized using a literature procedure for a compound similar to analog **107**.[172] A solution of compound **129** (0.30 g, 1.50 mmol) in THF (40 mL) was added to a stirred solution of $LiAlH_4$ (0.29 g, 7.50 mmol) in anhydrous THF (50 mL) at 0 ºC under an N_2 atmosphere. The reaction mixture was heated at reflux for 8 h, cooled to 0 °C (ice-bath), and quenched by addition of H_2O (0.3 mL), 15% NaOH (0.3 mL) and H_2O (1.5 mL). The suspension was filtered, and the residue was washed with Et_2O. The filtrate was extracted with Et_2O (3 x 10 mL). The combined organic portion was washed with brine (10 mL), dried (Na_2SO_4),

and evaporated under reduced pressure to yield 0.10 g (33%) of compound **130** as a white solid: mp 184-188 °C (lit.[171] mp 193-194 °C). IR (diamond, cm^{-1}) 3277 (-OH).

Ethyl 2-(1*H*-indol-3-yl)ethylcarbamate (131)

Compound **131** was synthesized using a literature procedure for the same compound.[172] Ethyl chloroformate (1.48 mL, 15.61 mmol) was added dropwise at 0 ºC (ice-bath) to a stirred solution of tryptamine (**105**) (2.5 g, 15.61 mmol) and Et_3N (2.17 mL, 15.61 mmol) in anhydrous CH_2Cl_2 (39 mL). The stirred reaction mixture was allowed to warm to room temperature. The organic portion was washed with H_2O (10 mL), 1M HCl (10 mL), 5% $NaHCO_3$ solution (10 mL), H_2O (10 mL), brine (10 mL), dried (Na_2SO_4), and evaporated under reduced pressure to yield 2.80 g (77%) as an orange-colored oil. The oil was purified using column chromatography (silica gel; EtOAc/Hexanes; 3:7) to yield 1.76 g (49%) of compound **131** as an orange-colored oil. IR (diamond, cm^{-1}) 1689 (-C=O), 3318 (-NH). Compound **131** was used in the preparation of compound **107**.

***N*,*N*-bis(3-(2-Ethyl)-2-methyl-6,7,8,9-tetrahydro-4*H*-pyrido[1,2-*a*]pyrimidin-4-onyl)tryptamine (132)**

3-(2-Chloroethyl)-2-methyl-6,7,8,9-tetrahydro-4*H*-pyrido[1,2-*a*]pyrimidin-4-one (0.10 g, 0.4 mmol) was added to a stirred suspension of tryptamine (**105**) (0.079 g, 0.44 mmol), KI (catalytic amount) and anhydrous K_2CO_3 (0.07 g, 0.44 mmol) in MeCN (3 mL) The stirred reaction mixture was heated in a sealed tube at 80 ºC for 5 days. The hot reaction mixture was filtered and the filtrate was evaporated under reduced pressure to give 0.15 g of a crude residue. The crude residue was

purified using a short column (silica gel; CH_2Cl_2/MeOH/NH_4OH; 8.5:1.5:0.1) to yield 0.03 g (13%) of compound **132** as a sticky white solid. ^{1}H NMR (DMSO-d_6) δ 1.73-1.85 (m, 8H, CH_2), 2.21 (s, 6H, CH_3), 2.62 (s, 8H, CH_2), 2.72-2.76 (t, 4H, CH_2), 2.83 (s, 4H, CH_2), 3.76-3.79 (t, 4H, CH_2, *J* = 6.2 Hz), 6.94-6.98 (t, 1H, ArH, *J* = 7.4 Hz), 7.03-7.07 (t, 1H, ArH, *J* = 7.5 Hz), 7.12 (s, 1H, ArH), 7.31-7.33 (d, 1H, ArH, *J* = 8.0 Hz), 7.52-7.54 (d, 1H, ArH, *J* = 7.8 Hz), 10.76 (s, 1H, NH). MS calculated $[M+H]^+$: 541.3213 MS found $[M+H]^+$: 541.3313.

***N*-Benzyltryptamine (133)**

Compound **133** is known and was synthesized using a literature procedure for the same compound.[218] $MgSO_4$ (0.01 g, 0.1 mmol), tryptamine (**105**) (0.16 g, 1.00 mmol), and benzaldehyde (0.14 g, 1.3 mmol) were added to EtOH (10 mL), and the stirred reaction mixture was heated at 60 ºC for 1 h. The reaction mixture was filtered and $NaBH_4$ (0.04 g, 1 mmol) was added to the filtrate. The reaction mixture was allowed to stir at room temperature for 1.5 h and was quenched by the addition of ice-H_2O at 0 ºC (ice-bath). The aqueous portion was extracted with CH_2Cl_2 (3x 5 mL), and the combined organic portion was washed with H_2O (5 mL), brine (5 mL), dried (Na_2SO_4), and evaporated under reduced pressure to yield 0.18 g (78%) of compound **133** as a brown-colored oil. NMR (DMSO-d_6) δ 2.77-2.88 (m, 4H, CH_2), 3.74 (s, 2H, CH_2), 6.93-6.97 (m, 1H, ArH), 7.03-7.07 (td, 1H, ArH, *J* = 1.1, 8.1 Hz), 7.12-7.13 (d, 1H, ArH, *J* = 2.3 Hz), 7.19-7.23 (m, 1H, ArH), 7.28-7.34 (m, 5H, ArH), 7.48-7.50 (d, 1H, ArH, *J* = 7.9 Hz). 10.76 (s, NH). Compound **133** was used in the preparation of compound **134**.

3-(2-((2-(1*H*-Indol-3-yl)ethyl)(benzyl)amino)ethyl)-2-methyl-6,7,8,9-tetrahydro-4*H*-pyrido[1,2-*a*]pyrimidin-4-one (134)

3-(2-Chloroethyl)-2-methyl-6,7,8,9-tetrahydro-4*H*-pyrido[1,2-*a*]pyrimidin-4-one (0.16 g, 0.73 mmol) was added to a stirred suspension of intermediate **133** (0.18 g, 0.73 mmol), anhydrous K_2CO_3 (0.10 g, 0.73 mmol) and KI (few crystals) in MeCN (15 mL) under an N_2 atmosphere. The stirred reaction mixture was heated at reflux for 48 h. The hot reaction mixture was filtered and the filtrate was evaporated under reduced pressure to give 0.24 g of a crude residue. The residue was dissolved in H_2O (~5 mL), and extracted with CH_2Cl_2 (3 x 5 mL). The combined organic portion was washed with H_2O (5 mL), brine (5 mL), dried (Na_2SO_4) and evaporated under reduced pressure to yield 0.20 g of a sticky, yellow-colored liquid that was purified using a short column (silica gel; CH_2Cl_2/MeOH/NH_4OH; 9:1:0.1) to afford 0.12 g of a liquid, that was dissolved in CH_2Cl_2 (2 mL), cooled to 0 °C (ice-bath), and treated with a saturated solution of gaseous HCl/EtOH, and then the reaction mixture was allowed to stir at room temperature overnight. The precipitate was collected by filtration to yield 0.07 g (20%) of compound **134** as a sticky, pale gray-colored solid. NMR (DMSO-d_6) δ 1.77-1.94 (m, 4H, CH_2), 2.36 (s, 3H, CH_3), 3.02-3.43 (m, 10 H, CH_2), 3.81-3.84 (t, 2H, CH_2, J = 6.3 Hz), 4.55-4.57 (d, 2H, CH_2, J = 5.2 Hz), 6.96-7.00 (m, 1H, ArH), 7.07-7.11 (m, 1H, ArH, J = 1.1, 8.1 Hz), 7.21 (d, 1H, ArH, J = 3.96 Hz), 7.35-7.37 (d, 1H, ArH, J = 8.1 Hz), 7.48-7.51 (m, 4H, ArH), 7.77-7.79 (m, 2H, ArH, J = 7.9 Hz). 11.01 (s, 1H, NH), 11.41 (brs, 1H, NH^+).

5-Chlorovaleroyl chloride (140)

Compound **140** was synthesized using a literature procedure for the same compound.[175] Thionyl chloride (2.0 mL, 28.09 mmol) was added to 5-chlorovaleric acid (**139**) (2.00 g, 14.64 mmol), and heated at reflux for 3 h under an N_2 atmosphere. The reaction mixture was allowed to cool to room temperature and the thionyl chloride was evaporated under reduced pressure to give 2.04 g (90%) of compound **140** as a crude yellow oil. Compound **140** was used without further purification in the next step. IR (diamond, cm^{-1}) 1791 (-C=O). Compound **140** was used in the preparation of compound **141**.

5-Chloro-1-phenyl-1-pentanone (141)

Compound **141** was synthesized using a literature procedure for the same compound.[176] $AlCl_3$ (1.89 g, 14.17 mmol) was added to a stirred solution of **140** (2.04 g, 13.16 mmol) in benzene (3.2 mL, 35.88 mmol) at 0 ºC (ice-bath). The reaction mixture was stirred at 0 ºC for 1 h, and was allowed to cool to room temperature and stirred for an additional hour. It was quenched by pouring into ice-H_2O, and the organic portion was separated. The aqueous portion was extracted with benzene (3 x 10 mL). The combined organic portion was washed with H_2O (10 mL), brine (10 mL), dried (Na_2SO_4), and concentrated under reduced pressure to yield 2.4 g of a crude pale brown solid: mp 42-43 ºC, that was recrystallized using hexane to give 2.2 g of a pale yellow solid: mp 43-44 ºC that was further purified by column chromatography (silica gel; hexanes/ EtOAc; 100:0 to 94:06) to yield 2.1 g (81%) of compound **141** as a pearly white solid: mp 49 ºC (lit.[176] mp 50-51 °C). ^{1}H NMR (DMSO-d_6) δ 1.70-1.84 (m, 4H, CH_2), 3.07-3.10 (t, 2H, CH_2, J = 6.8 Hz), 3.68-3.71 (t, 2H, CH_2, J = 6.4 Hz), 7.51-7.55 (t, 2H, ArCH, J = 7.4 Hz), 7.62-7.66 (t, 1H, ArCH, J = 7.4

Hz), 7.96-7.99 (d, 2H, ArCH, J = 7.1 Hz). Compound **141** was used in the preparation of compound **116**.

4-(4-Phenylpiperidin-1-yl)pyridin-2(1*H*)-one (150)

Compound **150** was unknown and was synthesized using a literature procedure for a similar compound.[204] A solution of **151** (0.11 g, 0.32 mmol) in EtOAc/MeOH (27 mL, 1/2) was hydrogenated (30-40 psi) using 10% Pd/C (0.01 g) as a catalyst at room temperature for 2 h. The reaction mixture was filtered over Celite and the filtrate was evaporated under reduced pressure to yield 0.07 g (86%) of compound **150** as a yellow-colored solid: mp 110-114 ºC. ^{1}H NMR (DMSO-d_6) δ 1.57-1.68 (m, 2H, CH_2), 1.82-1.85 (d, 2H, CH_2, J = 11.4 Hz), 2.77-2.83 (m, 1H, CH), 2.91-2.97 (t, 2H, CH_2, J = 11.5 Hz) 3.94-3.97 (d, 2H, CH_2, J = 13.3 Hz), 5.53 (s, 1H, ArH), 6.14-6.17 (dd, 1H, ArH, J = 2.4 Hz, 7.6 Hz), 7.16-7.32 (m, 6H, Ar H). IR (diamond, cm^{-1}) 1611 (-C=O), 2917 (-NH). Compound **150** was used in the preparation of compounds **153** and **154**.

2-(Benzyloxy)-4-(4-phenylpiperidin-1-yl)pyridine (151)

Compound **151** was not known and was synthesized using a procedure for a similar compound.[119] 4-Phenyl piperidine (1.71 g, 10.67 mmol), palladium diacetate (0.79 g, 3.53 mmol), BINAP (0.33 g, 0.53 mmol) and sodium *tert*-butoxide (1.38 g, 14.33 mmol) were added to a stirred solution of **152** (1.5 g, 5.73 mmol) in toluene (15 mL). The reaction mixture was heated in a sealed tube at 100 ºC for 27 h and filtered over Celite. The filtrate was diluted with water (~20 mL) and extracted with EtOAC (3x 20 mL). The combined organic portion was washed with H_2O (10 mL), brine (10 mL), dried (Na_2SO_4), and concentrated under reduced pressure to yield 2.01 g of a crude, yellow

oil that was further purified by column chromatography (silica gel; hexanes/ EtOAc; 100:0 to 94:06) to yield 0.43 g (22%) of compound **151** as a white solid: mp 106-108 ºC. ^{1}H NMR (DMSO-d_6) δ 1.62-1.69 (m, 2H, CH_2), 1.82-1.85 (d, 2H, CH_2, J = 12.12 Hz), 2.75-2.82 (m, 1H, CH), 2.89-2.96 (m, 2H, CH_2), 4.01-4.04 (d, 2H, CH_2, J = 13.3 Hz), 5.30 (s, 2H, CH_2), 6.23 (s, 1H, ArH), 6.60-6.62 (dd, 1H, ArH, J = 2.3 Hz, 6.2 Hz), 7.18-7.44 (m, 10H, Ar H), 7.80-7.82 (d, ArH, 1H, J = 6.2 Hz). Compound **151** was used in the preparation of compound **150**.

2-(Benzyloxy)-4-bromopyridine (152)

Compound **152** is known and was synthesized using a literature procedure for the same compound.[203] Sodium hydride (0.93 mg, 38.75 mmol) was added to a stirred solution of benzyl alcohol (2.65 mL, 25. 51 mmol) in THF (8 mL) at 0 ºC and was allowed to stir at room temperature for 15 min. 4-Bromo-2-chloro pyridine (**148**) (1.50 g, 7.79 mmol) in THF (2 mL) was added, the stirred reaction mixture was heated at reflux for 3 h, and quenched by the addition of H_2O (~10 mL). The aqueous portion was extracted with EtOAC (3x 10 mL). The combined organic portion was washed with H_2O (10 mL), brine (10 mL), dried (Na_2SO_4), and concentrated under reduced pressure to yield 2.20 g of a crude yellow oil that was further purified by column chromatography (silica gel; hexanes/ EtOAc; 100:0 to 80:20) to yield 1.5 g (73%) of compound **152** as a colorless oil. ^{1}H NMR (DMSO-d_6) δ 5.41 (s, 2H, CH_2), 7.26 (s, 1H, ArH), 7.30-7.31 (dd, 1H, ArH, J = 1.6 Hz, 5.5 Hz), 7.36-7.51 (m, 5H, Ar H), 8.14-8.16 (d, ArH, 1H, 5.5 Hz). Compound **152** was used in the preparation of compound **151**.

2-Butoxy-4-(4-phenylpiperidin-1-yl)pyridine (153)

Compound **153** was obtained as a side-product instead of compound **147** and was synthesized using a literature procedure for a similar compound.[219] Sodium hydride was added to a solution of compound **150** (0.22 g, 0.85 mmol) in DMF (10 mL) at 0 ºC under an N_2 atmosphere and was stirred at room temperature for 1 h. n-Butyl bomide (0.1 mL, 0.91 mmol) was added dropwise and the reaction mixture was heated at 103 ºC for 3 days. The reaction mixture was diluted with H_2O (~10 mL) and extracted with EtOAC (3x 10 mL). The combined organic portion was washed with H_2O (10 mL), brine (10 mL), dried (Na_2SO_4), and concentrated under reduced pressure to yield 0.16 g of a crude yellow oil that was further purified by column chromatography (silica gel; hexanes/ EtOAc; 100:0 to 80:20) to yield 0.04 g (17%) of compound **153** as a yellow-colored oil. ^{1}H NMR (DMSO-d_6) δ 0.91-0.95 (t, 3H, CH_3, J = 7.4 Hz), 1.25-1.27 (d, 1H, CH, J = 10 Hz), 1.38-1.46 (m, 2H, CH_2), 1.62-1.69 (m, 4H, CH_2), 1.82-1.85 (d, 2H, CH_2, J = 10.6 Hz), 2.76-2.81 (m, 1H, CH), 2.87-2.93 (m, 2H, CH_2), 3.99-4.02 (d, 2H, CH_2, J = 12.8 Hz), 4.17-4.20 (t, 2H, CH_2, J = 6.6 Hz), 6.12-6.13 (d, 1H, ArH, J = 2.2 Hz), 6.56-6.58 (dd, 1H, ArH, J = 2.2 Hz, 6.2 Hz), 7.16-7.32 (m, 5H, ArH), 7.77-7.78 (d, 1H, ArH, J = 6.1 Hz).

3-Chloro-4-(4-phenylpiperidin-1-yl)pyridin-2(1*H*)-one (154)

Compound **154** was unknown and was synthesized using a literature procedure for a similar compound.[119] *N*-Chlorosuccinimide (0.08 g, 0.63 mmol) was added to a stirred solution of Compound **150** (0.16 g, 0.63 mmol) in CH_2Cl_2 (30 mL). The reaction mixture was allowed to stir at room temperature for 10 min and was quenched by the addition of a saturated aqueous $NaHCO_3$ solution. The aqueous portion was extracted with CH_2Cl_2 (3 x 10 mL) and the combined organic

portion was washed with H_2O (10 mL), brine (10 mL), dried (Na_2SO_4), and concentrated under reduced pressure to yield 0.12 g of a crude residue that was was further purified by column chromatography (silica gel; CH_2Cl_2/ MeOH; 90:10) to yield 0.05 g (81%) of compound **154** as a white solid: mp 274 ºC. ^{1}H NMR (DMSO-d_6) δ 1.67-1.86 (m, 4H, CH_2), 2.65-2.73 (m, 1H, CH), 2.83-2.91 (t, 2H, CH_2, J = 11.55 Hz), 3.64-3.68 (d, 2H, CH_2, J = 12.3 Hz), 6.08-6.11 (d, 1H, ArH, J = 7.2 Hz), 6.14-6.17 (m, 6H, ArH).

(±)6-Fluoro-3-(piperidin-3-yl)benz[*d*]isoxazole Hydrochloride (155)

Compound **155** was synthesized using a literature procedure for a similar compound.[153] Compound **161** (0.07 g, 0.27 mmol) was added to a solution of HCl (3N, 1 mL) and EtOH (1 mL), and heated at reflux for 3 h. It was allowed to cool to room temperature and evaporated to dryness under reduced pressure to yield a crude yellow-colored solid (mp 258-260 °C) that was recrystallized from EtOH/H_2O to yield 0.05 g (74%) of compound **155** as a yellow-colored solid: mp 262-264 °C. ^{1}H NMR (DMSO-d_6) δ 1.78-1.92 (m, 3H, CH_2), 2.21-2.25 (d, 1H, CH_2, J = 13.2 Hz), 3.04 (s, 1H, CH), 3.27-3.34 (m, 2H, CH_2), 3.59-3.72 (m, 2H, CH_2), 7.34-7.39 (m, 1H, ArH), 7.75-7.78 (m, 1H, ArH), 8.13-8.16 (m, 1H, ArH), 9.25 (br s, 2H, NH^+) ; Anal. Calcd for ($C_{12}H_{13}N_2OF$•1HCl) C, 56.15; H, 5.50; N, 10.91. Found C, 56.11; H, 5.52; N, 10.84.

***N*-Formylpiperidine-3-carboxylic acid (157)**

Compound **157** was synthesized using a literature procedure for a similar compound.[143] A solution of HCOOH (9 mL, 222.98 mmol) and Ac_2O (22 mL, 222.98 mmol) was heated at 60 ºC for 1 h, cooled to 0 °C (ice-bath) and nipecotic acid (**156**) (5.00 g, 38.71 mmol) was added portion-wise.

The reaction mixture was allowed to stir at room temperature for 16 h. and concentrated under reduced pressure to yield a colorless oil that was crystallized using *i*-PrOH and diisopropyl ether to give a crude white solid (mp 110-112 °C). The solid was recrystallized using *i*-PrOH to yield 5.14 g (85%) of compound **157** as a white solid: mp 114 °C and used without further purification in the next step. Compound **157** was used in the preparation of compound **158**.

***N*-Formylpiperidine-3-carboxylic acid chloride (158)**

Compound **158** was synthesized using a literature procedure for a similar compound.[153] $SOCl_2$ (3 mL, 41.30 mmol) was added to **157** (2.00 g, 12.72 mmol) at 0 ºC (ice-bath) under an N_2 atmosphere. It was allowed to stir at room temperature for 6 h and the $SOCl_2$ was evaporated under reduced pressure to afford 2.18 g (98%) of compound **158** as a crude orange-colored oil that was verified spectrally and used without further characterization and purification in the next step. IR (diamond, cm^{-1}) 1668 (-C=O). Compound **158** was used in the preparation of compound **159**.

***N*-Formyl-3-(2,4-difluorobenzoyl)piperidine (159)**

Compound **159** was synthesized using a literature procedure for a similar compound.[153] Compound **158** (2.18 g, 12.41 mmol) was added dropwise to a stirred suspension of $AlCl_3$ (3.00 g, 22.50 mmol) suspended in 1,3-difluorobenzene (13 mL, 132.51 mmol) at 0 °C (ice-bath) under an N_2 atmosphere. The reaction mixture was heated at reflux for 22 h, allowed to cool to room temperature, and quenched by pouring into ice-H_2O (50 mL). The aqueous portion was extracted using $CHCl_3$ (3 x 15 mL) and the combined organic portion was washed with H_2O (10 mL), brine (10 mL), dried (Na_2SO_4), and evaporated under reduced pressure to yield 2.98 g (95%) of **159** as

an orange-colored oil that was used without further purification in the next step. Compound **159** was used in the preparation of compound **160**.

***N*-Formyl-3-((2,4- difluorophenyl)(hydroxyimino)methyl)piperidine (160)**

Compound **160** was synthesized using a literature procedure for a similar compound.[143] Hydroxylamine hydrochloride (2.37 g, 34.09 mmol) was added to a solution of **159** (2.89 g, 11.41 mmol) in EtOH (58 mL)and was followed by the addition of a solution of NaOH (1.39, 34.70 mmol) in H_2O (9 mL). The reaction mixture was heated at reflux for 96 h, allowed to cool to room temperature, and filtered. The filtrate was evaporated under reduced pressure to give a crude yellow-colored oil that was purified by column chromatography (silica gel; CH_2Cl_2/CH_3OH; 100:0 to 95:5) to afford 0.60 g (40%) of **160** as a yellow-colored solid: mp 158-160 °C. IR (diamond, cm^{-1}) 1639 (-C=N), 2864-3180 (-OH). Compound **160** was used in the preparation of compound **161**.

***N*-Formyl-3-(6-fluorobenz[*d*]isoxazol-3-yl)piperidine (161)**

Compound **161** was synthesized using a literature procedure for a similar compound.[153] A solution of **160** (0.59 g, 2.14 mmol) in DMF (3 mL) was added dropwise to a suspension of NaH (0.09 g, 3.63 mmol) in THF (5 mL) at 0 °C (ice-bath) under an N_2 atmosphere. The reaction mixture was heated at 75 °C for 4 h, allowed to cool to room temperature and poured into ice-H_2O (30 mL). The aqueous portion was extracted with EtOAc (3 x 15 mL) and the combined organic portion was washed with H_2O (10 mL), brine (10 mL), dried (Na_2SO_4) and evaporated under reduced pressure to give a crude yellow-colored solid that was purified by column chromatography (silica gel;

CH_2Cl_2/MeOH; 100:0 to 95:5) to afford 0.08 g (15%) of compound **161** as a pale yellow-colored solid: mp 104-106 ºC. Compound **161** was used in the preparation of compound **155**.

B. Radioligand binding studies

i. For risperidone (14), ketanserin (36), and compounds 60, 61, 65, 66, Ris/Ket (103) and Ket/Ris (104)

Radioligand binding studies of the compounds were conducted in Dr. Javier Gonzalez-Maeso's laboratory as previously reported.[141] Binding affinities of risperidone (**14**), ketanserin (**36**) and compounds **60**, **61**, **65**, **66**, Ris/Ket (**103**) and Ket/Ris (**104**) were determined by Dr. Jose L. Moreno.

ii. For compounds 57, 62, 63, 111, 112 and 155

Radioligand binding studies of the compounds were conducted in Dr. Javier Gonzalez-Maeso's laboratory. Binding affinities of analogs **62** and **63** were determined by Dr. Supriya A. Gaitonde.

The radioligand binding studies were performed in HEK 293 cells that stably express human 5-HT_{2A} receptors. The cell pellets were homogenized using a Teflon-glass grinder (50 up-and-down strokes) in 5 mL of binding buffer (5 mM Tris-HCl; pH 7.4). The volume was made up to 10 mL with binding buffer and the crude homogenate was centrifuged at 3000 rpm for 5 min at 4 °C. The supernatant was centrifuged at 18,000 rpm for 10 min at 4 °C. The resultant pellet (P_2 fraction) was washed with 10 mL of binding buffer (5 mM Tris-HCl pH 7.4) and re-centrifuged at 18,000 rpm for 15 minutes. Aliquots were stored at -80 °C until assay. Protein concentration was

determined using the Bio-Rad protein estimation assay. Curves were carried out by incubating each drug (10^{-10}-10^{-4} M; 13 concentrations) in binding buffer containing 5 nM [^{3}H]-ketanserin. Nonspecific binding was determined in the presence of 10 μM methysergide. Incubations were terminated by dilution with 200 μL ice-cold incubation buffer, and free ligand was separated from bound ligand by rapid filtration under vacuum through GF/C glass fiber filters using a microbeta filtermat-96 harvester (PerkinElmer). These filters were then rinsed twice with 200 μL of ice-cold incubation buffer, air-dried for 0.5 h, dried at 65 ºC for 1 h and counted for radioactivity by liquid scintillation spectrometry, using a MicroBeta2 detector (PerkinElmer). Radioligand binding data were analyzed by nonlinear regression by GraphPad PRISM (version 7 for Windows 10, GraphPad Software, La Jolla California, US).

C. Functional activity studies

The TEVC and calcium imaging assays were performed in Dr. Diomedes Logothetis's laboratory by Dr. Jason Younkin, Amr Ellaithy, and Dr. Lia Baki as previously reported.[141]

D. Molecular modeling studies

i. Docking studies at 5-HT$_{2A}$ receptors

The ligands were sketched in and energy minimized using the Tripos Force Field (Gasteiger-Hückel charges, distance-dependent dielectric constant = 4.0) in SYBYL X-2.1 (Tripos International). Docking studies at 5-HT$_{2A}$ receptors were conducted using the genetic algorithm docking program GOLD suite 5.4[187] (Cambridge Crystallographic Data Centre, Cambridge, UK), with ChemPLP as the chosen scoring function. The binding site was defined to include all amino

acid residues within a radius of 10 Å from Asp155 The docking poses were clustered (intracluster RMSD ≤ 2 Å) using a script that was provided by Dr. Philip Mosier. The top solutions were merged into homology models of the 5-HT_{2A} receptor and the receptor-ligand complexes were energy minimized using the Tripos Force Field (Gasteiger-Hückel charges, distance-dependent dielectric constant = 4.0) in SYBYL X-2.1 (Tripos International). HINT[188] analysis was performed in SYBYL-8.1 to quantify the receptor-ligand interactions observed in molecular modeling studies. PYMOL[220] was used to generate images.

ii. Homology modeling of $mGlu_2$ receptors

The amino acid sequences of the crystal structure of the $mGlu_5$ receptor (PDB ID: 4OO9) was retrieved as a FASTA file from the Protein Databank (PDB) The sequences retrieved consisted of a dimer and only residues from one monomer were retained. The sequence was prepared by removal of water molecules, ligand and other molecules. The amino acid sequence of the human $mGlu_2$ receptor was (entry code: Q14416), were retrieved as a FASTA files from the Universal Protein Resource (UniPort) Database. The amino acid sequences of the TMD of the $mGlu_5$ receptor and the $mGlu_2$ receptor were aligned using Clustal X 2.1.[178.] Homology models (100) of the TMD of the $mGlu_2$ receptor were generated using MODELLER v9.12[179] (University of California San Francisco, San Francisco, CA) Hydrogen atoms were added to the homology models and disulfide bonds were built using SYBYL-X 2.1 (Tripos International, St. Louis, MO, USA). Ramachandran plots using MolProbity[197] were generated to examine the models.

iii. Docking studies at $mGlu_2$ receptors

The ligands were sketched in and energy minimized using the Tripos Force Field (Gasteiger-Hückel charges, distance-dependent dielectric constant = 4.0) in SYBYL X-2.1 (Tripos International). Docking studies at $mGlu_2$ receptors were conducted using the genetic algorithm docking program GOLD suite 5.2[187] (Cambridge Crystallographic Data Centre, Cambridge, UK) with ChemPLP as the chosen scoring function. The binding site was defined to include all amino acid residues within a radius of 10 Å from Asn735. The docking poses were clustered (intracluster RMSD $\leq$ 2 Å) using a script that was provided by Dr. Philip Mosier. The top solutions were merged into homology models of the $mGlu_2$ receptor and the. The receptor-ligand complexes were energy minimized using the Tripos Force Field (Gasteiger-Hückel charges, distance-dependent dielectric constant = 4.0) in SYBYL X-2.1 (Tripos International).

HINT[188] analysis was performed in SYBYL-8.1 to quantify the receptor-ligand interactions observed in molecular modeling studies. PYMOL[220] was used to generate images.

iv. Distance measurements for 5-HT (6) and analogs 61, 63 and 155

A systematic search was performed on SYBYL-X 2.1 (Tripos International) to determine the lowest energy conformation of the molecules. The benzene ring centroid was defined as the aromatic center, and the distances of the aromatic centers from the nitrogen atoms (for 5-HT (**6**), analogs **61**, **63** and **155)** as well as the distances of the hydrogen bond acceptors from the nitrogen atom (for analog **61**) were measured using SYBYL-X 2.1.

BIBLIOGRAPHY

BIBLIOGRAPHY

1. Tamminga, C. A.; Medoff, D. R. The biology of schizophrenia. *Dialogues Clin. Neurosci.* **2000**, *2*, 339-348.
2. Faludi, G.; Dome, P.; Lazáry, J. Origins and perspectives of the schizophrenia research. *Neuropsychopharmacol. Hung.* **2011**, *13*, 185-192.
3. Laruelle, M.; Kegeles, L. S.; Abi-Dargham, A. Glutamate, dopamine, and schizophrenia. From pathophysiology to treatment. *Ann. N. Y. Acad. Sci.* **2003**, *1003*, 138-158.
4. Lang, U. E.; Puls, I.; Müller, D. J.; Strutz-Seebohm, N.; Gallinat, J. Molecular mechanisms of schizophrenia. *Cell. Physiol. Biochem.* **2007**, *20*, 687-702.
5. Eggers, A. E. A serotonin hypothesis of schizophrenia. *Med. Hypotheses* **2013**, *80*, 791-794.
6. Raedler, T. J.; Bymaster, F. P.; Tandon, R.; Copolov, D.; Dean, B. Towards a muscarinic hypothesis of schizophrenia. *Mol. Psychiatry* **2007**, *12*, 232-246.
7. Worrel, J. A.; Marken, P. A.; Beckman, S. E.; Ruehter, V. Atypical antipsychotic agents: A critical review. *Am. J. Health-Syst. Pharm.* **2000**, *57*, 238-255.

8. Agarwal, P.; Sarris, C. E.; Herschman, Y.; Agarwal, N.; Mammis, A. Schizophrenia and neurosurgery: A dark past with hope of a brighter future. *J. Clin. Neurosci.* **2016**, *34*, 53-58.
9. Pieters, T.; Majerus, B. The introduction of chlorpromazine in Belgium and the Netherlands (1951–1968); Tango between old and new treatment features. *Stud. Hist. Philos. Biol. Biomed. Sci.* **2011**, *42*, 443-452.
10. *Current Antipsychotics*, 1st ed.; Gross, G., Gerhard M. A., Eds; Handbook of Experimental Pharmacology; Springer: Berlin, Heidelberg, 2012; Vol. 212.
11. Pierre, J. M. Extrapyramidal symptoms with atypical antipsychotics: Incidence, prevention and management. *Drug Saf.* **2005**, *28*, 191-208.
12. Kane, J.; Honigfeld, G.; Singer, J.; Meltzer, H. Clozapine for the treatment-resistant schizophrenic: A double-blind comparison with chlorpromazine. *Arch. Gen. Psychiatry* **1988**, *45*, 789-796.
13. Shen, W. W. A history of antipsychotic drug development. *Compr. Psychiatry* **1999**, *40*, 407-414.
14. Schotte, A.; Janssen, P. F. M.; Gommeren, W.; Luyten, W. H. M. L.; Van Gompel, P.; Lesage, A. S.; De Loore, K.; Leysen, J. E. Risperidone compared with new and reference antipsychotic drugs: In vitro and in vivo receptor binding. *Psychopharmacology* **1996**, *124*, 57–73.
15. Megens, A. A. H. P.; Kennis, L. E. J. Risperidone and related $5HT_2/D_2$ antagonists: A new type of antipsychotic agent? *Prog. Med. Chem.* **1996**, *33*, 185-232.

16. Hasnain, M.; Vieweg, W. V. R.; Hollett, B. Weight gain and glucose dysregulation with second-generation antipsychotics and antidepressants: A review for primary care physicians. *Postgrad. Med.* **2012**, *124*, 154-167.
17. Jašović-Gašić, M.; Vuković, O.; Pantović, M.; Cvetić, T.; Marić-Bojović, N. Antipsychotics--history of development and field of indication, new wine--old glasses. *Psychiatr. Danubina.* **2012**, *24*, S342-S344.
18. Gonzalez-Maeso, J.; Ang, R. L.; Yuen, T.; Chan, P.; Weisstaub, N. V.; Lopez-Gimenez, J. F.; Zhou, M.; Okawa, Y.; Callado, L. F.; Milligan, G.; Gingrich, J. A.; Filizola, M.; Meana, J. J.; Sealfon, S. C. Identification of a serotonin/glutamate receptor complex implicated in psychosis. *Nature* **2008**, *452*, 93-97.
19. Moreno, J. L.; Miranda-Azpiazu, P.; García-Bea, A.; Younkin, J.; Cui, M.; Kozlenkov, A.; Ben-Ezra, A.; Voloudakis, G.; Fakira, A. K.; Baki, L.; Ge, Y.; Georgakopoulos, A.; Morón, J. A.; Milligan, G.; López-Giménez, J. F.; Robakis, N. K.; Logothetis, D. E.; Meana, J. J.; González-Maeso, J. Allosteric signaling through an $mGlu_2$ and $5\text{-}HT_{2A}$ heteromeric receptor complex and its potential contribution to schizophrenia. *Sci. Signal.* **2016**, *9*, 1-18.
20. Moreno, J. L.; Muguruza, C.; Umali, A.; Mortillo, S.; Holloway, T.; Pilar-Cuéllar, F.; Mocci, G.; Seto, J.; Callado, L. F.; Neve, R. L.; Milligan, G.; Sealfon, S. C.; López-Giménez, J. F.; Meana, J. J.; Benson, D. L.; González-Maeso, J. Identification of three residues essential for 5-hydroxytryptamine 2A-metabotropic glutamate 2 ($5\text{-}HT_{2A}\cdot mGlu_2$) receptor heteromerization and its psychoactive behavioral function. *J. Biol. Chem.* **2012**, *287*, 44301-44319.

21. Baki, L.; Fribourg, M.; Younkin, J.; Eltit, J. M.; Moreno, J. L.; Park, G.; Vysotskaya, Z.; Narahari, A.; Sealfon, S. C.; Gonzalez-Maeso, J.; Logothetis, D. E. Cross-signaling in metabotropic glutamate 2 and serotonin 2A receptor heteromers in mammalian cells. *Pflüg. Arch.* **2016**, *468*, 775-793.
22. Fribourg, M.; Moreno, J. L.; Holloway, T.; Provasi, D.; Baki, L.; Mahajan, R.; Park, G.; Adney, S. K.; Hatcher, C.; Eltit, J. M.; Ruta, J. D.; Albizu, L.; Li, Z.; Umali, A.; Shim, J.; Fabiato, A.; MacKerell, A. D., Jr.; Brezina, V.; Sealfon, S. C.; Filizola, M.; González-Maeso, J.; Logothetis, D. E. Decoding the signaling of a GPCR heteromeric complex reveals a unifying mechanism of action of antipsychotic drugs. *Cell* **2011**, *147*, 1011-1023.
23. Muguruza, C.; Meana, J. J.; Callado, L. F. Group II metabotropic glutamate receptors as targets for novel antipsychotic drugs. *Front. Pharmacol.* **2016**, *7*, 1-12.
24. World Health Organization. Mental Health. Schizophrenia Home Page. http://www.who.int/mental_health/management/schizophrenia/en/ (accessed April 20, 2017).
25. Jablensky, A. The diagnostic concept of schizophrenia: Its history, evolution, and future prospects. *Dialogues Clin. Neurosci.* **2010**, *12*, 271-287.
26. Kuhn, R.; Cahn, C. H. Eugen Bleuler's concepts of psychopathology. *Hist. Psychiatry* **2004**, *15*, 361-366.
27. American Psychiatric Association (2013). Diagnostic and Statistical Manual of Mental Disorders (5th ed.).
28. World Health Organization (1992). The ICD-10 Classification of Mental and Behavioral Disorders. Clinical Descriptions and Diagnostic Guidelines.

29. Nakazawa, K.; Zsiros, V.; Jiang, Z.; Nakao, K.; Kolata, S.; Zhang, S.; Belforte, J. E. GABAergic interneuron origin of schizophrenia pathophysiology. *Neuropharmacology* **2012**, *62*, 1574-1583.
30. Beaulieu, J.-M.; Espinoza, S.; Gainetdinov, R. R. Dopamine receptors – IUPHAR review 13. *Br. J. Pharmacol.* **2015**, *172*, 1-23.
31. Howes, O. D.; Kapur, S. The dopamine hypothesis of schizophrenia: Version III-The final common pathway. *Schizophr. Bull.* **2009**, *35*, 549-562.
32. Lieberman, J. A.; Kane, J. M.; Alvir, J. Provocative tests with psychostimulant drugs in schizophrenia. *Psychopharmacology* **1987**, *91*, 415-433.
33. Carlsson, A.; Lindqvist, M.; Magnusson, T. 3,4-Dihydroxyphenylalanine and 5-hydroxytryptophan as reserpine antagonists. *Nature* **1957**, *180*, 1200.
34. Seeman, P.; Lee, T. Antipsychotic drugs: Direct correlation between clinical potency and presynaptic action on dopamine neurons. *Science* **1975**, *188*, 1217-1219.
35. Davis, K. L.; Kahn, R. S.; Ko, G.; Davidson, M. Dopamine in schizophrenia: A review and reconceptualization. *Am. J. Psychiatry* **1991**, *148*, 1474-1486.
36. Howes, O. D.; Nour, M. M. Dopamine and the aberrant salience hypothesis of schizophrenia. *World Psychiatry* **2016**, *15*, 3-4.
37. Balu, D. T. The NMDA receptor and schizophrenia: From pathophysiology to treatment. *Adv. Pharmacol.* **2016**, *76*, 351-382.
38. Coyle, J. T.; Basu, A.; Benneyworth, M.; Balu, D.; Konopaske, G. Glutamatergic Synaptic Dysregulation in Schizophrenia: Therapeutic Implications. In *Novel Antischizophrenia*

Treatments, Geyer M. A.; Gross, G., Eds; Handbook Of Experimental Pharmacology; Springer: Berlin, Heidelberg, 2012; Vol. 213, pp 267-295.

39. Glennon, R. A.; Dukat, M. Serotonin Receptors and Drugs Affecting Serotonergic Neurotransmission. In *Foye's Textbook of Medicinal Chemistry*, 7th Ed.; Williams, D. A.; and Lemke, T.; Eds., Lippincott Williams and Wilkins: Baltimore, MD, 2013; pp 365-396.
40. Woolley, D. W.; Shaw, E. A biochemical and pharmacological suggestion about certain mental disorders. *Proc. Natl. Acad. Sci. U. S. A.* **1954**, *40*, 228-231.
41. Glennon, R. A. Do classical hallucinogens act as 5-HT_2 agonists or antagonists? *Neuropsychopharmacology* **1990**, *3*, 509-517.
42. Shaw, E.; Woolley, D. W. Some serotoninlike activities of lysergic acid diethylamide. *Science* **1956**, *124*, 121-122.
43. Aghajanian, G. K.; Marek, G. J. Serotonin model of schizophrenia: Emerging role of glutamate mechanisms. *Brain Res. Rev.* **2000**, *31*, 302-312.
44. Igbal, N.; van Praag, H. M. The role of serotonin in schizophrenia. *Eur. Neuropsychopharmacol.* **1995**, *5*, 11-23.
45. Meltzer, H. Y.; Matsubara, S.; Lee, J. C. Classification of typical and atypical antipsychotic drugs on the basis of dopamine D-1, D-2 and serotonin2 pKi values. *J. Pharmacol. Exp. Ther.* **1989**, *251*, 238-246.
46. Aghajanian, G. K.; Marek, G. J. Serotonin, via 5-HT_{2A} receptors, increases EPSCs in layer V pyramidal cells of prefrontal cortex by an asynchronous mode of glutamate release. *Brain Res.* **1999**, *825*, 161-171.

47. Aghajanian, G.; Marek, G. Serotonin induces excitatory postsynaptic potentials in apical dendrites of neocortical pyramidal cells. *Neuropharmacology* **1997**, *36*, 589-599.
48. Javitt, D. C. Glutamate and schizophrenia: Phencyclidine, N-methyl-D-aspartate receptors, and dopamine-glutamate interactions. *Int. Rev. Neurobiol.* **2007**, *78*, 69-108.
49. Meldrum, B. S. Glutamate as a neurotransmitter in the brain: Review of physiology and pathology. *J. Nutr.* **2000**, *130*, 1007S-1015S.
50. Nakanishi, S. Molecular diversity of glutamate receptors and implications for brain function. *Science* **1992**, *258*, 597-603.
51. Coyle, J. T. Glutamate and schizophrenia: Beyond the dopamine hypothesis. *Cell. Mol. Neurobiol.* **2006**, *26*, 363-382.
52. Luby, E. D.; Cohen, B. D.; Rosenbaum, G.; Gottlieb, J. S.; Kelley, R. Study of a new schizophrenomimetic drug; sernyl. *AMA Arch. Neurol. Psychiatry* **1959**, *81*, 363-369.
53. Javitt, D. C.; Zukin, S. R. Recent advances in the phencyclidine model of schizophrenia. *Am. J. Psychiatry* **1991**, *148*, 1301-1308.
54. Schwartz, T. L.; Sachdeva, S.; Stahl, S. M. Glutamate neurocircuitry: Theoretical underpinnings in schizophrenia. *Front. Pharmacol.* **2012**, *3*, 1-11.
55. Ellaithy, A.; Younkin, J.; Gonzalez-Maeso, J.; Logothetis, D. E. Positive allosteric modulators of metabotropic glutamate 2 receptors in schizophrenia treatment. *Trends Neurosci.* **2015**, *38*, 506-516.
56. Yuen, E. Y.; Jiang, Q.; Chen, P.; Feng, J.; Yan, Z. Activation of 5-$HT_{2A/C}$ receptors counteracts 5-HT_{1A} regulation of N-methyl-D-aspartate receptor channels in pyramidal neurons of prefrontal cortex. *J. Biol. Chem.* **2008**, *283*, 17194-17204.

57. Shu, Y.; Hasenstaub, A.; McCormick, D. A. Turning on and off recurrent balanced cortical activity. *Nature* **2003**, *423*, 288-293.

58. Huang, Z. J. Activity-dependent development of inhibitory synapses and innervation pattern: Role of GABA signalling and beyond. *J. Physiol.* **2009**, *587*, 1881-1888.

59. Guidotti, A.; Auta, J.; Davis, J. M.; Dong, E.; Grayson, D. R.; Veldic, M.; Zhang, X.; Costa, E. GABAergic dysfunction in schizophrenia: New treatment strategies on the horizon. *Psychopharmacology* **2005**, *180*, 191-205.

60. Bencherif, M.; Stachowiak, M. K.; Kucinski, A. J.; Lippiello, P. M. Alpha7 nicotinic cholinergic neuromodulation may reconcile multiple neurotransmitter hypotheses of schizophrenia. *Med. Hypotheses* **2012**, *78*, 594-600.

61. Ahnallen, C. G. The role of the α7 nicotinic receptor in cognitive processing of persons with schizophrenia. *Curr. Opin. Psychiatry* **2012**, *25*, 103-108.

62. Mirza, N. R.; Peters, D.; Sparks, R. G. Xanomeline and the antipsychotic potential of muscarinic receptor subtype selective agonists. *CNS Drug Rev.* **2003**, *9*, 159-186.

63. Boison, D. Adenosine as a neuromodulator in neurological diseases. *Curr. Opin. Pharmacol.* **2008**, *8*, 2–7.

64. Boison, D.; Singer, P.; Shen, H.-Y.; Feldon, J.; Yee, B. K. Adenosine hypothesis of schizophrenia - opportunities for pharmacotherapy. *Neuropharmacology* **2012**, *62*, 1527-1543.

65. Ashby, C. R.; Wang, R. Y. Pharmacological actions of the atypical antipsychotic drug clozapine: A review. *Synapse* **1996**, *24*, 349-394.

66. Svensson, T. H. α-Adrenoceptor modulation hypothesis of antipsychotic atypicality. *Prog. Neuro-Psychopharmacol. Biol. Psychiatry* **2003**, *27*, 1145-1158.

67. Nutt, D. J. Putting the "A" in atypical: Does α2-adrenoceptor antagonism account for the therapeutic advantage of new antipsychotics? *J. Psychopharmacol.* **1994**, *8*, 193-195.

68. Müller-Vahl, K. R.; Emrich, H. M. Cannabis and schizophrenia: Towards a cannabinoid hypothesis of schizophrenia. *Expert Rev. Neurother.* **2008**, *8*, 1037-1048.

69. Wyrofsky, R.; McGonigle, P.; Van Bockstaele, E. J. Drug discovery strategies that focus on the endocannabinoid signaling system in psychiatric disease. *Expert Opin. Drug Discovery* **2015**, *10*, 17-36.

70. Roser, P.; Vollenweider, F. X.; Kawohl, W. Potential antipsychotic properties of central cannabinoid (CB1) receptor antagonists. *World J. Biol. Psychiatry* **2010**, *11*, 208-219.

71. Kucharski, A. History of frontal lobotomy in the United States, 1935-1955. *Neurosurgery* **1984**, *14* , 765-772.

72. Bridges, P. K.; Bartlett, J. R. Psychosurgery: Yesterday and today. *Br. J. Psychiatry* **1977**, *131*, 249-260.

73. Tamminga, C. A. Treatment mechanisms: Traditional and new antipsychotic drugs. *Dialogues Clin. Neurosci.* **2000**, *2*, 281-286.

74. Awouters, F. H. L.; Lewi, P. J. Forty years of antipsychotic drug research – from haloperidol to paliperidone – with Dr. Paul Janssen. *Arzneimittelforschung* **2011**, *57*, 625-632.

75. Madras, B. K. History of the discovery of the antipsychotic dopamine D2 receptor: A basis for the dopamine hypothesis of schizophrenia. *J. Hist. Neurosci.* **2013**, *22*, 62-78.

76. Hippius, H. The history of clozapine. *Psychopharmacology* **1989**, *99*, S3-S5.

77. Keltner, N. L.; Johnson, V. Biological perspectives. Aripiprazole: A third generation of antipsychotics begins? *Perspect. Psychiatr. Care* **2002**, *38*, 157-159.

78. King, C.; Voruganti, L. N. What's in a name? The evolution of the nomenclature of antipsychotic drugs. *J. Psychiatry Neurosci.* **2002**, *27*, 168-175.

79. Horacek, J.; Bubenikova-Valesova, V.; Kopecek, M.; Palenicek, T.; Dockery, C.; Mohr, P.; Höschl, C. Mechanism of action of atypical antipsychotic drugs and the neurobiology of schizophrenia. *CNS Drugs* **2006**, *20*, 389-409.

80. Remington, G. Understanding antipsychotic "atypicality": A clinical and pharmacological moving target. *J. Psychiatry Neurosci.* **2003**, *28*, 275-284.

81. Geddes, J.; Freemantle, N.; Harrison, P.; Bebbington, P. Atypical antipsychotics in the treatment of schizophrenia: Systematic overview and meta-regression analysis. *BMJ* **2000**, *321*, 1371-1376.

82. Leucht, S.; Wahlbeck, K.; Hamann, J.; Kissling, W. New generation antipsychotics versus low-potency conventional antipsychotics: A systematic review and meta-analysis. *Lancet* **2003**, *361*, 1581-1589.

83. Davis, J. M.; Chen, N.; Glick, I. D. A meta-analysis of the efficacy of second-generation antipsychotics. *Arch. Gen. Psychiatry* **2003**, *60*, 553-564.

84. Makhinson, M. Biases in medication prescribing: The case of second-generation antipsychotics. *J. Psychiatr. Pract.* **2010**, *16*, 15-21.

85. Huttunen, M. The evolution of the serotonin-dopamine antagonist concept. *J. Clin. Psychopharmacol.* **1995**, *15*, 4S–10S.

86. Meltzer, H. Y. The mechanism of action of novel antipsychotic drugs. *Schizophr. Bull.* **1991**, *17*, 263-287.

87. Awouters, F.; Niemegeers, C. J. E.; Megens, A. A. H. P.; Meert, T. F.; Janssen, P. A. J. Pharmacological profile of ritanserin: A very specific central serotonin S_2-antagonist. *Drug Dev. Res.* **1988**, *15*, 61-73.

88. Meltzer, H.; Massey, B. The role of serotonin receptors in the action of atypical antipsychotic drugs. *Curr. Opin. Pharmacol.* **2011**, *11*, 59-67.

89. Kenakin, T. Efficacy as a vector: The relative prevalence and paucity of inverse agonism. *Mol. Pharmacol.* **2004**, *65*, 2-11.

90. Sullivan, L. C.; Clarke, W. P.; Berg, K. A. Atypical antipsychotics and inverse agonism at 5-HT_2 Receptors. *Curr. Pharm. Des.* **2015**, *21*, 3732-3738.

91. Schmidt, C. J.; Fadayel, G. M. The selective 5-HT_{2A} receptor antagonist, MDL 100,907, increases dopamine efflux in the prefrontal cortex of the rat. *Eur. J. Pharmacol.* **1995**, *273*, 273-279.

92. De Deurwaerdère, P.; Navailles, S.; Berg, K. A.; Clarke, W. P.; Spampinato, U. Constitutive activity of the serotonin2C receptor inhibits in vivo dopamine release in the rat striatum and nucleus accumbens. *J. Neurosci.* **2004**, *24*, 3235-3241.

93. Meltzer, H. Y.; Huang, M. In vivo actions of atypical antipsychotic drug on serotonergic and dopaminergic systems. *Prog. Brain Res.* **2008**, *172*, 177-197.

94. Gardell, L. R.; Vanover, K. E.; Pounds, L.; Johnson, R. W.; Barido, R.; Anderson, G. T.; Veinbergs, I.; Dyssegaard, A.; Brunmark, P.; Tabatabaei, A.; Davis, R. E.; Brann, M. R.; Hacksell, U.; Bonhaus, D. W. ACP-103, a 5-hydroxytryptamine 2A receptor inverse

agonist, improves the antipsychotic efficacy and side-effect profile of haloperidol and risperidone in experimental models. *J. Pharmacol. Exp. Ther.* **2007**, *322*, 862-870.

95. Mcfarland, K.; Price, D. L.; Bonhaus, D. W. Pimavanserin, a 5-HT_{2A} inverse agonist, reverses psychosis-like behaviors in a rodent model of Parkinson's disease. *Behav. Pharmacol.* **2011**, *22*, 681-692.
96. Price, D. L.; Bonhaus, D. W.; Mcfarland, K. Pimavanserin, a 5-HT_{2A} receptor inverse agonist, reverses psychosis-like behaviors in a rodent model of Alzheimer's disease. *Behav. Pharmacol.* **2012**, *23*, 426-433.
97. Stahl, S. M. Dopamine system stabilizers, aripiprazole, and the next generation of antipsychotics, part 1, "Goldilocks" actions at dopamine receptors. *J. Clin. Psychiatry* **2001**, *62*, 841-842.
98. Strange, P. G. Antipsychotic drug action: Antagonism, inverse agonism or partial agonism. *Trends Pharmacol. Sci.* **2008**, *29*, 314–321.
99. Di Sciascio, G.; Riva, M. A. Aripiprazole: From pharmacological profile to clinical use. *Neuropsychiatr. Dis. Treat.* **2015**, *11*, 2635-2647.
100. Urban, J. D.; Vargas, G. A.; von Zastrow, M.; Mailman, R. B. Aripiprazole has functionally selective actions at dopamine D_2 receptor-mediated signaling pathways. *Neuropsychopharmacology* **2006**, *32*, 67-77.
101. Mailman, R. B.; Murthy, V. Third generation antipsychotic drugs: Partial agonism or receptor functional selectivity? *Curr. Pharm. Des.* **2010**, *16*, 488-501.
102. Greig, S. L. Brexpiprazole: First global approval. *Drugs* **2015**, *75*, 1687-1697.

103. Gaddum, J. H.; Picarelli, Z. P. Two kinds of tryptamine receptor. *Br. J. Pharmacol. Chemother.* **1957**, *12*, 323-328.

104. Peroutka, S. J.; Snyder, S. H. Multiple serotonin receptors: Differential binding of [^{3}H]5-hydroxytryptamine, [^{3}H]lysergic acid diethylamide and [^{3}H]spiroperidol. *Mol. Pharmacol.* **1979**, *16*, 687-699.

105. Nichols, D. E.; Nichols, C. D. Serotonin receptors. *Chem. Rev.* **2008**, *108*, 1614-1641.

106. Branchek, T.; Adham, N.; Macchi, M.; Kao, H. T.; Hartig, P. R. [3H]-DOB(4-bromo-2,5-dimethoxyphenylisopropylamine) and [3H] ketanserin label two affinity states of the cloned human 5-hydroxytryptamine2 receptor. *Mol. Pharmacol.* **1990**, *38*, 604-609.

107. Barnes, N. M.; Sharp, T. A review of central 5-HT receptors and their function. *Neuropharmacology* **1999**, *38*, 1083-1152.

108. Leysen, J. E. 5-HT2 Receptors. *Curr. Drug Target: CNS Neurol. Disord.* **2004**, *3*, 11-26.

109. Glennon, R. A. Discriminative stimulus properties of the serotonergic agent 1-(2,5-dimethoxy-4-iodophenyl)-2-aminopropane (DOI). *Life Sci.* **1986**, *39*, 825-830.

110. Glennon, R. A. Serotonin receptors: Clinical implications. *Neurosci. Biobehav. Rev.* **1990**, *14*, 35-47.

111. Niswender, C. M.; Conn, P. J. Metabotropic glutamate receptors: Physiology, pharmacology, and disease. *Annu. Rev. Pharmacol. Toxicol.* **2010**, *50*, 295-322.

112. Gregory, K. J.; Dong, E. N.; Meiler, J.; Conn, P. J. Allosteric modulation of metabotropic glutamate receptors: Structural insights and therapeutic potential. *Neuropharmacology* **2011**, *60*, 66-81.

113. Conn, P. J.; Pin, J.-P. Pharmacology and functions of metabotropic glutamate receptors. *Annu. Rev. Pharmacol. Toxicol.* **1997**, *37*, 205-237.

114. Cartmell, J.; Schoepp, D. D. Regulation of neurotransmitter release by metabotropic glutamate receptors. *J. Neurochem.* **2000**, *75*, 889-907.

115. Wierońska, J. M.; Zorn, S. H.; Doller, D.; Pilc, A. Metabotropic glutamate receptors as targets for new antipsychotic drugs: Historical perspective and critical comparative assessment. *Pharmacol. Ther.* **2016**, *157*, 10-27.

116. Downing, A. M.; Kinon, B. J.; Millen, B. A.; Zhang, L.; Liu, L.; Morozova, M. A.; Brenner, R.; Rayle, T. J.; Nisenbaum, L.; Zhao, F.; Gomez, J. C. A double-blind, placebo-controlled comparator study of LY2140023 monohydrate in patients with schizophrenia. *BMC Psychiatry* **2014**, *14*, 351-362.

117. Stauffer, V. L.; Millen, B. A.; Andersen, S.; Kinon, B. J.; LaGrandeur, L.; Lindenmayer, J. P.; Gomez, J. C. Pomaglumetad methionil: No significant difference as an adjunctive treatment for patients with prominent negative symptoms of schizophrenia compared to placebo. *Schizophr. Res.* **2013**, *150*, 434-441.

118. Fell, M. J.; Svensson, K. A.; Johnson, B. G.; Schoepp, D. D. Evidence for the role of metabotropic glutamate (mGlu2) not mGlu3 receptors in the preclinical antipsychotic pharmacology of the mGlu2/3 receptor agonist (–)-(1R,4S,5S,6S)-4-amino-2-sulfonylbicyclo[3.1.0]hexane-4,6-dicarboxylic acid (LY404039). *J. Pharmacol. Exp. Ther.* **2008**, *326*, 209-217.

119. Cid, J. M.; Tresadern, G.; Duvey, G.; Lütjens, R.; Finn, T.; Rocher, J.-P.; Poli, S.; Vega, J. A.; de Lucas, A. I.; Matesanz, E.; Linares, M. L.; Andrés, J. I.; Alcazar, J.; Alonso, J. M.;

Macdonald, G. J.; Oehlrich, D.; Lavreysen, H.; Ahnaou, A.; Drinkenburg, W.; Mackie, C.; Pype, S.; Gallacher, D.; Trabanco, A. A. Discovery of 1-butyl-3-chloro-4-(4-phenyl-1-piperidinyl)-(1H)-pyridone (JNJ-40411813): A novel positive allosteric modulator of the metabotropic glutamate 2 receptor. *J. Med. Chem.* **2014**, *57*, 6495-6512.

120. Litman, R. E.; Smith, M. A.; Doherty, J. J.; Cross, A.; Raines, S.; Gertsik, L.; Zukin, S. R. AZD8529, a positive allosteric modulator at the mGluR2 receptor, does not improve symptoms in schizophrenia: A proof of principle study. *Schizophr. Res.* **2016**, *172*, 152-157.
121. Moreno, J. L.; Holloway, T.; Albizu, L.; Sealfon, S. C.; González-Maeso, J. Metabotropic glutamate $mGlu_2$ receptor is necessary for the pharmacological and behavioral effects induced by hallucinogenic 5-HT_{2A} receptor agonists. *Neurosci. Lett.* **2011**, *493*, 76-79.
122. Janssen, P. A.; Niemegeers, C. J.; Awouters, F.; Schellekens, K. H.; Megens, A. A.; Meert, T. F. Pharmacology of risperidone (R 64 766), a new antipsychotic with serotonin-S2 and dopamine-D2 antagonistic properties. *J. Pharmacol. Exp. Ther.* **1988**, *244*, 685-693.
123. Janssen P. A.; Niemegeers C. J.; Schellekens K. H. Is it possible to predict the clinical effects of neuroleptic drugs (major tranquillizers) from animal data? "Neuroleptic activity spectra" for rats. *ArzneimittelForschung* **1965**, *15*, 104-117.
124. Sugerman A. A. A pilot study of floropipamide (dipiperon). *Dis. Nerv. Syst.* **1964**, *25*, 355-358.
125. Awouters, F.; Niemegeers, C. J.; Megens, A. A.; Janssen, P. A. Functional interaction between serotonin-S2 and dopamine-D2 neurotransmission as revealed by selective

antagonism of hyper-reactivity to tryptamine and apomorphine. *J. Pharmacol. Exp. Ther.* **1990**, *254*, 945-951.

126. Ceulemans, D. L. S.; Gelders, Y. G.; Hoppenbrouwers, M.-L. J. A.; Reyntjens, A. J. M.; Janssen, P. A. J. Effect of serotonin antagonism in schizophrenia: A pilot study with setoperone. *Psychopharmacology* **1985**, *85*, 329-332.
127. Leysen, J. E.; Janssen, P. M. F.; Schotte, A.; Luyten, W. H. M. L.; Megens, A. A. H. P. Interaction of antipsychotic drugs with neurotransmitter receptor sites in vitro and in vivo in relation to pharmacological and clinical effects: Role of 5HT2 receptors. *Psychopharmacology* **1993**, *112*, S40-S54.
128. Megens, A. A. H. P.; Awouters, F. H. L. In vivo pharmacological profile of 9-hydroxyrisperidone, the major metabolite of the novel antipsychotic risperidone. *Drug Dev. Res.* **1994**, *33*, 399-412.
129. van Beijsterveldt, L. E. C.; Geerts, R. J. F.; Leysen, J. E.; Megens, A. A. H. P.; Van den Eynde, H. M. J.; Meuldermans, W. E. G.; Heykants, J. J. P. Regional brain distribution of risperidone and its active metabolite 9-hydroxy-risperidone in the rat. *Psychopharmacology* **1994**, *114*, 53-62.
130. Megens, A. A. H. P.; Awouters, F. H. L.; Schotte, A.; Meert, T. F.; Dugovic, C.; Niemegeers, C. J. E.; Leysen, J. E. Survey on the pharmacodynamics of the new antipsychotic risperidone. *Psychopharmacology* **1994**, *114*, 9-23.
131. Reyntjens, A.; Gelders, Y. G.; Hoppenbrouwers, M.-L. J. A.; Bussche, G. V. Thymosthenic effects of ritanserin (R 55667), a centrally acting serotonin-S2 receptor blocker. *Drug Dev. Res.* **1986**, *8*, 205-211.

132. Bersani, G.; Grispini, A.; Marini, S.; Pasini, A.; Valducci, P. M.; Ciani, N. Neuroleptic-induced extrapyramidal side effects: Clinical perspectives with ritanserin (R 55667), a new selective 5-HT_2 receptor blocking agent. *Curr. Ther. Res.* **1986**, *40*, 492-499.

133. Colpaert, F. C.; Meert, T. F.; Niemegeers, C. J. E.; Janssen, P. A. J. Behavioral and 5-HT antagonist effects of ritanserin: A pure and selective antagonist of LSD discrimination in rat. *Psychopharmacology* **1985**, *86*, 45–54.

134. Colpaert, F. C.; Niemegeers, C. J.; Janssen, P. A. A drug discrimination analysis of lysergic acid diethylamide (LSD): In vivo agonist and antagonist effects of purported 5-hydroxytryptamine antagonists and of pirenperone, a LSD-antagonist. *J. Pharmacol. Exp. Ther.* **1982**, *221*, 206-214

135. Weiner, D. M.; Burstein, E. S.; Nash, N.; Croston, G. E.; Currier, E. A.; Vanover, K. E.; Harvey, S. C.; Donohue, E.; Hansen, H. C.; Andersson, C. M.; Spalding, T. A.; Gibson, D. F. C.; Krebs-Thomson, K.; Powell, S. B.; Geyer, M. A.; Hacksell, U.; Brann, M. R. 5-Hydroxytryptamine2A receptor inverse agonists as antipsychotics. *J. Pharmacol. Exp. Ther.* **2001**, *299*, 268-276.

136. Akam, E.; Strange, P. G. Inverse agonist properties of atypical antipsychotic drugs. *Biochem. Pharmacol.* (*Amsterdam, Neth.*) **2004**, *67*, 2039-2045.

137. Glennon, R. A.; Young, R. *Drug Discrimination: Applications to Medicinal Chemistry and Drug Studies*; Wiley: Hoboken, NJ, 2011.

138. Herndon, J. L.; Ismaiel, A.; Ingher, S. P.; Teitler, M.; Glennon, R. A. Ketanserin analogs: Structure-affinity relationships for 5-HT_2 and 5-HT_{1C} serotonin receptor binding. *J. Med. Chem.* **1992**, *35*, 4903-4910.

139. Wang, C. D.; Gallaher, T. K.; Shih, J. C. Site-directed mutagenesis of the serotonin 5-hydroxytrypamine2 receptor: Identification of amino acids necessary for ligand binding and receptor activation. *Mol. Pharmacol.* **1993**, *43*, 931-940.

140. Iwamura, T.; Casey, C. T.; Young, R.; Dukat, M.; Teitler, M.; Fadden, J. S. P.; Glennon, R. A. 4-(6-Fluorobenzisoxazol-3-yl)piperidine, a risperidone metabolite with serotonergic activity of potential clinical significance. *Med. Chem. Res.* **1996**, *6*, 593-601.

141. Younkin, J.; Gaitonde, S. A.; Ellaithy, A.; Vekariya, R.; Baki, L.; Moreno, J. L.; Shah, S.; Drossopoulos, P.; Hideshima, K. S.; Eltit, J. M.; González-Maeso, J.; Logothetis, D. E.; Dukat, M.; Glennon, R. A. Reformulating a pharmacophore for 5-HT_{2A} serotonin receptor antagonists. *ACS Chem. Neurosci.* **2016**, *7*, 1292-1299.

142. Slanina, P.; Bartl, J. Process for making risperidone and intermediates thereof. U. S. Patent 7,405,298 B2, July 29, 2008.

143. Gaitonde, S. A. A Study of the Action of Risperidone at 5-HT_{2A} Receptors, Ph.D. Dissertation, Virginia Commonwealth University, Richmond, VA, 2016.

144. Clarke, H. T.; Gurin, S. Studies of crystalline vitamin B_1. XII. The sulfur-containing moiety. *J. Am. Chem. Soc.* **1935**, *57*, 1876-1881.

145. Tota, Y. A.; Elderfield, R. C. Synthesis of the pyrimidine analog of thiamin bromide. *J. Org. Chem.* **1942**, *7*, 309-312.

146. Linghong, X.; Bingsong, H.; Yuelian, X. Aryl acid pyrimidinyl methyl amides, pyridazinyl methyl amides and related compounds. WO 2004074259 A1. September 2, 2004.

147. Khurana, J. M.; Kukreja, G. nickel boride mediated reductive desulfurization of 2-thioxo-4(*3H*)-quinazolinones: A New synthesis of quinazolin-4(*3H*)-Ones and 2,3-dihydro-4(*1H*)-quinazolinones. *J. Heterocycl. Chem.* **2003**, *40*, 677-679.

148. Peng, K.-Y.; Chen, S.-A.; Fann, W.-S. Efficient light harvesting by sequential energy transfer across aggregates in polymers of finite conjugational segments with short aliphatic linkages. *J. Am. Chem. Soc.* **2001**, *123*, 11388-11397.

149. Casey, B. M.; Eakin, C. A.; Flowers II, R. A. Synthesis of γ-halogenated ketones via the Ce(IV)-mediated oxidative coupling of cyclobutanols and inorganic halides. *Tetrahedron Lett.* **2009**, *50*, 1264-1266.

150. Fujioka, H.; Komatsu, H.; Miyoshi, A.; Murai, K.; Kita, Y. Phenyliodine diacetate-mediated oxidative cleavage of cyclobutanols leading to γ-hydroxy ketones. *Tetrahedron Lett.* **2011**, *52*, 973-975.

151. Becker, K. B.; Boschung, A. F.; Geisel, M.; Grob, C. A. Nucleophilic reactions at tertiary carbon. Part 3. σ- and π-routes to the 9-decalyl cation. *Helv. Chim. Acta* **1973**, *56*, 2747-2759.

152. Wapenaar, H.; van der Wouden, P. E.; Groves, M. R.; Rotili, D.; Mai, A.; Dekker, F. J. Enzyme kinetics and inhibition of histone acetyltransferase KAT8. *Eur. J. Med. Chem.* **2015**, *105*, 289-296.

153. Strupczewski, J. T.; Bordeau, K. J.; Chiang, Y.; Glamkowski, E. J.; Conway, P. G.; Corbett, R.; Hartman, H. B.; Szewczak, M. R.; Wilmot, C. A.; Helsley, G. C. 3-[[(Aryloxy)alkyl]piperidinyl]-1,2-Benzisoxazoles as D_2/5-HT_2 antagonists with potential

atypical antipsychotic activity: Antipsychotic profile of iloperidone (HP 873). *J. Med. Chem.* **1995**, *38*, 1119-1131.

154. Ebersole, B. J.; Visiers, I.; Weinstein, H.; Sealfon, S. C. Molecular basis of partial agonism: Orientation of indoleamine ligands in the binding pocket of the human serotonin 5-HT_{2A} receptor determines relative efficacy. *Mol. Pharmacol.* **2003**, *63*, 36-43.
155. Blough, B. E.; Landavazo, A.; Partilla, J. S.; Decker, A. M.; Page, K. M.; Baumann, M. H.; Rothman, R. B. Alpha-ethyltryptamines as dual dopamine–serotonin releasers. *Bioorg. Med. Chem. Lett.* **2014**, *24*, 4754-4758.
156. Mokrosz, M. J.; Strekowski, L.; Kozak, W. X.; Duszyńska, B.; Bojarski, A. J.; Kłodzinska, A.; Czarny, A.; Cegła, M. T.; Dereń-Wesołek, A.; Chojnacka-Wójcik, E.; Dove, S.; Mokrosz, J. L. Structure-activity relationship studies of CNS Agents, Part 25: 4,6-Di(heteroaryl)-2-(*N*-methylpiperazino)pyrimidines as new, potent 5-HT_{2A} receptor ligands: A verification of the topographic model. *Arch. Pharm. (Weinheim, Ger.)* **1995**, *328*, 659-666.
157. Westkaemper, R. B.; Glennon, R. A. Application of ligand SAR, receptor modeling and receptor mutagenesis to the discovery and development of a new class of 5-HT_{2A} ligands. *Curr. Top. Med. Chem.* **2002**, *2*, 575-598.
158. Höltje, H.-D.; Jendretzki, U. K. Construction of a detailed serotoninergic 5-HT_{2A} receptor model. *Arch. Pharm. (Weinheim, Ger.)* **1995**, *328*, 577-584.
159. Andersen, K.; Liljefors, T.; Gundertofte, K.; Perregaard, J.; Bogeso, K. P. Development of a receptor-interaction model for serotonin 5-HT2 receptor antagonists. Predicting selectivity with respect to dopamine D2 receptors. *J. Med. Chem.* **1994**, *37*, 950-962.

160. Kongsamut, S.; Roehr, J. E.; Cai, J.; Hartman, H. B.; Weissensee, P.; Kerman, L. L.; Tang, L.; Sandrasagra, A. Iloperidone binding to human and rat dopamine and 5-HT receptors. *Eur. J. Pharmacol.* **1996**, *317*, 417-423.

161. Kalkman, H. O.; Subramanian, N.; Hoyer, D. Extended radioligand binding profile of iloperidone: A broad spectrum dopamine/serotonin/norepinephrine receptor antagonist for the management of psychotic disorders. *Neuropsychopharmacology* **2001**, *25*, 904-914.

162. Speeter, M. E.; Anthony, W. C. The action of oxalyl chloride on indoles: A new approach to tryptamines. *J. Am. Chem. Soc.* **1954**, *76*, 6208-6210.

163. Blair, J. B.; Kurrasch-Orbaugh, D.; Marona-Lewicka, D.; Cumbay, M. G.; Watts, V. J.; Barker, E. L.; Nichols, D. E. Effect of ring fluorination on the pharmacology of hallucinogenic tryptamines. *J. Med. Chem.* **2000**, *43*, 4701-4710.

164. Shaw, K. N. F.; McMillan, A.; Gudmundson, A. G.; Armstrong, M. D. Preparation and properties of β-3-indolyl compounds related to tryptophan metabolism. *J. Org. Chem.* **1958**, *23*, 1171-1178.

165. Akihiro, T.; Masahiro, N.; Hisae, O.; Tomotaka, Y.; Mami, M.; Hideo, M. Indazole Compound and Pharmaceutical Use Thereof. EP1714961 A4, October 25, 2006.

166. Muratore, M. E.; Holloway, C. A.; Pilling, A. W.; Storer, R. I.; Trevitt, G.; Dixon, D. J. Enantioselective brønsted acid-catalyzed N-acyliminium cyclization cascades. *J. Am. Chem. Soc.* **2009**, *131*, 10796-10797.

167. Schumacher, R. W.; Davidson, B. S. Synthesis of didemnolines A-D, N9-substituted β-carboline alkaloids from the marine *Ascidian Didemnum* Sp. *Tetrahedron* **1999**, *55*, 935-942.

168. Tulyaganov, T. S.; Ibragimov, A. A.; Yunusov, S. Y. Alkaloids of *Nitraria Komarovii*. IV. Total synthesis of komarovine and komarovidine. *Chem. Nat. Compd.* **1981**, *17*, 149–152.

169. Guinchard, X.; Vallée, Y.; Denis, J.-N. Total syntheses of brominated marine sponge alkaloids. *Org. Lett.* **2007**, *9*, 3761-3764.

170. Stauffer, R. Synthèse de nouvelles tryptamines substituées. *Helv. Chim. Acta* **1966**, *49*, 1199-1203.

171. Speeter, M. E.; Anthony, W. C. Production of certain tryptamines and compounds produced in the process. US Patent 2870162 A, January 20, 1959.

172. Ignatenko, V. A.; Zhang, P.; Viswanathan, R. Step-economic synthesis of (±)-debromoflustramine A using indole C3 activation strategy. *Tetrahedron Lett.* **2011**, *52*, 1269-1272.

173. Rusterholz, D. B.; Barfknecht, C. F.; Clemens, J. A. Ergoline congeners as potential inhibitors of prolactin release 2. *J. Med. Chem.* **1976**, *19*, 99-102.

174. Kennis, L. E J; Vandenberk, J. 3-Piperidinyl-substituted 1,2-benzisoxazoles and 1,2-benzisothiazoles. U. S. Patent 4804663 A, February 14, 1989.

175. Aicher, T. D.; Chicarelli, M. J.; Hinklin, R. J.; Hongqvi, T.; Wallace, O. B. Cycloalkyl lactam derivatives as inhibitors of 11-beta hydroxysteroid dehydrogenase 1. WO 2006068991 A1, June 29, 2006.

176. Komissarov, V. V.; Kritzyn, A. M. Polymethylene derivatives of nucleic bases bearing ω-functional groups. VIII. ω-Oxo-ω-phenylalkylpyrimidines and purines. *Russ. J. Bioorg. Chem.* **2010**, *36*, 477–487.

177. Wacker, D.; Wang, C.; Katritch, V.; Han, G. W.; Huang, X.-P.; Vardy, E.; McCorvy, J. D.; Jiang, Y.; Chu, M.; Siu, F. Y.; Liu, W.; Xu, H. E.; Cherezov, V.; Roth, B. L.; Stevens, R. C. Structural features for functional selectivity at serotonin receptors. *Science* **2013**, *340*, 615-619.

178. Larkin, M. A.; Blackshields, G.; Brown, N. P.; Chenna, R.; McGettigan, P. A.; McWilliam, H.; Valentin, F.; Wallace, I. M.; Wilm, A.; Lopez, R.; Thompson, J. D.; Gibson, T. J.; Higgins, D. G. Clustal W and Clustal X version 2.0. *Bioinformatics* **2007**, *23*, 2947-2948.

179. Eswar, N.; Webb, B.; Marti-Renom, M. A.; Madhusudhan, M. S.; Eramian, D.; Shen, M.; Pieper, U.; Sali, A. Comparative protein structure modeling using MODELLER. *Curr. Protoc. Protein Sci.* **2007**, 2.9.1-2.9.31.

180. Muntasir, H. A.; Rashid, M.; Komiyama, T.; Kawakami, J.; Nagatomo, T. Identification of amino acid residues important for sarpogrelate binding to the human 5-hydroxytryptamine2A serotonin receptor. *J. Pharmacol. Sci.* **2006**, *102*, 55-63.

181. Kristiansen, K.; Kroeze, W. K.; Willins, D. L.; Gelber, E. I.; Savage, J. E.; Glennon, R. A.; Roth, B. L. A highly conserved aspartic acid (Asp-155) anchors the terminal amine moiety of tryptamines and is involved in membrane targeting of the 5-HT_{2A} serotonin receptor but does not participate in activation via a "salt-bridge disruption" mechanism. *J. Pharmacol. Exp. Ther.* **2000**, *293*, 735-746.

182. Almaula, N.; Ebersole, B. J.; Zhang, D.; Weinstein, H.; Sealfon, S. C. Mapping the binding site pocket of the serotonin 5-hydroxytryptamine$_{2A}$ receptor: $Ser^{3.36(159)}$ provides a second

interaction site for the protonated amine of serotonin but not of lysergic acid diethylamide or bufotenin. *J. Biol. Chem.* **1996**, *271*, 14672-14675.

183. Braden, M. R.; Nichols, D. E. Assessment of the roles of serines 5.43(239) and 5.46(242) for binding and potency of agonist ligands at the human serotonin 5-HT_{2A} receptor. *Mol. Pharmacol.* **2007**, *72*, 1200-1209.

184. Roth, B. L.; Shoham, M.; Choudhary, M. S.; Khan, N. Identification of conserved aromatic residues essential for agonist binding and second messenger production at 5-hydroxytryptamine$_{2A}$ receptors. *Mol. Pharmacol.* **1997**, *52*, 259-266.

185. Choudhary, M. S.; Craigo, S.; Roth, B. L. A single point mutation (Phe340 -->Leu340) of a conserved phenylalanine abolishes 4-[^{125}I]iodo-(2,5-dimethoxy)phenylisopropylamine and [^{3}H]mesulergine but not [^{3}H]ketanserin binding to 5-hydroxytryptamine2 receptors. *Mol. Pharmacol.* **1993**, *43*, 755-761.

186. Choudhary, M. S.; Sachs, N.; Uluer, A.; Glennon, R. A.; Westkaemper, R. B.; Roth, B. L. Differential ergoline and ergopeptine binding to 5-hydroxytryptamine2A receptors: Ergolines require an aromatic residue at position 340 for high affinity binding. *Mol. Pharmacol.* **1995**, *47*, 450-457.

187. Jones, G.; Willett, P.; Glen, R. C.; Leach, A. R.; Taylor, R. Development and validation of a genetic algorithm for flexible docking. *J. Mol. Biol.* **1997**, *267*, 727-748.

188. Kellogg, G. E.; Abraham, D. J. Hydrophobicity: Is log$P_{o/w}$ more than the sum of its parts? *Eur. J. Med. Chem.* **2000**, *35*, 651-661.

189. Cashman, D. J.; Scarsdale, J. N.; Kellogg, G. E. Hydropathic analysis of the free energy differences in anthracycline antibiotic binding to DNA. *Nucleic Acids Res.* **2003**, *31*, 4410–4416.

190. Cozzini, P.; Fornabaio, M.; Marabotti, A.; Abraham, D. J.; Kellogg, G. E.; Mozzarelli, A. Simple, intuitive calculations of free energy of binding for protein-ligand complexes. 1. Models without explicit constrained water. *J. Med. Chem.* **2002**, *45*, 2469-2483

191. Kanagarajadurai, K.; Malini, M.; Bhattacharya, A.; Panicker, M. M.; Sowdhamini, R. Molecular modeling and docking studies of human 5-hydroxytryptamine 2A ($5\text{-}HT_{2A}$) receptor for the identification of hotspots for ligand binding. *Mol. Biosyst.* **2009**, *5*, 1877-1888.

192. Schaffhauser, H.; Rowe, B. A.; Morales, S.; Chavez-Noriega, L. E.; Yin, R.; Jachec, C.; Rao, S. P.; Bain, G.; Pinkerton, A. B.; Vernier, J.-M.; Bristow, L. J.; Varney, M. A.; Daggett, L. P. Pharmacological characterization and identification of amino acids involved in the positive modulation of metabotropic glutamate receptor subtype 2. *Mol. Pharmacol.* **2003**, *64*, 798-810.

193. Hemstapat, K.; Da Costa, H.; Nong, Y.; Brady, A. E.; Luo, Q.; Niswender, C. M.; Tamagnan, G. D.; Conn, P. J. A novel family of potent negative allosteric modulators of group II metabotropic glutamate receptors. *J. Pharmacol. Exp. Ther.* **2007**, *322*, 254-264.

194. Lundström, L.; Bissantz, C.; Beck, J.; Wettstein, J.; Woltering, T.; Wichmann, J.; Gatti, S. Structural determinants of allosteric antagonism at metabotropic glutamate receptor 2: Mechanistic studies with new potent negative allosteric modulators. *Br. J. Pharmacol.* **2011**, *164*, 521-537.

195. Monn, J. A.; Prieto, L.; Taboada, L.; Hao, J.; Reinhard, M. R.; Henry, S. S.; Beadle, C. D.; Walton, L.; Man, T.; Rudyk, H.; Clark, B.; Tupper, D.; Baker, S. R.; Lamas, C.; Montero, C.; Marcos, A.; Blanco, J.; Bures, M.; Clawson, D. K.; Atwell, S.; Lu, F.; Wang, J.; Russell, M.; Heinz, B. A.; Wang, X.; Carter, J. H.; Getman, B. G.; Catlow, J. T.; Swanson, S.; Johnson, B. G.; Shaw, D. B.; McKinzie, D. L. Synthesis and pharmacological characterization of *C*4-(thiotriazolyl)-substituted-2-aminobicyclo[3.1.0]hexane-2,6-dicarboxylates. Identification of (1*R*,2*S*,4*R*,5*R*,6*R*)-2-Amino-4-(1*H*-1,2,4-Triazol-3-ylsulfanyl)bicyclo[3.1.0]hexane-2,6-dicarboxylic Acid (LY2812223), a highly potent, functionally selective $mGlu_2$ receptor agonist. *J. Med. Chem.* **2015**, *58*, 7526-7548.

196. Dore, A. S.; Okrasa, K.; Patel, J. C.; Serrano-Vega, M.; Bennett, K.; Cooke, R. M.; Errey, J. C.; Jazayeri, A.; Khan, S.; Tehan, B.; Weir, M.; Wiggin, G. R.; Marshall, F. H. Structure of class C GPCR metabotropic glutamate receptor 5 transmembrane domain. *Nature* **2014**, *511*, 557-562.

197. Lovell, S. C.; Davis, I. W.; Arendall, W. B.; de Bakker, P. I. W.; Word, J. M.; Prisant, M. G.; Richardson, J. S.; Richardson, D. C. Structure validation by Cα geometry: Φ,ψ and Cβ deviation. *Proteins* **2003**, *50*, 437-450.

198. Farinha, A.; Lavreysen, H.; Peeters, L.; Russo, B.; Masure, S.; Trabanco, A. A.; Cid, J.; Tresadern, G. Molecular determinants of positive allosteric modulation of the human metabotropic glutamate receptor 2. *Br. J. Pharmacol.* **2015**, *172*, 2383-2396.

199. Lundström, L.; Bissantz, C.; Beck, J.; Dellenbach, M.; Woltering, T. J.; Wichmann, J.; Gatti, S. Reprint of pharmacological and molecular characterization of the positive

allosteric modulators of metabotropic glutamate receptor 2. *Neuropharmacology* **2017**, *115*, 115-127.

200. Georg, J.; Lothar, L.; Eric; V.; Juergen, W. Imidazoles. U. S. Patent 2011015202 A1, January 20, 2011.

201. Bourgeois, W.; Seela, F. Synthesis of ara-3,7-dideazaadenosine and related pyrrolo[3,2-c]pyridine D-arabinofuranosides. *J. Chem. Soc., Perkin Trans. 1* **1991**, 279-283.

202. Mekheimer, R. A.; Refaey, S. M.; Sadek, K. U.; Hameed, A. M. A.; Ibrahim, M. A.; Shah, A. Fused quinoline heterocycles VIII. Synthesis of polyfunctionally substituted pyrazolo[4,3-c]quinol in-4(5*H*)-ones. *J. Chem. Res.* **2008**, *2008*, 735-737.

203. Kenichi, N.; Hidemasa, K.; Masakazu, S.; Yuko, N.; Tatsuya, K.; Tatsuya, S. Pesticide. WO2013027660 A1, February 28, 2013.

204. Micale, N.; Ettari, R.; Lavecchia, A.; Di Giovanni, C.; Scarbaci, K.; Troiano, V.; Grasso, S.; Novellino, E.; Schirmeister, T.; Zappalà, M. Development of peptidomimetic boronates as proteasome inhibitors. *Eur. J. Med. Chem.* **2013**, *64*, 23-34.

205. Hao, X.; Xu, Z.; Lu, H.; Dai, X.; Yang, T.; Lin, X.; Ren, F. Mild and regioselective n-alkylation of 2-pyridones in water. *Org. Lett.* **2015**, *17*, 3382-3385.

206. Runyon, S. P.; Mosier, P. D.; Roth, B. L.; Glennon, R. A.; Westkaemper, R. B. Potential modes of interaction of 9-aminomethyl-9,10-dihydroanthracene (AMDA) derivatives with the 5-HT_{2A} receptor: A ligand structure-affinity relationship, receptor mutagenesis and receptor modeling investigation. *J. Med. Chem.* **2008**, *51*, 6808-6828.

207. Xiong, Z.; Du, P.; Li, B.; Zhen, X.; Fu, U. Discovery of a novel 5-HT_{2A} inhibitor by pharmacophore-based virtual screening. *Chem. Res. Chin. Univ.* **2011**, *27*, 655-660.

208. Runyon, S. P.; Peddi, S.; Savage, J. E.; Roth, B. L.; Glennon, R. A.; Westkaemper, R. B. Geometry-affinity relationships of the selective serotonin receptor ligand 9-(aminomethyl)-9,10-dihydroanthracene. *J. Med. Chem.* **2002**, *45*, 1656-1664.

209. Sekhar, K. V. G. C.; Vyas, D. R. K.; Nagesh, H. N.; Rao, V. S. Pharmacophore hypothesis for atypical antipsychotics. *Bull. Korean Chem. Soc.* **2012**, *33*, 2930-2936.

210. Awadallah, M. F. Synthesis, pharmacophore modeling, and biological evaluation of novel 5*H*-thiazolo[3,2-a]pyrimidin-5-one derivatives as 5-HT_{2A} receptor antagonists. *Sci. Pharm.* **2008**, *76*, 415-438.

211. Kołaczkowski, M.; Mierzejewski, P.; Bieńkowski, P.; Wesołowska, A.; Newman-Tancredi, A. ADN-1184 A monoaminergic ligand with 5-HT(6/7) receptor antagonist activity: Pharmacological profile and potential therapeutic utility. *Br. J. Pharmacol.* **2014**, *171*, 973-984.

212. Gobbi, L.; Jaeschke, G.; Roche, O.; Rodriguez, S. R. M; Steward, L. Dual modulators of 5-HT_{2A} and D_3 Receptors. WO2009013212 A3, June 11, 2009.

213. Uto, Y. 1,2-Benzisoxazole compounds: A patent review (2009 - 2014). *Expert Opin. Ther. Pat.* **2015**, *25*, 643-662.

214. Dumas, D. J. Total synthesis of peramine. *J. Org. Chem.* **1988**, *53*, 4650-4653.

215. Torres-Gómez, H.; Lehmkuhl, K.; Frehland, B.; Daniliuc, C.; Schepmann, D.; Ehrhardt, C.; Wünsch, B. Stereoselective synthesis and pharmacological evaluation of [4.3.3]propellan-8-amines as analogs of adamantanamines. *Bioorg. Med. Chem.* **2015**, *23*, 4277-4285.

216. Aubry, C.; Wilson, A. J.; Emmerson, D.; Murphy, E.; Chan, Y. Y.; Dickens, M. P.; García, M. D.; Jenkins, P. R.; Mahale, S.; Chaudhuri, B. Fascaplysin-inspired diindolyls as selective inhibitors of CDK4/cyclin D1. *Bioorg. Med. Chem.* **2009**, *17*, 6073-6084.

217. Martins, C. P. B.; Freeman, S.; Alder, J. F.; Brandt, S. D. Characterisation of a proposed internet synthesis of *N*,*N*-dimethyltryptamine using liquid chromatography/electrospray ionisation tandem mass spectrometry. *J. Chromatogr. A* **2009**, *1216*, 6119-6123.

218. Song, H.; Yang, J.; Chen, W.; Qin, Y. Synthesis of chiral 3-substituted hexahydropyrroloindoline via intermolecular cyclopropanation. *Org. Lett.* **2006**, *8*, 6011-6014.

219. Bartkovitz, D. J.; Chu, X. -J.; Ding, Q.; Jiang, N.; Liu, J. -J.; Ross, T. M.; Zhang, J.; Zhang, Z. Substituted pyrrolidine-2-carboxamides. WO2011098398 A1, August 18, 2011.

220. The PyMOL Molecular Graphics System, Version 1.3 Schrödinger, LLC.

APPENDIX A

Analog **155** (Figure A1) has a chiral carbon atom, and can have multiple conformational isomers. A systematic search was performed using SYBYL-X 2.1 (Tripos International) to determine the lowest energy conformations of analog **155**. Figure A1 illustrates the bonds that were set as rotatable bonds (RB) as well as the closure bond. The increment value, and the maximum energy difference, were set as 10 degrees and 9999 kcal/mol, respectively. Default options were used for the other parameters. The benzene-ring centroid was defined as the aromatic center, and the distances of the aromatic centers from the nitrogen atoms were also measured as part of the systematic search. The systematic search was performed on the *S* equatorial, *R* axial, *R* equatorial, and *S* axial isomers of **155**, and the results of the conformational search are tabulated in Tables A1, A2, A3 and A4, respectively. In the lowest energy conformations of the *S* equatorial, *R* axial, *R* equatorial, and *S* axial isomers of analog **155**, the piperidine ring was in a chair conformation, and are shown in Figure A2.

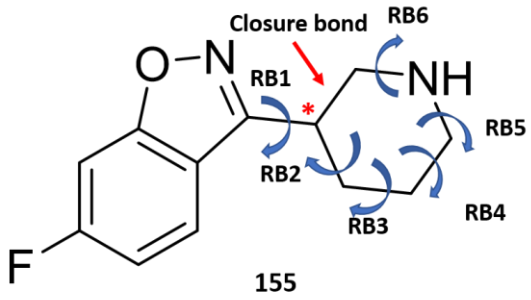

Figure A1. Analog **155**. Blue arrows indicate rotatable bonds (RB).

Table A1. Results of the systematic search for *S* equatorial-**155**.

Name	RB1*	RB2*	RB3*	RB4*	RB5*	RB6*	Energy (kcal/mol)	Distance (Å)**
1. CNF_15	**280**	**56.3**	**303.6**	**56.8**	**302**	**58**	**15.5630**	**5.75**
2. CNF_1	270	56.3	303.6	56.8	302	58	15.6464	5.85
3. CNF_14	290	56.3	303.6	56.8	302	58	15.6809	5.65
4. CNF_8	200	56.3	303.6	56.8	302	58	15.7319	6.35
5. CNF_2	260	56.3	303.6	56.8	302	58	15.7662	5.95
6. CNF_7	210	56.3	303.6	56.8	302	58	15.7855	6.25
7. CNF_6	220	56.3	303.6	56.8	302	58	15.8622	6.25
8. CNF_3	250	56.3	303.6	56.8	302	58	15.8743	5.95
9. CNF_9	190	56.3	303.6	56.8	302	58	15.8863	6.35
10. CNF_5	230	56.3	303.6	56.8	302	58	15.9212	6.15
11. CNF_4	240	56.3	303.6	56.8	302	58	15.9315	6.05
12. CNF_13	300	56.3	303.6	56.8	302	58	16.9391	5.55
13. CNF_10	180	56.3	303.6	56.8	302	58	17.2677	6.35
14. CNF_12	60	56.3	303.6	56.8	302	58	17.3462	5.55
15. CNF_11	170	336.3	323.6	66.8	332	328	27.2139	5.45

***RB:** rotatable bond (degrees). **Aromatic (benzene-ring) to amine distance.

Table A2. Results of the systematic search for *R* axial-**155**.

Name	RB1*	RB6*	RB5*	RB4*	RB3*	RB2*	Energy (kcal/mol)	Distance (Å)**
1. CNF_1	**161.7**	**303.3**	**58.5**	**301.9**	**56.2**	**304.4**	**15.2224**	**5.75**
2. CNF_62	171.7	303.3	58.5	301.9	56.2	304.4	15.4034	5.75
3. CNF_60	181.7	303.3	58.5	301.9	56.2	304.4	17.1884	5.65
4. CNF_37	81.7	23.3	38.5	291.9	26.2	34.4	23.6635	6.05
5. CNF_41	71.7	23.3	38.5	291.9	26.2	34.4	23.6724	5.95
6. CNF_33	91.7	23.3	38.5	291.9	26.2	34.4	23.6975	6.15
7. CNF_36	81.7	33.3	28.5	291.9	36.2	24.4	23.7202	6.05
8. CNF_32	91.7	33.3	28.5	291.9	36.2	24.4	23.7492	6.15
9. CNF_29	101.7	23.3	38.5	291.9	26.2	34.4	23.7506	6.25
10. CNF_40	71.7	33.3	28.5	291.9	36.2	24.4	23.7628	5.95
11. CNF_28	101.7	33.3	28.5	291.9	36.2	24.4	23.802	6.25
12. CNF_23	111.7	23.3	38.5	291.9	26.2	34.4	23.8169	6.35
13. CNF_45	61.7	23.3	38.5	291.9	26.2	34.4	23.8227	5.85
14. CNF_22	111.7	33.3	28.5	291.9	36.2	24.4	23.8653	6.35
15. CNF_17	121.7	23.3	38.5	291.9	26.2	34.4	23.8978	6.35
16. CNF_16	121.7	33.3	28.5	291.9	36.2	24.4	23.9309	6.35
17. CNF_10	131.7	33.3	28.5	291.9	36.2	24.4	24.0114	6.45
18. CNF_11	131.7	23.3	38.5	291.9	26.2	34.4	24.0238	6.45
19. CNF_5	151.7	323.3	68.5	331.9	326.2	64.4	24.0278	6.05

20. CNF_2	161.7	323.3	68.5	331.9	326.2	64.4	24.0727	6.05
21. CNF_44	61.7	33.3	28.5	291.9	36.2	24.4	24.085	5.85
22. CNF_8	141.7	323.3	68.5	331.9	326.2	64.4	24.0919	6.05
23. CNF_14	131.7	323.3	68.5	331.9	326.2	64.4	24.2301	6.05
24. CNF_7	141.7	333.3	68.5	321.9	336.2	64.4	24.2679	6.15
25. CNF_64	171.7	323.3	68.5	331.9	326.2	64.4	24.2811	5.95
26. CNF_4	151.7	333.3	68.5	321.9	336.2	64.4	24.2888	6.15
27. CNF_58	301.7	23.3	38.5	291.9	26.2	34.4	24.3342	5.35
28. CNF_49	51.7	23.3	38.5	291.9	26.2	34.4	24.3522	5.75
29. CNF_13	131.7	333.3	68.5	321.9	336.2	64.4	24.3568	6.15
30. CNF_20	121.7	323.3	68.5	331.9	326.2	64.4	24.4141	5.95
31. CNF_19	121.7	333.3	68.5	321.9	336.2	64.4	24.5013	6.05
32. CNF_26	111.7	323.3	68.5	331.9	326.2	64.4	24.6469	5.95
33. CNF_25	111.7	333.3	68.5	321.9	336.2	64.4	24.6739	6.05
34. CNF_57	301.7	33.3	28.5	291.9	36.2	24.4	24.7407	5.45
35. CNF_48	51.7	33.3	28.5	291.9	36.2	24.4	25.2815	5.75
36. CNF_51	41.7	23.3	38.5	291.9	26.2	34.4	25.5312	5.65
37. CNF_54	311.7	23.3	38.5	291.9	26.2	34.4	26.7319	5.25
38. CNF_35	81.7	43.3	18.5	291.9	46.2	14.4	27.2489	6.05
39. CNF_39	71.7	43.3	18.5	291.9	46.2	14.4	27.2763	5.95
40. CNF_31	91.7	43.3	18.5	291.9	46.2	14.4	27.3276	6.15
41. CNF_42	71.7	13.3	48.5	291.9	16.2	44.4	27.3566	5.95

42. CNF_46	61.7	13.3	48.5	291.9	16.2	44.4	27.3805	5.85
43. CNF_38	81.7	13.3	48.5	291.9	16.2	44.4	27.4161	6.05
44. CNF_27	101.7	43.3	18.5	291.9	46.2	14.4	27.4313	6.25
45. CNF_34	91.7	13.3	48.5	291.9	16.2	44.4	27.5012	6.15
46. CNF_21	111.7	43.3	18.5	291.9	46.2	14.4	27.5322	6.25
47. CNF_30	101.7	13.3	48.5	291.9	16.2	44.4	27.5977	6.25
48. CNF_15	121.7	43.3	18.5	291.9	46.2	14.4	27.6072	6.35
49. CNF_9	131.7	43.3	18.5	291.9	46.2	14.4	27.6525	6.45
50. CNF_50	51.7	13.3	48.5	291.9	16.2	44.4	27.6563	5.75
51. CNF_6	141.7	43.3	18.5	291.9	46.2	14.4	27.6825	6.45
52. CNF_3	151.7	43.3	18.5	291.9	46.2	14.4	27.6952	6.45
53. CNF_24	111.7	13.3	48.5	291.9	16.2	44.4	27.6983	6.35
54. CNF_43	61.7	43.3	18.5	291.9	46.2	14.4	27.7931	5.85
55. CNF_53	31.7	23.3	38.5	291.9	26.2	34.4	27.7996	5.55
56. CNF_18	121.7	13.3	48.5	291.9	16.2	44.4	27.8048	6.35
57. CNF_63	171.7	43.3	18.5	291.9	46.2	14.4	27.8064	6.45
58. CNF_12	131.7	13.3	48.5	291.9	16.2	44.4	27.9582	6.45
59. CNF_59	301.7	13.3	48.5	291.9	16.2	44.4	28.0038	5.15
60. CNF_56	301.7	43.3	18.5	291.9	46.2	14.4	28.6003	5.65
61. CNF_52	41.7	13.3	48.5	291.9	16.2	44.4	28.6801	5.65
62. CNF_55	311.7	13.3	48.5	291.9	16.2	44.4	29.0222	5.15
63. CNF_61	181.7	43.3	18.5	291.9	46.2	14.4	29.2778	6.45

64. CNF_47	51.7	43.3	18.5	291.9	46.2	14.4	30.2279	5.75

***RB:** rotatable bond (degrees). **Aromatic (benzene-ring) to amine distance.

Table A3. Results of the systematic search for *R* equatorial-**155**.

Name	RB1*	RB2*	RB3*	RB4*	RB5*	RB6*	Energy (kcal/mol)	Distance (Å)**
1. CNF_1	**283.2**	**56.9**	**301.6**	**58.2**	**303.3**	**56.1**	**15.558**	**6.45**
2. CNF_2	273.2	56.9	301.6	58.2	303.3	56.1	15.6152	6.45
3. CNF_11	203.2	56.9	301.6	58.2	303.3	56.1	15.7263	5.95
4. CNF_4	263.2	56.9	301.6	58.2	303.3	56.1	15.7295	6.45
5. CNF_12	193.2	56.9	301.6	58.2	303.3	56.1	15.7835	5.85
6. CNF_10	213.2	56.9	301.6	58.2	303.3	56.1	15.793	6.05
7. CNF_16	293.2	56.9	301.6	58.2	303.3	56.1	15.8182	6.45
8. CNF_6	253.2	56.9	301.6	58.2	303.3	56.1	15.8422	6.35
9. CNF_9	223.2	56.9	301.6	58.2	303.3	56.1	15.8683	6.15
10. CNF_7	243.2	56.9	301.6	58.2	303.3	56.1	15.9138	6.25
11. CNF_8	233.2	56.9	301.6	58.2	303.3	56.1	15.9189	6.25
12. CNF_13	183.2	56.9	301.6	58.2	303.3	56.1	16.6131	5.85
13. CNF_14	63.2	56.9	301.6	58.2	303.3	56.1	17.2443	5.75
14. CNF_15	303.2	56.9	301.6	58.2	303.3	56.1	17.891	6.45
15. CNF_3	273.2	346.9	311.6	68.2	343.3	316.1	27.2003	6.25
16. CNF_5	263.2	346.9	311.6	68.2	343.3	316.1	27.3223	6.25

***RB:** rotatable bond (degrees). **Aromatic (benzene-ring) to amine distance.

Table A4. Results of the systematic search for *S* axial-**155**.

Name	RB1*	RB2*	RB3*	RB4*	RB5*	RB6*	Energy (kcal/mol)	Distance (Å)**
1. CNF_1	**80**	**54.9**	**299.7**	**60.2**	**304.7**	**52.2**	**15.9379**	**5.85**
2. CNF_3	70	54.9	299.7	60.2	304.7	52.2	15.9942	5.85
3. CNF_41	90	54.9	299.7	60.2	304.7	52.2	16.0544	5.85
4. CNF_37	100	54.9	299.7	60.2	304.7	52.2	16.2338	5.85
5. CNF_33	110	54.9	299.7	60.2	304.7	52.2	16.4354	5.85
6. CNF_12	170	54.9	299.7	60.2	304.7	52.2	16.4431	5.05
7. CNF_29	120	54.9	299.7	60.2	304.7	52.2	16.6118	5.75
8. CNF_25	130	54.9	299.7	60.2	304.7	52.2	16.7173	5.65
9. CNF_5	60	54.9	299.7	60.2	304.7	52.2	16.8652	5.75
10. CNF_8	180	54.9	299.7	60.2	304.7	52.2	18.6755	4.85
11. CNF_18	160	334.9	69.7	320.2	334.7	62.2	23.6483	6.05
12. CNF_15	170	334.9	69.7	320.2	334.7	62.2	23.7422	5.95
13. CNF_21	150	334.9	69.7	320.2	334.7	62.2	23.7704	6.15
14. CNF_24	140	334.9	69.7	320.2	334.7	62.2	23.9774	6.15
15. CNF_28	130	334.9	69.7	320.2	334.7	62.2	24.1841	6.25
16. CNF_16	160	34.9	289.7	30.2	34.7	292.2	24.3245	5.55
17. CNF_32	120	334.9	69.7	320.2	334.7	62.2	24.3255	6.35

18. CNF_19	150	34.9	289.7	30.2	34.7	292.2	24.3952	5.65
19. CNF_36	110	334.9	69.7	320.2	334.7	62.2	24.3987	6.35
20. CNF_11	180	334.9	69.7	320.2	334.7	62.2	24.4115	5.75
21. CNF_13	170	34.9	289.7	30.2	34.7	292.2	24.448	5.45
22. CNF_42	90	34.9	289.7	30.2	34.7	292.2	24.4602	6.15
23. CNF_40	100	334.9	69.7	320.2	334.7	62.2	24.4681	6.45
24. CNF_2	80	34.9	289.7	30.2	34.7	292.2	24.4715	6.05
25. CNF_22	140	34.9	289.7	30.2	34.7	292.2	24.5117	5.85
26. CNF_38	100	34.9	289.7	30.2	34.7	292.2	24.5393	6.05
27. CNF_4	70	34.9	289.7	30.2	34.7	292.2	24.6103	6.05
28. CNF_26	130	34.9	289.7	30.2	34.7	292.2	24.6265	5.95
29. CNF_34	110	34.9	289.7	30.2	34.7	292.2	24.64	6.05
30. CNF_30	120	34.9	289.7	30.2	34.7	292.2	24.6809	6.05
31. CNF_9	180	34.9	289.7	30.2	34.7	292.2	25.7056	5.25
32. CNF_7	190	334.9	69.7	320.2	334.7	62.2	26.3994	5.65
33. CNF_14	170	4.9	299.7	60.2	354.7	312.2	26.7008	5.75
34. CNF_17	160	4.9	299.7	60.2	354.7	312.2	26.7645	5.85
35. CNF_10	180	4.9	299.7	60.2	354.7	312.2	26.8825	5.65
36. CNF_20	150	4.9	299.7	60.2	354.7	312.2	26.8877	6.05
37. CNF_23	140	4.9	299.7	60.2	354.7	312.2	27.0264	6.15
38. CNF_27	130	4.9	299.7	60.2	354.7	312.2	27.1553	6.15
39. CNF_31	120	4.9	299.7	60.2	354.7	312.2	27.2394	6.25

40. CNF_35	110	4.9	299.7	60.2	354.7	312.2	27.2777	6.35
41. CNF_39	100	4.9	299.7	60.2	354.7	312.2	27.3496	6.35
42. CNF_6	190	4.9	299.7	60.2	354.7	312.2	28.1301	5.55

***RB:** rotatable bond (degrees). **Aromatic (benzene-ring) to amine distance.

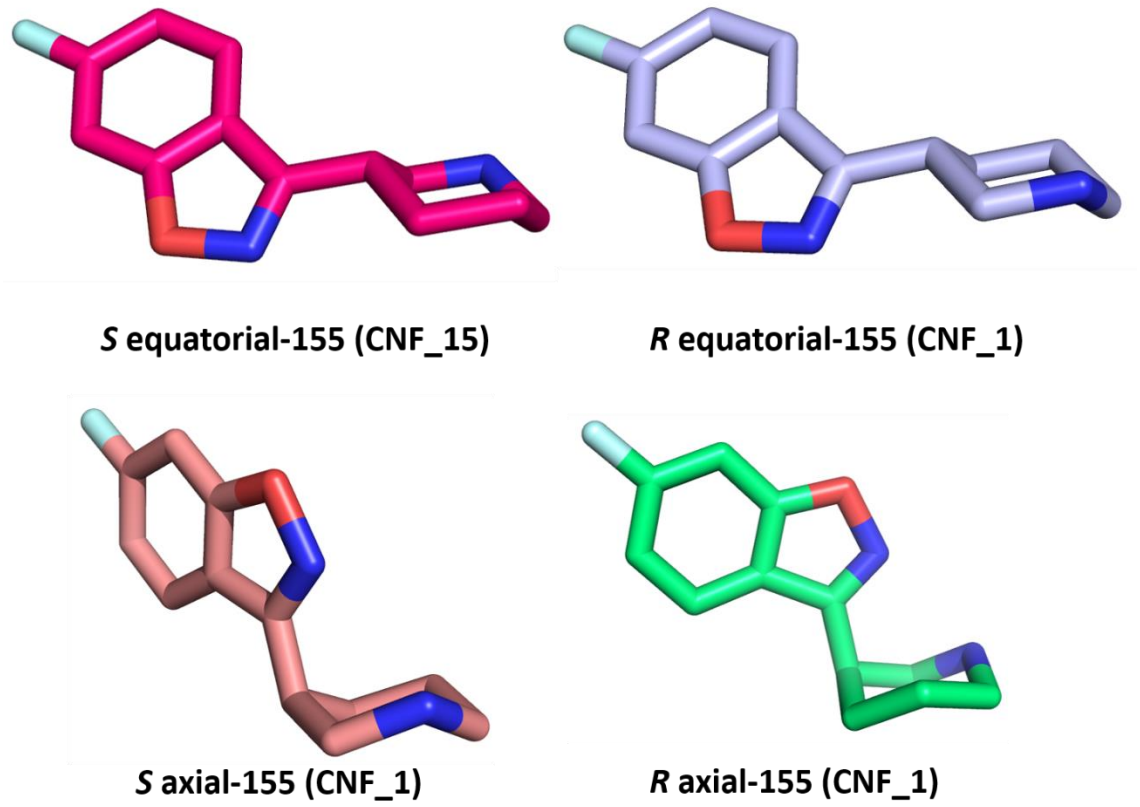

Figure A2. The lowest energy conformers of *S* equatorial-**155** (CNF_15; pink), *R* equatorial **155** (CNF_1; violet), *S* axial-**155** (CNF_1; salmon), and *R* axial-**155** (CNF_1; green).

Discussion

The systematic search on *S*-equatorial **155** and *R*-equatorial **155** resulted in only 15 (Table A1), and 16 (Table A3) isomers, respectively. Hence, we modified the Van der Waals radius scale factors general parameter to 0.7, and performed the systematic search as previously described. This

change resulted in 123 isomers for both *S*-equatorial **155** and *R*-equatorial **155**. The lowest energy conformer for the *S*-equatorial isomer had the same energy as CNF_15 (Table A1), however, the distance of the aromatic (benzene-ring centroid) center from the amine increased to 5.95 Å. The lowest energy conformer for the *R*-equatorial isomer had the same energy and aromatic center (benzene-ring centroid) to amine distance as CNF_1 (Table A3).

VITA

Urjita H. Shah was born on March 4, 1990 to Harsh D. Shah and Seema H. Shah in Mumbai, India. She received her Bachelor in Pharmaceutical Sciences degree from the University of Mumbai in July 2012, following which she enrolled in the doctoral program in the Department of Medicinal Chemistry, School of Pharmacy at Virginia Commonwealth University.